UiO : University of Oslo

Krister Gjestvang Grønlien

Sustainable use of rest raw materials: Properties of collagen from turkey (*Meleagris gallopavo*) and potential pharmaceutical and biomedical applications

Thesis submitted for the degree of Philosophiae Doctor

Department of Pharmacy
Faculty of Mathematics and Natural Sciences

2021

Preface

This thesis is submitted in partial fulfillment of the requirements for the degree of *Philosophiae Doctor* at the Department of Pharmacy, University of Oslo. The research presented here was conducted at the University of Oslo, Nofima AS and at Nordic Institute of Dental Materials AS, under the supervision of Professor Hanne Hjorth Tønnesen, Dr. Scient. Mona Elisabeth Pedersen, Dr. Scient. Ellen Bruzell and Ph.D. Håkon Valen.

Acknowledgements

First, I want to thank my main supervisor, Professor Hanne Hjorth Tønnesen. It has been a pleasure working with you and the rest of the PharmaLuxLab research group throughout these years. Thank you for always having an open door and for sharing your knowledge with me. Thank you for believing in me and my research.

I would also like to express my gratitude to my co-supervisors Mona Elisabeth Pedersen, Ellen Bruzell and Håkon Valen. Thank you for your commitment to the project. Your knowledge from other scientific areas than pharmaceutics has been invaluable.

During my first years of the PhD project, Professor Emeritus Jan Karlsen was a co-supervisor and an extensive part of the project and the ideas behind the research. Unfortunately, Jan passed away 21.03.2019. I want to express my gratitude to all the knowledge and ideas he shared with me.

Bente Amalie Breiby, Ivar Grove and Tove Larsen, Ragnhild Stenberg Berg, Nina Solberg and Inger-Sofie Dragland, thank you for all technical assistance.

Julia, Raj and Helene, thank you for being the best office mates, and together with Anca, Joseph and Bjarke the best colleagues I could get. Thank you for your friendship and your social encouragement.

I want to thank all my co-authors and colleagues at Nofima AS and NIOM AS for technical assistance, valuable discussions and for welcoming me to your labs. I am also very grateful to Norilia AS for supporting the work by donation of rest raw materials and funding of analytical kits.

Mom and dad, I can not thank you enough. Your support throughout my childhood, youth and studies has been the best. I have been so lucky growing up with you, Even and my grandparents. Thank you!

Last, but not least I want to thank Janine for always supporting me throughout these years. I love you.

Krister Gjestvang Grønlien
Oslo, March 2021

List of Papers

Paper I

Grønlien, K. G., Pedersen, M. E., Sanden, K. W., Høst, V., Karlsen, J. and Tønnesen, H. H. "Collagen from Turkey (*Meleagris gallopavo*) tendon: A promising sustainable biomaterial for pharmaceutical use". In: *Sustainable Chemistry and Pharmacy*. Vol. 13, (2019), article 100166. DOI: 10.1016/j.scp.2019.100166.

Paper II

Grønlien, K. G., Pedersen, M. E. and Tønnesen, H. H. "A natural deep eutectic solvent (NADES) as potential excipient in collagen-based products". In: *International Journal of Biological Macromolecules*. Vol. 156, (2020), pp. 394–402. DOI: 10.1016/j.ijbiomac.2020.04.026.

Paper III

Grønlien, K. G., Pedersen, M. E., Rønning, S. B., Solberg, N. and Tønnesen, H. H. "Tuning of 2D cultured human fibroblast behavior using lumichrome photocrosslinked collagen hydrogels". Submitted to *International Journal of Biological Macromolecules*.

Paper IV

Grønlien, K. G., Valen, H., Bruzell, E. and Tønnesen H. H. "Bacterial phototoxicity of lumichrome photocrosslinked collagen hydrogels". Manuscript in preparation for *Photochemical & Photobiological Sciences*.

Other co-authored papers

Thapa, R. K., Cazzador, F., Grønlien, K. G. and Tønnesen, H. H. "Effect of curcumin and cosolvents on the micellization of Pluronic F127 in aqueous solution". In: *Colloids and Surfaces B: Biointerfaces*. Vol. 195, (2020), article 111250. DOI: 10.1016/j.colsurfb.2020.111250.

Nystedt, H. L., Grønlien, K. G. and Tønnesen, H. H. "Interactions of natural deep eutectic solvents (NADES) with artificial and natural membranes". In: *Journal of Molecular Liquids*. Vol. 328, (2021), article 115452. DOI: 10.1016/j.molliq.2021.115452.

Abbreviations

$^1O_2$	singlet oxygen
AFM	atomic force microscopy
AI	avian influenza
α-SMA	α-smooth muscle actin
aPDT	antimicrobial photodynamic therapy
BHI	brain heart infusion
BSE	bovine spongiform encephalopathy
CD	cyclodextrin(s)
CE	complexation efficiency
CX	citric acid and xylitol in the molar ratio 1:1
CFU	colony forming unit(s)
DES	deep eutectic solvent(s)
DMEM	Dulbecco's modified Eagle's medium
DPBS	Dulbecco's phosphate buffered saline
DSC	differential scanning calorimetry
E	Young's modulus
ECM	extracellular matrix
ER	endoplasmic reticulum
F-actin	filamentous actin
FDA	US Food and Drug Administration
FMD	foot-and-mouth disease
FT-IR	fourier transform infrared spectroscopy
GRAS	generally recognized as safe
HPβCD	(2-hydroxypropyl)-β-cyclodextrin
HPγCD	(2-hydroxypropyl)-γ-cyclodextrin
HPLC	high-performance liquid chromatography
IC	internal conversion
ISC	intersystem crossing
$K_{1:1}$	complexation stability constant
LC	lumichrome
LF	lumiflavin
MMP	matrix metalloproteinase

mRNA	messenger ribonucleic acid
M_W	molecular weight
NADES	natural deep eutectic solvent(s)
OD	optical density
PBS	phosphate buffered saline
PCL	prilocaine hydrochloride
PCR	polymerase chain reaction
PEG	polyethylene glycol
PDT	photodynamic therapy
PS	photosensitizer
RF	riboflavin
ROS	reactive oxygen species
RT-qPCR	reverse transcriptase quantitative polymerase chain reaction
S. aureus	*Staphylococcus aureus*
SEM	scanning electron microscopy
SDC-4	syndecan-4
TEM	transmission electron microscopy
T_g	glass transition temperature
TGA	thermogravimetric analysis
TIMP	tissue inhibitor of matrix metalloproteinase
T_m	melting point *or* major transition
T_s	minor transition
TSE	transmittable spongiform encephalopathy
UV	ultraviolet
UV-CD	ultraviolet circular dichroism
VR	vibrational relaxation
WHC	water holding capacity

Abstract

The 2030 Agenda for Sustainable Development, adopted by all members of the United Nations, includes goals to secure an increased responsibility in the use and consumption of meat products. The global demand and increase in production and consumption of such products have lead to the accumulation of large amounts of organic waste, i.e., rest raw materials after the edible part is used. Rest raw materials such as skin, bones and tendons are often rich in fibrous proteins, in particular collagen. The aim of the present thesis was to investigate how rest raw materials from Norwegian industrially produced turkey (*Meleagris gallopavo*) could be utilized as a source of collagen suitable for use in pharmaceutical and biomedical applications. Further, the aim was to investigate the suitability of new environmentally friendly solvents and natural crosslinkers as sustainable formulation strategies.

Collagen was isolated and characterized with respect to properties describing the protein's molecular functions, stability and biocompatibility. Properties studied confirmed the suitability of the isolated collagen for further use in formulation of pharmaceutical and biomedical products. The isolated collagen was used in preparation of formulations relevant for pharmaceutical (drug delivery) and biomedical (tissue engineering and wound healing) applications. Hydrogels, sponges and freeze-dried sheets were prepared.

Hydrogels were prepared by neutralization and optional photochemical crosslinking of acidic collagen solutions. Photochemical crosslinking was performed by application of riboflavin and its photo-oxidation product, lumichrome. The mechanical properties, water holding capacity and enzymatic degradation profile were investigated. Cell studies were performed to evaluate biocompatibility and behavior of fibroblasts on the hydrogels in 2D. The results indicated that the hydrogels may be suitable for biomedical applications, such as skin tissue engineering and wound healing. The dual effect of lumichrome as a photochemical crosslinker and a photosensitizer in antibacterial applications was studied and indicated a potential for the hydrogels in such applications. Freeze-dried sponges were prepared from riboflavin crosslinked hydrogels. The morphology, thermal stability and release of an active pharmaceutical ingredient were investigated. The results indicated that the sponges could be suitable for further development into scaffolds for cells.

Natural deep eutectic solvents (NADES) have proven to be suitable as alternatives to conventional solvents. The NADES can also possess antibacterial properties (either alone or in combination with photosensitizers and light). A combination of collagen and NADES has the potential to add the unique wound healing properties of collagen to the antibacterial properties of the NADES. The molecular properties of collagen in the NADES were studied. While the

collagen seemed to unfold and degrade in undiluted NADES, a highly diluted NADES preserved the triple helical structure of the protein. The combination of diluted NADES and collagen was further investigated as combinations in collagen formulations. Freeze-drying of collagen-NADES solutions resulted in thin sheets with NADES concentrated within the protein structure, increasing the plasticity of the material.

The findings in the present thesis provide the basis for further use of turkey rest raw materials in pharmaceutical and biomedical applications, and suggests the isolation of collagen as an sustainable alternative in waste management.

Contents

List of Figures

List of Tables

Chapter 1

Introduction

Good health, clean water, clean energy and responsible consumption and production are goals included in the 2030 Agenda for Sustainable Development, adopted by all member states of the United Nations [1]. Important areas of action for these goals are the responsible use and consumption of meat products, reduced environmental pollution and circular bioeconomy. The global demand and increase in production and consumption of meat products have lead to the accumulation of large amounts of organic waste and byproducts, which will have impact on the Sustainable Development goals [2–4]. The organic waste and byproducts include the remains after industrial production of meat, poultry and fish products [4]. The waste management continues to be an important issue related to environmental pollution [5]. The slaughterhouse waste is often utilized as source for renewable energy, such as the production of biofuel, in pet food, but also incinerated without energy recovery [6]. Examples of successful use of waste and byproducts in the development of new products are extraction of eggshell membrane to produce biomedical scaffolds, development of wood adhesives from animal-based proteins and isolation of collagen from connective tissue for both food and non-food applications such as sausage casings and the production of biomedical devices, respectively [6–8].

The remains from the food production after the edible part is utilized are defined as rest raw materials. Examples of such materials are skin, bones and tendons [9]. These materials are rich in fibrous proteins, in particular collagen. Collagen has previously been isolated from bovine, porcine, equine, avian and aquatic species [10–14]. In this thesis, collagen was isolated from turkey (*Meleagris gallopavo*) rest raw material and characterized with respect to potential use in pharmaceutical and biomedical applications.

1.1 Collagen

Collagen is the major fibrous component and protein in both human and animal connective tissue, constituting about 20-30% of the total protein weight. Collagen has in its native form a characteristic triple helical structure formed by three α-chains held together by hydrogen bonds (Figure 1.1). The α-chains are built up by repeating triplets of the amino acid sequence glycine-X-Y, where X and Y are often proline and its metabolite hydroxyproline [15].

1.1.1 Molecular properties and biosynthesis

The most common collagen-producing cells are fibroblasts. These cells are found in connective tissue throughout the body and produce extracellular matrix (ECM)

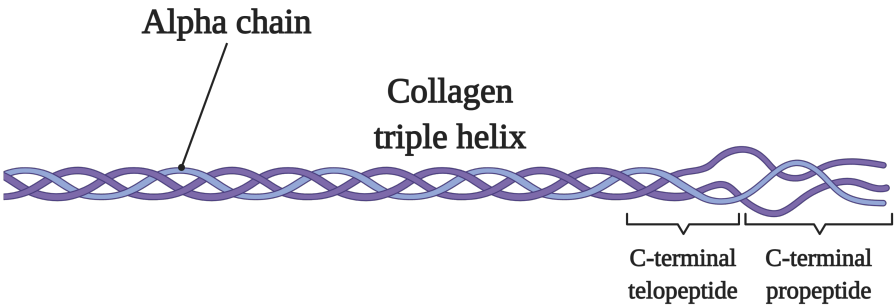

Figure 1.1: Illustration of a collagen type I molecule, consisting of three alpha chains (two α_1(I) and one α_2(I)) forming a helix with a c-terminal propeptide and telopeptide. The telopeptide is cleaved off during pepsin treatment. (Created with BioRender.com).

components [16]. In the nuclei of the fibroblasts, genes for the pro-α chains are transcribed producing mRNA. The translation of the mRNA is done by ribosomes in the cytoplasm, and the pre-pro-polypeptide chain is produced. The post-translational modifications of collagen start in the endoplasmic reticulum (ER) of the cells. Important steps of the modification include removal of the signal peptide on the N-terminal, hydroxylation of the amino acids lysine and proline by hydroxylase enzymes requiring ascorbic acid (vitamin C) as a co-factor, and the glycosylation of hydroxylated lysine [17, 18]. Winding of the α-chains into a triple helix produces a collagen molecule with non-helical terminal peptides called procollagen. After synthesis of procollagen, the molecule will move out of the ER and move over the Golgi stacks before the propeptides are removed by peptidases in the extracellular space [18, 19]. This produces a collagen molecule able to assemble into fibrils. At this stage, the endings of the molecule consist of non-helical telopeptides [20]. The telopeptides are important for the assembling into higher order structures of collagen as fibrils and fibers. However, the telopeptides are a limitation for the use of the material in biomedical applications by being the major source of potential immunogenicity. The telopeptides can further be cleaved off during pepsin treatment, producing atelocollagen. The amino acid tyrosine is located within the telopeptides, and cleavage of these will result in a low tyrosine content of the molecule [13, 21]. In its post-translational form, collagen is approximately 300 nm in length, 1.6 nm in diameter and has a molecular weight (M_W) of approximately 300 000 Da [22, 23].

1.1.2 Physicochemical properties and methods for characterization of collagen

The physicochemical properties of collagen are important for the function and potential use in biomedical products. Collagen is often characterized with respect

to amino acid composition, strand composition, viscosity, spectral properties, thermal behavior and enzymatic degradability/resistance.

The properties of collagen differ quite much between species and source within the specimen. Hence, collagen is classified into different types. At least 29 variants of collagen have been identified to date. The types differ in origin, structure and their ability to form fibrils [15, 23]. They are further divided into six groups describing their respective functions; fibrillar collagens, fibril associated collagens with interrupted triple helices, beaded filament, basement membrane collagens, short chain collagens and transmembrane collagens [24]. The most abundant group of collagens are fibrillar collagens (including type I, II, III, V, XI, XXIV and XXVII), which are the main focus of the present thesis. Fibrillar collagens are distributed across connective tissues, with type I found in bone, skin and tendons, type II specific to cartilage and type III as the major structural component in hollow organs and skin, but is also found in tendons [24, 25]. The other fibrillar collagens are present to a lesser extent. Structural information of collagen can be achieved through mass spectroscopy methods and gel electrophoresis of isolated collagen [26].

The amino acid composition of collagen determines many of the other physicochemical properties. Some amino acids are important for the formation of the helical structure of the molecule (among others alanine, phenylalanine and tyrosine), while other amino acids are sterically hindered in participating in the helix formation [27]. Further, some amino acids are eliminated from the molecule during production and post-translational modifications, for example pepsin treatment. As described above, the tyrosine moieties of collagen are located in the non-helical telopeptides of the collagen molecule, and are cleaved off during pepsin treatment. The role of the telopeptides is still partially unknown, but they are known to be involved in the stabilization of the molecule and ability to form fibrils [20]. The amino acid content varies between animal species, and by the source of isolation [28].

The structural properties of collagen may further be examined by studying the spectral properties. Collagen has two characteristic UV-absorption maxima at approximately 230 and 250-280 nm. These are related to the absorption by the triple helix and aromatic amino acid residues (phenylalanine and tyrosine), respectively [29, 30]. The helical integrity and unfolding can further be studied by measuring differential absorption of circular polarized light through circular dichroism methods (UV-CD) [26]. The absorption of infrared light ($\geq$ 700 nm) measured by fourier transform infrared spectroscopy (FT-IR) can be used to study the collagen composition and analyze differences in collagen types [31, 32]. This will give information about vibrational bands related to the specific biochemical composition of the molecule [33]. FT-IR may further be used to monitor changes in the composition following modification and formulation of the protein [11]. Collagen has the unique ability to form fibers by self-assembly after production and secretion to the extracellular space *in vivo*. This forms the physical basis for tensile strength in tissues [34]. The kinetics of fibril formation may be monitored *in vitro* by recording the increase in absorption at 313 nm due to increased turbidity [35]. The fibril formation under increasing temperature

can also be followed by UV-CD combined with signal-processing algorithms [36].

The thermal behavior of a protein is crucial for the stability of the protein structure. Denaturation is the process where a protein loses its quaternary, tertiary and secondary structure after being exposed to an external factor, such as temperature and pH. For collagen, denaturation means the loss of the triple helical structure with helix-to-coil transformation of the molecule [37]. The denaturation temperature of collagen can be attributed to the content of the amino acids proline, hydroxyproline and hydroxylysine [38]. A higher proline and hydroxyproline content stabilizes the native collagen helices, increasing the denaturation temperature [39]. The denaturation temperature is further influenced by the isoelectric point and swelling abilities, with lower denaturation temperature at higher swelling [21]. For biomedical use, the collagen should have a denaturation temperature above the human body temperature to avoid protein denaturation [40]. Crosslinking of collagen will influence the denaturation temperature. An increased crosslinking will lead to a higher denaturation temperature, possibly due to dehydration of the fibers [41]. Human collagen has been studied and shown to have a denaturation temperature below the body temperature [42]. This means that the collagen should be unstable at body temperature, but is in fact stabilized by the formation of crosslinked fibers [42]. Changes in collagen stability have been postulated to play a role in certain diseases, for example *osteogenesis imperfecta*. The pathophysiology of this disease involves abnormalities in the collagen molecule with the absence of one of the collagen α-chain types. This will result in an triple helical molecule with reduced crosslinking functionality and furthermore a lower denaturation temperature [41, 42]. The denaturation temperature of collagen is related to the body temperature for the respective species [43]. Among the most used sources for collagen, the denaturation temperatures range from 36.3 °C for calf skin, 37.0 °C for pig skin, and 44.0 °C for chicken keel bone [12, 40]. Collagen from different fish species has, however, shown quite low denaturation temperatures, i.e., $\leq$ 15.2 °C below mammal species [14]. In the present thesis, collagen was isolated from turkey (*Meleagris gallopavo*). Turkeys have an average body temperature of 41.1 °C, which should indicate excellent thermal stability of collagen [44]. A recent study has proved that the thermally induced denaturation of collagen can be restored to some degree by the application of ultra-high pressure treatment. The effect is, however, lost for high thermally denatured collagen [45]. Thermal denaturation of proteins can be measured by calorimetric methods.

Collagen and collagen preparations can also be studied on a morphological level. The structure of collagen differs based on the area of presence. For instance, collagen in tendons forms thick fibers, while collagen in the corneal component of the eye forms sheets of thin fibers providing strength and optical transparency [46]. Typical methods for such studies are atomic force microscopy (AFM), scanning or transmission electron microscopy (SEM/TEM) and light microscopy [26]. AFM will reveal structure at nano-level, and is able to distinguish the individual fibers and monomers, and is further used to perform force measurements [26, 47]. SEM is used to study the microstructure of collagen fibrils and fibers bundled together [26, 48]. SEM can further be used in characterization of collagen preparations by

analysis of structure and pore formation after, e.g., freeze-drying [26, 49]. TEM can be used to observe the fibril structure down to 10 nm [48]. Light microscopy is mostly used to observe interactions between biomaterials and cells, such as cell distribution and replication [26].

1.1.3 Applications and challenges for the use of collagen isolated from rest raw materials

Collagen is a widely used protein in pharmaceutical, biomedical, cosmetic and food industry. Applications in pharmaceutical industry include drug delivery systems, such as freeze-dried products (sponges and sheets), eye shields, films and hydrogels [50]. In tissue engineering and wound healing, collagen is used as a scaffold for cell growth [51]. Cosmetic applications of collagen utilize its ability to bind water in skin care products [52]. Food applications include sausage casings and functional food packaging films [53, 54]. Advantages and disadvantages of the biomedical and pharmaceutical application of collagen from rest raw materials are summarized in Table 1.1.

Table 1.1: Main advantages and disadvantages of the pharmaceutical and biomedical application of collagen from rest raw materials. Partially adapted from [19, 50].

Advantages	**Disadvantages**
• Good availability and can be isolated from rest raw materials • High degree of biocompatibility • Biodegradable • Low antigenicity after post-translational modification • Can be crosslinked to improve mechanical and functional properties • Can be formulated as films, hydrogels, sponges and beads	• High cost of purified collagen • Variable composition (e.g., crosslinking, molecular weight, solubility) • Sterilization of isolated material and prepared products can be a challenge • Risk of containing transmissible diseases (TSE, BSE, FMD, AI) • Low viscosity and mechanical strength of solutions and constructs

Degradation products of collagen are widely used in the pharmaceutical, cosmetic, health and food industry [55]. Thermal denaturation of collagen leads to an uncoiling of the triple-helical structure and partial hydrolysis, producing fragments called gelatin. Gelatin is widely used in the food industry in both the production of confections and as thickening agents in products, for instance in cheese and yoghurt. It is further used in the drug industry in capsules and tablets and in production of hydrogels for biotechnology purposes [56]. Another decomposition product of collagen is hydrolyzed collagen (also called collagen hydrolysate, gelatin hydrolysate or collagen peptides). Hydrolyzed collagen is a polypeptide made by enzymatic or acidic hydrolysis of collagen or denatured

collagen [55, 57]. Hydrolysis can be controlled to produce hydrolysates with desirable properties, such as specific chain length and molecular weight [58]. Gelatin and hydrolysates are widely used in the cosmetic industry as viscosity modulating and moisturizing excipients and in the production of supplement products. Some health product suppliers even use native collagen in their products, claiming positive effects on skin and joints by oral ingestion. Dietary supplements (neutraceuticals) containing collagen and gelatin for improving skin and joint health have a rather disputed effect, due to further degradation in the stomach by pH and enzymes before the amino acids can be absorbed. However, some studies including hydrolyzed collagen show beneficial health effects [59, 60].

A general concern regarding the use of rest raw material from the meat industry is the risk that the material contains transmissible diseases. This includes transmissible spongiform encephalopathy (TSE), bovine spongiform encephalopathy (BSE), foot-and-mouth disease (FMD) and avian influenza (AI) [10, 61, 62]. The risk is, however, eliminated or strongly reduced by the correct treatment of the material prior to isolation or use. However, inactivation of pathogens by sterilization will in most cases involve the use of high temperatures, leading to protein denaturation. Sterilization of collagen-based materials is therefore challenging. Conventional sterilization techniques based on high temperature or gamma irradiation have limitations, such as denaturation and changes in the amino acid structure [27]. Collagen is further susceptible to UV irradiation [63]. Alternative sterilization methods that will preserve material structure and properties are supercritical CO_2, acid treatment (with peracetic acid) and the use of gas plasma [21, 64, 65]. Ethanol is also used for sterilization of collagen-based products, without any noticeable structural or functional changes, but may not be sufficient to remove bacterial and fungal spores and endotoxins [21, 65]. Aquatic sources, such as fish and jellyfish, and plant-derived recombinant collagen have been investigated as potential alternatives to mammal collagen to avoid issues related to transmissible diseases and religious preferences [14, 66, 67]. Both porcine collagen and gelatin are classified as "Generally recognized as safe" (GRAS) by the US Food and Drug Administration (FDA) for use in food applications.

Applications of collagen discussed in the present thesis include drug delivery, wound healing and tissue fabrication. Other current and tentative applications are mentioned throughout the thesis. Figure 1.2 shows examples of current and tentative applications of collagen.

1.2 Skin, wounds and infections

The importance of collagen for the skin structure is emphasized by its presence in skin and importance for the skin function. Collagen is a major constituent of the skin as one of the proteins responsible for skin strength, elasticity and cellular support [68].

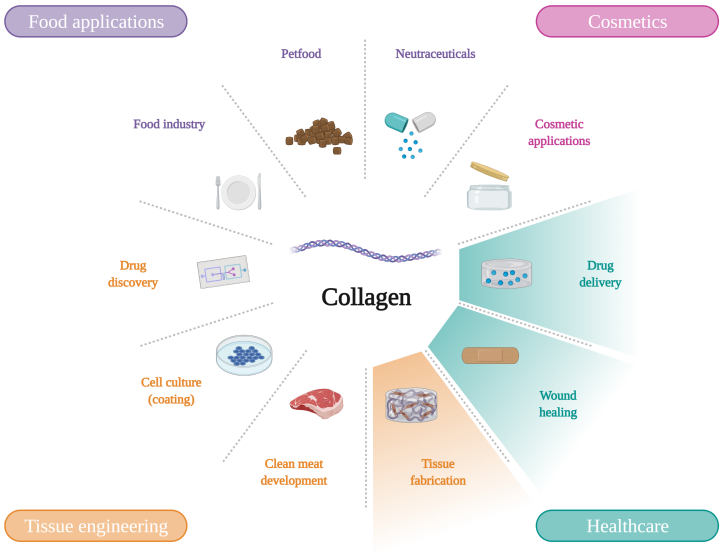

Figure 1.2: Examples of current and tentative applications of collagen. Applications discussed in this thesis are highlighted. (Created with BioRender.com).

1.2.1 Skin structure and function

The skin is the largest organ of the human body and has important protective and sensory functions. These include a barrier function against the external environment, preventing body moisture loss and acting as a sensory organ reacting to external stimulus and temperature [69]. The skin is made up of three main layers; epidermis, dermis and subcutis (sometimes referred to as the hypodermis) (Figure 1.3). The epidermis is the outermost layer consisting of keratinocytes producing keratin and melanocytes producing the pigment melanin. Other cells important for the epidermis are the antigen presenting Langerhans cells which are responsible for the immune system of the skin [70, 71]. The second outermost skin layer is the dermis, which is the layer important for the strength and elasticity of the skin. This layer consists mainly of fibroblast cells and fibrous proteins, such as collagen and elastin [69, 70]. Collagen can account for up to 70-80% of the dry weight of the dermis [68]. Subcutis is the deepest skin layer. This layer consists of mostly adipose tissue, with adipocytes, fibroblasts and macrophages being the most prominent cell types [69, 70].

1.2.2 Wounds and wound healing

The skin can easily be damaged, thereby reducing the barrier function against the external environment including particles, microorganisms and physical factors

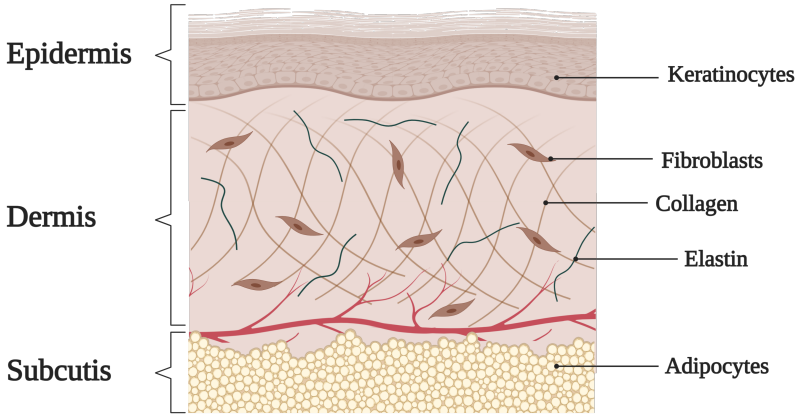

Figure 1.3: Simplified schematic of the skin composition. Other components such as Langerhans cells, melanocytes, hair follicles, pili muscles and sweat glands are not included for simplification. (Created with BioRender.com).

[72]. Examples of skin damage are skin burns and wounds (trauma). Chronic wounds are today one of the largest burdens to the healthcare system [73]. Together with an increasing bacterial resistance against antibiotics, chronic wounds have become one of the leading causes of death worldwide [74]. Wounds may be the result of underlying diseases, such as atopic dermatitis, diabetes, skin infections and vasculopathy [72]. Because of the complexity of wound pathophysiology and healing, only the theory and mechanisms relevant for the current work will be presented in this thesis.

Wound healing involves cascades of events, multiple cell types, enzymes and growth factors. A simplified overview of the stages of wound healing and their major cellular components following injury is given in Figure 1.4. The process is divided into defined (but overlapping) events, including bleeding, clot formation, inflammation, re-epithelialization, angiogenesis, granulation tissue formation, wound contraction, scar formation and tissue remodeling [75, 76]. The invasion of cells, among others the fibroblasts, is important for migration and proliferation into the wound site and synthesis of extracellular macromolecules [19, 77]. Other cells involved in the wound healing process include blood platelets, inflammatory cells, keratinocytes and endothelial cells [75, 76]. Proteolytic enzymes play a major role in the modification of the ECM allowing cell migration and remodeling of the skin. These include matrix metalloproteinases (MMPs) and tissue inhibitors of MMPs (TIMPs) [78, 79]. MMPs are divided into types classified by their substrates and function. There are numerous MMPs involved in the wound healing process. Some of the important MMPs for wound healing include MMP-1, which is responsible for promoting keratinocyte migration on fibrillar collagen, MMP-2, which accelerates cell migration, MMP-8, which cleaves the collagens in the wound site and MMP-9, which promotes cell migration

and re-epithelialization [80]. Another important regulator of cell adhesion and migration is syndecan-4 (SDC-4). SDC-4 is a cell receptor protein, which is a target for MMP-2 activity. MMPs will cleave off the extracellular domain of SDC-4, fine tuning its biological activity [81]. SDC-4 is shown to be important for the wound healing process by the ability to interact with ECM ligands, morphogenes and cytokines that are important regulators of tissue regeneration [81, 82].

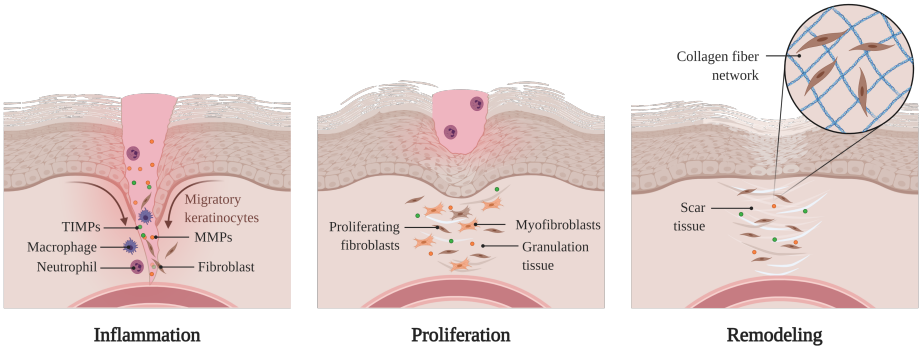

Figure 1.4: Simplified overview of the stages of wound healing and their major cellular components following injury. (Adapted and modified from "Wound Healing", by BioRender.com (2021). Retrieved from https://app.biorender.com/biorender-templates).

During the granulation tissue formation event of the wound healing, the fibroblasts are further activated into myofibroblasts. These cells are important for production and organization of the ECM [83]. Despite being important for the healing process, the myofibroblasts are further involved in less desirable processes such as wound contraction and scarring of tissue. Insufficient differentiation of fibroblasts will, however, prevent the normal healing process [83]. Myofibroblasts are identified by their production of α-smooth muscle actin (α-SMA), an actin isoform normally found in vascular smooth muscle cells [83, 84]. The exact role of α-SMA expressed by myofibroblasts is still not clear, but loss of α-SMA has resulted in impaired wound healing [84].

When skin damage does not heal within a predictable amount of time, it is defined as a chronic wound. On a molecular level, chronic wounds are characterized by an imbalance of certain enzymes and growth factors involved in the healing process [85]. The condition may further be a result of underlying diseases. Another part of the pathophysiology of wounds and diseased skin is infections. Chronic wounds, for instance diabetic ulcers, venous ulcers and pressure ulcers are related with an increased susceptibility to infections [86]. Bacterial infections may cause wound deterioration, which will slow down the healing process and prevent wound closure [86, 87]. The most common bacteria found in chronic wounds and diseased skin are *Pseudomonas aeruginosa* and *Staphylococcus aureus* [86, 88].

1.2.3 Collagen and collagen-based dressings in wound healing

Collagen has multiple important roles in the wound healing process. One of the first events after injury is the formation of blood clots. Collagen triple helices have hemostatic properties by arginine residues interacting with platelets and contributing to the formation of blood clots [89]. During the late events of the wound healing, collagen is degraded by the proteolytic enzymes to smaller fragments, which may work by chemotaxis to cells involved in the wound healing and rebuilding of the ECM [90, 91]. Further, collagen is involved in the formation of scar tissue, which mostly consists of collagen fiber networks [92]. Besides the function as a scaffold for cell invasion, collagen is also important for the mechanical strength of the tissue [93]. In chronic wounds the deposition of new collagen is delayed or prevented due to an imbalance between MMPs and TIMPs that result in a higher degree of collagen degradation than collagen neosynthesis [94, 95]. Collagen wound dressings can work as a sacrificial substrate for the excess MMPs towards degradation, protecting the inherent collagen of the skin [94, 95]. The use of native collagen in wound dressings can exploit the triple helical domain to be a target for elastases, protecting elastin and collagen in the skin [94]. Collagen wound dressings may also allow promotion of the natural wound healing process optimal for infiltration by fibroblasts and macrophages by providing a porous 3D matrix [94]. Native non-denatured collagen with an intact triple helix is therefore desirable in development of wound healing products. Collagen wound dressings have been prepared as hydrogels, freeze-dried sponges and casted as films [92]. Hydrogels are particularly interesting in wound healing applications due to a high degree of biocompatibility and high moisture content, which will provide good healing conditions [96]. Hydrogel preparations will further act as a physical barrier against secondary infections [92].

1.3 Tissue engineering and drug delivery

Tissue engineering techniques are interesting and highly relevant for the treatment of a variety of diseases, including dermal loss and wound healing, mimicking native organs and structures of the body. Tissue engineering is the creation of new tissues based on biomaterials and cells for therapeutic reconstruction in the human body. Cells in artificial scaffolds are stimulated through a combination of molecular and mechanical signals to produce tissue mimicking human tissue [97]. Tissue engineering is dependent on scaffolds for optimal cell growth. These formulations are further interesting in drug delivery. The concepts of tissue engineering and biofabrication are illustrated in Figure 1.5.

Scaffolds (or templates) are constructs made of polymeric biomaterials and their functions in tissue engineering are to give structural support for cell attachment and provide sufficient oxygen and nutrition exchange to promote cell proliferation and tissue development [98, 99]. Scaffolds are further relevant for controlled drug delivery by spatial and temporal control over the drug release [100]. Scaffolds can be fabricated in multiple ways, and a common feature is the ability to support cell growth. Examples of scaffolds used in tissue engineering

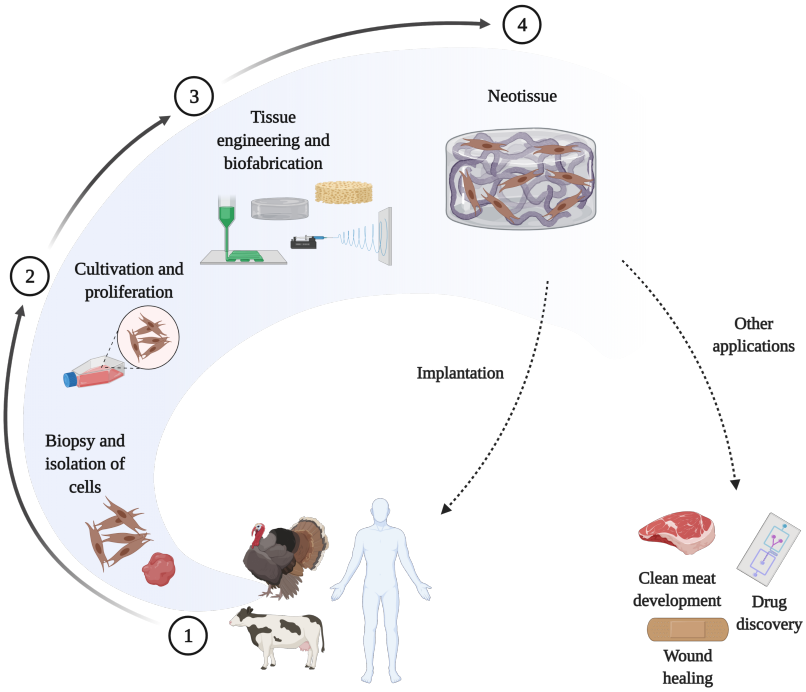

Figure 1.5: Schematic of the concept of tissue engineering and biofabrication. Cells isolated from biopsies can be cultivated and proliferated. Further, fabrication of constructs can be performed and combined with the cells to form neotissue. The newly formed tissue can be used for implantation to treat diseases or other applications such as development of lab grown meat, in wound healing or in drug discovery. (Created with BioRender.com).

are hydrogels and pre-made porous scaffolds, such as electrospun sheets or freeze-dried sponges [101]. Hydrogels can be made of natural or synthetic materials, resulting in high water holding constructs. They can be designed to exhibit desirable properties with controlled transport of nutrients, oxygen and signalling molecules. Further, they can be tailored to mimic tissue and be favorable for specific cell types [102]. For example, self-assembled hydrogels may produce thinner fibers with structures similar to the ECM. This will promote proliferation and migration of cells involved in ECM production [103, 104]. The mechanical properties of hydrogels can be tailored by inducing crosslinking of the polymer or protein [105]. Hydrogels may further be formulated to respond to external stimuli including light, pH, temperature or enzymatic environment as "smart" hydrogels [106]. Nanofibrous scaffolds are also interesting in tissue engineering. Such scaffolds may be produced by electrospinning and electrospraying techniques

[99]. An advantage is the large surface-to-area ratio, which potentially will allow for high absorption of proteins, presenting more binding sites to cell membrane receptors [103]. The resulting scaffolds can be tailored by using different polymer blends and by fine tuning the production parameters. Electrospun nanofibrous scaffolds have been used in tissue engineering of tissues, such as bone tissue, nerve tissue, cartilage and skin, in addition to being used as delivery systems for a variety of drugs [99].

Biofabrication is an evolving research field involving different techniques to produce functional products based on living cells, bioactive molecules and biomaterials. These techniques include 3D bioprinting, bioassembly or other automated methods to obtain tissue constructs [107]. One of the most recent definitions of biofabrication is *"The automated generation of biologically functional products with structural organization from living cells, bioactive molecules, biomaterials, cell aggregates such as micro-tissues, or hybrid cell-material constructs, through bioprinting or bioassembly and subsequent tissue maturation processes"* [107]. Biofabrication differs from classical tissue engineering by including cells in the fabrication step of the material. Bioprinting is one of the most used techniques in biofabrication. The fabrication steps involve computational design, computer-controlled techniques and layer-by-layer deposition of a bioink to produce a construct of a biological entity [108]. Bioink is a term used for materials suitable for biofabrication by bioprinting with cells. However, many of the materials used in bioprinting can as well be used without cells to make biomimicking constructs and scaffolds where seeding of the scaffolds with cells can be performed after the printing, if desired. These materials are called biomaterial inks [109]. Electrospinning (solution or melt electrospinning) has also been studied as a biofabrication technique, with cells maintaining their viability to some extent after fabrication [110, 111]. Other interesting biofabrication techniques are microfluidics and laser-assisted techniques [110].

Apart from fabrication of scaffolds serving new tissue for the therapeutic reconstruction of the human body, tissue engineering can be used in a variety of industries. Tissue engineering has recently been in the spotlight in the food industry. The increase in meat consumption and population growth have created a need for alternative protein sources to produce enough food. With the exception of plant-based alternatives, the concepts of clean meat and cultured meat have gained attention to solve this problem [112, 113]. These concepts use tissue engineering applications and animal cells to produce neotissue suitable for consumption. Challenges for these products include retaining structural functions, incorporation of fat, achieving desired taste and appearance, and making an affordable product [112]. Another potential application area for tissue engineering is drug discovery. Tissue engineering has been investigated as an alternative to animal experiments. So far, most of the transitions from animal experiments to tissue engineering have been done for toxicological testing of drugs and drug formulations on skin [114]. Recently, the development of bioprinted constructs has gained attention for *in vitro* drug screening as alternative to time- and resource consuming pre-clinical and clinical testing [115]. Challenges for these constructs include low mechanical strength, inadequate *in vitro-in vivo*

correlation and lack of certain functions such as vascularization [116, 117].

1.3.1 Material properties in tissue engineering

Materials for tissue engineering applications should have properties compatible with the desired target environment and target cells. Natural polymers and proteins (collagen, elastin, silk fibroin), synthetic polymers (poly(lactic-coglycolic) acid, polyanhydrides), carbohydrates (chitosan, alginate) and some inorganic materials (hydroxyapatite) have been studied for tissue engineering applications [118]. For optimal function, the materials should have mechanical properties close to the mimicking tissue [118]. Desirable properties include a not too weak material, with a certain elasticity. The material should further be biocompatible, and in most cases, biodegradable [98]. The material should be able to deliver signalling molecules and mechanical signals to stimulate cells in a controlled and desirable way after fabrication of scaffolds [119].

1.3.2 Collagen in tissue engineering and biofabrication

Collagen has been investigated thoroughly as a material for tissue engineering applications, including biofabrication techniques such as bioprinting and self assembly [51, 120, 121]. The almost ubiquitous presence of collagen in the body makes it interesting in tissue engineering [51]. The main limitation for the use is low mechanical strength of prepared constructs [122]. This has been attempted solved by increasing the collagen concentration, using biocomposites, forming the structures directly into a supportive gelatin slurry bath (commonly known as FRESH bioprinting) or inducing crosslinking reactions before or after fabrication of constructs to modify the physicochemical properties of the protein [101, 123–125]. Crosslinking can enhance the proteins' chemical stability, thermal stability, swelling properties, mechanical properties and pore size of constructs [100, 126, 127]. Crosslinking of proteins can be performed by physical or chemical crosslinking methods, which both have their respective advantages and limitations.

Physical crosslinking can be achieved by neutralization of an acidic collagen solution and heating to body temperature (or close to the denaturation temperature) to induce self assembly [128]. The main limitation of physical crosslinking is restricted tunability of the physicochemical properties, including mechanical strength, swelling abilities and water holding capacities [128]. For physically crosslinked collagen, a change in protein concentration is one of the few possible ways to optimize the physicochemical properties. Recent studies have, however, shown that the modulation of collagen by cyclodextrin complexation can be applied to tailor biomimetic cornea implants for the eye and modulate cell activity [129, 130]. Cyclodextrins (CDs) are cyclic oligosaccharides with a hydrophobic inner and a hydrophilic outer structure [131]. They will bind to aromatic residues on the collagen molecule resulting in increased viscosity through collagen self-assembly. This has proved to reduce the fibril diameter during gelation and provide increased viscosity, mechanical strength and transparency

of the gels [130]. These properties may be desirable in tissue engineering applications, especially for the eye [132]. Modulation with CDs will further allow to sequester growth factors [129].

Chemical crosslinking of collagen will allow for tunability of the physicochemical properties. The mechanism of chemical crosslinking involves the creation of covalent crosslinks between the side chains of the collagen molecule (lysyl residues, carboxyl groups or H-bonds) [127, 128]. The main limitation of chemical crosslinking is potential toxicity from the crosslinking agents, making the reaction less relevant for biomedical applications. Further, the kinetics of the reaction is hard to control. Crosslinking agents for chemical crosslinking include glutaraldehyde, carbodiimide or enzymes for enzymatic catalysis, such as transglutaminase [127]. Photochemical crosslinking is another type of crosslinking reaction, suitable for crosslinking of collagen constructs. This type of crosslinking has advantages over conventional chemical crosslinking. Photochemical crosslinking requires a photosensitive compound and absorption of optical radiation. Photoreactivity of photosensitizing compounds and the mechanisms of photochemical crosslinking will be introduced in Section 1.4.

1.3.3 Collagen in drug delivery applications

Pharmaceutical drug delivery systems of collagen share many of the same characteristics as materials and scaffolds for tissue engineering. Further, delivery of bioactive molecules and drugs are sometimes combined with tissue engineering techniques [100, 133, 134]. Examples of drug delivery systems based on collagen are hydrogels, freeze-dried sponges, films and composite formulations [135]. Drugs may be incorporated by physical entrapment in the collagen network or with chemical bonding between the drug and collagen. Chemical bonds include covalent linkage, electrostatic interaction or hydrophobic association [100]. An example of hydrophobic interactions is complexation by CDs, which is used in tissue engineering applications with collagen as described above. This will not chemically change the hydrogel, but increase the solubility of active ingredients within the vehicle [100, 129].

Collagen hydrogels and films have been investigated as potential drug delivery systems for antimicrobial substances and analgesic substances, and also delivery of cells and growth factors in tissue engineering [100, 129, 136–138]. Freeze-dried collagen sponges have been developed for the sustained release of ibuprofen and chloramphenicol by varying the extent of crosslinking [139, 140]. The drug release from a collagen preparations can be influenced by several factors, such as porosity, density and crosslinking of the material [100]. The pore size of the collagen network and the drug size affects the diffusion of a drug through a hydrogel. Drugs smaller than the pore size will rapidly diffuse out of the gel, while larger drugs and biomolecules will have a slower diffusion. If drugs are linked to or immobilized in the protein matrix, the diffusion may be affected by degradation, swelling and deformation [100]. The same will apply to sponges, with an initial swelling phase. An example of a hypothetical drug delivery system based on collagen is a formulation with two drugs for wound healing where one drug

should have immediately release, and the other sustained release. A potential mechanism is desorption and fast diffusion of non-linked drugs upon contact with wound fluids, followed by hydration and swelling of the wound dressing. Drugs linked to the collagen fibrils can further be released by slow diffusion from the formulation or potential erosion of the matrix by degradation with proteases, e.g., collagenases. Collagen formulations can take advantage of the beneficial properties of collagen, such as good biocompatibility and biodegradability.

1.4 Photochemical reactions and antimicrobial photodynamic therapy

In the development of collagen-based formulations for potential use in tissue engineering and wound healing, it may be necessary to crosslink the constructs to develop products tailored for these applications. Photocrosslinking and incorporation of photocrosslinkers are relevant in the production of biomedical devices with enhanced durability and antibacterial properties. These products require the absorption of photons of certain wavelengths and energy to induce the excitation of a photosensitive molecule (i.e., photosensitizer, PS).

1.4.1 Photoreactivity of photosensitizing compounds

The photophysical processes that can occur following the photon absorption by a PS can be described by a Jablonski diagram (Figure 1.6).

The absorbed photon energy raises one valence electron in the PS molecule to an outer shell. In this state, the valence electrons of the PS have antiparallel spin. The exited states (S_1, S_2 and T_1) of the PS are unstable, and the energy may be eliminated by radiative or non-radiative transitions to lower energy levels. The exited PS may decay from higher to lower vibrational energy states by non-radiative emission of heat, i.e., vibrational relaxation (VR) and from the exited state to its ground state by internal conversion (IC). The radiative transitions include fluorescence from the excited singlet state. Another reaction is the intersystem crossing (ISC) between the singlet state of a molecule to the triplet state. This involves a spin-forbidden conversion of one of the valence electrons of the molecule into parallel spin. In the triplet state, the energy may be lost by radiative decay by phosphorescence or by electron (type I) or energy (type II) transfer to a substrate. This will lead to the generation of oxygen radicals, reactive oxygen species (ROS) and singlet oxygen ($^1O_2$). [141–144].

Oxygen is by its nature a triplet in its ground state (electron spins are parallel), and can thereby be spin-matched with the triplet exited PS and react by direct energy transfer. Through a type II photochemical reaction, the triplet oxygen will receive enough energy to be exited into a singlet state ($^1O_2$). The highly reactive $^1O_2$ may react with biological components such as cell walls, lipids, enzymes, proteins and DNA [141, 142]. This can lead to cell death (e.g., killing of cancer cells or bacteria).

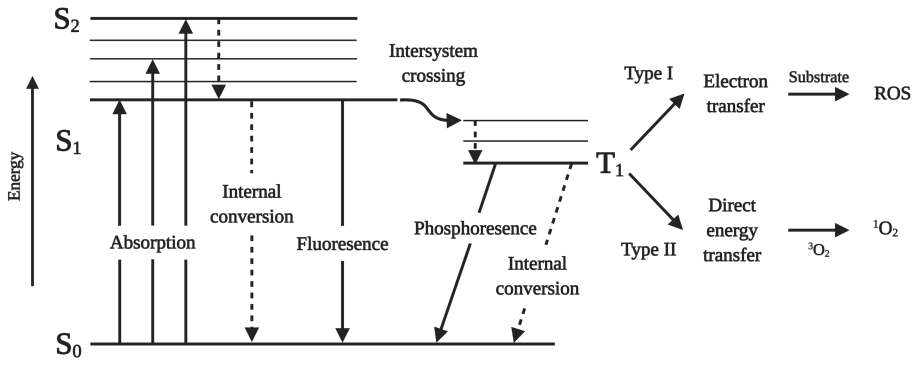

Figure 1.6: Simplified Jablonski diagram showing photophysical processes that can occur following photon absorption by a PS. S_0 is the ground state of the PS. S_1, S_2 and T_1 are the exited singlet states and triplet state, respectively. In the T_1 state, the PS may undergo Type I and/or Type II reactions, resulting in electron transfer or direct energy transfer producing reactive oxygen species (ROS) or singlet oxygen ($^1O_2$), respectively. Adapted from [145]. (Created with BioRender.com).

1.4.2 Photochemical crosslinking

Photochemical reactions can be used to crosslink proteins and polymers. Photochemical crosslinking (further called photocrosslinking) is achieved by irradiation of a material in the presence of a PS. One of the advantages with photochemical crosslinking compared to chemical crosslinking is the possibility to trigger the crosslinking reaction at a desired time. Common PS used in photocrosslinking of proteins are Igracure 2959, Eosin Y, ruthenium-compounds, riboflavin and rose bengal [146]. Mechanisms in photocrosslinking include photo-oxidation and covalent bonding between amino acids, methacrolyl modification of the proteins to increase the number of photocrosslinkable sites or use of photons to induce conformational changes in the protein [146–148].

The mechanisms of photocrosslinking of collagen have previously been discussed and thoroughly studied by several research groups [126, 149]. The crosslinking effect is postulated to involve the formation of ROS and $^1O_2$ by the exited PS, resulting in photo-oxidation. This hypothesis is supported by the ability of quenchers to inhibit the photocrosslinking. The crosslinking reaction will lead to covalent bonding between amino acids of collagen fibrils [150].

1.4.3 Antimicrobial photodynamic therapy

Antimicrobial photodynamic therapy (aPDT) is the killing of microorganisms by the combination of a dye (a PS) and optical radiation. This technique has been known and used for over 100 years, but has recently gained new interest after the

increasing incidents of bacterial resistance to antibiotics [151]. The application of aPDT has been postulated as an alternative to antibiotics in the treatment of localized infections. The bacterial phototoxicity is caused by either type I and/or II photochemical reactions resulting in a non-specific damage to the microorganism [152]. The exited PS in the triplet state will react with oxygen and produce $^1O_2$, ROS or other reactive photoproducts. Thus, the PS used in aPDT should be an efficient source of $^1O_2$ and/or ROS when irradiated at selected wavelengths [153]. Further, the PS should have a high affinity for microbial cells. ROS and $^1O_2$ may cause damage to biomolecules on the membrane or inside the bacteria cells, eventually killing the bacteria [151, 153]. Most aPDT PS are water soluble, cationic compounds absorbing visible light up to 600 nm [154]. Red light ($>$ 600 nm) will penetrate deeper into the skin than, e.g., blue light ($\sim$ 450 nm). However, the use of lower wavelengths in aPDT may be an alternative to minimize light penetration into healthy skin [155]. aPDT has a broad spectrum of action against bacteria, virus, fungi, yeasts and parasites [152]. Since the killing of microorganisms involves non-specific mechanisms, it is less likely to induce development of treatment resistance [156, 157]. This has, however, been discussed [158]. The clinical application areas are limited to localized infections where irradiation of the PS can be performed. Thus, infected wounds, eye infections and infections in the oral cavity are potential application areas. Other cavities can also be treated by use of fiber optics, such as infections in the bladder. aPDT may further be combined with conventional antimicrobial agents to treat more complicated bacterial infections [159]. A pre-treatment with irradiation of a PS before the use of conventional antimicrobial agents may weaken the bacteria, leading to complete killing and less resistance [159]. aPDT has also shown effect against antimicrobial resistant bacteria *in vitro*, in larvae models and on human epithelial surfaces [158, 160].

1.4.4 Photosensitizers: riboflavin and lumichrome

In the present work, riboflavin (RF) and lumichrome (LC) were used as PS (Figure 1.7). RF was used as a PS in photocrosslinking of collagen in preparation of freeze-dried scaffolds, LC was investigated as a potential PS in photocrosslinking of collagen hydrogels, which was further investigated as a potential formulation for aPDT applications.

RF is a water soluble vitamin (vitamin B_2), which is produced in small amounts by gut bacteria. It is classified chemically as an isoalloxazine [161]. RF is ubiquitous in food, supplying the human body with sufficient amounts to function as co-enzymes in cells [162]. RF has previously been investigated as a potential PS in photocrosslinking of collagen in biofabrication applications [120]. Further, RF has been used as a PS in photodecontamination of blood products by adding RF to the blood component followed by UVA irradiation [163]. RF was first described as a photocrosslinker of collagen for the treatment of the eye disease keratoconus by *Wollensak et al.* in 2003 [164]. Keratoconus is a disease where the cornea in the eye is thinning and bulges outward into a cone shape. RF eye drops are applied to the affected eye prior to irradiation with

UVA. This leads to an *in situ* crosslinking of the collagen in the cornea [165, 166]. Irradiation of RF results in photodegradation to LC in acidic and neutral solutions or lumiflavin (LF) in alkaline solutions [167, 168]. Both LC and LF are more photostable than their precursor and are efficient photogenerators of $^1O_2$ [168–170].

LC is classified as an alloxazine, structurally similar to isoalloxazines, but with different spectral and photophysical properties [171]. It is regarded as a natural compound in human body, plants and bacteria [172, 173]. LC has a low water solubility ($\sim 10^{-5}$ M), which limits the use in pharmaceutical applications [174]. This has, however, been solved by using solubility enhancers, like co-solvents and surfactants like polyethylene glycol (PEG), Pluronics® and by the formation of CD inclusion complexes [169]. LC is an effective $^1O_2$ generator, and is more photostable and more lipophilic than its precursor. These properties are beneficial for a PS in aPDT [153, 158, 168, 169]. A high lipophilicity will potentially favor the uptake in a lipophilic bacterial membrane. The absorption spectrum of LC extends to $\sim$ 450 nm. This will restrict the application mainly to superficial infections [175].

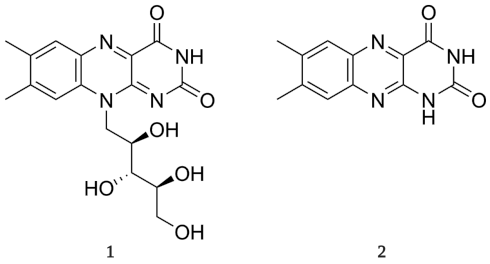

Figure 1.7: Molecular structure of riboflavin (1) and lumichrome (2).

1.5 Sustainable technology – Natural deep eutectic solvents

Sustainable technology is about minimizing the environmental footprint by responsible development, production, use and consumption of products, food, energy and environmental resources. The 2030 Agenda for Sustainable Development emphasizes sustainable consumption and production, reduced use of chemicals and the challenge of antibiotic resistance [1, 176]. The concept of using rest raw material from industrial meat production combined with natural endogenous PS in aPDT meets some of these criteria. Another environmental concern regarding the development of new drugs and biomedical products is the use of organic and inorganic solvents. In the past decade, new alternatives to conventional solvents have emerged, including eutectic solvents [177].

1.5.1 Eutectic solvents

An eutectic solvent, mixture or system is a homogeneous mixture of two or more components, which has a lower melting point (T_m) than any of the components alone. Their formation can be explained by a phase diagram (Figure 1.8). The two (or more) individual components (A and B) are normally in the solid state when they are separate at a certain temperature, but become liquid when they are combined at a specific molar ratio (i.e., eutectic point). The eutectic mixture has unique properties relative to the individual components [178].

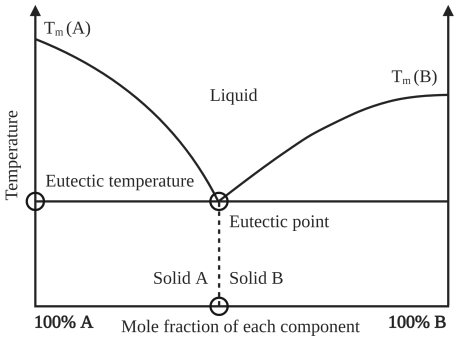

Figure 1.8: Phase diagram explaining the formation of eutectic mixtures. Adapted from [178]. (Created with BioRender.com).

1.5.2 Natural deep eutectic solvents

Eutectic systems with a large depression of the melting point are called deep eutectic solvents (DES) [178]. Natural deep eutectic solvents (NADES) were first described in 2011 and postulated as a third class of liquids in organisms, different from water and lipids, which is present in all living cells [179]. NADES generally consist of plant based primary metabolites, for instance organic acids, amino acids, sugars, polyols and tertiary amines. Examples of components are glucose, fructose, sucrose, trehalose, xylitol, glycerol, choline chloride, betaine, citric acid, malic acid, maleic acid, proline and serine [180]. In nature, NADES have been postulated a central role in the plants' ability to survive extreme conditions, such as cold and drought [179]. The discovery of NADES, the apparent abilities in nature, and previously known applications for DES have resulted in the discovery of many application areas for NADES. They have especially been utilized in the extraction of bioactive compounds [181]. NADES have further been reported to solubilize a wide range of hydrophilic and hydrophobic compounds. Both small molecules including itraconazole, curcumin and porphyrins, and proteins, such as gluten and laccases have been dissolved in NADES [181–188]. NADES can be considered as potential sustainable alternatives to organic and inorganic solvents in many fields.

NADES can be prepared by different methods, resulting in eutectics with a wide range of properties. The most frequent used preparation methods include melting a mixture of the components (heating method) or dissolving the individual components in water followed by water evaporation (the vacuum evaporation method) [189]. FT-IR and ^{1}H NMR studies have revealed that the individual components become strongly bound in a supramolecular H-bonding network [190]. The resulting eutectic solvents are viscous, colorless, transparent liquids. The viscosity is tailored by the inclusion of water in the network [189]. DES and NADES have been used in diluted and undiluted forms. Some studies report that the supramolecular structure of the solvents may rupture by dilution above 50% (v/v) [190]. However, other studies show unique effects by the NADES diluted up to 1:200 [191].

Certain NADES have shown antibacterial properties alone, or in combination with optical radiation in the absence or presence of PS. In combination with optical radiation and PS, the production of toxic ROS may work together with the intrinsic NADES properties. The proposed mechanisms of the antibacterial effects of NADES involve chelation of outer bacterial membrane-bound cations and dissolution of bacterial membrane components. The antibacterial properties can also be due to a pH effect of acidic NADES. The enhanced bacterial phototoxic effect in combination with PS and optical radiation may also be due to weakening of the bacteria prior to irradiation [191]. The combination of NADES with aPDT or conventional antibiotics may contribute to a reduction in antimicrobial resistance to antibiotics by utilizing different non-specific killing mechanisms [159]. NADES have also shown antifungal and antioxidative properties [192].

The biocompatibility and toxicity of NADES have been under investigation [192, 193]. Studies indicate that NADES containing organic acids are generally more cytotoxic than neutral NADES [192, 193]. However, the acidic NADES seem to have a higher bacterial toxicity, which leads to a risk-benefit assessment if used in medicinal products. The toxicity of several DES and their individual components have previously been studied. The toxicity of the individual components have shown to be lowered upon incorporation in the eutectic network [194]. The wide range of eutectic mixtures makes a general assumption about the toxicity impossible. Toxicity of the eutectic mixtures and their individual components will also vary depending on the route of administration. Further studies on the toxicity including *in vivo* studies have to be performed to assess the safety of use of the individual NADES.

The unique properties of NADES such as bacterial toxicity and the ability to dissolve a wide range of substances make them interesting as excipients in pharmaceutical preparations. In the present thesis, one NADES was investigated as a potential excipient in collagen-based preparations. The combination was proposed as a new sustainable concept for potential use in antimicrobial products, e.g., for treatment of infected wounds.

1.6 Summary of Papers

Paper I focuses on the characterization of collagen from turkey (*Meleagris gallopavo*), and the potential use as a biomaterial in pharmaceutical preparations. Collagen is the major fibrous component and protein in human and animal connective tissue. The industrial production of meat and poultry products results in large amounts of organic waste, including rest raw materials rich in collagen. Collagen has previously been applied in medical preparations, including wound dressings and in tissue engineering. The aim of this paper was to isolate and characterize collagen from turkey and investigate the potential for the protein as a biomaterial for pharmaceutical use. Structural analysis indicated that the collagen isolated could be classified as a mixture of type I and III with an estimated molecular weight of 477.3 kDa. The isolated collagen demonstrated excellent thermal stability, among the highest reported for collagen, with a denaturation temperature at 44.5 °C. A denaturation temperature above the human body temperature may be desirable in medical preparations to maintain the native collagen structure during application. Cell studies indicated good cytocompatiblity of turkey collagen. Gelling of the collagen followed by freeze-drying to porous scaffolds illustrated the suitability of the material in pharmaceutical preparations. The resulting scaffolds exhibited enhanced mechanical and structural properties when photocrosslinked with riboflavin. *In vitro* drug release studies of the model drug prilocaine hydrochloride showed significant differences between the release from scaffolds and aqueous solutions of the drug. The release was, however, not significantly different between the physically and photochemically crosslinked formulations, most likely due to the formation of larger pore structures in the latter. Altogether, the results indicated that the isolated collagen may be suitable as a sustainable biomaterial for pharmaceutical use.

Paper II demonstrates how a natural deep eutectic solvent (NADES) influences the structural behavior of collagen and evaluates the potential of NADES as excipients in collagen-based formulations. NADES have previously shown antibacterial properties alone or in combination with photosensitizers and light. A combination of collagen and NADES add the unique wound healing properties of collagen to the antibacterial effect of certain NADES. To make a successful combination, it is important to understand the structural properties of collagen in the NADES. Collagen is normally dissolved in weak acids, giving viscous solutions for use in formulations. In this study, collagen was dissolved in an acidic NADES and characterized with respect to structural, spectroscopic, calorimetric and viscometric properties. Collagen isolated with and without pepsin, resulting in different compositions, were examined. The amino acid content of collagen will influence its spectral properties. Tyrosine residues are normally excised together with the non-helical telopeptides of the protein after pepsin treatment. Spectroscopic

studies of the collagens applied in this study revealed that tyrosine was present both before and after pepsin treatment, despite the removal of the telopeptides in the latter samples. Both collagen types were susceptible to unfolding in the selected, undiluted NADES, but retained more of the structural properties in diluted NADES. This was confirmed by studies of the secondary protein structure by SDS-PAGE, thermal properties by nano DSC and spectroscopic properties. Results indicated that the eutectic network of the NADES was preserved up to 1:200 dilution in water. Freeze-dried collagen sheets containing the selected NADES were prepared as a potential wound dressing formulation. The freeze-drying process up-concentrated the NADES within the protein structure. The results on the molecular structure and mechanical properties of collagen-NADES sheets were consistent with the spectroscopic and thermal observations on the collagen-NADES solutions, indicating that the structural properties of collagen was maintained in NADES dilutions $\geq$ 1:50. FT-IR results demonstrated a loss of the amide I and II signal in the spectrum at low dilutions of the NADES. These amides are related to the helix-conformation. The studies on mechanical properties revealed that NADES may further be used as a plasticizer in collagen sheet formulations. Mechanical force-displacement studies showed that a 1:100 dilution of the selected NADES was an optimal solvent for the preparation of collagen-NADES sheets. Further, this dilution retained the structural properties of native collagen. The combination of collagen and aqueous dilutions of the selected NADES seemed suitable for further development into topical preparations.

Paper III describes how the photosensitizing compound lumichrome can be used as a photocrosslinker for collagen to produce hydrogels with unique properties tuning the behavior of 2D cultured human fibroblasts. The use of collagen in biomedical applications has been considered limited due to low viscosity and slow gelation. In this paper we applied lumichrome, a photochemical degradation product of riboflavin, to efficiently crosslink collagen, even at low temperatures. Lumichrome has previously been studied for its photosensitizing properties in antimicrobial photodynamic therapy. A limitation for the use of lumichrome is the low aqueous solubility, which in the present work has been addressed by the complexation with cyclodextrins. Cyclodextrins can further be used to modulate collagen to increase viscosity and fibril organization. Lumichrome photocrosslinking of the collagen hydrogels reduced the gelation time from several minutes to 10 s prior to optional physical crosslinking. The prepared hydrogels were compared with riboflavin photocrosslinked hydrogels and physically crosslinked hydrogels. The material properties of the hydrogels were studied. Lumichrome photocrosslinking resulted in hydrogels with the highest water holding capacity and elasticity. These properties may be desirable in wound healing and tissue engineering applications. Fibroblasts were seeded on the hydrogels. Cell morphology, cell viability, enzyme expression and secretion of proteins involved in extracellular matrix production and

differentiation were monitored, as well as expression of corresponding genes. The fibroblasts seeded on the lumichrome hydrogels exhibited a myofibroblastic phenotype, expressed by α-SMA fibers and pan-cadherin. Results on mRNA and protein expression for SDC-4 and MMP-2 indicated a low adhesive and a more migratory behavior. The study showed that lumichrome photocrosslinking of collagen offers a good alternative to other crosslinking methods.

Paper IV demonstrates the bacterial phototoxicity of lumichrome photocrosslinked collagen gels. Collagen preparations, and particularly hydrogels, have shown to be effective in the treatment of wounds by being a sacrificial material against proteolytic enzymes and by chemotaxis of cells involved in the wound healing process. Their high degree of biocompatibility and high moisture content will provide good conditions for a humid healing environment. Collagen preparations have previously been combined with antibiotics to produce antibacterial drug formulations. However, the increasing resistance against antibiotics requires new and innovative antibacterial treatment alternatives. Antimicrobial photodynamic therapy has been investigated as an alternative antibacterial treatment for topical infections combining photosensitizers with optical radiation to produce oxygen species toxic to bacteria. The aim of this paper was to investigate the bacterial phototoxicity of the lumichrome photocrosslinked collagen hydrogels developed in **Paper III**. The dual effect of lumichrome in collagen hydrogels, both as a photocrosslinker of collagen and photosensitizer for antimicrobial applications was demonstrated. Despite a more than 2-fold higher concentration of lumichrome in hydrogels prepared with (2-hydroxypropyl)-β-cyclodextrin (HPβCD) compared to (2-hydroxypropyl)-γ-cyclodextrin (HPγCD), the hydrogels exhibited approximately similar bacterial phototoxicity in *Staphylococcus aureus*. The lumichrome release profile from the gels showed a similar percentage cumulative release after 4 h. The phototoxic effect was therefore attributed to a higher complexation efficiency and stability of the HPβCD complex, resulting in a lower singlet oxygen production for complexed lumichrome. The study is a proof of concept for possible application of an endogenous photocrosslinker in combination with a biopolymer in applications such as antimicrobial photodynamic therapy after further development.

Chapter 2

Aim of the project

The overall aim of the project was to investigate how rest raw material from Norwegian industrially produced turkey (*Meleagris gallopavo*) could be utilized as a source of collagen suitable for use in pharmaceutical (e.g., topical preparations) and biomedical (e.g., tissue engineering) preparations.

The specific aims of the work were to:

- investigate the suitability of collagen from turkey (*Meleagris gallopavo*) as a biomaterial in pharmaceutical preparations (**Paper I**)
- investigate the physicochemical properties of collagen in an eutectic solvent and aqueous dilutions thereof to identify potential combinations suitable in pharmaceutical preparations (**Paper II**)
- use lumichrome as a photocrosslinker of collagen hydrogels, to produce a material with adequate biocompatibility, biodegradability and bacterial phototoxicity suitable for tissue engineering and wound healing (**Paper III and IV**)

Chapter 3

General experimental conditions

A brief description of main materials and methods used in **Papers I-IV** is given below. Further details can be found in the individual papers.

3.1 Materials

The collagen used in the present work was isolated from industrially produced turkey (*Meleagris gallopavo*) rest raw material. In brief, turkey tendons were manually cleaned and freeze-dried for 48 h. A 0.5 M acetic acid solution with pepsin (1:10) was added to enzymatically hydrolyze the material. The hydrolyzed material was centrifuged, and the supernatant was collected. The collagen was precipitated by the addition of 4 M NaCl (1:3) and centrifuged. The collagen was re-solubilized in 0.5 M acetic acid and dialyzed against distilled water for 3 days. The dialyzed collagen was freeze-dried to obtain a dry material. Other reagents were of analytical grade and were purchased from Merck KGaA (Darmstadt, Germany). Bacterial medium and components were all purchased from Thermo Fischer Scientific (Waltham, MA, USA) or VWR International, LLC (Radnor, PA, USA). The isolation method is described in detail in **Paper I**.

3.2 Preparation of samples and formulations

3.2.1 Collagen solutions

Collagen solutions were prepared by dissolving the collagen in the relevant solvent. Collagen was dissolved in 20 mM acetic acid (**Paper I, III and IV**), or in a NADES based on citric acid and xylitol (in the molar ratio 1:1 of the individual components), referred to as CX and aqueous dilutions thereof (**Paper II**) under stirring (500 rpm) overnight. The preparation of NADES CX and the aqueous dilutions are described in **Paper II**.

3.2.2 Collagen hydrogels

Collagen hydrogels (**Paper I, III and IV**) were prepared by physical or photochemical crosslinking methods.

Physically crosslinked hydrogels (Col gels) were prepared by dissolving collagen in 20 mM acetic acid over 24 h. The collagen solution was neutralized to pH 7.4 by the addition of 10X PBS (0.1 × final volume of the combined solution) and 1 M NaOH (0.023 × volume of added collagen solution) and diluted with Milli-Q water to desired collagen concentration. The neutralized solution was incubated in the dark at 37 °C for 90 min to initiate gelling and self-assembly of the collagen.

Riboflavin photocrosslinked hydrogels (RF gels) were prepared by a two-step gelation and photocrosslinking method (**Paper I and III**). The hydrogels were prepared as for the Col gels, except for the addition of riboflavin 5'-monophosphate sodium salt to a final concentration of 0.01% (w/v) (265 µM). The neutralized solution (pH 7.4) was incubated in the dark at 37 °C for 1 h to initiate gelling and self-assembly of the collagen. The collagen hydrogels were exposed to UVA irradiation (Ralutec 9W/78, Radium, Germany, λ_{max} = 365 nm, 2.94 mW/cm^2) in a chamber (Polylux-PT, Dreve, Germany) for 4 min (0.7 J/cm^2) to form interhelical crosslinks. The crosslinking procedure was completed by incubating the hydrogels in the dark at 37 °C for 30 min.

Lumichrome photocrosslinked hydrogels (LC gels) were prepared by a direct photocrosslinking method (Figure 3.1) (**Paper III and IV**). (2-hydroxypropyl)-β-cyclodextrin (HPβCD, International Specialty Products, Köln, Germany) or (2-hydroxypropyl)-γ-cyclodextrin (HPγCD, Wacker Chemie AG, Burghausen, Germany) was dissolved in 20 mM acetic acid to a final concentration of 5% (w/v). LC was dissolved in the acidic CD solution to a final concentration of 250 µM or 100 µM for HPβCD and HPγCD, respectively. Collagen was dissolved in the acidic LC-CD solution with over 24 h. The collagen solution was neutralized to pH 7.4 by the addition of 10X phosphate buffered saline (PBS) (0.1 × final volume of the combined solution), 1 M NaOH (0.023 × volume of added collagen-LC-CD solution) and Milli-Q water to desired collagen concentration, 200 µM (in 5% HPβCD) or 80 µM (in 5% HPγCD) LC. The neutralized solutions were crosslinked by irradiation with blue light (Bio X, Cellink, Gothenburg, Sweden, λ_{max} = 405 nm, 17.8 mW/cm^2) for 10 s (0.2 J/cm^2) directly after neutralization. The gels were incubated at 37 °C for 90 min to complete the crosslinking procedure. To distinguish the effects of LC and HPβCD in cell studies, CD-modulated collagen hydrogels (CD gels) were prepared with 5% HPβCD added to 20 mM acetic acid without LC and photocrosslinking (**Paper III**).

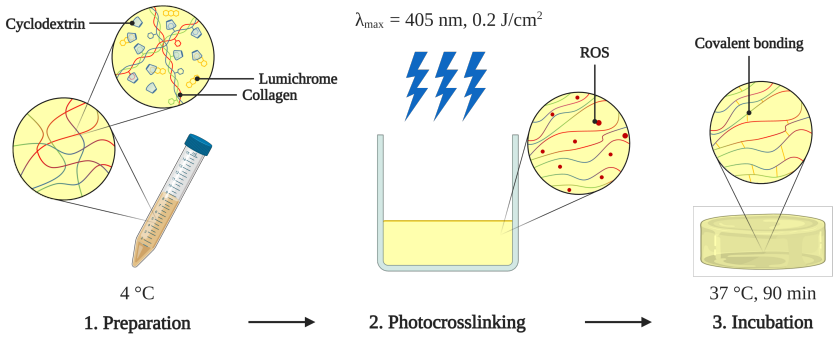

Figure 3.1: Schematic illustration of the preparation of LC gels. A solution of collagen with cyclodextrin complexed LC was prepared. Neutralization and irradiation produce ROS, contributing to the formation of covalent bonding between collagen fibrils to produce a firm gel. (Created with BioRender.com).

3.2.3 Collagen freeze-dried products (sponges and sheets)

Collagen sponges were prepared by freeze-drying of RF gels (**Paper I**). Sponges were prepared with prilocaine hydrochloride (PCL) as a model drug. The PCL was dissolved in the gel solution under the neutralization procedure to a final concentration of 5 mg/ml. The gels were frozen at -80 °C for 1 h prior to freeze-drying at 0.0019 mbar for 20 h, including 1 h final drying at 0.0010 mbar (Alpha 2-4 LD Plus Freeze Dryer, Martin Christ, Osterodeam Harz, Germany).

Collagen sheets were prepared by freeze-drying of the collagen-NADES solutions (**Paper II**). The solutions were transferred to a 6-well multiplate (Corning Life Sciences, Tewksbury, MA, USA) (2 ml) and freeze-dried in order to form sheets. The solutions were frozen at -80 °C for 1 h prior to freeze-drying at 0.0019 mbar for 20 h, including 1 h final drying at 0.0010 mbar (Alpha 2-4 LD Plus Freeze Dryer, Martin Christ, Osterodeam Harz, Germany).

3.3 Methods

3.3.1 Characterization of isolated collagen

Collagen from turkey was characterized with respect to its physicochemical properties in dry (freeze-dried) state and in solution in **Paper I**. Methods used, and described in the paper, included a total collagen quantification assay (Sircol^{TM} Soluble Collagen Assay), measurement of intrinsic viscosity and estimation of average molecular weight, sodium dodecyl sulphate-polyacrylamide gel electrophoresis (SDS-PAGE), circular dichroism, nano differential scanning calorimetry (nano DSC), fourier transform infrared spectroscopy (FT-IR), morphology studies (SEM) and a cell viability assay.

The behavior of the isolated turkey collagen and a commercially available collagen from calf skin in NADES CX and aqueous dilutions thereof were assessed by studying viscometric, calorimetric (nano DSC), structural (SDS-PAGE) and spectral properties (absorbance and fluorescence) in **Paper II**.

3.3.2 Characterization of formulations

The sponges prepared in **Paper I** were characterized with respect to mechanical properties (compression), thermal stability (DSC and TGA), morphology (SEM) and *in vitro* drug release (Franz cell diffusion). Estimated average pore size was quantified using ImageJ [195]. Presented value was calculated from the average pore size of the total of 20 randomly chosen pores.

The collagen sheets prepared in **Paper II** were characterized with respect to molecular composition (FT-IR) and mechanical properties (puncture test).

The collagen gels prepared in **Paper III and IV** were characterized with respect to mechanical properties (macroindentation), water holding capacity (centrifugal dehydration), enzyme-mediated scaffold degradation (collagenase digestion) and *in vitro* drug release (gel diffusion in well plate inserts). LC gels were evaluated for their bacterial phototoxicity.

3.3.3 Cell culture studies

Cell studies were conducted to evaluate the cytocompatibility of the isolated collagen in **Paper I** and cytocompatibility, cellular behavior and secretion of proteins and mRNA expression for cells seeded on hydrogels in **Paper III**.

Human primary dermal fibroblasts (PCS-201-012™, ATCC®, Manassas, VA, USA) were cultured in Dulbecco's modified Eagle's medium (DMEM) supplemented with 10% (v/v) fetal bovine serum (FBS), 100 U/ml penicillin, 100 μg/ml streptomycin and 250 μg/ml fungizone in tissue culture flasks. The cells were maintained at 37 °C in a humidified atmosphere of 5% CO_2 and routinely sub-cultivated twice a week. Cells between passages 3-10 were used.

Cytocompatibility studies of the isolated collagen in **Paper I** were conducted by adding collagen to fibroblasts plated on microtiter plates. The collagen was not dissolved before addition to the wells, to mimic use under relevant biological conditions. Cell viability was measured with a commercial assay (CellTiter-Glo® Luminescent Cell Viability Assay, Promega, Madison, WI, USA).

Cell studies on fibroblast behavior in **Paper III** was conducted by seeding cells onto hydrogels. Cytocompatibility was evaluated by live-dead staining of the cell nuclei. Immunofluorescent staining and imaging were used to examine stress fibers, differentiation and expression of α-smooth muscle actin (α-SMA) and pan-cadherin. Commercial enzyme-linked immunosorbent assays (ELISAs) were used to measure protein secretion of matrix metalloproteinase-2 (MMP-2), tissue inhibitor of metalloproteinase-2 (TIMP-2) and shed syndecan-4 (SDC-4). RNA extraction and reverse transcriptase quantitative polymerase chain reaction (RT-qPCR) were used to evaluate gene expression of *ACTA2* (α-SMA), *SDC4* and *COL1A2*. The RT-qPCR results were evaluated according to the MIQE guidelines [196]. Experiments were performed in triplicate and repeated three times.

3.3.4 Bacterial phototoxicity studies

To evaluate the bacterial phototoxicity of the LC gels developed in **Paper III** on planktonic *Staphylococcus aureus*, a hydrogel diffusion method was applied in **Paper IV**. A schematic illustration of the procedure is given in Figure 3.2.

Hydrogels (250 μl) were prepared as described above in 24-well cell culture inserts (Falcon®, Corning Inc. Life Sciences, Corning, NY, USA) with 3.0 μm pores and 8.0×10^5 pores/cm^2. The diffusion area of the inserts was 0.33 cm^2. *S. aureus* strain Newman was cultured overnight in brain heart infusion (BHI, Oxoid Ltd., Basingstoke, UK) broth at 37 °C in a 5% CO_2 supplemented atmosphere. The bacterial suspension was centrifuged and the supernatant was discarded. The bacteria were redispersed in Dulbecco's PBS (DPBS, Lonza, Verviers, Belgium) with 100 mg/l $MgCl_2$ and 130 mg/l $CaCl_2$ to an optical density at 600 nm (OD_{600}) of 1.0, corresponding to approximately 3.0×10^8 colony forming units (CFU)/ml. Each well of a 24-well plate was added 1 ml of a 1:10 dilution of OD_{600} 1.0 inoculum before the insertion of the cell culture inserts containing gels. The gels were incubated with the bacteria for 3 h, following the removal of

the inserts containing the remaining gel. The remaining bacterial suspension was then subjected to UVA irradiation (Ralutec 9W/78, Radium, Germany, λ_{max} = 365 nm, 5.1 ± 0.3 mW/cm^2 at level of wells) in a chamber (Polylux-PT, Dreve, Germany) for 30 min (9 J/cm^2). Colonies of surviving bacteria were calculated after serial dilution in PBS and plating on BHI agar plates incubated overnight at 37 °C in 5% CO_2 supplemented atmosphere. Experiments were performed in triplicate and repeated three times.

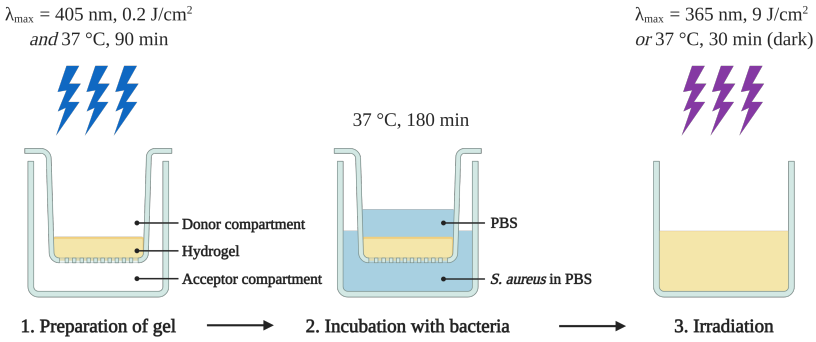

Figure 3.2: Schematic illustration of the studies on bacterial phototoxic effect of LC photocrosslinked collagen hydrogels. Gels were prepared in cell culture inserts and photocrosslinked. *S. aureus* suspended in PBS was added to the well plate. PBS was added to the cell culture insert. After incubation, the cell culture insert was removed and the bacterial suspension was exposed to UVA irradiation followed by calculation of surviving bacteria colonies after serial dilution. (Created with BioRender.com).

Chapter 4

Discussion of the main results

In the present thesis, collagen from turkey (*Meleagris gallopavo*) was investigated for its suitability as a biomaterial in drug delivery and biomedical applications. The isolated collagen was characterized in dry form, in acidic solution and solubilized in a NADES. Further, relevant formulation techniques were applied to obtain collagen preparations with potential applications in drug delivery, tissue engineering and wound healing. The importance of the use of sustainable materials and formulation techniques was emphasized in the present work. A summary of the main aims, achievements and future considerations are summarized in Table 4.1.

4.1 Characterization of collagen from turkey

4.1.1 Physicochemical properties of isolated collagen

Collagen was isolated from turkey tendon and characterized with respect to its physicochemical properties in freeze-dried and dissolved (acidic solution) form (**Paper I**). Due to the large differences in the composition of collagen between species and source within the specimen, it was important to thoroughly study properties relevant for the application in biomaterials. This included the purity, composition and thermal properties as summarized in Table 4.2.

The quantification of total collagen content in solution indicated that the collagen was isolated with high purity. Isolation procedures involving pepsin are known to increase the yield and cleave non-helical telopeptide moieties of the protein [13, 20]. This will further lead to a product with low immunogenicity and good biocompatibility [20]. One of the leading definitions of biocompatibility states that *"the biocompatibility of a material is the ability to perform an appropriate host response in a specific situation or application"* [197]. Biocompatibility studies usually include investigation of histopathological changes in host, which was exposed to a material for an extended period of time. Host response is a measure of biocompatibility. Cytocompatibility (cell response) is a particular case of biocompatibility, which is the wider term. A good biocompatibility is desirable for biomaterials for pharmaceutical use [98, 198]. The cytocompatibility of this collagen in relevant concentrations (0.5-3.0 mg/ml) was confirmed by an *in vitro* viability study on human primary dermal fibroblasts. The results showed a slight decrease in viability with increasing collagen concentration (although not significant). However, this was attributed to the increasing bulk volume of the collagen and/or quenching of the luminescence signal from the viability assay.

Collagen type I has been considered as the gold standard for tissue engineering applications due to low antigenicity and ability to form fibrils [199]. Type I and

Table 4.1: Summary of aims, achieved results and considerations.

Aims	**Achievements**	**Considerations**
Isolate a collagen material with properties suitable for pharmaceutical and biomedical applications.	Isolation of collagen with high purity, high thermal stability and a high degree of cytocompatibility.	Other properties, such as amino acid content should be investigated to get a more holistic characterization.
Prepare a collagen hydrogel suitable for biomedical applications, such as tissue engineering and wound healing.	Reduced gelation time and stronger hydrogels by LC photocrosslinking. Tuned fibroblast behavior to a more migratory myofibroblastic phenotype in 2D.	Fibril organization and pore size should be further investigated. Seeding cells in 3D can represent a more realistic environment for tissue engineering applications.
Investigate the dual effect (photocrosslinking and bacterial phototoxicity) of LC-collagen hydrogels.	Similar bacterial phototoxicity of hydrogels despite different LC concentrations (i.e., excipient-dependent formation of $^1O_2$).	Optimization of irradiation dosimetry, LC dose and studies in other bacteria and biofilms should be performed.
Prepare a freeze-dried drug delivery system of collagen, which by photocrosslinking should control the release of an active pharmaceutical ingredient.	Formation of sponges by RF photocrosslinking and freeze-drying with enhanced mechanical properties.	Further studies investigating how the photocrosslinking can be optimized to control the release of active pharmaceutical ingredients.
Investigate the properties of collagen in a NADES to evaluate the potential for the combination in pharmaceutical and biomedical applications.	Fragmentation of collagen in concentrated NADES. Preservation of collagen structure in highly diluted NADES.	Investigate combinations with other NADES and evaluate and find stable combinations suitable for further development of products.
Assess the best combination of collagen and the NADES for a formulation with potential use in wound healing.	Formation of freeze-dried collagen-NADES sheets with increased plasticity and preserved collagen structure.	Cell- and bacterial studies confirming suitability of the sheets in biomedical settings should be performed.

Table 4.2: Summary of physicochemical properties of collagen isolated from turkey.

Properties	**Result**
Purity	$103.1 \pm 3.1\%$.
Intrinsic viscosity	19.76 dl/g
Estimated molecular weight (M_W)	477.3 kDa
Type (SDS-PAGE)	Type I and III (α_1(I), α_1(III), α_2(I), β, γ)
Transition temperature (minor, T_s)	38.3 °C
Transition temperature (major, T_m)	44.5 °C
Composition (FT-IR)	Amide A (3324 cm^{-1}), amide B (2938 cm^{-1}), amide I (1658 cm^{-1}), amide II (1548 cm^{-1}), amide III (1234 cm^{-1})
Protein conformation (UV-CD)	Abs_{max} 221.5 nm, Abs_{min} 197 nm, Crossover 214 nm

III are also the major collagen types in the ECM and the most important types in the wound healing process [199, 200]. The present collagen was identified as collagen type I and III by SDS-PAGE separation of the α-chains. This agrees with the general presence of type I and III collagen in tendons and ligaments [24, 25]. Indications of crosslinks between the collagen chains were observed by the presence of β- and γ-bands. These bands corresponded to crosslinking between the α-chains or intermolecular crosslinking between collagen molecules [63]. The crosslinking was further confirmed by the estimated average M_W of 477.3 kDa, which was higher than expected. SEM images of the isolated collagen revealed fibrils and sheet-like structures (see figure in Section 4.2.2). FT-IR spectroscopy was applied to further determine the structural features of the isolated collagen. The FT-IR spectra displayed signals characteristic for collagen, including absorption bands for amide A, B, I, II and III (Table 4.2). Amide I, II and III are related to the secondary polypeptide conformation of proteins, and especially the α-helix conformation in collagen [11]. In short, the FT-IR results indicated that the native structure of collagen was preserved. The preservation of the triple helix was further confirmed by the UV-CD measurements exhibiting peaks, which are characteristic for the triple helical conformation [40]. Native collagen is preferred in wound healing applications by being a target for proteolytic enzymes and in tissue engineering applications by being a matrix for cell proliferation [94].

Knowledge about the thermal stability is important to evaluate how the preparation methods and potential applications can affect the collagen structure. Calorimetric analysis were performed by nano DSC on acidic solutions of collagen

to evaluate the thermal stability and determine the denaturation temperature. The thermal denaturation of the isolated collagen occurred in two steps with a minor transition (T_s) at 38.3 °C and a major transition (T_m) at 44.5 °C. A three-state model has been proposed to describe the thermal denaturation of proteins. This includes a thermodynamic step from native to unfolded protein and a kinetically controlled step from unfolded protein to denatured protein (N $\leftrightarrow$ U $\rightarrow$ D) [201]. This model has been evaluated and found to be the best model for thermal unfolding of collagen where the reversible unfolding step is related to melting of small parts of the triple helix (T_s), and the denaturation step (T_m) describes irreversible unfolding to monocoils [37, 202]. The values for T_s and T_m were among the highest values reported in the literature for acidic collagen solutions and emphasize that turkey collagen has superior thermal stability compared to collagen from other species. As described in the introduction, the amino acid content may contribute to the denaturation temperature. However, the amino acid sequence was not studied in detail in the present work. The collagen demonstrated partial refolding after extensive heating (10 °C above the recorded T_m). The denaturation occurring at the T_m of collagen is related to the formation of gelatin fragments, which apparently were formed to a certain extent despite partial refolding [42]. The refolding may be due to the applied pressure in the nano DSC capillary chamber, as discussed in a recent study [45]. Results from the investigation of the integrity of the collagen helix as a function of increasing temperature by UV-CD were consistent with the postulated biphasic thermal transition mechanism.

The high purity, composition and thermal stability of the isolated collagen were considered as properties desirable in biomedical and pharmaceutical preparations. Thus, the material was further evaluated in the preparation of potential collagen formulations and scaffolds.

4.1.2 Physicochemical properties of collagen dissolved in NADES CX

NADES are prepared from natural substances and secondary metabolites and are considered as alternatives to conventional solvents. The possibility to use NADES as "green" sustainable solvents and excipients in collagen formulations was therefore assessed (**Paper II**). Some NADES have demonstrated antibacterial properties in previous studies in our lab [191]. Further, NADES have been utilized in the preparation of functionalized electrospun fibers for drug delivery, which could be interesting for future applications of collagen [203, 204]. NADES CX was selected in the present work based on previous results on antibacterial activity and preliminary studies on the collagen dissolving abilities. The pH of NADES CX and aqueous dilutions thereof ranged from 0.2 (undiluted) to 2.4 (dilutions 1:100 and 1:200). Collagen from turkey tendon (isolated and characterized in the present work; pepsin treated) and collagen from calf skin (commercially available; isolated without pepsin) were compared in the experiments to assess the behavior of collagen with different origin and composition in the selected NADES. Pepsin treatment of the turkey collagen would remove the non-helical

telopeptides, and reduce the content of certain amino acids, such as tyrosine, which may alter the physicochemical properties of the protein compared to non-pepsin treated samples [20]. The physical and spectral properties of collagen from turkey- and calf collagen dissolved in NADES CX and aqueous dilutions thereof are presented in Table 4.3 and 4.4, respectively.

UV absorbance and fluorescence data revealed the presence of tyrosine in both samples, despite pepsin treatment of the turkey collagen, which should remove tyrosine. This indicates that the telopeptides are not completely excised by pepsin treatment [205]. The telopeptides are further rich in phenylalanine (which is the precursor of tyrosine) [206]. Absorption peaks at 268, 265 and 258 nm indicate the presence of phenylalanine [205]. The absorption peak (265 nm) of phenylalanine was the highest intensity peak in the calf collagen, indicating the presence of telopeptides. Hypsochromic (blue shift) and hyperchromic (increase in absorbance) shifts were detected upon dilution of the samples, and are hypothesized to be due to the uncoiling of the protein helix [207, 208]. However, these shifts may also indicate a weakening of the NADES hydrogen bond network, leading to increased stabilization of the dissolved protein. The preservation of the eutectic network upon dilution has been a topic of discussion and some literature claims that the network is absent at high dilutions [190]. The present results indicate that the network is maintained up to 200-fold dilution, which is consistent with previous findings in our lab [191].

Further details on the collagen structure were obtained by fluorescence spectroscopy. Excitation at 270 nm should induce tyrosine fluorescence with a maximum emission near 305 nm. However, unusual tyrosine emission at longer wavelengths (330-350 nm) are reported in proteins and has been ascribed to tyrosinate emission [209]. Tyrosine emerged as the main peak in collagen from calf, while tyrosinate was dominating in collagen from turkey. The emission maximum in turkey samples (i.e., i.e., tyrosine/tyrosinate fluorescence) indicated a bathochromic shift (red shift) with increasing NADES dilution. This confirms a weakening of the NADES network and stabilization of the collagen hypothesized above [210]. Dissolving collagen in aqueous dilutions of NADES may alter the conformation of the protein due to the presence of a supramolecular H-bonding network and a low pH. This was confirmed by a linear decrease in the tyrosinate emission (corrected for the variation in absorbance) as a function of decreased viscosity in diluted NADES samples. The tyrosine emission in calf collagen was, however, virtually independent of NADES concentration. Both the fluorescence measurements and the absorbance spectra indicated that tyrosine was more exposed to the aqueous phase of the environment in samples containing turkey collagen than calf collagen.

Measurements of the fluorescence anisotropy were performed to study the folding of the collagen. The rotational motions of the fluorophores determining the anisotropy relies on the size, shape and extent of aggregation of the molecule. The steady-state fluorescence anisotropy of tyrosinate emission was independent of the supramolecular structure, pH and viscosity of the solvent in turkey collagen samples. This indicated that the tyrosinate residues were not deeply embedded in these samples [211]. The fluorescence anisotropy from tyrosine emission in

Table 4.3: Physical and spectral properties of collagen from turkey tendon dissolved in NADES CX and aqueous dilutions thereof.

Solvent (dilution)	**Viscosity**	T_s [a]	T_m [b]	λ_{Abs} [c]	λ_{Em} [d]	**Anis.** [e]	**FI** [f]**/Abs** [g]
NADES CX	-	-	-	281 (259, 265, 269) nm	319 nm	0.12 ± 0.01	6.40×10^5
NADES CX (1:1)	8.35 mPa·s	-	-	249 (280) nm	335 nm	0.12 ± 0.04	4.23×10^5
NADES CX (1:10)	6.50 mPa·s	33.8 °C	38.3 °C	242 (280) nm	(297) 333 nm	0.13 ± 0.01	2.52×10^5
NADES CX (1:50)	5.69 mPa·s	34.8 °C	40.3 °C	234 (280) nm	(297) 334 nm	0.12 ± 0.01	2.36×10^5
NADES CX (1:100)	5.12 mPa·s	35.1 °C	40.9 °C	231 (280) nm	(301) 339 nm	0.12 ± 0.01	3.08×10^5
NADES CX (1:200)	4.64 mPa·s	35.7 °C	41.7 °C	228 (280) nm	(297) 336 nm	0.12 ± 0.01	1.48×10^5
Acetic acid (20 mM)	5.42 mPa·s	38.5 °C	44.2 °C	223 (∼ 275) nm	(298) 333 nm	0.10 ± 0.02	3.30×10^5

Table 4.4: Physical and spectral properties of collagen from calf skin dissolved in NADES CX and aqueous dilutions thereof.

Solvent (dilution)	**Viscosity**	T_s [a]	T_m [b]	λ_{Abs} [c]	λ_{Em} [d]	**Anis.** [e]	**FI** [f]**/Abs** [g]
NADES CX	-	-	-	265 (258, 268, 275, 281) nm	303 nm	0.12 ± 0.02	3.26×10^5
NADES CX (1:1)	6.67 mPa·s	-	-	249 (278) nm	300 nm	0.13 ± 0.02	0.68×10^5
NADES CX (1:10)	5.52 mPa·s	-	35.7 °C	243 (278) nm	301 nm	0.18 ± 0.02	0.29×10^5
NADES CX (1:50)	5.19 mPa·s	34.1 °C	39.6 °C	231 (282) nm	297 nm	0.20 ± 0.01	1.01×10^5
NADES CX (1:100)	4.86 mPa·s	34.4 °C	39.9 °C	230 (280) nm	298 nm	0.20 ± 0.01	0.46×10^5
NADES CX (1:200)	4.54 mPa·s	34.1 °C	40.0 °C	230 (279) nm	300 nm	0.21 ± 0.01	0.32×10^5
Acetic acid (20 mM)	5.43 mPa·s	36.9 °C	42.6 °C	221 (∼ 275 nm)	296 nm	0.22 ± 0.01	1.33×10^5

[a]Minor transition, [b]Major transition, [c]Absorption wavelength, [d]Emission wavelength (λ_{Ex} = 270 nm), [e]Anisotropy (λ_{Ex} = 295 and 270 nm for turkey collagen and calf skin collagen, respectively), [f]Fluorescence intensity, [g]Absorption intensity.

calf skin collagen was, on the other hand, dependent on the NADES dilution as an inverse function of the viscosity. This indicated a conformational change of the protein upon dilution of the NADES. In very dilute NADES samples (i.e., 1:200), the anisotropy was virtually similar to samples in 0.02 M acetic acid representing a stable collagen structure.

The SDS-PAGE pattern of the collagens dissolved in aqueous dilutions of NADES CX revealed differences in the protein fragmentation upon dilution. The pattern confirmed the unfolding and degradation of the collagens in low dilutions ($\leq$ 1:50) of NADES CX at room temperature. Further, the importance of the telopeptides for the stability of the molecules were emphasized. Collagen from calf with intact telopeptides showed less degradation than telopeptide-excised collagen from turkey. It was hypothesized that the degradation and apparent changes in the protein conformation were due to changes in the supramolecular network of NADES combined with changes in pH.

The thermal stability was evaluated by nano DSC. The denaturation temperature showed a linear increase as a function of increased pH between NADES dilution 1:10 and 1:100. This indicated a stabilization of the collagen structure with increasing pH. Low pH (i.e., $\leq$ 1) causes partial denaturation of the collagen, which can explain the absence of minor transitions prior to the main transition at lower dilutions [212]. This was consistent with the SDS-PAGE results that indicated a fragmentation of these samples.

NADES CX contains xylitol. The presence of polyols, such as xylitol, in a collagen solution has previously shown a stabilizing effect on the triple helix through binding of the polyol to the collagen molecule [213]. However, our study indicated a destabilizing effect of the collagen with increasing NADES concentration. A possible explanation can be that the binding of xylitol in a supramolecular network of hydrogen bonds in NADES can change its ability to form intermolecular bonds with collagen.

Our research group has recently investigated the interactions of NADES with artificial and natural membranes, including the effect of several NADES on liposomes and pig skin (study not included in this thesis) [214]. Collagen is a major constituent of the skin, as mentioned in the introduction. The main findings in the study included a stabilizing effect by NADES on liposome membranes and a slightly reduced permeability of a model drug through pig skin, most likely caused by H-bonding between NADES and the skin proteins. These results are important to further develop combinations of NADES for pharmaceutical purposes.

The unique ability of NADES to dissolve a wide range of substances, combined with their physicochemical properties (e.g., viscosity, pH and antimicrobial properties) make NADES interesting as vehicles in drug delivery. Possible formulations could include sprays, freeze dried sheets and electrospun nanofibers. Formulations for wound treatment should retain the chemotactic properties of collagen either as a native collagen or as peptide fragments [19, 215].

4.2 Characterization of collagen formulations

Collagen was in the present thesis formulated into sponges for modified release of a local anesthetic, sheets for potential use in infected wounds and hydrogels with increased durability and water holding capacity for potential use in wound healing and tissue engineering. Collagen from turkey isolated in **Paper I** was used in all the preparations. Photographs of the respective formulations are presented in Figure 4.1.

Figure 4.1: Photographs of collagen formulations prepared in **Paper I-IV**. From left to right: RF photocrosslinked collagen sponges, collagen-NADES sheets and LC photocrosslinked collagen hydrogels.

4.2.1 Collagen hydrogels

Collagen hydrogels seem promising within a range of application areas, including drug delivery, tissue engineering and wound healing [96, 100, 102]. In **Paper I**, hydrogels were prepared by RF photocrosslinking of collagen solutions. This resulted in apparently stiff and durable gels. Non-irradiated hydrogels appeared weak. The gel properties were not further investigated before freeze-drying into collagen sponges. Challenges associated with the RF photocrosslinking method include a potential radiation attenuation due to highly absorbing components (inner filter effect) caused by the high RF concentration, and a time-consuming irradiation procedure. Further, RF photocrosslinking of collagen may cause heterogeneity in the crosslinks formed by a limited reaction depth of around 300 μm [149]. Previous studies in our lab have proved that photodegradation of RF produces LC, which is more photostable and a more effective $^1O_2$ generator than its precursor [168]. LC was therefore investigated as a potential PS in photocrosslinking of collagen (**Paper III**). Physical properties of the resulting hydrogels and their effect on primary dermal fibroblasts were investigated. Furthermore, the release of LC and potential bacterial phototoxicity of the hydrogels were investigated in **Paper IV**. The photocrosslinking time could be reduced from several minutes to 10 s by changing from RF to LC. A short irradiation time is beneficial in combination with cells for application as bioinks.

Collagen hydrogels were in the present work prepared both by physical crosslinking (with and without CD modulation) and LC and RF photocrosslink-

ing. The physically crosslinked hydrogels and RF photocrosslinked hydrogels were prepared as described in the literature [150]. LC photocrosslinking of collagen hydrogels were, however, performed for the first time in the present work. Thus, an optimization study was performed to evaluate the optimal LC concentration and irradiation source for the preparation of those hydrogels. The viscosity before and directly after irradiation was measured. Collagen solutions with 10% (w/v) HPβCD and 500 μM LC exhibited a viscosity of 122.8 mPa·s before photocrosslinking and 942.0 ± 366.5 mPa·s after being exposed to UVA (Bio X, Cellink, Gothenburg, Sweden, 10 s, $\lambda_{max} = 365$ nm). The large variation in the viscosity after crosslinking was ascribed to precipitation of the collagen in solution within a few minutes after neutralization, despite being prepared on ice. The CD concentration (and subsequently the LC concentration) was therefore reduced. Collagen solutions with 5% (w/v) HPβCD and 250 μM LC exhibited a viscosity of 998.6 ± 55.2 mPa·s after irradiation, while a change in the irradiation procedure to exposing the solution to blue light (10 s, $\lambda_{max} = 405$ nm) increased the viscosity to 1818 ± 83.8 mPa·s. Due to a superior viscosity and reproducible results compared to the other formulations, it was decided to continue with this formulation in the further studies.

Material properties

The measured material properties of the hydrogels prepared in **Paper III** are presented in Table 4.5.

Tissue engineering applications require biomaterials with a certain elasticity. Ideally, a scaffold should have material properties consistent with the application site [216]. The complex elasticity of native tissue is difficult to replicate, and this has been considered as one of the major challenges in tissue engineering [217]. The LC gels had a low initial stress ($\leq$ 1% strain), high Young's modulus (20% strain) and high viscosity, corresponding to a soft material with elastic properties at low strains [218]. RF gels displayed the highest initial stress, but a lower Young's modulus than LC gels. The physically crosslinked hydrogels (Col gels and CD gels) were in general weak and displayed low Young's moduli. The elasticity of skin ranges from $<$ 10 kPa to $>$ 100 kPa depending on, among others, subject age, skin thickness and test parameters [219, 220]. Both LC- and RF gels displayed Young's moduli within the range, indicating a suitability in biomaterials for skin applications.

LC gels exhibited high biodegradability, reflected in the lowest collagenase resistance of the hydrogels studied. This indicated a lower crosslinking density than the other hydrogels, which was confirmed by a higher water holding capacity [221]. The retention of water in the hydrogels can be desirable in tissue engineering applications, facilitating the diffusion and retention of nutritional components. Ophthalmic applications, such as hydrogel contact lenses are dependent on a high water retention capacity to secure oxygen passing to the corneal layer [222, 223]. The collagenase effect is, however, also dependent on the availability of the sites of cleavage. The use of CDs together with LC photocrosslinking seemingly reduced the fibril diameter and increased the

Table 4.5: Physical properties of collagen hydrogels.

Sample	**WHC**[a]	***E***[b]	**Collagenase resistance**[c]
Col gels	2.67 ± 0.53%	3.50 ± 0.21 kPa	31.08 ± 7.68%
CD gels	5.12 ± 2.80%	3.90 ± 0.40 kPa	32.21 ± 10.32%
LC gels	44.97 ± 3.04%	62.30 ± 7.95 kPa	15.18 ± N.A.%
RF gels	2.57 ± 0.06%	30.88 ± 0.51 kPa	62.47 ± 1.14%

[a]Water holding capacity, [b]Young's modulus (20% strain), [c]Remaining gel (12 h)

organization into collagen fibril alignments [130]. This was further expressed after LC photocrosslinking. A change in the fibril alignment can influence the digestion of the collagen molecules, possibly explaining the increased susceptibility to collagenase degradation in LC gels [224].

Reduced fibril diameter and organized molecule alignment were further confirmed by the formation of transparent LC gels. Good optical properties of the scaffolds are usually not a requirement in tissue engineering applications. However, certain application areas may require transparency, such as eye treatment with corneal shields/lenses [222, 223, 225]. Further, photocrosslinking of gels requires a transparent material to avoid radiation attenuation due to light scattering or highly absorbing materials (inner filter effect). An inner filter effect will in the worst case prevent homogeneous crosslinking throughout the material [226]. LC gels prepared by photocrosslinking prior to incubation were clearly more transparent than Col gels and RF gels (Figure 4.2). A change in the crosslinking procedure from photocrosslinking before to mid-way during the incubation, resulted in more translucent gels.

Figure 4.2: Photographs of collagen hydrogel formulations, illustrating the difference in optical properties. From left to right: Col gel, LC gel, CD gel and RF gel.

The presence of LC induced photocrosslinking and gelation of the collagen solution after only 10 s exposure to blue light. A recent study has shown that it is possible to induce fiber-like aggregation and gelation of collagen by UV-irradiation at low temperatures. However, the total required irradiation time for these gels were 60 min [227]. The gels were formed as a result of crosslinking and degradation of the protein. A long irradiation time limits the potential of

co-seeding cells with the gels and biofabrication of cell-laden bioinks. Blue light is not only less destabilizing than UV to collagen, but is less harmful to cells. This is desirable if the formulation is intended to be used in bioprinting [226]. Some studies also show reduced proliferation of fibroblasts after being irradiated with blue light, however, the effect will be dose dependent [228].

LC photocrosslinking of collagen has been performed by application of two types of LC-CD complexes (LC-HPβCD and LC-HPγCD). The CDs had different complexation efficiency (CE), which limited the amount of LC used in the crosslinking reaction. There were no noticeable differences in the mechanical properties between the hydrogels prepared with HPβCD and HPγCD. The influence on the hydrogel properties and behavior of cells seeded on the hydrogels prepared with HPγCD or other CDs must be studied further in a similar way as hydrogels prepared with HPβCD to compare their potential application in tissue engineering and wound healing.

Cell experiments

The effect of the developed LC gels on primary dermal fibroblasts was thoroughly studied with respect to cell morphology, expression of proteolytic enzymes and proteins involved in the ECM production (**Paper III**). The results from the characterization of the collagen hydrogel scaffolds indicated a suitability in tissue engineering and wound healing applications [216]. Thus, the cellular behavior, including the secretion of proteins involved in ECM production and differentiation was monitored, together with the expression of corresponding genes.

Live/dead staining of cells seeded on LC gels, Col gels and CD gels revealed a high viability of cells, demonstrated by the low appearance of dead cells. The viability of fibroblasts seeded on RF gels was, however, dramatically reduced (no viable cells detected). The reason for this is unknown. The only differences between the RF gels and Col gels were the addition of 0.01% (w/v) RF and photocrosslinking of the constructs after 1 h incubation in the former. All hydrogels were further incubated for 30 min prior to seeding of cells. A potential explanation for the death of the cells seeded on RF gels is the presence of trace amounts of long-lived ROS (hydrogen peroxide, H_2O_2) formed during the long irradiation time, resulting in a toxic environment for the seeded cells. RF gels were not included in further cell studies.

Hydrogel scaffolds for tissue engineering and wound healing applications should provide structural support and stimulate cells to express signals to control the production of the ECM, such as biodegradation, similar to the natural remodeling process [98]. Further, the balance between migration and adhesion of cells in a scaffold is important. Thus, cells seeded should adhere to the scaffold and migrate onto, or through the scaffold [216]. The cells seeded on LC gels seemed to be self-organized into cell clusters with an elongated morphology and more prominent intracellular stress fibers (filamentous actin, F-actin) compared to cells seeded on Col gels and CD gels (Figure 4.4). Cells on Col gels and CD gels were evenly distributed throughout the hydrogel surface. Cell clustering is dependent

on ECM properties, growth factors and cell-cell interactions and stabilization. The clustering can further be an indication of collective migration of the cells. The redistribution of actin stress fibers is a morpohological characteristic observed in less adhesive and more migratory cells [229, 230]. SDC-4 is a regulator of focal adhesion and actin-cytoskeletal organization formation in fibroblasts. SDC-4 shedding of its ectodomain results in an altered distribution of cytoskeletal components followed by a loss of adhesion and gain of migratory capacities. The measurement of SDC-4 levels in cell media can thereby be an indication of migratory behavior of cells on a substrate. The levels of SDC-4 was higher (although not significant) in LC and CD gels, compared to Col gels (Figure 4.3). Furthermore, the concentrations of MMP-2 and TIMP-2 in the cell media were measured. Fibroblasts seeded on LC gels had the highest MMP-2/TIMP-2 ratio. The ratio indicated a balance in the expression of the proteins leading towards MMP-2 for cells seeded on all the gels. The role of MMPs and TIMPs in tissue regeneration has previously been investigated [231]. The presence of MMPs is important for the (re)-generation of tissue. An imbalance between the MMPs and TIMPs can, however, be destructive for the tissue. In our study, the levels of MMP-2 and TIMP-2 were lower for LC gels, despite the highest MMP-2/TIMP-2 ratio. MMP-2 is also known to target SDC-4 causing shedding, which is necessary for migration. An elevated MMP-2/TIMP-2 ratio is therefore also indirectly an indication of migratory properties.

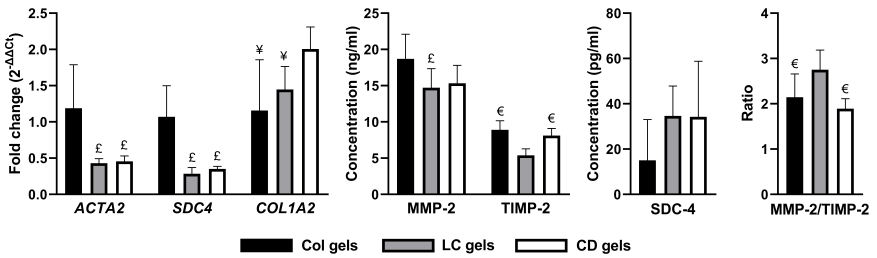

Figure 4.3: mRNA expression and secretion of proteins involved in extracellular matrix production and differentiation. mRNA expression is presented as the normalized mRNA (fold change) in cells seeded on hydrogels relative to expression for cells seeded on Col gels. Protein secretion is presented as the average protein concentration. The MMP-2/TIMP-2 ratio was calculated based on the secretion of protein into the cell media. Black: Col gels; gray: LC gels; white: CD gels. $^{£}P < 0.05$ compared to Col gels; $^{¥}P < 0.05$ compared to CD gels; $^{€}P < 0.05$ compared to LC gels.

The differentiation of fibroblasts into myofibroblasts is critical for the formation of granulation tissue and production of ECM [83]. The expression of α-SMA is a measure of the differentiation of the fibroblasts. The mRNA expression of the α-SMA gene (*ACTA2*) was over 2-fold higher in Col gels than LC and CD gels. However, immunostaining displayed the most mature organization of

α-SMA for fibroblasts seeded on the LC gels (Figure 4.4). Immunostaining of pan-cadherin, a cell adhesion protein related to myofibroblast differentiation, showed a more prominent expression in fibroblasts seeded on the LC gels (Figure 4.4). The summarized results indicated that the onset of myofibroblast differentiation was earlier in fibroblasts grown on LC gels, reflecting the observed down-regulation of α-SMA at mRNA level (Figure 4.3).

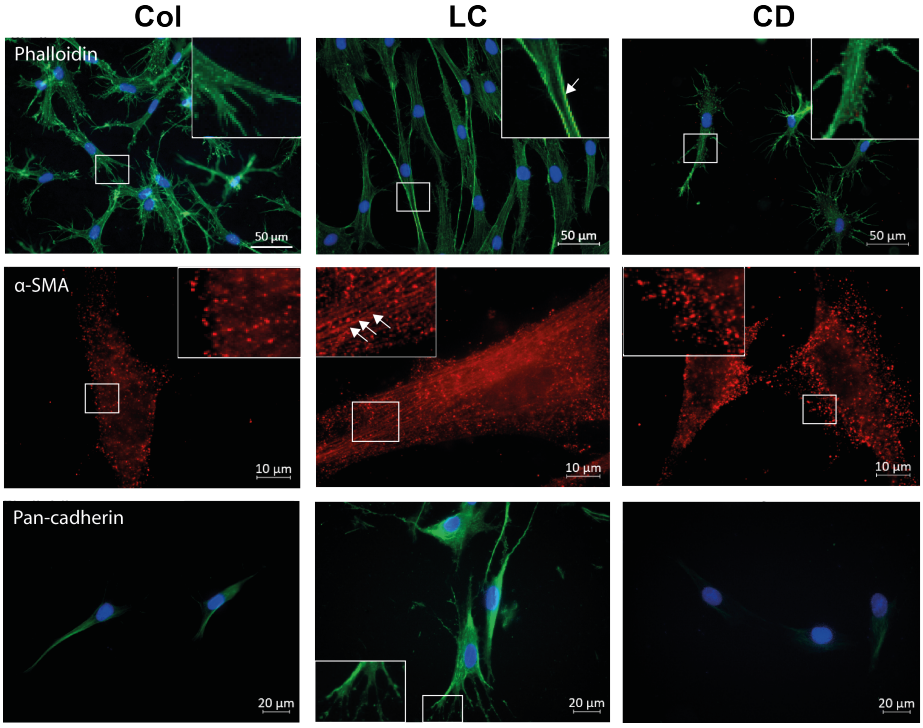

Figure 4.4: Fluorescence microscopy images of fibroblasts seeded on collagen hydrogels. Upper panel: Fluorescence microscopy of F-actin (phalloidin: green; cell nuclei: blue); Mid panel: Immunostaining of α-SMA (red); Lower panel: Immunostaining of pan-cadherin (green; cell nuclei: blue). Secondary antibody controls were included and the results are presented in **Paper III**.

The *COL1A2* gene codes for the production of the α_2-chain of the collagen type I molecule. Measurements of the mRNA-expression of *COL1A2* were included in the study to investigate the effect of the crosslinking on the collagen production from the fibroblasts. The *COL1A2* mRNA expression was significantly highest for fibroblasts seeded on CD gels, with LC gels and Col gels having lower and quite similar expression. The results may be affected by the level of TIMP-2 and SDC-4. These proteins are known to regulate the *COL1A2* mRNA expression via different pathways [232, 233]. The differentiation of fibroblasts into myofibroblasts has also shown to affect the collagen production

following a low mRNA expression, correlating with the results in the present study [233].

Cells experiments on fibroblasts seeded in the well plates in the absence of hydrogels (performed as a control, not included in the paper) showed normal cell behavior with a equal level of MMP-2 and TIMP-2, similar SDC-4 shedding to the cells seeded on hydrogels, low *ACTA2* mRNA expression and high *COL1A2* mRNA expression. Immunofluorescent staining of α-SMA and pan-cadherin was not performed in these samples.

The fibroblasts were in the present thesis, seeded on top of the hydrogel in 2D. The translation of the present results to the proposed applications (in 3D) must therefore be taken into consideration. Cells cultured on hydrogels in 2D are in general less constrained and 3D cultures may model the architecture of tissues in a more accurate way. However, 2D environments may be more relevant for certain applications, such as epithelial surfaces, i.e., the skin [104].

LC release and bacterial phototoxicity experiments

Collagen hydrogels prepared by LC photocrosslinking exhibited physical properties and induced cellular responses which may be beneficial in biomedical applications. The application of hydrogels to a wound can protect the wound site against infections, but collagen alone has, however, no antibacterial properties. Hydrogels have been suggested as promising formulations for aPDT applications [234]. The presence of a PS with phototoxic effect (i.e., LC) in the hydrogels may be an advantage in the treatment of localized infections, such as keratitis, superficial skin infections and infections in the oral cavity. The phototoxic properties of the LC gels were tested against planktonic *S. aureus* in **Paper IV**. Previous studies on the bacterial phototoxicity of LC have been performed with either pure aqueous solutions of the substance or in inclusion complexes and micelles. The reduction in number of bacteria was dependent on the solubilization method [169]. Parameters and results from the release and bacterial phototoxicity experiments in the present study are summarized in Table 4.6.

Hydrogels containing either HPβCD or HPγCD were prepared to assess the influence of complexation agents on the release of LC from the formulations. The LC-HPβCD complex has a complexation efficiency (CE) and stability constant ($K_{1:1}$) twice the values of the LC-HPγCD complex (CE = 0.0165 compared to 0.0034 and $K_{1:1}$ = 412 compared to 85 M^{-1}, respectively) [235]. Thus, the

Table 4.6: Summary of formulation parameters and results from the LC release experiments (**Paper IV**).

		Remaining LC in compartment (4 h)		
Sample	**LC in gel**	**Donor**	**Acceptor**	**Gel**
HPβCD	200 μM	32.60 ± 0.15%	30.15 ± 1.67%	37.16 ± 1.79%
HPγCD	80 μM	35.47 ± 0.77%	33.76 ± 5.71%	30.77 ± 5.13%

amount of LC complexed in HPγCD was reduced compared to the amount in HPβCD. The percentage cumulative release of LC was, however, not significantly different between the two gels after 4h.

An approximately two-fold higher concentration of LC in hydrogels prepared with HPβCD should indicate a higher phototoxicity. However, there was no significant difference between the bacterial phototoxic effect caused by hydrogels prepared with HPβCD and HPγCD. The log reduction was 0.82 and 0.77 corresponding to a total bacterial survival of 28.9 $\pm$ 12.1% and 33.4 $\pm$ 13.8% for formulations containing HPβCD and HPγCD, respectively. Formulations of PS-CD inclusion complexes are known to reduce the production of $^1O_2$, probably due to the low diffusion rate of ground state O_2 into the CD cavity [236, 237]. Furthermore, $^1O_2$ generated within the CD cavity can be quenched by the CDs. The higher $K_{1:1}$ of LC-HPβCD compared to LC-HPγCD indicated that LC was retained to a greater extent in the HPβCD cavity after the release from the hydrogels than its counterpart. This suggests that the similar phototoxicity observed for the two formulations, despite the difference in PS concentration, can be explained by the difference in LC-CD complexation.

The results from the phototoxicity studies showed that LC photocrosslinking of hydrogels for application in wound healing can benefit from the dual effect of LC in collagen hydrogels, both as a crosslinking agent and as a PS in antibacterial treatment of infections. The combination of LC and CDs may further be tailored to increase the phototoxicity, either by varying CDs and LC concentration or in combination with a conventional antibiotic, e.g., chloramphenicol. The latter will weaken the bacteria by aPDT before complete eradication with an antibiotic agent. The present bacterial phototoxicity study is a proof of concept for the application of an endogenous photocrosslinker in combination with a biopolymer in aPDT.

4.2.2 Collagen sponges

Freeze-drying of collagen gels prepared in **Paper I** resulted in the formation of cylindrical sponges. PCL was included as a model drug. Photocrosslinking by irradiation of the gels after 1 h incubation at 37.0 °C prior to freeze-drying was performed to enhance mechanical properties and attempt to modify the release of PCL. No significant difference in the release of PCL was detected between irradiated and non-irradiated formulations. However, there was a difference in the release between sponges and a solution of the drug. The delayed release observed from sponges could be ascribed to the diffusion of drug from the swollen sponge upon hydration rather than physical or chemical entrapment of the drug [100]. The release was not significantly changed after photochemical crosslinking.

RF photocrosslinking of the formulation increased the mechanical strength more than 2-fold compared to non-irradiated sponges. Non-irradiated samples exhibited stress of 1.79 $\pm$ 0.20 kPa at 50% strain, while irradiation increased the stress to 3.74 $\pm$ 0.94 kPa under similar conditions. The high standard deviation was ascribed to the inner filter effect leading to heterogeneity in the crosslinks formed, as previously discussed.

Photocrosslinking of the gels prior to freeze-drying resulted in the formation of pores and stabilizing fibrils between the pores of the sponge. During freeze-drying, pores are formed by large-growing ice crystals that appear during the initial freezing step. This will segregate the collagen fibrils and compress them into thin sheets. After the ice crystals sublimate during freeze-drying, empty spaces are formed [238]. Photocrosslinking of the gel before freeze-drying will stabilize the porous fibril network. The photocrosslinking led to the formation of fibril-stabilized pores with an estimated average diameter of 392 ± 139 μm. The non-irradiated sponges exhibited a collapsed pore structure with fewer visible fibrils, and the average pore size could not be measured. The changes in morphology after photocrosslinking may be favorable in tissue engineering applications where cell movement and sufficient exchange of nutrients and oxygen are crucial [105, 239]. Further, the pore structure may absorb excessive wound exudate. This results in swollen hydrogels, which adhere to the wound bed and protect the wound site against exogenous factors, such as bacteria. The irradiated sponges absorbed water but retained their shape upon dispersion in aqueous solution. SEM images of the isolated collagen, RF photocrosslinked collagen sponges and non-irradiated collagen sponges are presented in Figure 4.5.

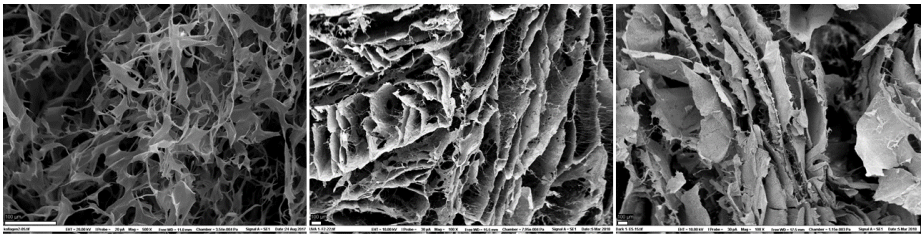

Figure 4.5: SEM images of collagen and collagen sponges prepared in **Paper I**. From left to right: isolated collagen from turkey, cross section of RF photocrosslinked collagen sponge and non-irradiated collagen sponge. Scale bars 100 μm.

The photocrosslinking of the sponges further changed the thermal properties of the formulation. TGA measurements demonstrated a significant weight loss upon heating of the sponges ascribed to both the decomposition of PCL and collagen. The results were, however, similar for all sponge samples. Thermal studies by DSC revealed that non-irradiated sponges exhibited a lower shrinkage temperature (57.1 ± 1.9 °C) than RF photocrosslinked sponges (63.5 ± 2.5 °C). The shrinkage temperature of collagen corresponds to the loss of the triple helical structure [240]. This indicated a stabilization of the formulation by photocrosslinking [41].

4.2.3 Collagen-NADES sheets

Collagen sheets are another type of scaffold, which can be produced by freeze-drying. In the present thesis, collagen-NADES sheets were prepared as an example of a collagen material containing a NADES (**Paper II**). The sheets were prepared from turkey and calf skin collagen, respectively.

The molecular composition of the collagen-NADES sheets were assessed by FT-IR spectroscopy. The sheets containing NADES were compared to control samples without NADES, both prepared by freeze-drying of acidic collagen solutions. The control sample maintained the molecular characteristics of the solid collagen (i.e., amide A, B, I, II and III). Samples prepared with NADES CX 1:1 and 1:10 displayed weak or no amide I and II signals. These amides are associated with the helix conformation of collagen, and a loss of these functions are related to the uncoiling or degradation of the collagen helix [11]. Samples prepared with aqueous dilutions 1:50-1:200 of NADES CX exhibited bands related to the molecular characteristics of collagen triple helix. A band at approximately 1714 cm^{-1} was observed in all samples containing NADES. The presence of citric acid in the NADES can induce a shift of the C=O stretching signal from approximately 1692 cm^{-1} to 1714 cm^{-1} by hydrogen bonding [241].

Freeze-dried collagen sheets are normally brittle and have poor mechanical properties in the absence of crosslinking. Thus, the incorporation of substances such as plasticizers are necessary. The use of a plasticizer may increase mechanical properties, such a toughness and resistance to cracking [242]. NADES at low dilutions ($\leq$ 1:10) lead to the formation of a sticky mass, impossible to handle. Perforation tests of the collagen-NADES sheets were performed. However, only sheets prepared from turkey collagen could be analyzed because sheets prepared from calf collagen were sticking to the container. This may indicate that the isolation method and the amino acid composition of the collagen is crucial for the ability to form sheets prepared with NADES. Incorporation of NADES to the turkey collagen sheets increased the maximum force of indentation prior perforation of the sheets from 0.10 $\pm$ 0.01 (control sample without NADES) to 0.46 $\pm$ 0.07 N (sheets prepared with NADES dilution 1:100). The displacement before perforation was increased from 1.80 $\pm$ 0.12 to 4.94 $\pm$ 0.65 mm. The introduction of NADES to the sheets had apparently a plasticizing effect on the formulation. Further dilution of NADES prior to dissolving collagen and freeze-drying sheets decreased both the force and displacement. Hence, a 1:100 dilution of NADES CX was the optimal solvent, giving the best mechanical properties of the resulting product.

The effect of the NADES on the collagen sheets was attributed to the up-concentration by evaporation, leaving concentrated NADES within the protein structure. Further, the presence of xylitol and citric acid may have affected the collagen structure. As discussed previously, xylitol alone was postulated to stabilize the collagen structure. However, the tightly bound hydrogen network may affect this ability. Both xylitol and citric acid have previously been evaluated as excipients in protein sheets. Xylitol was demonstrated to have plasticizing properties when added to squid protein films, while citric acid has

been investigated as a potential natural crosslinking agent of collagen sheets [243, 244]. Other DES and NADES, such as choline chloride combined with urea, citric acid and glycerol have been investigated for their plasticizing properties on polymer formulations. Results from these studies point towards a potential use of the eutectic mixtures in production of eco-friendly bio-based plastics [245]. The use of the present NADES can further be interesting in wound dressings by inhibition of biofilm formation. Xylitol has shown biofilm inhibition by reduced bacterial viability, reduced content of polysaccharides and tightness of biofilm attachment [246].

The use of a 1:100 dilution of NADES CX was considered the best alternative for preparation of collagen-NADES sheets. The presence of the NADES within the sheets may further allow for inclusion of additional compounds (e.g., drugs) with low aqueous solubility to enhance the potential antibacterial effect.

4.3 Sustainability and relevance of the present work

The current attention in bioeconomy research is focused on alternative sources to conventional products, such as alternative feedstocks from waste and rest raw materials [247]. The use of sustainable materials in the production of new biomedical devices are demanded, and the isolation of collagen can improve the circular bioeconomical aspects related to the increasing meat consumption and amounts of rest raw materials from poultry [248]. Collagen has already been predicted a future as an excipient in pharmaceutical and biomedical applications, but the clinical applications have been prevented by challenges such as the risk of containing transmissible diseases and by religious and dietary preferences. The use of poultry rest raw material lowers the risk of transmitting TSE, BSE and FMD, and is generally more accepted in different diets [249].

The interest in the use of NADES as an alternative to conventional solvents is increasing, especially for the extraction of plant metabolites. A few products containing NADES have been introduced on the market, especially within cosmetics [250, 251]. The present study demonstrated that collagen could be dissolved in NADES. Concentrated NADES induced some degradation of the collagen molecule. However, highly diluted NADES could be applied without major induction of changes in the collagen structure. This makes the addition of small amounts of NADES to collagen preparations, such as hydrogels, possible. NADES can by this be used as a solubilizer for, e.g., poorly aqueous soluble drugs or PS in hydrogels, but also contribute to antibacterial properties of the formulation. NADES in higher concentrations may induce fragmentation of collagen. Further studies on these degradation products have to be performed to identify potential bioactive collagen peptides formed in the presence of NADES.

The areas of focus for research within life sciences at University of Oslo (UiO:Life Science) have sustainability as an overarching topic, aiming to fulfill several of the goals in the 2030 Agenda for Sustainable Development [252]. The use of rest raw materials and "green" chemicals, such as NADES and endogenous PS matches one of the three pillars of UiO:Life Science strategy by

promoting innovation related to environment and health. Further, the challenge of increasing antimicrobial resistance is emphasized as a field of research. This has been addressed in the present thesis by application of NADES and endogenous PS as a new approach to fight bacterial infections.

Chapter 5

Concluding remarks

The present thesis aimed to investigate the potential use of rest raw materials from Norwegian industrially produced turkey (*Meleagris gallopavo*) in pharmaceutical and biomedical applications. Further, sustainable alternatives to organic solvents, artificial polymers, toxic crosslinkers and conventional antibiotics were addressed.

Collagen was isolated with high purity. The protein exhibited a high thermal stability and had a composition which indicated a suitability in applications such as drug delivery, tissue engineering and wound healing. Different formulations based on the isolated collagen were prepared, including hydrogels, freeze-dried sponges and sheets. The hydrogels demonstrated suitability for the growth of human dermal fibroblast. Photocrosslinking increased the mechanical strength of the hydrogels. The application of LC as a photocrosslinker reduced the required irradiation time from minutes to only 10 s, which is favorable in preparation of cell-laden hydrogels and development of bioinks. Cells seeded on these gels had a migratory myofibroblastic phenotype. Studies on the release of LC from the hydrogels in combination with bacterial phototoxicity studies were performed as a proof of concept and demonstrated a dual function of LC in the hydrogels, both as a photocrosslinker of collagen and as a PS for antimicrobial applications. Sponges prepared from collagen hydrogels exhibited properties favorable for potential use as a scaffold. RF photocrosslinking of hydrogels before freeze-drying increased the mechanical properties of the resulting product. Sustained release of the hydrophilic model drug, prilocaine hydrochloride, was observed from the sponges. Studies on the morphology of the photochemically crosslinked sponges indicated a pore size optimal for cell growth and nutrition exchange and thereby a potential application as a scaffold.

A NADES based on citric acid and xylitol was evaluated as a sustainable solvent for collagen. Both acid soluble and pepsin soluble collagen were included in the study. Collagen exhibited variable unfolding properties depending both on its isolation method/source and the degree of NADES dilution. While the collagen seemed to unfold and degrade in undiluted NADES, a highly diluted NADES preserved the triple helical structure of the protein. Further, freeze-dried products of collagen in aqueous dilutions of the NADES were prepared. A 1:100 dilution of the NADES appeared to be the optimal concentration for retaining the molecular functions of collagen and increasing the mechanical strength of the formed sheets.

Rest raw material from industrial turkey production seems to be a relevant source for isolation of collagen with high purity. The application of natural and endogenous PS in photocrosslinking, and the combination of collagen with certain NADES are promising and sustainable alternatives to conventional crosslinking agents and solvents, respectively.

Chapter 6

Future perspectives

- Collagen has a great potential in biomedical applications (e.g., tissue engineering, wound healing and biofabrication) due to its biocompatibility, biodegradability and natural function as a structural component in the body. The present work demonstrated the use of rest raw material from turkey as a source of collagen. Further optimization and up-scaling of the production method have to be performed to achieve a cost-effective product.

- Sterilization of collagen and collagen preparations are challenging. Conventional sterilization techniques, such as the use of high temperatures or gamma irradiation can lead to conformational changes in the protein structure. Alternative sterilization methods that preserve the triple helical collagen structure and retain its physicochemical properties should be established.

- The use of collagen in biofabrication applications (e.g., bioprinting) has been considered as limited due to slow gelation and low viscosity. A bioink must be printable and allow for sufficient nutrient and oxygen exchange to maintain cell viability. The viscosity of bioinks should therefore be as low as possible while maintaining the printed structure. In this thesis, LC photocrosslinking at short irradiation times was used to induce crosslinking and stabilize the collagen gel structure. The results were promising for the potential application of collagen. The new crosslinking procedure must be optimized for bioink formulations. 3D cell culture experiments will add further information on the suitability of the gels for tissue engineering applications.

- LC photocrosslinking reduced the irradiation time needed for gelation of collagen from minutes to 10 s compared to conventional photocrosslinkers. Treatment of the eye disease keratoconus is thereby another possible target for this crosslinking reaction *in vivo*. Photocrosslinking of collagen in the cornea is painful due to a long irradiation time ($\sim$ 1 h), especially for postoperative patients, and requires active pain management. Based on our preliminary results, an eye drop formulation containing LC can be convenient due to the short irradiation time to achieve collagen photocrosslinking. Further experiments *in vitro* on ocular cells followed by *in vivo* studies should be performed to evaluate the clinical relevance.

- In the present thesis, a NADES was combined with collagen as a template for antibacterial products suitable in, e.g., wound healing. The concept

should be further explored, e.g., by inclusion of other NADES. The unique properties of NADES, both as a "green" solvent and as an antibacterial component combined with the wound healing properties of collagen could lead to development of new wound dressings based on innovative production technology such as electrospun shell-core materials.

- Formulations prepared in the present thesis were characterized with respect to their physicochemical properties, and cell studies were performed in case of the hydrogels. Further cell studies followed by *in vivo* experiments in, e.g., animal models are needed to achieve clinical translation of the formulations investigated in the present thesis.

Bibliography

[1] United Nations, General Assembly. *Transforming our world: the 2030 Agenda for Sustainable Development*. Sept. 25, 2015.

[2] Stevens, J. R. et al. "The rise of aquaculture by-products: Increasing food production, value, and sustainability through strategic utilisation". In: *Mar. Policy* vol. 90 (2018), pp. 115–124. DOI: 10.1016/j.marpol.2017.12.027.

[3] Stiborova, H. et al. "Waste products from the poultry industry: a source of high-value dietary supplements". In: *J. Chem. Technol. Biotechnol* vol. 95, no. 4 (2020), pp. 985–992. DOI: 10.1002/jctb.6131.

[4] Irastorza, A. et al. "The versatility of collagen and chitosan: from food to biomedical applications". In: *Food Hydrocoll.* (2021), p. 106633. DOI: 10.1016/j.foodhyd.2021.106633.

[5] Bustillo-Lecompte, C. F. and Mehrvar, M. "Slaughterhouse wastewater characteristics, treatment, and management in the meat processing industry: A review on trends and advances". In: *J. Environ. Manage.* vol. 161 (2015), pp. 287–302. DOI: 10.1016/j.jenvman.2015.07.008.

[6] Adhikari, B. B., Chae, M., and Bressler, D. C. "Utilization of Slaughterhouse Waste in Value-Added Applications: Recent Advances in the Development of Wood Adhesives". In: *Polymers* vol. 10, no. 2 (2018). DOI: 10.3390/polym10020176.

[7] Rønning, S. B. et al. "Processed Eggshell Membrane Powder Is a Promising Biomaterial for Use in Tissue Engineering". In: *Int. J. Mol. Sci.* vol. 21, no. 21 (2020). DOI: 10.3390/ijms21218130.

[8] Mokrejs, P. et al. "Extraction of collagen and gelatine from meat industry by-products for food and non food uses". In: *Waste Manag. Res.* vol. 27, no. 1 (2009), pp. 31–37. DOI: 10.1177/0734242X07081483.

[9] Jayathilakan, K. et al. "Utilization of byproducts and waste materials from meat, poultry and fish processing industries: a review". In: *J. Food Sci. Technol.* vol. 49, no. 3 (2012), pp. 278–293. DOI: 10.1007/s13197-011-0290-7.

[10] Parenteau-Bareil, R. et al. "Comparative study of bovine, porcine and avian collagens for the production of a tissue engineered dermis". In: *Acta Biomater.* vol. 7, no. 10 (2011), pp. 3757–3765. DOI: 10.1016/j.actbio.2011.06.020.

[11] Terzi, A. et al. "Effects of processing on structural, mechanical and biological properties of collagen-based substrates for regenerative medicine". In: *Sci. Rep.* vol. 8, no. 1 (2018), p. 1429. DOI: 10.1038/s41598-018-19786-0.

[12] Yousefi, M., Ariffin, F., and Huda, N. “An alternative source of type I collagen based on by-product with higher thermal stability”. In: *Food Hydrocoll.* vol. 63 (2017), pp. 372–382. DOI: 10.1016/j.foodhyd.2016.09.029.

[13] Zhang, J. and Duan, R. “Characterisation of acid-soluble and pepsin-solubilised collagen from frog (Rana nigromaculata) skin”. In: *Int. J. Biol. Macromol.* vol. 101 (2017), pp. 638–642. DOI: 10.1016/j.ijbiomac.2017.03.143.

[14] Sotelo, C. G. et al. “Characterization of Collagen from Different Discarded Fish Species of the West Coast of the Iberian Peninsula”. In: *J. Aquat. Food Prod. T.* vol. 25, no. 3 (2016), pp. 388–399. DOI: 10.1080/10498850.2013.865283.

[15] Shoulders, M. D. and Raines, R. T. “Collagen structure and stability”. In: *Annu. Rev. Biochem.* vol. 78 (2009), pp. 929–958. DOI: 10.1146/annurev.biochem.77.032207.120833.

[16] Kendall, R. T. and Feghali-Bostwick, C. A. “Fibroblasts in fibrosis: novel roles and mediators”. In: *Front. Pharmacol.* vol. 5, no. 123 (2014). DOI: 10.3389/fphar.2014.00123.

[17] Stefanovic, B. “RNA protein interactions governing expression of the most abundant protein in human body, type I collagen”. In: *Wiley Interdiscip. Rev.: RNA* vol. 4, no. 5 (2013), pp. 535–545. DOI: 10.1002/wrna.1177.

[18] Canty, E. G. and Kadler, K. E. “Procollagen trafficking, processing and fibrillogenesis”. In: *J. Cell Sci.* vol. 118, no. 7 (2005), pp. 1341–1353. DOI: 10.1242/jcs.01731.

[19] Chattopadhyay, S. and Raines, R. T. “Collagen-based biomaterials for wound healing.” In: *Biopolymers* vol. 101, no. 8 (2014), pp. 821–833. DOI: 10.1002/bip.22486.

[20] Holmes, R. et al. “Influence of telopeptides on the structural and physical properties of polymeric and monomeric acid-soluble type I collagen”. In: *Mater. Sci. Eng., C* vol. 77 (2017), pp. 823–827. DOI: 10.1016/j.msec.2017.03.267.

[21] Meyer, M. “Processing of collagen based biomaterials and the resulting materials properties”. In: *Biomed. Eng. Online* vol. 18, no. 1 (2019), p. 24. DOI: 10.1186/s12938-019-0647-0.

[22] Chang, S.-W. and Buehler, M. J. “Molecular biomechanics of collagen molecules”. In: *Mater. Today* vol. 17, no. 2 (2014), pp. 70–76. DOI: 10.1016/j.mattod.2014.01.019.

[23] Sorushanova, A. et al. “The Collagen Suprafamily: From Biosynthesis to Advanced Biomaterial Development”. In: *Adv. Mater.* vol. 31, no. 1 (2019), p. 1801651. DOI: 10.1002/adma.201801651.

[24] Sherman, V. R., Yang, W., and Meyers, M. A. “The materials science of collagen”. In: *J. Mech. Behav. Biomed. Mater.* vol. 52 (2015), pp. 22–50. DOI: 10.1016/j.jmbbm.2015.05.023.

[25] Buckley, M. R. et al. “Distributions of types I, II and III collagen by region in the human supraspinatus tendon”. In: *Connect. Tissue Res.* vol. 54, no. 6 (2013), pp. 374–379. DOI: 10.3109/03008207.2013.847096.

[26] Abraham, L. C. et al. “Guide to collagen characterization for biomaterial studies”. In: *J. Biomed. Mater. Res. Part B Appl. Biomater.* vol. 87B, no. 1 (2008), pp. 264–285. DOI: 10.1002/jbm.b.31078.

[27] Gauza-Włodarczyk, M., Kubisz, L., and Włodarczyk, D. “Amino acid composition in determination of collagen origin and assessment of physical factors effects”. In: *Int. J. Biol. Macromol.* vol. 104 (2017), pp. 987–991. DOI: 10.1016/j.ijbiomac.2017.07.013.

[28] Angele, P. et al. “Influence of different collagen species on physico-chemical properties of crosslinked collagen matrices”. In: *Biomaterials* vol. 25, no. 14 (2004), pp. 2831–2841. DOI: 10.1016/j.biomaterials.2003.09.066.

[29] Ju, H. et al. “Comparison of the Structural Characteristics of Native Collagen Fibrils Derived from Bovine Tendons using Two Different Methods: Modified Acid-Solubilized and Pepsin-Aided Extraction”. In: *Materials* vol. 13, no. 2 (2020). DOI: 10.3390/ma13020358.

[30] Sionkowska, A. “Modification of collagen films by ultraviolet irradiation”. In: *Polym. Degrad. Stab.* vol. 68, no. 2 (2000), pp. 147–151. DOI: 10.1016/S0141-3910(99)00176-7.

[31] Doyle, B. B., Bendit, E. G., and Blout, E. R. “Infrared spectroscopy of collagen and collagen-like polypeptides”. In: *Biopolymers* vol. 14, no. 5 (1975), pp. 937–957. DOI: 10.1002/bip.1975.360140505.

[32] Belbachir, K. et al. “Collagen types analysis and differentiation by FTIR spectroscopy”. In: *Anal. Bioanal. Chem.* vol. 395, no. 3 (2009), pp. 829–837. DOI: 10.1007/s00216-009-3019-y.

[33] Riaz, T. et al. “FTIR analysis of natural and synthetic collagen”. In: *Appl. Spectrosc. Rev.* vol. 53, no. 9 (2018), pp. 703–746. DOI: 10.1080/05704928.2018.1426595.

[34] Notbohm, H. et al. “In vitro formation and aggregation of heterotypic collagen I and III fibrils”. In: *Int. J. Biol. Macromol.* vol. 15, no. 5 (1993), pp. 299–304. DOI: 10.1016/0141-8130(93)90030-P.

[35] Williams, B. R. et al. “Collagen fibril formation. Optimal in vitro conditions and preliminary kinetic results”. In: *J. Biol. Chem.* vol. 253, no. 18 (1978), pp. 6578–85.

[36] Drzewiecki, K. E. et al. “Circular Dichroism Spectroscopy of Collagen Fibrillogenesis: A New Use for an Old Technique”. In: *Biophys. J.* vol. 111, no. 11 (2016), pp. 2377–2386. DOI: 10.1016/j.bpj.2016.10.023.

[37] Liu, Y. et al. “Double thermal transitions of type I collagen in acidic solution”. In: *J. Biomol. Struct. Dyn.* vol. 31, no. 8 (2013), pp. 862–873. DOI: 10.1080/07391102.2012.715042.

[38] Persikov, A. V., Ramshaw, J. A. M., and Brodsky, B. "Prediction of collagen stability from amino acid sequence". In: *J. Biol. Chem.* vol. 280, no. 19 (2005), pp. 19343–19349. DOI: 10.1074/jbc.M501657200.

[39] Krane, S. M. "The importance of proline residues in the structure, stability and susceptibility to proteolytic degradation of collagens". In: *Amino Acids* vol. 35, no. 4 (2008), p. 703. DOI: 10.1007/s00726-008-0073-2.

[40] Losso, J. N. and Ogawa, M. "Thermal Stability of Chicken Keel Bone Collagen". In: *J. Food Biochem.* vol. 38, no. 3 (2014), pp. 345–351. DOI: 10.1111/jfbc.12059.

[41] Miles, C. A. et al. "The Increase in Denaturation Temperature Following Cross-linking of Collagen is Caused by Dehydration of the Fibres". In: *J. Mol. Biol.* vol. 346, no. 2 (2005), pp. 551–556. DOI: 10.1016/j.jmb.2004.12.001.

[42] Leikina, E. et al. "Type I collagen is thermally unstable at body temperature". In: *Proc. Natl. Acad. Sci. U. S. A.* vol. 99, no. 3 (2002), pp. 1314–1318. DOI: 10.1073/pnas.032307099.

[43] Privalov, P. L. "Stability of Proteins: Proteins which do not Present a Single Cooperative System". In: *Adv. Protein Chem.* Ed. by Anfinsen, C. B., Edsall, J. T., and Richards, F. M. Vol. 35. Academic Press, 1982, pp. 1–104. DOI: 10.1016/S0065-3233(08)60468-4.

[44] Wilson, W. O. and Woodard, A. "Some factors affecting body temperature of turkeys". In: *Poult. Sci.* vol. 34, no. 2 (1955), pp. 369–371. DOI: 10.3382/ps.0340369.

[45] Sun, M. et al. "Structure Restoration of Thermally Denatured Collagen by Ultrahigh Pressure Treatment". In: *Food Bioproc. Tech.* vol. 13, no. 2 (2020), pp. 367–378. DOI: 10.1007/s11947-019-02389-6.

[46] Jansen, K. A. et al. "The Role of Network Architecture in Collagen Mechanics". In: *Biophys. J.* vol. 114, no. 11 (2018), pp. 2665–2678. DOI: 10.1016/j.bpj.2018.04.043.

[47] Bozec, L. and Horton, M. "Topography and Mechanical Properties of Single Molecules of Type I Collagen Using Atomic Force Microscopy". In: *Biophys. J.* vol. 88, no. 6 (2005), pp. 4223–4231. DOI: 10.1529/biophysj.104.055228.

[48] Zhu, S. et al. "Self-assembly of collagen-based biomaterials: preparation, characterizations and biomedical applications". In: *J. Mater. Chem. B* vol. 6, no. 18 (2018), pp. 2650–2676. DOI: 10.1039/C7TB02999C.

[49] Tamaddon, M. et al. "Characterisation of freeze-dried type II collagen and chondroitin sulfate scaffolds". In: *J. Mater. Sci.: Mater. Med.* vol. 24, no. 5 (2013), pp. 1153–1165. DOI: 10.1007/s10856-013-4882-9.

[50] Lee, C. H., Singla, A., and Lee, Y. "Biomedical applications of collagen". In: *Int. J. Pharm.* vol. 221, no. 1 (2001), pp. 1–22. DOI: 10.1016/S0378-5173(01)00691-3.

[51] Dong, C. and Lv, Y. "Application of Collagen Scaffold in Tissue Engineering: Recent Advances and New Perspectives". In: *Polymers* vol. 8, no. 2 (2016), p. 42. DOI: 10.3390/polym8020042.

[52] Sionkowska, A. et al. "Collagen Based Materials in Cosmetic Applications: A Review". In: *Materials* vol. 13, no. 19 (2020), p. 4217. DOI: 10.3390/ma13194217.

[53] Wang, L.-F. and Rhim, J.-W. "Preparation and application of agar/alginate/collagen ternary blend functional food packaging films". In: *Int. J. Biol. Macromol.* vol. 80 (2015), pp. 460–468. DOI: 10.1016/j.ijbiomac.2015.07.007.

[54] Suurs, P. and Barbut, S. "Collagen use for co-extruded sausage casings – A review". In: *Trends Food Sci. Technol.* vol. 102 (2020), pp. 91–101. DOI: 10.1016/j.tifs.2020.06.011.

[55] Liu, D. et al. "Collagen and gelatin". In: *Annu. Rev. Food Sci. Technol.* vol. 6 (2015), pp. 527–557. DOI: 10.1146/annurev-food-031414-111800.

[56] Bagal-Kestwal, D. R., Pan, M., and Chiang, B.-H. "Properties and Applications of Gelatin, Pectin, and Carrageenan Gels". In: *Bio Monomers for Green Polymeric Composite Materials*. 2019, pp. 117–140. DOI: 10.1002/9781119301714.ch6.

[57] León-López, A. et al. "Hydrolyzed Collagen-Sources and Applications". In: *Molecules* vol. 24, no. 22 (2019), p. 4031. DOI: 10.3390/molecules24224031.

[58] Hong, H. et al. "Preparation of low-molecular-weight, collagen hydrolysates (peptides): Current progress, challenges, and future perspectives". In: *Food Chem.* vol. 301 (2019), p. 125222. DOI: 10.1016/j.foodchem.2019.125222.

[59] Sontakke, S. B. et al. "Orally Available Collagen Tripeptide: Enzymatic Stability, Intestinal Permeability, and Absorption of Gly-Pro-Hyp and Pro-Hyp". In: *J. Agric. Food. Chem.* vol. 64, no. 38 (2016), pp. 7127–7133. DOI: 10.1021/acs.jafc.6b02955.

[60] Ito, N., Seki, S., and Ueda, F. "Effects of Composite Supplement Containing Collagen Peptide and Ornithine on Skin Conditions and Plasma IGF-1 Levels—A Randomized, Double-Blind, Placebo-Controlled Trial". In: *Mar. Drugs* vol. 16, no. 12 (2018), p. 482. DOI: 10.3390/md16120482.

[61] Li, H. et al. "Studies on bullfrog skin collagen". In: *Food Chem.* vol. 84, no. 1 (2004), pp. 65–69. DOI: 10.1016/S0308-8146(03)00167-5.

[62] Beato, M. S., Capua, I., and Alexander, D. J. "Avian influenza viruses in poultry products: a review". In: *Avian Pathol.* vol. 38, no. 3 (2009), pp. 193–200. DOI: 10.1080/03079450902912200.

[63] Rabotyagova, O. S., Cebe, P., and Kaplan, D. L. "Collagen structural hierarchy and susceptibility to degradation by ultraviolet radiation". In: *Mater. Sci. Eng., C* vol. 28, no. 8 (2008), pp. 1420–1429. DOI: 10.1016/j.msec.2008.03.012.

[64] Herdegen, V. et al. “Sterilization of Medical Products from Collagen by Means of Supercritical CO2”. In: *Chem. Eng. Technol.* vol. 37, no. 11 (2014), pp. 1891–1895. DOI: 10.1002/ceat.201300679.

[65] Delgado, L. M., Pandit, A., and Zeugolis, D. I. “Influence of sterilisation methods on collagen-based devices stability and properties”. In: *Expert Rev. Med. Devices* vol. 11, no. 3 (2014), pp. 305–314. DOI: 10.1586/17434440.2014.900436.

[66] Khong, N. M. H. et al. “Improved collagen extraction from jellyfish (Acromitus hardenbergi) with increased physical-induced solubilization processes”. In: *Food Chem.* vol. 251 (2018), pp. 41–50. DOI: 10.1016/j.foodchem.2017.12.083.

[67] Wang, T. et al. “Production of recombinant collagen: state of the art and challenges”. In: *Eng. Biol.* vol. 1, no. 1 (2017), pp. 18–23. DOI: 10.1049/enb.2017.0003.

[68] Aziz, J. et al. “Molecular Mechanisms of Stress-Responsive Changes in Collagen and Elastin Networks in Skin”. In: *Skin Pharmacol. Physiol.* vol. 29, no. 4 (2016), pp. 190–203. DOI: 10.1159/000447017.

[69] Elias, P. M. “Skin barrier function”. In: *Curr. Allergy Asthma Rep.* vol. 8, no. 4 (2008), pp. 299–305. DOI: 10.1007/s11882-008-0048-0.

[70] Venus, M., Waterman, J., and McNab, I. “Basic physiology of the skin”. In: *Surgery (Oxford)* vol. 28, no. 10 (2010), pp. 469–472. DOI: 10.1016/j.mpsur.2010.07.011.

[71] Nguyen, A. V. and Soulika, A. M. “The Dynamics of the Skin’s Immune System”. In: *Int. J. Mol. Sci.* vol. 20, no. 8 (2019), p. 1811. DOI: 10.3390/ijms20081811.

[72] Proksch, E., Brandner, J. M., and Jensen, J.-M. “The skin: an indispensable barrier”. In: *Exp. Dermatol.* vol. 17, no. 12 (2008), pp. 1063–1072. DOI: 10.1111/j.1600-0625.2008.00786.x.

[73] Järbrink, K. et al. “The humanistic and economic burden of chronic wounds: a protocol for a systematic review”. In: *Syst. Rev.* vol. 6, no. 1 (2017), p. 15. DOI: 10.1186/s13643-016-0400-8.

[74] Escandon, J. et al. “High mortality in patients with chronic wounds”. In: *Wound Repair Regen.* vol. 19, no. 4 (2011), pp. 526–528. DOI: 10.1111/j.1524-475X.2011.00699.x.

[75] Blakytny, R. and Jude, E. “The molecular biology of chronic wounds and delayed healing in diabetes”. In: *Diabet. Med.* vol. 23, no. 6 (2006), pp. 594–608. DOI: 10.1111/j.1464-5491.2006.01773.x.

[76] Enoch, S. and Leaper, D. J. “Basic science of wound healing”. In: *Surgery (Oxford)* vol. 26, no. 2 (2008), pp. 31–37. DOI: 10.1016/j.mpsur.2007.11.005.

[77] Wilkinson, H. N. and Hardman, M. J. "Wound healing: cellular mechanisms and pathological outcomes". In: *Open Biol.* vol. 10, no. 9 (2020), p. 200223. DOI: 10.1098/rsob.200223.

[78] Rohani, M. G. and Parks, W. C. "Matrix remodeling by MMPs during wound repair". In: *Matrix Biol.* vol. 44-46 (2015), pp. 113–121. DOI: 10.1016/j.matbio.2015.03.002.

[79] Shaw, T. J. and Martin, P. "Wound repair at a glance". In: *J. Cell Sci.* vol. 122, no. 18 (2009), pp. 3209–3213. DOI: 10.1242/jcs.031187.

[80] Caley, M. P., Martins, V. L. C., and O'Toole, E. A. "Metalloproteinases and Wound Healing". In: *Adv. Wound Care* vol. 4, no. 4 (2015), pp. 225–234. DOI: 10.1089/wound.2014.0581.

[81] Chung, H. et al. "Minireview: Syndecans and their crucial roles during tissue regeneration". In: *FEBS Lett.* vol. 590, no. 15 (2016), pp. 2408–2417. DOI: 10.1002/1873-3468.12280.

[82] Vuong, T. T. et al. "Syndecan-4 Is a Major Syndecan in Primary Human Endothelial Cells In Vitro, Modulated by Inflammatory Stimuli and Involved in Wound Healing". In: *J. Histochem. Cytochem.* vol. 63, no. 4 (2015), pp. 280–292. DOI: 10.1369/0022155415568995.

[83] Hinz, B. "The role of myofibroblasts in wound healing". In: *Curr. Res. Transl. Med.* vol. 64, no. 4 (2016), pp. 171–177. DOI: 10.1016/j.retram.2016.09.003.

[84] Shinde, A. V., Humeres, C., and Frangogiannis, N. G. "The role of α-smooth muscle actin in fibroblast-mediated matrix contraction and remodeling". In: *Biochim. Biophys. Acta Mol. Basis Dis.* vol. 1863, no. 1 (2017), pp. 298–309. DOI: 10.1016/j.bbadis.2016.11.006.

[85] Mustoe, T. A., O'Shaughnessy, K., and Kloeters, O. "Chronic wound pathogenesis and current treatment strategies: a unifying hypothesis". In: *Plast. Reconstr. Surg.* vol. 117, no. 7 Suppl (2006), 35s–41s. DOI: 10.1097/01.prs.0000225431.63010.1b.

[86] Serra, R. et al. "Chronic wound infections: the role of Pseudomonas aeruginosa and Staphylococcus aureus". In: *Expert Rev. Anti Infect. Ther.* vol. 13, no. 5 (2015), pp. 605–613. DOI: 10.1586/14787210.2015.1023291.

[87] Roy, S. et al. "Staphylococcus aureus Biofilm Infection Compromises Wound Healing by Causing Deficiencies in Granulation Tissue Collagen". In: *Ann. Surg.* vol. 271, no. 6 (2020), pp. 1174–1185. DOI: 10.1097/sla.0000000000003053.

[88] Jinnestål, C. L. et al. "Skin barrier impairment correlates with cutaneous Staphylococcus aureus colonization and sensitization to skin-associated microbial antigens in adult patients with atopic dermatitis". In: *Int. J. Dermatol.* vol. 53, no. 1 (2014), pp. 27–33. DOI: 10.1111/ijd.12198.

[89] Wang, C.-L. et al. “Collagen-induced platelet aggregation and release. I effects of side-chain modifications and role of arginyl residues”. In: *Biochim. Biophys. Acta, Gen. Subj.* vol. 544, no. 3 (1978), pp. 555–567. DOI: 10.1016/0304-4165(78)90330-6.

[90] Postlethwaite, A. E., Seyer, J. M., and Kang, A. H. “Chemotactic attraction of human fibroblasts to type I, II, and III collagens and collagen-derived peptides”. In: *Proc. Natl. Acad. Sci. U. S. A.* vol. 75, no. 2 (1978), pp. 871–875. DOI: 10.1073/pnas.75.2.871.

[91] Banerjee, P., Suguna, L., and Shanthi, C. “Wound healing activity of a collagen-derived cryptic peptide”. In: *Amino Acids* vol. 47, no. 2 (2015), pp. 317–328. DOI: 10.1007/s00726-014-1860-6.

[92] Purna, S. K. and Babu, M. “Collagen based dressings–a review”. In: *Burns* vol. 26, no. 1 (2000), pp. 54–62. DOI: 10.1016/s0305-4179(99)00103-5.

[93] Oxlund, H. et al. “Collagen Deposition and Mechanical Strength of Colon Anastomoses and Skin Incisional Wounds of Rats”. In: *J. Surg. Res.* vol. 66, no. 1 (1996), pp. 25–30. DOI: 10.1006/jsre.1996.0367.

[94] Fleck, C. A. and Simman, R. “Modern Collagen Wound Dressings: Function and Purpose”. In: *J. Am. Col. Certif. Wound Spec.* vol. 2, no. 3 (2010), pp. 50–54. DOI: 10.1016/j.jcws.2010.12.003.

[95] McCarty, S. M. and Percival, S. L. “Proteases and Delayed Wound Healing”. In: *Adv. Wound Care* vol. 2, no. 8 (2013), pp. 438–447. DOI: 10.1089/wound.2012.0370.

[96] Xiang, J., Shen, L., and Hong, Y. “Status and future scope of hydrogels in wound healing: Synthesis, materials and evaluation”. In: *Eur. Polym. J.* vol. 130 (2020), p. 109609. DOI: 10.1016/j.eurpolymj.2020.109609.

[97] Williams, D. F. “To engineer is to create: the link between engineering and regeneration”. In: *Trends Biotechnol.* vol. 24, no. 1 (2006), pp. 4–8. DOI: 10.1016/j.tibtech.2005.10.006.

[98] Chan, B. P. and Leong, K. W. “Scaffolding in tissue engineering: general approaches and tissue-specific considerations”. In: *Eur. Spine J.* vol. 17 Suppl 4, no. Suppl 4 (2008), pp. 467–479. DOI: 10.1007/s00586-008-0745-3.

[99] Rahmati, M. et al. “Electrospinning for tissue engineering applications”. In: *Prog. Mater Sci.* (2020), p. 100721. DOI: 10.1016/j.pmatsci.2020.100721.

[100] Li, J. and Mooney, D. J. “Designing hydrogels for controlled drug delivery”. In: *Nat. Rev. Mater.* vol. 1 (2016), p. 16071. DOI: 10.1038/natrevmats.2016.71.

[101] Chan, B. P. and So, K. F. “Photochemical crosslinking improves the physicochemical properties of collagen scaffolds”. In: *J. Biomed. Mater. Res. Part A* vol. 75A, no. 3 (2005), pp. 689–701. DOI: 10.1002/jbm.a.30469.

[102] Drury, J. L. and Mooney, D. J. "Hydrogels for tissue engineering: scaffold design variables and applications". In: *Biomaterials* vol. 24, no. 24 (2003), pp. 4337–4351. DOI: 10.1016/S0142-9612(03)00340-5.

[103] Stevens, M. M. and George, J. H. "Exploring and Engineering the Cell Surface Interface". In: *Science* vol. 310, no. 5751 (2005), pp. 1135–1138. DOI: 10.1126/science.1106587.

[104] Caliari, S. R. and Burdick, J. A. "A practical guide to hydrogels for cell culture". In: *Nat. Methods* vol. 13, no. 5 (2016), pp. 405–414. DOI: 10.1038/nmeth.3839.

[105] Davidenko, N. et al. "Control of crosslinking for tailoring collagen-based scaffolds stability and mechanics". In: *Acta Biomater.* vol. 25 (2015), pp. 131–42. DOI: 10.1016/j.actbio.2015.07.034.

[106] Mantha, S. et al. "Smart Hydrogels in Tissue Engineering and Regenerative Medicine". In: *Materials* vol. 12, no. 20 (2019), p. 3323. DOI: 10.3390/ma12203323.

[107] Groll, J. et al. "Biofabrication: reappraising the definition of an evolving field". In: *Biofabrication* vol. 8, no. 1 (2016), p. 013001. DOI: 10.1088/1758-5090/8/1/013001.

[108] Sun, W. et al. "The bioprinting roadmap". In: *Biofabrication* vol. 12, no. 2 (2020), p. 022002. DOI: 10.1088/1758-5090/ab5158.

[109] Groll, J. et al. "A definition of bioinks and their distinction from biomaterial inks". In: *Biofabrication* vol. 11, no. 1 (2018), p. 013001. DOI: 10.1088/1758-5090/aaec52.

[110] Moroni, L. et al. "Biofabrication: A Guide to Technology and Terminology". In: *Trends Biotechnol.* vol. 36, no. 4 (2018), pp. 384–402. DOI: 10.1016/j.tibtech.2017.10.015.

[111] Hong, J. et al. "Cell-Electrospinning and Its Application for Tissue Engineering". In: *Int. J. Mol. Sci.* vol. 20, no. 24 (2019), p. 6208.

[112] Ben-Arye, T. and Levenberg, S. "Tissue Engineering for Clean Meat Production". In: *Front. Sustainable Food Syst.* vol. 3, no. 46 (2019). DOI: 10.3389/fsufs.2019.00046.

[113] Bhat, Z. F., Kumar, S., and Fayaz, H. "In vitro meat production: Challenges and benefits over conventional meat production". In: *J. Integr. Agric.* vol. 14, no. 2 (2015), pp. 241–248. DOI: 10.1016/S2095-3119(14)60887-X.

[114] Vries, R. B. de et al. "The potential of tissue engineering for developing alternatives to animal experiments: a systematic review". In: *J. Tissue Eng. Regener. Med.* vol. 9, no. 7 (2015), pp. 771–778. DOI: 10.1002/term.1703.

[115] Satpathy, A. et al. "Developments with 3D bioprinting for novel drug discovery". In: *Expert Opin. Drug Discovery* vol. 13, no. 12 (2018), pp. 1115–1129. DOI: 10.1080/17460441.2018.1542427.

[116] Peng, W. et al. “3D bioprinting for drug discovery and development in pharmaceutics”. In: *Acta Biomater.* vol. 57 (2017), pp. 26–46. DOI: 10.1016/j.actbio.2017.05.025.

[117] Nie, J. et al. “Grafting of 3D Bioprinting to In Vitro Drug Screening: A Review”. In: *Adv. Healthcare Mater.* vol. 9, no. 7 (2020), p. 1901773. DOI: 10.1002/adhm.201901773.

[118] Kohane, D. S. and Langer, R. “Polymeric Biomaterials in Tissue Engineering”. In: *Pediatr. Res.* vol. 63, no. 5 (2008), pp. 487–491. DOI: 10.1203/01.pdr.0000305937.26105.e7.

[119] Williams, D. F. “To engineer is to create: the link between engineering and regeneration”. In: *Trends Biotechnol.* vol. 24, no. 1 (2006), pp. 4–8. DOI: 10.1016/j.tibtech.2005.10.006.

[120] Diamantides, N. et al. “Correlating rheological properties and printability of collagen bioinks: the effects of riboflavin photocrosslinking and pH”. In: *Biofabrication* vol. 9, no. 3 (2017), p. 034102. DOI: 10.1088/1758-5090/aa780f.

[121] Shahin-Shamsabadi, A. and Selvaganapathy, P. R. “A rapid biofabrication technique for self-assembled collagen-based multicellular and heterogeneous 3D tissue constructs”. In: *Acta Biomater.* vol. 92 (2019), pp. 172–183. DOI: 10.1016/j.actbio.2019.05.024.

[122] Matteo, A. and Mantovani, D. “Tailoring Mechanical Properties of Collagen-Based Scaffolds for Vascular Tissue Engineering: The Effects of pH, Temperature and Ionic Strength on Gelation”. In: *Polymers* vol. 2 (2010). DOI: 10.3390/polym2040664.

[123] Hinton, T. J. et al. “Three-dimensional printing of complex biological structures by freeform reversible embedding of suspended hydrogels”. In: *Sci. Adv.* vol. 1, no. 9 (2015), e1500758. DOI: 10.1126/sciadv.1500758.

[124] Drzewiecki, K. E. et al. “A thermoreversible, photocrosslinkable collagen bio-ink for free-form fabrication of scaffolds for regenerative medicine”. In: *Technology* vol. 5, no. 4 (2017), pp. 185–195. DOI: 10.1142/S2339547817500091.

[125] Osidak, E. O. et al. “Viscoll collagen solution as a novel bioink for direct 3D bioprinting”. In: *J. Mater. Sci. Mater. Med.* vol. 30, no. 3 (2019), p. 31. DOI: 10.1007/s10856-019-6233-y.

[126] Tirella, A., Liberto, T., and Ahluwalia, A. “Riboflavin and collagen: New crosslinking methods to tailor the stiffness of hydrogels”. In: *Mater. Lett.* vol. 74 (2012), pp. 58–61. DOI: 10.1016/j.matlet.2012.01.036.

[127] Rýglová, Š., Braun, M., and Suchy, T. “Collagen and Its Modifications-Crucial Aspects with Concern to Its Processing and Analysis”. In: *Macromol. Mater. Eng.* vol. 302 (2017), p. 1600460. DOI: 10.1002/mame.201600460.

[128] Chuang, C.-H. et al. “Comparison of covalently and physically cross-linked collagen hydrogels on mediating vascular network formation for engineering adipose tissue”. In: *Artif. Cells Nanomed. Biotechnol.* vol. 46, no. sup3 (2018), S434–S447. DOI: 10.1080/21691401.2018.1499660.

[129] Grier, W. K. et al. “Incorporating β-cyclodextrin into collagen scaffolds to sequester growth factors and modulate mesenchymal stem cell activity”. In: *Acta Biomater.* vol. 76 (2018), pp. 116–125. DOI: 10.1016/j.actbio.2018.06.033.

[130] Majumdar, S. et al. “Cyclodextrin Modulated Type I Collagen Self-Assembly to Engineer Biomimetic Cornea Implants”. In: *Adv. Funct. Mater.* vol. 28, no. 41 (2018), p. 1804076. DOI: 10.1002/adfm.201804076.

[131] Kurkov, S. V. and Loftsson, T. “Cyclodextrins”. In: *Int. J. Pharm.* vol. 453, no. 1 (2013), pp. 167–180. DOI: 10.1016/j.ijpharm.2012.06.055.

[132] Fernandes-Cunha, G. M. et al. “In situ-forming collagen hydrogel crosslinked via multi-functional PEG as a matrix therapy for corneal defects”. In: *Sci. Rep.* vol. 10, no. 1 (2020), p. 16671. DOI: 10.1038/s41598-020-72978-5.

[133] Rambhia, K. J. and Ma, P. X. “Controlled drug release for tissue engineering”. In: *J. Controlled Release* vol. 219 (2015), pp. 119–128. DOI: 10.1016/j.jconrel.2015.08.049.

[134] Park, J. W., Hwang, S. R., and Yoon, I.-S. “Advanced Growth Factor Delivery Systems in Wound Management and Skin Regeneration”. In: *Molecules* vol. 22, no. 8 (2017), p. 1259. DOI: 10.3390/molecules22081259.

[135] Friess, W. “Collagen–biomaterial for drug delivery”. In: *Eur. J. Pharm. Biopharm.* vol. 45, no. 2 (1998), pp. 113–36. DOI: 10.1016/s0939-6411(98)00017-4.

[136] Chen, Y. et al. “An antibacterial collagen membrane crosslinked by the inclusion complex of β-cyclodextrin dialdehyde and ofloxacin for bacterial keratitis”. In: *RSC Adv.* vol. 8, no. 32 (2018), pp. 18153–18162. DOI: 10.1039/C8RA02160K.

[137] Sahiner, M., Alpaslan, D., and Bitlisli, B. O. “Collagen-based hydrogel films as drug-delivery devices with antimicrobial properties”. In: *Polym. Bull.* vol. 71, no. 11 (2014), pp. 3017–3033. DOI: 10.1007/s00289-014-1235-x.

[138] Xeroudaki, M. et al. “A porous collagen-based hydrogel and implantation method for corneal stromal regeneration and sustained local drug delivery”. In: *Sci. Rep.* vol. 10, no. 1 (2020), p. 16936. DOI: 10.1038/s41598-020-73730-9.

[139] Tihan, G. T. et al. “Chloramphenicol collagen sponges for local drug delivery in dentistry”. In: *C. R. Chim.* vol. 18, no. 9 (2015), pp. 986–992. DOI: 10.1016/j.crci.2015.06.004.

[140] Tihan, G. T. et al. “Collagen-based biomaterials for ibuprofen delivery”. In: *C. R. Chim.* vol. 19, no. 3 (2016), pp. 390–394. DOI: 10.1016/j.crci.2015.09.008.

[141] Moore, D. “Photophysical and Photochemical Aspects of Drug Stability”. In: *Photostability of drugs and drug formulations*. Ed. by Tønnesen, H. H. CRC Press, 2004, pp. 9–40. DOI: 10.1201/9781420023596.ch2.

[142] Baptista, M. S. et al. “Type I and Type II Photosensitized Oxidation Reactions: Guidelines and Mechanistic Pathways”. In: *Photochem. Photobiol.* vol. 93, no. 4 (2017), pp. 912–919. DOI: 10.1111/php.12716.

[143] Oleinick, N. L. *Basic photosensitization*. 2011. URL: http://photobiology.info/Oleinick.html (visited on 04/02/2021).

[144] Visser, A. J. and Rolinski, O. J. *Basic photophysics*. 2014. URL: http://photobiology.info/Visser-Rolinski.html (visited on 04/02/2021).

[145] Nishiyama, N. et al. “Design and development of dendrimer photosensitizer-incorporated polymeric micelles for enhanced photodynamic therapy”. In: *Adv. Drug Delivery Rev.* vol. 61, no. 4 (2009), pp. 327–38. DOI: 10.1016/j.addr.2009.01.004.

[146] Mu, X. et al. “Photo-Crosslinked Silk Fibroin for 3D Printing”. In: *Polymers* vol. 12, no. 12 (2020), p. 2936. DOI: 10.3390/polym12122936.

[147] Hägglund, P., Mariotti, M., and Davies, M. J. “Identification and characterization of protein cross-links induced by oxidative reactions”. In: *Expert Rev. Proteomics* vol. 15, no. 8 (2018), pp. 665–681. DOI: 10.1080/14789450.2018.1509710.

[148] Yue, K. et al. “Structural analysis of photocrosslinkable methacryloyl-modified protein derivatives”. In: *Biomaterials* vol. 139 (2017), pp. 163–171. DOI: 10.1016/j.biomaterials.2017.04.050.

[149] Hapach, L. A. et al. “Manipulation of in vitro collagen matrix architecture for scaffolds of improved physiological relevance”. In: *Phys. Biol.* vol. 12, no. 6 (2015), p. 061002. DOI: 10.1088/1478-3975/12/6/061002.

[150] Heo, J. et al. “Riboflavin-induced photo-crosslinking of collagen hydrogel and its application in meniscus tissue engineering”. In: *J. Control Release* vol. 6, no. 2 (2016), pp. 148–158. DOI: 10.1007/s13346-015-0224-4.

[151] Jori, G. et al. “Photodynamic therapy in the treatment of microbial infections: basic principles and perspective applications”. In: *Lasers Surg. Med.* vol. 38, no. 5 (2006), pp. 468–81. DOI: 10.1002/lsm.20361.

[152] Hamblin, M. R. “Antimicrobial photodynamic inactivation: a bright new technique to kill resistant microbes”. In: *Curr. Opin. Microbiol.* vol. 33 (2016), pp. 67–73. DOI: 10.1016/j.mib.2016.06.008.

[153] Carrera, E. T. et al. “The application of antimicrobial photodynamic therapy (aPDT) in dentistry: a critical review”. In: *Laser Phys.* vol. 26, no. 12 (2016), p. 123001. DOI: 10.1088/1054-660X/26/12/123001.

[154] Yin, R. and R. Hamblin, M. "Antimicrobial Photosensitizers: Drug Discovery Under the Spotlight". In: *Curr. Med. Chem.* vol. 22, no. 18 (2015), pp. 2159–2185. DOI: 10.2174/0929867322666150319120134.

[155] Wegener, M. et al. "Photocontrol of Antibacterial Activity: Shifting from UV to Red Light Activation". In: *J. Am. Chem. Soc.* vol. 139, no. 49 (2017), pp. 17979–17986. DOI: 10.1021/jacs.7b09281.

[156] Tavares, A. et al. "Antimicrobial photodynamic therapy: study of bacterial recovery viability and potential development of resistance after treatment". In: *Mar. Drugs* vol. 8, no. 1 (2010), pp. 91–105. DOI: 10.3390/md8010091.

[157] Ikai, H. et al. "In vitro evaluation of the risk of inducing bacterial resistance to disinfection treatment with photolysis of hydrogen peroxide". In: *PLoS One* vol. 8, no. 11 (2013), e81316. DOI: 10.1371/journal.pone.0081316.

[158] Cieplik, F. et al. "Antimicrobial photodynamic therapy – what we know and what we don't". In: *Crit. Rev. Microbiol.* vol. 44, no. 5 (2018), pp. 571–589. DOI: 10.1080/1040841X.2018.1467876.

[159] Pérez-Laguna, V. et al. "A combination of photodynamic therapy and antimicrobial compounds to treat skin and mucosal infections: a systematic review". In: *Photochem. Photobiol. Sci.* vol. 18, no. 5 (2019), pp. 1020–1029. DOI: 10.1039/C8PP00534F.

[160] Garcez, A. et al. "Effects of antimicrobial photodynamic therapy on antibiotic-resistant Escherichia coli". In: *Photodiagn. Photodyn. Ther.* vol. 32 (2020), p. 102029. DOI: 10.1016/j.pdpdt.2020.102029.

[161] *PubChem Compound Summary for CID 493570, Riboflavin.* National Center for Biotechnology Information. Feb. 2, 2021. URL: https://pubchem.ncbi.nlm.nih.gov/compound/Riboflavin.

[162] Cardoso, D. R., Libardi, S. H., and Skibsted, L. H. "Riboflavin as a photosensitizer. Effects on human health and food quality". In: *Food Funct.* vol. 3, no. 5 (2012), pp. 487–502. DOI: 10.1039/C2FO10246C.

[163] Ruane, P. H. et al. "Photochemical inactivation of selected viruses and bacteria in platelet concentrates using riboflavin and light". In: *Transfusion* vol. 44, no. 6 (2004), pp. 877–885. DOI: 10.1111/j.1537-2995.2004.03355.x.

[164] Wollensak, G., Spoerl, E., and Seiler, T. "Riboflavin/ultraviolet-A–induced collagen crosslinking for the treatment of keratoconus". In: *Am. J. Ophthalmol.* vol. 135, no. 5 (2003), pp. 620–627. DOI: 10.1016/s0002-9394(02)02220-1.

[165] Kamaev, P. et al. "Photochemical Kinetics of Corneal Cross-Linking with Riboflavin". In: *Investig. Ophthalmol. Vis. Sci.* vol. 53, no. 4 (2012), pp. 2360–2367. DOI: 10.1167/iovs.11-9385.

[166] Sorkin, N. and Varssano, D. "Corneal Collagen Crosslinking: A Systematic Review". In: *Ophthalmologica* vol. 232, no. 1 (2014), pp. 10–27. DOI: 10.1159/000357979.

[167] Huang, R., Kim, H. J., and Min, D. B. "Photosensitizing Effect of Riboflavin, Lumiflavin, and Lumichrome on the Generation of Volatiles in Soy Milk". In: *J. Agric. Food Chem.* vol. 54, no. 6 (2006), pp. 2359–2364. DOI: 10.1021/jf052448v.

[168] Remucal, C. K. and McNeill, K. "Photosensitized Amino Acid Degradation in the Presence of Riboflavin and Its Derivatives". In: *Environ. Sci. Technol.* vol. 45, no. 12 (2011), pp. 5230–5237. DOI: 10.1021/es200411a.

[169] Bergh, V. J. V. et al. "Influence of formulation on photoinactivation of bacteria by lumichrome". In: *Pharmazie* vol. 70, no. 9 (2015), pp. 574–580. DOI: 10.1691/ph.2015.5006.

[170] Edwards, A. M. et al. "Photochemical and pharmacokinetic properties of selected flavins". In: *J. Photochem. Photobiol. B* vol. 48, no. 1 (1999), pp. 36–41. DOI: 10.1016/s1011-1344(99)00006-8.

[171] *PubChem Compound Summary for CID 5326566, Lumichrome*. National Center for Biotechnology Information. Feb. 2, 2021. URL: https://pubchem.ncbi.nlm.nih.gov/compound/Lumichrome.

[172] Hardwick, C. C. et al. "Separation, identification and quantification of riboflavin and its photoproducts in blood products using high-performance liquid chromatography with fluorescence detection: a method to support pathogen reduction technology". In: *Photochem. Photobiol.* vol. 80, no. 3 (2004), pp. 609–15. DOI: 10.1562/2004-04-14-tsn-139.

[173] Gouws, L. et al. "The plant growth promoting substance, lumichrome, mimics starch and ethylene-associated symbiotic responses in lotus and tomato roots". In: *Front. Plant Sci.* vol. 3, no. 120 (2012). DOI: 10.3389/fpls.2012.00120.

[174] Lilletvedt, M., Kristensen, S., and Tønnesen, H. H. "Lumichrome complexation by cyclodextrins: influence of pharmaceutical excipients". In: *Pharmazie* vol. 65, no. 12 (2010), pp. 871–6. DOI: 10.1691/ph.2010.0680.

[175] Sowa, P. et al. "Review paperOptical radiation in modern medicine". In: *Postepy Dermatol. Alergol.* vol. 30, no. 4 (2013), pp. 246–251. DOI: 10.5114/pdia.2013.37035.

[176] Gajdács, M. et al. "Antimicrobial Resistance in the Context of the Sustainable Development Goals: A Brief Review". In: *Eur. J. Investig. Health Psychol. Educ.* vol. 11, no. 1 (2021), pp. 71–82. DOI: 10.3390/ejihpe11010006.

[177] Khandelwal, S., Tailor, Y. K., and Kumar, M. "Deep eutectic solvents (DESs) as eco-friendly and sustainable solvent/catalyst systems in organic transformations". In: *J. Mol. Liq.* vol. 215 (2016), pp. 345–386. DOI: 10.1016/j.molliq.2015.12.015.

[178] Smith, E. L., Abbott, A. P., and Ryder, K. S. "Deep Eutectic Solvents (DESs) and Their Applications". In: *Chem. Rev.* vol. 114, no. 21 (2014), pp. 11060–11082. DOI: 10.1021/cr300162p.

[179] Choi, Y. H. et al. “Are natural deep eutectic solvents the missing link in understanding cellular metabolism and physiology?” In: *Plant Physiol.* vol. 156, no. 4 (2011), pp. 1701–1705. DOI: 10.1104/pp.111.178426.

[180] Dai, Y. et al. “Natural deep eutectic solvents as new potential media for green technology”. In: *Anal. Chim. Acta* vol. 766 (2013), pp. 61–8. DOI: 10.1016/j.aca.2012.12.019.

[181] Choi, Y. H. and Verpoorte, R. “Green solvents for the extraction of bioactive compounds from natural products using ionic liquids and deep eutectic solvents”. In: *Curr. Opin. Food Sci.* vol. 26 (2019), pp. 87–93. DOI: 10.1016/j.cofs.2019.04.003.

[182] Morrison, H. G., Sun, C. C., and Neervannan, S. “Characterization of thermal behavior of deep eutectic solvents and their potential as drug solubilization vehicles”. In: *Int. J. Pharm.* vol. 378, no. 1 (2009), pp. 136–139. DOI: 10.1016/j.ijpharm.2009.05.039.

[183] Wikene, K. O., Bruzell, E., and Tonnesen, H. H. “Characterization and antimicrobial phototoxicity of curcumin dissolved in natural deep eutectic solvents”. In: *Eur. J. Pharm. Sci.* vol. 80 (2015), pp. 26–32. DOI: 10.1016/j.ejps.2015.09.013.

[184] Wikene, K. O., Bruzell, E., and Tonnesen, H. H. “Improved antibacterial phototoxicity of a neutral porphyrin in natural deep eutectic solvents”. In: *J. Photochem. Photobiol. B* vol. 148 (2015), pp. 188–196. DOI: 10.1016/j.jphotobiol.2015.04.022.

[185] Wikene, K. O. et al. “Physicochemical characterisation and antimicrobial phototoxicity of an anionic porphyrin in natural deep eutectic solvents”. In: *Eur. J. Pharm. Biopharm.* vol. 105 (2016), pp. 75–84. DOI: 10.1016/j.ejpb.2016.06.001.

[186] Lores, H. et al. “Natural deep eutectic solvents in combination with ultrasonic energy as a green approach for solubilisation of proteins: application to gluten determination by immunoassay”. In: *Talanta* vol. 162 (2017), pp. 453–459. DOI: 10.1016/j.talanta.2016.10.078.

[187] Khodaverdian, S. et al. “Activity, stability and structure of laccase in betaine based natural deep eutectic solvents”. In: *Int. J. Biol. Macromol.* vol. 107, no. Pt B (2018), pp. 2574–2579. DOI: 10.1016/j.ijbiomac.2017.10.144.

[188] Esquembre, R. et al. “Thermal unfolding and refolding of lysozyme in deep eutectic solvents and their aqueous dilutions”. In: *Phys. Chem. Chem. Phys.* vol. 15, no. 27 (2013), pp. 11248–56. DOI: 10.1039/c3cp44299c.

[189] Liu, Y. et al. “Natural Deep Eutectic Solvents: Properties, Applications, and Perspectives”. In: *J. Nat. Prod.* vol. 81, no. 3 (2018), pp. 679–690. DOI: 10.1021/acs.jnatprod.7b00945.

[190] Dai, Y. et al. “Tailoring properties of natural deep eutectic solvents with water to facilitate their applications”. In: *Food Chem* vol. 187 (2015), pp. 14–9. DOI: 10.1016/j.foodchem.2015.03.123.

[191] Wikene, K. O. et al. “Investigation of the antimicrobial effect of natural deep eutectic solvents (NADES) as solvents in antimicrobial photodynamic therapy”. In: *J. Photochem. Photobiol. B* vol. 171 (2017), pp. 27–33. DOI: 10.1016/j.jphotobiol.2017.04.030.

[192] Radosevic, K. et al. “Antimicrobial, cytotoxic and antioxidative evaluation of natural deep eutectic solvents”. In: *Environ. Sci. Pollut. Res. Int.* vol. 25, no. 14 (2018), pp. 14188–14196. DOI: 10.1007/s11356-018-1669-z.

[193] Hayyan, M. et al. “Natural deep eutectic solvents: cytotoxic profile”. In: *SpringerPlus* vol. 5, no. 1 (2016), pp. 913–913. DOI: 10.1186/s40064-016-2575-9.

[194] Wen, Q. et al. “Assessing the toxicity and biodegradability of deep eutectic solvents”. In: *Chemosphere* vol. 132 (2015), pp. 63–69. DOI: 10.1016/j.chemosphere.2015.02.061.

[195] Schneider, C. A., Rasband, W. S., and Eliceiri, K. W. “NIH Image to ImageJ: 25 years of image analysis”. In: *Nat. Methods* vol. 9, no. 7 (2012), pp. 671–675. DOI: 10.1038/nmeth.2089.

[196] Bustin, S. A. et al. “MIQE précis: Practical implementation of minimum standard guidelines for fluorescence-based quantitative real-time PCR experiments”. In: *BMC Mol. Biol.* vol. 11, no. 1 (2010), p. 74. DOI: 10.1186/1471-2199-11-74.

[197] Williams, D. F. *The Williams dictionary of biomaterials*. Liverpool University Press, 1999.

[198] Williams, D. F. “On the mechanisms of biocompatibility”. In: *Biomaterials* vol. 29, no. 20 (2008), pp. 2941–2953. DOI: 10.1016/j.biomaterials.2008.04.023.

[199] Parenteau-Bareil, R., Gauvin, R., and Berthod, F. “Collagen-Based Biomaterials for Tissue Engineering Applications”. In: *Materials* vol. 3, no. 3 (2010). DOI: 10.3390/ma3031863.

[200] Tottoli, E. M. et al. “Skin Wound Healing Process and New Emerging Technologies for Skin Wound Care and Regeneration”. In: *Pharmaceutics* vol. 12, no. 8 (2020), p. 735. DOI: 10.3390/pharmaceutics12080735.

[201] Lumry, R. and Eyring, H. “Conformation Changes of Proteins”. In: *J. Phys. Chem.* vol. 58, no. 2 (1954), pp. 110–120. DOI: 10.1021/j150512a005.

[202] Liu, W. and Li, G. “Non-isothermal kinetic analysis of the thermal denaturation of type I collagen in solution using isoconversional and multivariate non-linear regression methods”. In: *Polym. Degrad. Stab.* vol. 95, no. 12 (2010), pp. 2233–2240. DOI: 10.1016/j.polymdegradstab.2010.09.012.

[203] Mano, F. et al. “Production of poly(vinyl alcohol) (PVA) fibers with encapsulated natural deep eutectic solvent (NADES) using electrospinning”. In: *ACS Sustain. Chem. Eng.* vol. 3, no. 10 (2015), pp. 2504–2509. DOI: 10.1021/acssuschemeng.5b00613.

[204] Mano, F. et al. “Production of Electrospun Fast-Dissolving Drug Delivery Systems with Therapeutic Eutectic Systems Encapsulated in Gelatin”. In: *AAPS PharmSciTech* vol. 18, no. 7 (2017), pp. 2579–2585. DOI: 10.1208/s12249-016-0703-z.

[205] Na, G. C. “UV spectroscopic characterization of type I collagen”. In: *Collagen Rel. Res.* vol. 8, no. 4 (1988), pp. 315–330. DOI: 10.1016/S0174-173X(88)80003-7.

[206] Sassi, M. L. et al. “Immunochemical characterization of assay for carboxyterminal telopeptide of human type I collagen: loss of antigenicity by treatment with cathepsin K”. In: *Bone* vol. 26, no. 4 (2000), pp. 367–373. DOI: 10.1016/S8756-3282(00)00235-0.

[207] Menter, J. M. “Temperature dependence of collagen fluorescence”. In: *Photochem. Photobiol. Sci.* vol. 5, no. 4 (2006), pp. 403–410. DOI: 10.1039/B516429J.

[208] Lindy, S. et al. “Hyperchromic effect of collagen induced by human collagenase”. In: *Eur. J. Biochem.* vol. 156, no. 1 (1986), pp. 1–4. DOI: 10.1111/j.1432-1033.1986.tb09539.x.

[209] Pundak, S. and Roche, R. S. “Tyrosine and tyrosinate fluorescence of bovine testes calmodulin: calcium and pH dependence”. In: *Biochemistry* vol. 23, no. 7 (1984), pp. 1549–1555. DOI: 10.1021/bi00302a032.

[210] Lucas, L. H. et al. “Probing protein structure and dynamics by second-derivative ultraviolet absorption analysis of cation-pi interactions”. In: *Protein Sci.* vol. 15, no. 10 (2006), pp. 2228–2243. DOI: 10.1110/ps.062133706.

[211] Lakowicz, J. R. *Principles of fluorescence spectroscopy*. 3rd. New York: Springer, 2006.

[212] Montero, P., Jiménez-Colmenero, F., and Borderìas, J. “Effect of pH and the presence of NaCl on some hydration properties of collagenous material from trout (Salmo irideus Gibb) muscle and skin”. In: *J. Sci. Food Agric.* vol. 54, no. 1 (1991), pp. 137–146. DOI: 10.1002/jsfa.2740540115.

[213] Usha, R. et al. “Role of polyols (erythritol, xylitol and sorbitol) on the structural stabilization of collagen”. In: *Chem. Phys. Lett.* vol. 430, no. 4 (2006), pp. 391–396. DOI: 10.1016/j.cplett.2006.09.023.

[214] Nystedt, H. L., Grønlien, K. G., and Tønnesen, H. H. “Interactions of natural deep eutectic solvents (NADES) with artificial and natural membranes”. In: *J. Mol. Liq.* vol. 328 (2021), p. 115452. DOI: 10.1016/j.molliq.2021.115452.

[215] Albini, A., Adelmann-Grill, B. C., and Müller, P. K. “Fibroblast Chemotaxis”. In: *Collagen Rel. Res.* vol. 5, no. 3 (1985), pp. 283–296. DOI: 10.1016/S0174-173X(85)80018-2.

[216] O’Brien, F. J. “Biomaterials & scaffolds for tissue engineering”. In: *Mater. Today* vol. 14, no. 3 (2011), pp. 88–95. DOI: 10.1016/S1369-7021(11)70058-X.

[217] Chen, Q., Liang, S., and Thouas, G. A. "Elastomeric biomaterials for tissue engineering". In: *Prog. Polym. Sci.* vol. 38, no. 3 (2013), pp. 584–671. DOI: 10.1016/j.progpolymsci.2012.05.003.

[218] Lee, D., Zhang, H., and Ryu, S. "Elastic Modulus Measurement of Hydrogels". In: *Cellulose-Based Superabsorbent Hydrogels*. Ed. by Mondal, M. I. H. Cham: Springer International Publishing, 2018, pp. 1–21. DOI: 10.1007/978-3-319-76573-0_60-1.

[219] Li, C. et al. "Determining elastic properties of skin by measuring surface waves from an impulse mechanical stimulus using phase-sensitive optical coherence tomography". In: *J. R. Soc. Interface* vol. 9, no. 70 (2012), pp. 831–841. DOI: 10.1098/rsif.2011.0583.

[220] Delalleau, A. et al. "Characterization of the mechanical properties of skin by inverse analysis combined with the indentation test". In: *J. Biomech.* vol. 39, no. 9 (2006), pp. 1603–1610. DOI: 10.1016/j.jbiomech.2005.05.001.

[221] Kudo, K. et al. "Structural changes of water in poly(vinyl alcohol) hydrogel during dehydration". In: *J. Chem. Phys.* vol. 140, no. 4 (2014), p. 044909. DOI: 10.1063/1.4862996.

[222] Kirchhof, S., Goepferich, A. M., and Brandl, F. P. "Hydrogels in ophthalmic applications". In: *Eur. J. Pharm. Biopharm* vol. 95 (2015), pp. 227–238. DOI: 10.1016/j.ejpb.2015.05.016.

[223] Chatterjee, S. et al. "Advances in chemistry and composition of soft materials for drug releasing contact lenses". In: *RSC Adv.* vol. 10, no. 60 (2020), pp. 36751–36777. DOI: 10.1039/D0RA06681H.

[224] Perumal, S., Antipova, O., and Orgel, J. P. R. O. "Collagen fibril architecture, domain organization, and triple-helical conformation govern its proteolysis". In: *Proc. Natl. Acad. Sci. U.S.A* vol. 105, no. 8 (2008), pp. 2824–2829. DOI: 10.1073/pnas.0710588105.

[225] Hong, H. et al. "Ultra-stiff compressed collagen for corneal perforation patch graft realized by in situ photochemical crosslinking". In: *Biofabrication* vol. 12, no. 4 (2020), p. 045030. DOI: 10.1088/1758-5090/abb52a.

[226] Knowlton, S. et al. "Photocrosslinking-based bioprinting: Examining crosslinking schemes". In: *Bioprinting* vol. 5 (2017), pp. 10–18. DOI: 10.1016/j.bprint.2017.03.001.

[227] Xu, C. et al. "Induction of fiber-like aggregation and gelation of collagen by ultraviolet irradiation at low temperature". In: *Int. J. Biol. Macromol.* vol. 153 (2020), pp. 232–239. DOI: 10.1016/j.ijbiomac.2020.03.012.

[228] Opländer, C. et al. "Effects of blue light irradiation on human dermal fibroblasts". In: *J. Photochem. Photobiol. B, Biol.* vol. 103, no. 2 (2011), pp. 118–125. DOI: 10.1016/j.jphotobiol.2011.02.018.

[229] Rodríguez Fernández, J. L. et al. "Suppression of vinculin expression by antisense transfection confers changes in cell morphology, motility, and anchorage-dependent growth of 3T3 cells". In: *J. Cell Biol.* vol. 122, no. 6 (1993), pp. 1285–94. DOI: 10.1083/jcb.122.6.1285.

[230] Acharya, P. S. et al. “Fibroblast migration is mediated by CD44-dependent TGF beta activation”. In: *J. Cell Sci.* vol. 121, no. Pt 9 (2008), pp. 1393–402. DOI: 10.1242/jcs.021683.

[231] Bellayr, I. H., Mu, X., and Li, Y. “Biochemical insights into the role of matrix metalloproteinases in regeneration: challenges and recent developments”. In: *Future Med. Chem.* vol. 1, no. 6 (2009), pp. 1095–1111. DOI: 10.4155/fmc.09.83.

[232] Dohi, T. et al. “Tissue Inhibitor of Metalloproteinase-2 Suppresses Collagen Synthesis in Cultured Keloid Fibroblasts”. In: *Plast. Reconstr. Surg.* vol. 3, no. 9 (2015), e520–e520. DOI: 10.1097/GOX.0000000000000503.

[233] Herum, K. M. et al. “Syndecan-4 signaling via NFAT regulates extracellular matrix production and cardiac myofibroblast differentiation in response to mechanical stress”. In: *J. Mol. Cell Cardiol.* vol. 54 (2013), pp. 73–81. DOI: 10.1016/j.yjmcc.2012.11.006.

[234] Leung, B. et al. “Development of thermosensitive hydrogel containing methylene blue for topical antimicrobial photodynamic therapy”. In: *J. Photochem. Photobiol. B, Biol.* vol. 203 (2020), p. 111776. DOI: 10.1016/j.jphotobiol.2020.111776.

[235] Bergh, V. J. V. “Pharmaceutical preformulation and formulation of an alloxazine and a porphyrin-type photosensitizer”. University of Oslo, Faculty of Mathematics and Natural Sciences, School of Pharmacy. Thesis. 2017.

[236] Lang, K., Mosinger, J., and Wagnerová, D. M. “Photophysical properties of porphyrinoid sensitizers non-covalently bound to host molecules; models for photodynamic therapy”. In: *Coord. Chem. Rev.* vol. 248, no. 3 (2004), pp. 321–350. DOI: 10.1016/j.ccr.2004.02.004.

[237] Slavětínská, L., Mosinger, J., and Kubát, P. “Supramolecular carriers of singlet oxygen: Photosensitized formation and thermal decomposition of endoperoxides in the presence of cyclodextrins”. In: *J. Photochem. Photobiol. A, Chem.* vol. 195, no. 1 (2008), pp. 1–9. DOI: 10.1016/j.jphotochem.2007.09.007.

[238] O’Brien, F. J. et al. “Influence of freezing rate on pore structure in freeze-dried collagen-GAG scaffolds”. In: *Biomaterials* vol. 25, no. 6 (2004), pp. 1077–1086. DOI: 10.1016/S0142-9612(03)00630-6.

[239] Murphy, C. M. and O’Brien, F. J. “Understanding the effect of mean pore size on cell activity in collagen-glycosaminoglycan scaffolds”. In: *Cell Adhes. Migr.* vol. 4, no. 3 (2010), pp. 377–381. DOI: 10.4161/cam.4.3.11747.

[240] Ashokkumar, M. et al. “Three-Dimensional Porous Sponges from Collagen Biowastes”. In: *ACS Appl. Mater. Interfaces* vol. 8, no. 23 (2016), pp. 14836–14844. DOI: 10.1021/acsami.6b04582.

[241] Santana, A. P. R. et al. “Natural deep eutectic solvents for sample preparation prior to elemental analysis by plasma-based techniques”. In: *Talanta* vol. 199 (2019), pp. 361–369. DOI: 10.1016/j.talanta.2019.02.083.

[242] Vieira, M. G. A. et al. “Natural-based plasticizers and biopolymer films: A review”. In: *Eur. Polym. J.* vol. 47, no. 3 (2011), pp. 254–263. DOI: 10.1016/j.eurpolymj.2010.12.011.

[243] Murrieta-Martínez, C. et al. “Effect of different polyalcohols as plasticizers on the functional properties of squid protein film (Dosidicus Gigas)”. In: *Coatings* vol. 9, no. 2 (2019), p. 77. DOI: 10.3390/coatings9020077.

[244] Andonegi, M., Caba, K. de la, and Guerrero, P. “Effect of citric acid on collagen sheets processed by compression”. In: *Food Hydrocoll.* vol. 100 (2020), p. 105427. DOI: 10.1016/j.foodhyd.2019.105427.

[245] Gouveia, T. I. A. et al. “A new approach to develop biodegradable films based on thermoplastic pectin”. In: *Food Hydrocoll.* vol. 97 (2019), p. 105175. DOI: 10.1016/j.foodhyd.2019.105175.

[246] Loimaranta, V. et al. “Xylitol and erythritol inhibit real-time biofilm formation of Streptococcus mutans”. In: *BMC Microbiol.* vol. 20, no. 1 (2020), p. 184. DOI: 10.1186/s12866-020-01867-8.

[247] Stegmann, P., Londo, M., and Junginger, M. “The circular bioeconomy: Its elements and role in European bioeconomy clusters”. In: *Resour. Conserv. Recycl. X* vol. 6 (2020), p. 100029. DOI: 10.1016/j.rcrx.2019.100029.

[248] Li, Y.-C. E. “Sustainable Biomass Materials for Biomedical Applications”. In: *ACS Biomater. Sci. Eng.* vol. 5, no. 5 (2019), pp. 2079–2092. DOI: 10.1021/acsbiomaterials.8b01634.

[249] Moore, J. et al. “Studies of the transmissibility of the agent of bovine spongiform encephalopathy to the domestic chicken”. In: *BMC Res. Notes* vol. 4, no. 1 (2011), p. 501. DOI: 10.1186/1756-0500-4-501.

[250] Vanda, H. et al. “Natural Deep Eutectic Solvents: From Their Discovery to Their Applications”. In: *Deep Eutectic Solvents*. 2019, pp. 61–81. DOI: 10.1002/9783527818488.ch4.

[251] Manuela, P. et al. “Biological activity and sensory evaluation of cocoa by-products NADES extracts used in food fortification”. In: *Innov. Food Sci. Emerg. Technol.* vol. 66 (2020), p. 102514. DOI: 10.1016/j.ifset.2020.102514.

[252] University of Oslo. *UiO strategy for the life sciences*. 2016. URL: https://www.uio.no/english/research/strategic-research-areas/life-science/about/strategy/ (visited on 10/03/2021).

Papers

Paper I

Collagen from Turkey (*Meleagris gallopavo*) tendon: A promising sustainable biomaterial for pharmaceutical use

Krister Gjestvang Grønlien, Mona Elisabeth Pedersen, Karen Wahlstrøm Sanden, Vibeke Høst, Jan Karlsen, Hanne Hjorth Tønnesen

Published in *Sustainable Chemistry and Pharmacy*, September 2019, volume 13, article 100166. DOI: 10.1016/j.scp.2019.100166.

Sustainable Chemistry and Pharmacy 13 (2019) 100166

Contents lists available at ScienceDirect

Sustainable Chemistry and Pharmacy

journal homepage: http://www.elsevier.com/locate/scp

Collagen from Turkey (*Meleagris gallopavo*) tendon: A promising sustainable biomaterial for pharmaceutical use

Krister Gjestvang Grønlien [a,*], Mona Elisabeth Pedersen [b], Karen Wahlstrøm Sanden [b], Vibeke Høst [b], Jan Karlsen [a,1], Hanne Hjorth Tønnesen [a]

[a] Section for Pharmaceutics and Social Pharmacy, Department of Pharmacy, University of Oslo, P.O. Box 1068 Blindern, NO-0316, Oslo, Norway
[b] Nofima AS, P.O. Box 210, NO-1431, Ås, Norway

ARTICLE INFO

Keywords:
Collagen
Rest raw material
Characterization
Drug delivery

ABSTRACT

Collagen is the major fibrillar component and protein in both human and animal connective tissue. It is applied in medical preparations, e.g. wound dressings and tissue engineering. Meat and poultry production industries result in large amounts of organic waste, rich in collagen. Our aim was to isolate and characterize pepsin soluble collagen from turkey tendon. Structural analysis indicated the presence of α-chains from both collagen type I and III, β-dimers and γ-trimers, consistent with the estimated molecular weight of 477.3 kDa. Circular dichroism spectroscopy confirmed an intact triple helix. The collagen demonstrated excellent thermal stability, with denaturation temperatures (T_{max}) at 38.5 °C and 44.5 °C and partial refolding after extensive heating. Biocompatibility was confirmed through cell viability tests. The collagen was investigated for its potential drug carrier ability. Freeze dried collagen scaffolds containing prilocaine hydrochloride and riboflavin were prepared in the presence or absence of photo-crosslinking. Photochemical crosslinking was confirmed by SEM and enhanced mechanical properties were observed. Scaffolds had a significant slower *in vitro* release of the active ingredient than a reference solution. Altogether, our study suggests collagen from turkey tendon as a promising sustainable biomaterial for pharmaceutical use.

1. Introduction

Industrial production of meat and poultry products results in large amounts of organic waste. The waste is today often utilized as biofuel and in production of pet food, but also incinerated without energy recovery (Jayathilakan et al., 2012). However, there is a huge potential in the application of rest raw materials from food production industries for new and innovative purposes. Rest raw materials are defined as remains from the food production after the edible part is utilized. The increasing production and consumption of poultry, including turkey (*Meleagris gallopavo*), results in an increasing amount of rest raw material such as skin, tendons and bones i.e., materials that are rich in the protein collagen.

Collagen is the major fibrillar component and protein in both human and animal connective tissue, constituting about 20–30% of the total body protein weight. Collagen has a characteristic triple helix structure formed by three α-chains held together by hydrogen bonds in its native form. The α-chains consist of repeating triplets of the amino acids Glycine-X-Y, where X and Y are often proline and the imino acid hydroxyproline, respectively. Nonhelical telopeptides are attached to the ends of the collagen molecule. These telopeptides are the major source of antigenicity, but can be removed by pepsin digestion to produce atelocollagen, which is considered as biocompatible and is well tolerated by the human body. Collagen is classified into different types, and at least 28 variants of collagen have been identified. The types differ in origin, structure and their ability to form fibrils (Shoulders and Raines, 2009). Collagen has several potential applications in the food, medical, pharmaceutical and cosmetic industries.

Collagen from several different species has been evaluated for application in cosmetics and pharmaceutical preparations. Collagen isolated from avian sources has several beneficial properties compared to collagen from e.g. pigs, cattle and aquatic species. Due to the lack of diseases like bovine spongiform encephalopathy (BSE), transmissible spongiform encephalopathy (TSE) and foot-and-mouth disease (FMD),

* Corresponding author.
E-mail address: k.g.gronlien@farmasi.uio.no (K.G. Grønlien).
[1] Deceased 21 March 2019.

https://doi.org/10.1016/j.scp.2019.100166
Received 8 May 2019; Received in revised form 8 August 2019; Accepted 8 August 2019
Available online 12 August 2019

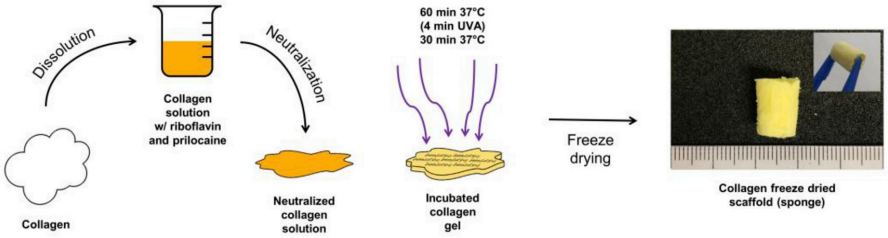

Fig. 1. Schematic showing the formation of the collagen freeze dried scaffolds (sponges).

avian sources can be regarded as safer than pigs and cattle although avian influenza (AI) can be a challenge (Li et al., 2004; Parenteau-Bareil et al., 2011; Pantin-Jackwood et al., 2017). Collagen is classified as "Generally Recognized as Safe" (GRAS) by the US Food and Drug Administration (FDA). There is an increasing interest for collagen from aquatic species as an alternative to collagen from mammal species, due to the various diseases and religious preferences. However, the use of aquatic collagen is limited by relatively poor thermal stability. With respect to cosmetic and medical applications, the collagen to be used should have a denaturation temperature above the human body temperature to avoid protein denaturation. Avian species are known to have a higher body temperature than mammal species, aquatic species and humans and thereby a higher denaturation temperature (Prinzinger et al., 1991; Varriale and Bernardi, 2006). Collagen from different fish species has shown a denaturation temperature $\leq$15.2 °C below mammal species (Sotelo et al., 2016). A previous study showed that pepsin soluble collagen type I isolated from quails' feet exhibited high thermal stability with a denaturation temperature of 38.3 °C, compared to calf skin (36.3 °C) and pig skin collagen (37.0 °C) (Yousefi et al., 2017). Collagen from chicken bone is reported to have a denaturation temperature at 44.0 °C, which was claimed to be the highest denaturation temperature for vertebrate collagen at the time of publication (Losso and Ogawa, 2014). The average body temperature of turkey is determined to 41.1 °C, which should indicate excellent thermal stability (Wilson and Woodard, 1955). Collagen from turkey has, however, not been thoroughly investigated for potential use in medicine or pharmacy.

Gels, sponges and shields are examples of medicinal and pharmaceutical products based on collagen. Collagen is used in tissue engineering as surgical suture, hemostatic agent, skin- and other tissue replacement (Chattopadhyay and Raines, 2014; Farndale, 2006). Collagen is known to have excellent wound healing properties because of its biocompatibility, biodegradability and chemotactic properties to cells involved in production of extracellular matrix (Chattopadhyay and Raines, 2014; Postlethwaite et al., 1978). Further, collagen can be used in the preparation of drug delivery devices. Examples are hydrogels and freeze-dried scaffolds (sponges). Hydrogels are composed of a crosslinked polymer network that contains a large amount of water. Drug molecules can be incorporated in the polymer network by covalent linkage, electrostatic interactions, hydrophobic association or by physical entrapment in the polymer network (Li and Mooney, 2016). Collagen is soluble in acids and is easily crosslinked by neutralization and self-assembly into fibrils at 37 °C. The mechanical properties and pore size of collagen hydrogels can be altered by a change in collagen concentration and further crosslinking by a chemical or photochemical process. Chemical crosslinkers like glutaraldehyde and epoxy compounds are often cytotoxic and not suitable for medicinal use. Photochemical crosslinkers are activated upon irradiation with the appropriate wavelength. Riboflavin (Vitamin B_2) is known to induce photochemical polymerization and interhelical crosslinking between the collagen molecules when exposed to UVA or blue light (Heo et al., 2016; Tirella et al., 2012). Riboflavin is an endogenous compound and is GRAS classified. A photochemical crosslinker can be added to the formulation at an early stage in the production. This is an advantage compared to chemical crosslinkers, which need to be added at the time of crosslinking. Collagen sponges can be formed by freeze drying of the photochemically crosslinked gels. Another approach is to stabilize and crosslink collagen with nanoparticles or make nanocomposites. This can be illustrated by the formation of novel functional biocomposites with improved surface area and porosity, like collagen sponges with iron oxide nanoparticles or iron encapsulated carbon nanoparticles for various environmental, energy and biorelated applications (Ashokkumar et al., 2016; Telay Mekonnen et al., 2019). Another example is the formation of nanocomposites with collagen and silica for wound healing (Desimone et al., 2011). Further, collagen is often used in a composite together with hydroxyapatite for bone tissue engineering (Kane et al., 2015). All of these techniques result in crosslinked materials with increased thermal properties, increased mechanical strength and improved porosity. Recently, the use of collagen alone and in polymer blends in bioinks for bioprinting and tissue engineering has gained attention. With bioprinting, the scaffold can be tailored to increase cell migration and proliferation (Rider et al., 2018).

In the present study, collagen was isolated from turkey rest raw material and characterized with respect to physicochemical properties and drug carrier ability. The biocompatibility was assessed with viability studies on human primary dermal fibroblasts treated with the isolated material. A freeze-dried scaffold (sponge) containing riboflavin as a photochemical crosslinker and prilocaine hydrochloride as a model drug was prepared (Fig. 1). The morphology was examined, and the *in vitro* release profile of the active ingredient was recorded. Our data reveal the potential for turkey tendon collagen as a promising sustainable material for drug delivery.

2. Materials and methods

All experiments were performed at 25 °C unless other stated.

2.1. Raw materials, chemicals and reagents

Rest raw material from industrially produced turkey (*Meleagris gallopavo*) was kindly provided by Norilia AS (Oslo, Norway). The raw material was stored at −20 °C until further preparation. All reagents were of analytical grade and were purchased from either Sigma-Aldrich Chemical Company (St. Louis, MO, USA) or Merck KGaA (Darmstadt, Germany). Cell medium and components were all purchased from Thermo Fischer Scientific (Waltham, MA, USA). Viability assay was purchased from Promega Corporation (Madison, WI, USA).

2.2. Preparation of pepsin-solubilized collagen from Turkey tendon

Frozen turkey tendons were thawed and manually cleaned with a scalpel to remove any remaining meat. The cleaned material was cut into smaller pieces and freeze dried for 48 h (Alpha 1–2 LD Plus Freeze Fryer, Martin Christ, Germany). Acetic acid solution (0.5 M) with pepsin (1:10) was added and the material was hydrolyzed enzymatically for

48 h at 4 °C with stirring. The mixture was then centrifuged at 4 °C and 20 000×*g* for 1 h (Avanti J-26 XP, Beckman Coulter, Brea, CA, USA). The supernatant was collected and transferred to new vials. NaCl (4 M) was added to the supernatant in a 1:3 ratio and kept on ice for 24 h to precipitate collagen. The solution was thereafter centrifuged at 20 000×*g* and 4 °C for 1 h and the sediment was further removed and replaced with 0.5 M acetic acid for re-solubilization. The mixture was dialyzed against distilled water for 3 days with change of medium every 24 h. The dialyzed solution was frozen to −40 °C and freeze dried for 96 h (Gamma 1–16 LSC Freeze dryer, Martin Christ, Germany).

2.3. Characterization of collagen

2.3.1. Total collagen quantification

The concentration of collagen was measured using the Sircol™ Soluble Collagen Assay (Biocolor Ltd., Carrickfergus, UK). Colorimetric detection of collagen was performed according to the manufacturer's protocol. In brief, 1.0 ml of the dye (Sirius Red) was added to 100 µl diluted collagen solution (approximately 10 µg collagen). The solution was agitated for 30 min followed by centrifugation at 10 000×*g* for 10 min. The dye-protein complex-pellet formed was collected and washed with 750 µl of the provided Acid-Salt Wash reagent. The pellet was once again collected and dissolved in 1.0 ml of the provided alkaline solution to release the dye. The absorbance was measured at 550 nm by an UV-VIS spectrophotometer (UV–2401PC, Shimadzu, Kyoto, Japan). Reagent blank was 0.5 M acetic acid. A calibration curve was prepared using bovine collagen type I (total amount in the samples was 5–15 µg). The assay does not discriminate between the different types of collagen.

The Sircol™ dye exclusively binds to collagen and the assay was used to assess the purity of the isolated material by comparing the amount of raw material to the total collagen quantified (Fauzi et al., 2016). Collagen isolated from turkey tendon was dissolved in 20 mM acetic acid to a concentration of 1.0 mg/ml. The collagen concentration was determined by the Sircol™ Assay to assess the purity of the isolated material and the recovery of collagen after filtration (5 µm Versapor® Membrane, Pall Corporation, MI, USA).

2.3.2. Collagen viscosity and molecular weight

Collagen isolated from turkey tendon was dissolved in 0.5 M acetic acid to a concentration of 0.5 mg/ml. The solution was diluted to concentrations between 0.1 and 0.5 mg/ml. Acetic acid (0.5 M) was used as negative control. The viscosity of the solutions was determined with an Anton Paar Rheometer (Anton Paar Physica MCR301 Rheometer, Germany). Samples of 10 ml were measured with a double gap concentric cylinder (DG26.7) at 25 °C with a shear rate of 10 s^{-1}. The intrinsic viscosity of collagen was calculated from the dynamic viscosity (Kulicke and Clasen, 2004). The average molecular weight was then estimated from the intrinsic viscosity according to the Kuhn-Mark-Houwink-Sakurada equation (Equation (1)):

$$[\eta] = KM^{\alpha} \quad (1)$$

where η is the intrinsic viscosity, M is the average molecular weight, K and α are values specific for the polymer or protein (1.86×10^{-19} and 1.8 for collagen, respectively) (Nishihara and Doty, 1958).

2.3.3. Sodium dodecyl sulphate-polyacrylamide gel electrophoresis (SDS-PAGE)

SDS-gel electrophoresis is a common method for determination of collagen polypeptide chains (Cliche et al., 2003; Rabotyagova et al., 2008). 20 µg of freeze dried collagen material was solubilized in 7 M Urea/2 M Thiourea, 2% CHAPS, 1% dithiothreitol before adding sample buffer to a final concentration of 0.05% Tris-HCl pH 6.8, 7% glycerol, 0.07 M dithiothreitol, 1% (w/v) SDS and 0.001% bromophenol blue. The samples were then pre-heated to 50 °C for 10 min and separated by SDS-PAGE by use of 4–12% Bis-Tris gels (Invitrogen, MD, USA), NuPAGE® MOPS SDS running buffer (Invitrogen, MD, USA) and Novex XCell II apparatus (Invitrogen, MD, USA). Protein bands were visualized by Coomassie Staining and molecular weight determined by use of Benchmark prestained protein ladder (Novex, Life technologies, 10 748–010) run simultaneously on the gel.

2.3.4. Circular dichroism (CD)

The molecular conformation and denaturation temperature were assessed by CD spectra using a spectropolarimeter (Jasco J-810, Easton, MD, USA). Collagen was dissolved in 20 mM acetic acid to a concentration of 0.15 mg/ml and placed into a quartz cell with a path length of 1 mm. The spectrum from 180 to 250 nm was recorded with an interval of 0.5 nm and scanning speed of 50 nm/min under nitrogen atmosphere at 20 °C. To determine the denaturation temperature, the rotatory angle at a fixed wavelength of 221 nm was recorded with heating from 20 to 60 °C at a constant heating rate of 2 °C/min. The triple helix content of native collagen was adjusted to be 100%, and the value of the denaturated collagen to be 0%. Denaturation temperature was defined as the temperature that gave the midpoint of ellipticities between 20 and 60 °C.

2.3.5. Nano differential scanning calorimetry (nano DSC)

Nano differential scanning calorimetry (nano DSC) experiments were performed using a Nano DSC 602 000 differential scanning calorimeter (TA Instruments, Lindon, UT, USA) with a capillary cell volume of 0.300 ml. DSC thermograms were recorded for 1.5 mg/ml collagen solutions in 20 mM acetic acid at a constant heating rate of 2 °C/min and 3 atm in the temperature range of 20–60 °C. Acetic acid (20 mM) was used as reference. The transition temperature of collagen was defined at the maximum of the transition peak after baseline subtraction. To assess the renaturation properties of the isolated collagen, the sample was dissolved in 20 mM acetic acid at 5 °C. The solution was heated to 55 °C, cooled to 5 °C and left in the nano DSC capillary cell for 2 weeks followed by heating to 55 °C. A sample stored at 4 °C was used as reference.

The results were processed by application of the NanoAnalyze software (TA Instruments). The partial specific heat capacity of collagen was determined from the estimated molecular weight and a partial specific volume of 0.700 ml/g (Noda, 1972). The results were fitted to a two-state trimer-to-monomer model. The deviation between the recorded data and the modulated data was $\leq$ 3%.

2.3.6. Fourier transform infrared spectroscopy (FT-IR)

FT-IR spectra were acquired with a PerkinElmer Spotlight 400 FT-IR imaging system coupled to an optical IR spotlight microscope (PerkinElmer, Shelton, CO, USA). The sample (collagen) was placed on a ZnSe substrate and put under the microscope. The area selected for measurement was a thin part of the sample, approximately 5–10 µm thick. Single element absorbance spectra were recorded in the range from 4000 to 750 cm^{-1} using a mercury cadmium telluride (MCT) detector, and with a spectral resolution of 4 cm^{-1}. For each pixel, 32 scans were obtained. The microscope was sealed with a custom-made box, and both microscope and spectrometer were purged with dry air to reduce the spectral contribution from water vapor and CO_2. A background spectrum/image of the ZnSe substrate was recorded before each sample measurement. The spectra were preprocessed by extended multiplicative signal corrections (EMSC) in The Unscrambler version 9.2 (Camo Process AS, Oslo, Norway) to remove multiplicative and wavenumber-independent and dependent baselines (Afseth and Kohler, 2012).

2.3.7. Cell culture

Human primary dermal fibroblasts (ATCC, Manassas, VA, USA) were cultured in Dulbecco's modified Eagle's medium (DMEM) supplemented with 10% fetal bovine serum (FBS), 100 U/ml penicillin, 100 µg/ml streptomycin and 250 µg/ml fungizone in tissue culture flasks. The cells were maintained at 37 °C in a humidified atmosphere of 5% CO_2. The cells were routinely sub-cultivated twice a week. The cells were

examined by a Leica DM IL LED light microscope (Leica Microsystems Nussloch GmbH, Nuβloch, Germany) during incubation. Cells between passages 3–10 were used in these experiments.

2.3.8. Cell viability

Evaluation of biocompatibility (viability) of collagen from turkey tendon was conducted for 48 h on proliferating cells. Fibroblasts were plated onto 96-well white opaque microtiter plates at a concentration of 3000 cells/well in medium with 2% FBS and incubated for approximately 24 h. The medium was then replaced with fresh medium. Collagen from turkey tendon was added to the wells in a concentration of 0.5, 1.0, 2.0 and 3.0 mg/ml and further incubated for 48 h. The samples were handled aseptic between isolation and the viability test. To mimic use under relevant biological conditions, the collagen was not dissolved before addition to the wells. Cell viability was measured with the Cell Titer-Glo Luminescent Cell Viability Assay (Promega, Madison, WI, USA) according to the manufacturer's protocol. The luminescence intensity was detected using a Synergy H1 Hybrid Multi-Mode Microplate Reader (Biotek, Bad Friedrichshall, Germany).

2.4. Preparation of drug loaded freeze dried scaffolds (sponges) of collagen from Turkey

Drug loaded freeze dried scaffolds of collagen i.e., collagen sponges, were prepared by a two-step gelation and crosslinking method. Prilocaine hydrochloride (PCL) was selected as a model drug ($M_w = 256.77$ g/mol). Collagen from turkey tendon was dissolved in 20 mM acetic acid over 24 h to a concentration of 5 mg/ml and filtered (5 μm Versapor® Membrane, Pall Corporation, MI, USA). PCL was mixed with the collagen solution to a final concentration of 5 mg/ml. The collagen-PCL solution was neutralized with 10X phosphate buffered saline (PBS) (0.1 × final volume) and 1 M NaOH (0.023 × volume of collagen solution) and diluted with Milli-Q water to a final concentration of 1X PBS and 2.5 mg/ml collagen. Riboflavin 5′-monophosphate sodium salt was added as a crosslinking agent to a final concentration of 0.01% (w/v) (Heo et al., 2016). The solution was incubated in the dark at 37 °C for 60 min to form intrahelical crosslinks and initiate gelling of the collagen. The collagen gels were irradiated with UVA ($\lambda_{max} = 365$ nm, 2.94 mW/cm^2) (Polylux-PT, Dreve, Germany), for 4 min to form interhelical crosslinks (i.e., a photochemically crosslinked gel). The crosslinking procedure was then completed by incubating the gels in the dark at 37 °C for 30 min. The non-irradiated gels were produced by mixing PCL with the collagen solution, addition of riboflavin, neutralization of the solution and incubation in the dark at 37 °C for 90 min.

All the gels were freeze dried in order to form sponges. The gels were frozen at −80 °C for 1 h prior to freeze drying at 0.0019 mbar for 20 h, including 1 h final drying at 0.0010 mbar (Alpha 2–4 LD Plus Freeze Fryer, Martin Christ, Germany).

2.5. Characterization of the drug loaded freeze dried scaffolds (sponges)

2.5.1. In vitro release study of prilocaine hydrochloride from collagen sponges

Irradiated and non-irradiated collagen sponges were tested for *in vitro* release of the active ingredient (PCL). The study was performed using Franz diffusion cells (PermeGear, Hellertown, PA, USA). The diffusion area of the cell was 1.00 cm^2 and the receptor compartment had a capacity of 7.8 ml. Sink conditions were maintained.

Nylon membrane filters (0.45 μm Whatman™ Nylon membrane filters, GE Healthcare UK Ltd., Buckinghamshire, UK) were saturated with receptor medium (PBS) for 1 h prior to the experiment. The cells were filled with receptor medium and the membrane was mounted between the donor and the receptor compartment. The sponge was transferred from the container in which it was freeze dried to the donor chamber, and the container was rinsed with 1 ml Milli-Q water which was transferred to the donor chamber of the Franz cell. PCL was dissolved in PBS to a concentration of 5 mg/ml and 1 ml was added to the donor chamber of the Franz cell to serve as a positive control (a solution of the drug). The receptor medium was continuously stirred at 500 rpm. The receptor medium was kept at 32 ± 1 °C. Samples of 100 μl were withdrawn after 0.25, 0.33, 0.42, 0.5, 0.75, 1.0, 1.5, 2.0, 2.5, 3.0, 3.5, 4.0, 5.0, 6.0 and 24 h and diluted 1:1 with the HPLC mobile phase to a total volume of 200 μl. Fresh receptor medium was added to the receptor chamber to replace the sample volume withdrawn.

PLC was quantified by reversed-phase HPLC. The analysis was conducted with isocratic elution with a mobile phase consisting of 0.1 M acetate buffer pH 3.8 and methanol (60:40). A C_{18} column (Nova-pak®, Waters Corporation, Milford, MA, USA) was used with a column temperature of 30 °C. The retention time of PCL at 1 ml/min flow was approximately 2.8 min under the given experimental conditions. All quantitative experiments were performed in triplicate unless otherwise stated.

2.5.2. Environmental scanning electron microscopy (ESEM)

ESEM imaging of freeze dried collagen isolated from turkey tendon and sponges prepared from the isolated collagen was performed using an Environmental Scanning Electron Microscope (Zeiss EVO-50-EP, Carl Zeiss SMT Ltd, Coldhams Lane, Cambridge, UK). The samples were mounted on an aluminum stub using double-sided tape coated with carbon and coated with gold/palladium using a Sputter Coater (SC7640 Sputter Coater, Quorium Technologies).

2.5.3. Mechanical properties

Mechanical properties of the derived sponges were studied using a TA-XT2i Texture Analyser (Stable Micro Systems, Haslemere, UK) in compression mode. The sponges were exposed to constant pressure at 0.1 mm/s to 10, 30 and 50% strain. The stress (kPa) was calculated by the force and load bearing area (A) of the sponges (r = 4 mm, A = 50.24 mm^2) and plotted against the strain.

2.5.4. Thermogravimetric analysis (TGA)

Thermogravimetric analysis (TGA) were performed on the derived sponges using a TG 209F1 Libra (Netzsch-Gerätebau GmbH, Selb, Germany) under nitrogen purge (50 ml/min). TGA thermograms were recorded for samples between 5 and 10 mg at a constant heating rate of 10 °C/min in the temperature range 25–800 °C. The transition temperatures were defined as the onset temperature of the transition.

2.5.5. Differential scanning calorimetry (DSC)

Differential scanning calorimetry (DSC) experiments were performed on the derived sponges using a DSC822^e Differential Scanning Calorimeter (Mettler Toledo Intl. Inc., Greifensee, Switzerland) under dry nitrogen purge (80 ml/min). DSC thermograms were recorded for samples between 0.5 and 2 mg at a constant heating rate of 10 °C/min in the temperature range 25–400 °C. The samples were placed in aluminum sample pans with a pierced lid. An empty pan was used as reference. The transition temperature of collagen in the sponges was defined at the minimum of the transition peak when integrated.

2.6. Statistical analysis

The data was presented as mean ± highest deviation from three independent experiments. Statistical analyses were performed using Students t-test ($p < 0.05$).

3. Results and discussion

3.1. Characterization of collagen

3.1.1. Total collagen quantification and estimated molecular weight

Collagen was isolated with pepsin in weak acetic acid. Pepsin is

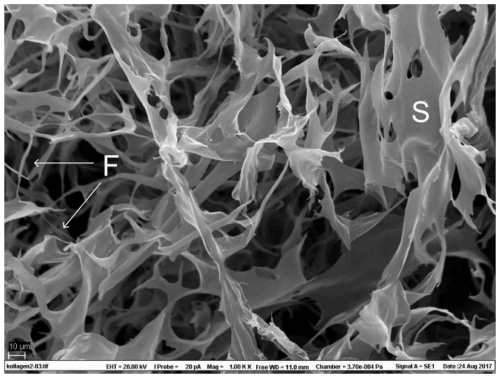

Fig. 2. ESEM image of freeze dried collagen extracted from turkey tendon at 1000X magnification (scale bar = 10 μm). Examples on collagen sheets and fibers are marked S and F, respectively.

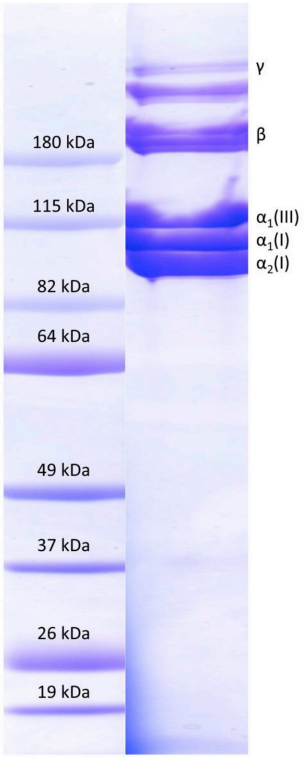

Fig. 3. SDS-PAGE of collagen from turkey tendon stained with Comassie Brilliant Blue. α, β and γ represent monomeric, dimeric and trimeric forms of the collagen molecules, respectively. Molecular weight standard (Benchmark prestained protein ladder) is shown to the left.

known to increase the yield of acid soluble crosslinked collagen and further to cleave the nonhelical telopeptide moieties of collagen, which leads to a product with good biocompatibility (Delgado et al., 2017). The purity of collagen was determined to 103.1 ± 3.1%, which indicated

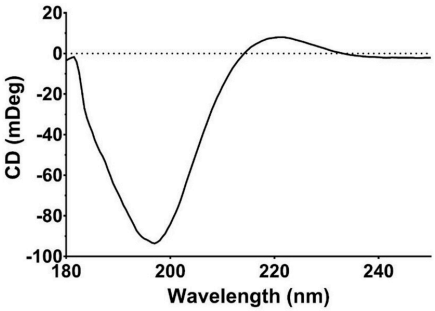

Fig. 4. CD spectrum of collagen from turkey tendon; 0.15 mg/ml in 20 mM acetic acid at 20 °C (50 nm/min). Rotary maximum = 221.5 nm, rotary minimum = 197 nm, crossover point = 214 nm.

that the isolated material solely consisted of collagen. The recovery of collagen was 95.7 ± 6.1% after filtration.

The intrinsic viscosity was found to be 19.76 dl/g. The average molecular weight was estimated to be 477.3 kDa. A standard collagen molecule is typically 300 kDa where each of the alpha strands are approximately 100 kDa (Shoulders and Raines, 2009). A higher molecular weight indicates the presence of interhelical crosslinks between the collagen molecules and formation of di- and trimers (Silver and Garg, 1997). The ESEM images of freeze dried pure collagen demonstrated the presence of both collagen sheets and fibers and confirmed the presence of interhelical crosslinks (Fig. 2).

3.1.2. SDS-PAGE pattern and CD spectroscopy of isolated collagen

The SDS-PAGE pattern indicated the presence of α-chains from both collagen type I and III (Rabotyagova et al., 2008; Han et al., 2018; Shikh Alsook et al., 2015) (Fig. 3). Different bands of high molecular weights around 115 kDa and above 180 kDa were detected. Previous SDS-gel electrophoresis studies of native collagen type I from tendon have revealed migration of reduced collagen type I into monomeric α1-and α2-chains in lower ranges approximately around 110 and 120, and β-band and γ-band above 240 kDa (Han et al., 2018; Rabotyagova et al., 2008; Shikh Alsook et al., 2015). Both types of collagen have previously been identified in tendons (Zhang et al., 2005).

The presence of β-dimers indicated intrahelical crosslinks between the collagen α-chains. The presence of γ-trimers indicated intrahelical crosslinking between the three collagen α-chains or intermolecular crosslinking between collagen molecules (Lewis and Piez, 1964). This is consistent with the high molecular weight as discussed above. ESEM analysis revealed fibrillary and sheet-like structures of freeze dried pure collagen supporting intermolecular crosslinks.

The CD spectrum of collagen showed a negative peak between 180 and 214 nm. The rotatory maximum was found at 221.5 nm, a minimum at 197 nm and a crossover point at 214 nm, which is characteristic for a triple helical conformation (Wang et al., 2014; Losso and Ogawa, 2014) (Fig. 4). This further emphasized the intact structure of isolated collagen.

3.1.3. Thermal properties of isolated collagen

The thermal denaturation of turkey collagen occurred in two steps with a minor transition (T_s) at 38.3 °C and a major transition (T_m) at 44.5 °C under the current experimental conditions (Fig. 5). The minor transition has previously been reported to be caused by collagen fibril depolymerization and melting of small parts of the triple helix structure, while the major transition was reported to be caused by denaturation of the triple helix to form monocoils (Liu et al., 2013). The transition at 44.5 °C was just above the turkey body temperature of 41.1 °C and is together with collagen from chicken keel bone among the highest

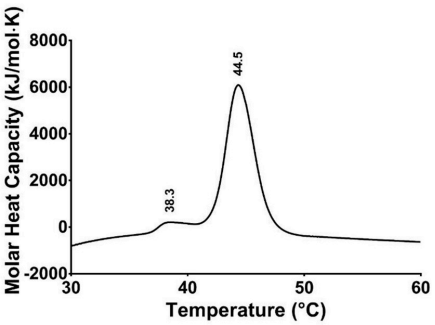

Fig. 5. Nano DSC thermogram of collagen from turkey tendon; 1.5 mg/ml in 20 mM acetic acid at heating rate 2 °C/min (baseline not subtracted).

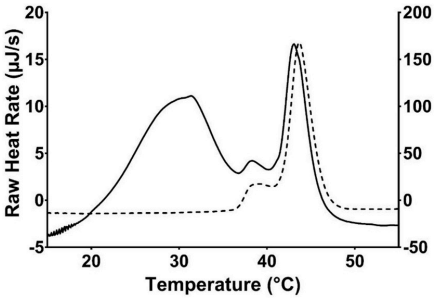

Fig. 6. Renaturation properties of collagen from turkey tendon (baseline subtracted). Left axis; partially renaturated collagen (solid line), right axis; collagen sample stored at 4 °C for the same time period (dashed line).

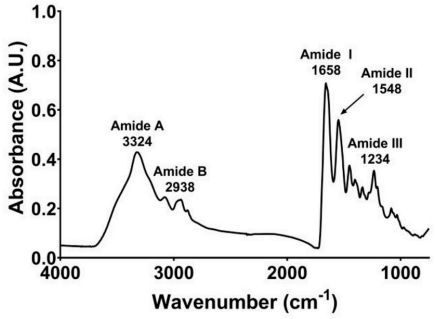

Fig. 7. FTIR spectrum of collagen from turkey tendon.

reported denaturation temperatures for collagen (Losso and Ogawa, 2014). A high denaturation temperature can be attributed to the imino acid content (hydroxyproline and hydroxylysine) of collagen (Persikov et al., 2005). However, the amino acid content was not investigated in detail in the present study. An extensive crosslinking of the collagen molecule can also contribute to a high denaturation temperature (Wright and Humphrey, 2002).

Two thermal transitions with T_s between 36.1 and 38.4 °C and T_m between 41.4 and 44.1 °C were observed in all samples (Fig. S1 A and B). The transition temperature for both transitions was dependent on the heating rate and shifted to a higher temperature when the heating rate increased. The transition temperature was a linear function of the logarithm of the heating rate (Figure S1 C). This indicated that the native protein was not in equilibrium with the unfolded protein, even at low heating rates (0.015 °C/min) and the unfolding was kinetically controlled (Liu et al., 2013). It is considered that such slow kinetics can be caused by a large activation energy or the many steps and complexity of the collagen unfolding (Leikina et al., 2002).

The helicity curve of collagen (Fig. S2) showed a biphasic transition, which is consistent with the two transitions from the nano DSC experiments (Fig. 5). The helicity went from 100% to 0% during the temperature interval 37–47 °C, which matched the onset temperature of the minor transition and offset temperature of the major transition, respectively, in the nano DSC experiments and confirmed the high denaturation temperature.

Collagen melting and denaturation has been described both as an irreversible rate-limited process with first-order reaction kinetics and Arrhenius dependency, and as a reversible process with an apparent irreversibility due to extremely slow equilibrium kinetics (Leikina et al., 2002). Lumry and Eyring (1954) proposed a three-state model for the thermal denaturation of proteins, involving a thermodynamic step and a kinetically controlled step (Equation (2)):

$$N \leftrightarrow U \rightarrow D \quad (2)$$

where N is the protein in its native form, U is the unfolded triple helix form and D is the denaturated form of the protein (Lumry and Eyring, 1954). This model has been evaluated to be the best model for the thermal denaturation of collagen (Liu and Li, 2010). The minor transition observed in the thermogram of collagen can thereby be assigned to the reversible step, while the major transition can be assigned the irreversible denaturation step in the Lumry-Eyring model (Liu et al., 2013).

According to Leikina et al., (2002) the peak transition temperature below 44.5 °C, i.e., T_m of collagen, is related to formation of gelatin fragments. Partial refolding of collagen with formation of gelatin fragments was demonstrated by a renaturation study (Fig. 6). The refolding capability was apparently maintained even when the sample was heated to 55 °C. Irreversible refolding of collagen has been reported when the molecule is heated above 55 °C (Liu et al., 2013). Temperatures above this value could be avoided in a pharmaceutical context unless heating is the only option for sterilization (Wright and Humphrey, 2002).

3.1.4. FT-IR analysis

The FT-IR spectrum of the isolated collagen included the bands of amide A (3324 cm^{-1}), amide B (2938 cm^{-1}), amide I (1658 cm^{-1}), amide II (1548 cm^{-1}) and amide III (1234 cm^{-1}) (Fig. 7).

The amide A band of collagen has been associated with the NH-stretching frequency and is usually found at 3325-3330 cm^{-1}. The position is shifted towards a lower frequency, around 3300 cm^{-1}, if the NH group of a protein or peptide is involved in a hydrogen bond (Doyle et al., 1975). However, NH-stretching occuring in the range 3400–3440 cm^{-1} indicates a free NH group (Wang et al., 2014). Collagen from turkey tendon was found to have an amide A band at 3324 cm^{-1}, which was an indication of hydrogen bonding (Doyle et al., 1975). The amide B band position of collagen from turkey tendon was observed at 2938 cm^{-1}. This band could be related to the asymmetrical stretch of CH_2 (Fauzi et al., 2016).

The amide I, II and III bands are related to the secondary polypeptide conformation of proteins. The amide I band of collagen has previously been reported at 1650-1688 cm^{-1} (Doyle et al., 1975). In the present study the amide I band was identified at 1658 cm^{-1}, which indicated the existence of non-equivalent C=O bonds. The band was asymmetrical, which is typical for collagens (Terzi et al., 2018). The amide II band of collagen is usually found at 1530-1540 cm^{-1}, however, if the material is partially hydrated, the band moves to higher frequencies around 1550 cm^{-1} (Doyle et al., 1975). The present collagen was found to have an amide II band at 1548 cm^{-1}, which further indicated a partially hydrated material. The amide II band is associated with N–H bend coupled

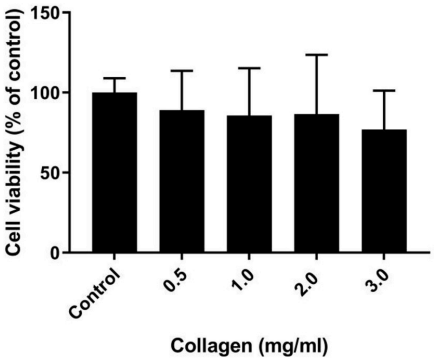

Fig. 8. Viability (i.e. the amount of ATP present) of human primary dermal fibroblasts treated with different collagen concentrations and without (control). The data is presented as the mean of three independent cell culture experiments seeded out in triplicates.

with C–N stretching. The amide III band of collagen is associated with N–H bend coupled with C–N stretch and indicates the presence of a helical structure. The amide III bands in our samples were identified around 1234 cm^{-1} and confirmed the native structure of the collagen triple helix (Terzi et al., 2018; Gąsior-Głogowska et al., 2010).

3.1.5. In vitro biocompatibility assessment of isolated collagen

The addition of collagen to primary human fibroblasts did not significantly affect the cell viability (i.e., the amount of ATP present) after 48 h at any of the concentrations of the isolated collagen compared to the control (Fig. 8). However, the viability showed a slight decrease with increasing collagen concentration. Collagen is supposed to be biocompatible and non-toxic to cells. The variance in the results can therefore be attributed to the increasing bulk volume of collagen in the well and/or a quenching of the luminescence from the luciferase in the viability assay. The results demonstrated good *in vitro* biocompatibility of the isolated collagen at concentrations relevant for production of freeze dried scaffolds.

3.2. Characterization of collagen freeze dried scaffolds (sponges)

3.2.1. Mechanical properties

Freeze dried scaffolds prepared in the presence or absence of photo-crosslinking resulted in sponges with different mechanical properties. The mechanical property studies of the sponges showed a clear difference between the stress at 10, 30 and 50% strain of the irradiated and non-irradiated sponges, respectively. The irradiated sponges had a stress varying between 1.35 ± 0.72 kPa at 10% strain, 2.08 ± 0.58 kPa at 30% strain and 3.74 ± 0.94 kPa at 50% strain. The non-irradiated sponges had a stress varying between 0.22 ± 0.03 kPa at 10% strain, 0.77 ± 0.17 kPa at 30% strain and 1.79 ± 0.20 kPa at 50% strain (Fig. 9 A and B). The variance within the irradiated samples can be attributed to an inhomogeneous photochemical crosslinking throughout the sample, due to a filter effect. This can in the future be addressed by making thinner sponges with a larger irradiation surface area. The flattening of the curve, especially for the irradiated sponges at strain $\geq$ 30%, can be attributed to the bending of the sponge, rather than direct compression. This happened to all the irradiated sponge samples at $>$ 30% strain. Upon dispersion in aqueous solution, the irradiated sponges retained their structure, while the non-irradiated sponges disintegrated.

3.2.2. Thermal stability of collagen sponges

Thermal stability studies of the two different sponges by TGA showed a significant weight loss with onset at approximately 173 °C and a small weight loss with onset at approximately 285 °C. The major weight loss was ascribed to PCL, while the small weight loss was ascribed to the decomposition of collagen (Fig. S3) (Schmidt et al., 2004; Ashokkumar et al., 2016). The results showed no differences in the thermal stability between the samples. However, the DSC results revealed differences with the irradiated sponges exhibiting a transition at 63.5 ± 2.5 °C compared to the non-irradiated sponges with a very weak transition at 57.1 ± 1.9 °C (Fig. S4). The transition corresponds to a shrinkage and the loss of the triple helical structure of collagen (Ashokkumar et al., 2016; Pietrucha, 2005). The transition around 40 °C was ascribed to PCL.

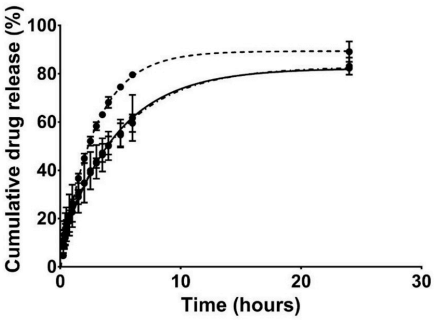

Fig. 10. *In vitro* release curves of prilocaine hydrochloride from irradiated collagen sponges (solid line), non-irradiated collagen sponges (dash-dotted line) and a solution of the drug (dashed line). The first two curves are superimposed.

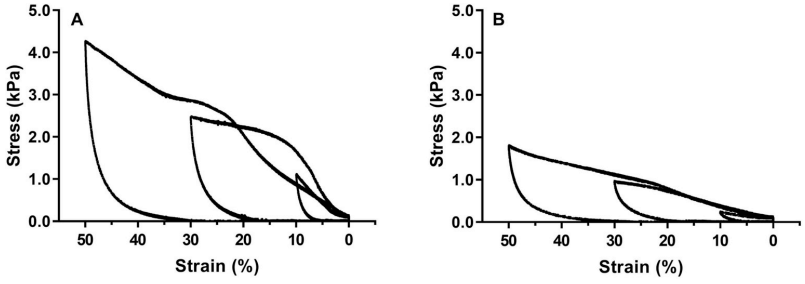

Fig. 9. Representative figures of compressive stress-strain curves of collagen sponges at 10, 30 and 50% strain. A: irradiated collagen sponges, B: non-irradiated collagen sponges.

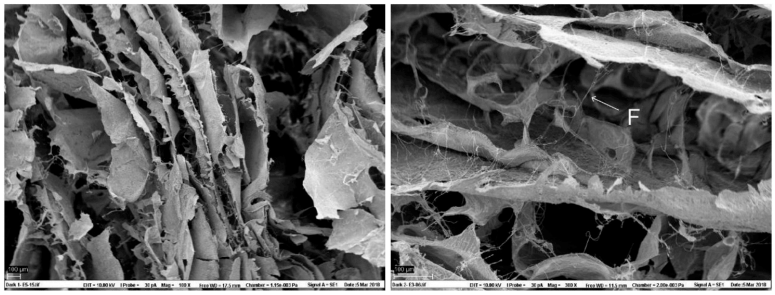

Fig. 11. Cross section of non-irradiated collagen sponges at 100X (left) and 300X (right) magnification (scale bars = 100 μm). The images show collapsed pore structures and few fibrils (F) to stabilize the pores.

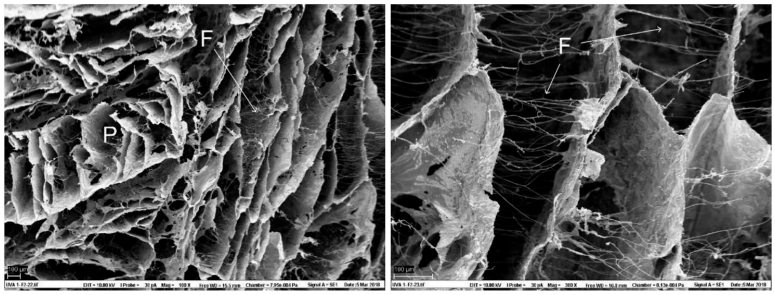

Fig. 12. Cross section of irradiated collagen sponges at 100X (left) and 300X (right) magnification (scale bars = 100 μm). The images show formation of more and smaller pores (P) compared to the non-irradiated sponges. The right image shows formation of fibrils (F) stabilizing the pores.

3.2.3. In vitro release study of prilocaine hydrochloride from collagen sponges

There was a significant slower release of PCL from the sponges compared to the membrane passage of a solution of the drug (Fig. 10). The difference between irradiated and non-irradiated sponges was however, not significant. The sustained release of the model drug from the sponge can be explained by diffusion through the hydrogel that was formed upon hydration of the sponge (Li and Mooney, 2016; Tihan et al., 2016). The slower release achieved from the sponges can be beneficial for applications where a prolonged effect of the active ingredient is requested, like a pain-relieving agent or a local anesthetic like our model drug. For other types of drugs, e.g. a photosensitizer for localized antimicrobial photodynamic therapy, a fast release will be desired. PCL is water soluble and can easily be quantified with a chromatographic method. PCL and riboflavin have no overlap in their respective absorption spectra. PCL was regarded as stable under the applied polymerization conditions, i.e., the degradation was ≤6%, and the substance served as a relevant and convenient model drug in the current experiments.

3.2.4. Morphology of collagen sponges

The ESEM images and structure of the sponge indicated that the degree of crosslinking was higher for the irradiated sponges than the non-irradiated sponges due to the photopolymerization of collagen fibrils in the presence of riboflavin (Figs. 11 and 12). The irradiated material showed a more rigid structure. The pores formed by crosslinking were probably too large to retain and control the release of the selected model drug which is a small molecule with $M_w = 256.8$ g/mol. During freeze drying, ice grows into large crystals, segregating the solute and compress it into thin sheets. Once the ice sublimate, empty spaces (i.e., pores) are formed. The pore size and mechanical properties of the collagen sponges could be altered by increasing the collagen concentration and/or change the polymerization conditions (Tirella et al., 2012). This was, however, not performed in the current study, but will be investigated as the next step. The pore size and scaffold architecture will directly affect the mechanical stability of the scaffold and behavior of cells migrating into the device. Cell migration is dependent on that the specific surface area of the scaffold is large enough for cells to attach, e.g. a high number of pores per unit area. However, the pores must be large enough to facilitate cell migration and cell nutrition exchange. The pore size estimated from the ESEM images of irradiated sponges was within the optimal pore size reported in the literature for cell attachment and proliferation (approximately 250–500 μm) (Murphy and O'Brien, 2010; Loh and Choong, 2013; Davidenko et al., 2015). It might therefore be difficult to achieve a pore size small enough to obtain controlled release of low-molecular weight probes (≈ 500 g/mol), but sponges for controlled release of larger molecules, polymeric compounds, peptides and proteins could be achieved by an optimization of the production method.

4. Conclusions

Collagen of high purity was isolated from turkey tendons by application of acetic acid and pepsin. The collagen was identified as type I and III. CD and FT-IR studies confirmed that the native triple helix structure was preserved after isolation. The collagen demonstrated high thermal stability, among the highest reported for vertebras, and good biocompatibility. An *in vitro* release test showed promising results for the application of freeze dried collagen scaffolds as a drug delivery system. There was a significant difference between the release rate of the model drug from the sponges and from a solution. Photochemical polymerization of the sponges increased the mechanical properties and made the product easier to handle. The properties of the isolated material and of the preliminary formulations make this collagen a

promising candidate as excipient in pharmaceutical as well as cosmetic products.

Acknowledgments

The authors are grateful to Bente Amalie Breiby, Tove Larsen and Julia Fredrika Alopaeus, Department of Pharmacy, University of Oslo, Per Eugen Kristiansen, Department of Biosciences, University of Oslo, Ingrid Marie Bergh Bakke, Department of Chemistry, University of Oslo and Ragnhild Stenberg Berg, Nofima AS for technical support. Turkey tendon by-products and financial support for isolation of collagen from turkey were contributed by Norilia AS. The ESEM instrument was borrowed from the Imaging Centre of the Norwegian University of Life Sciences.

Appendix A. Supplementary data

Supplementary data to this article can be found online at https://doi.org/10.1016/j.scp.2019.100166.

Conflicts of interest

The authors declare that they have no conflict of interest.

Funding

This work was supported by Norilia AS (Oslo, Norway).

Disclosure statement

Conceptualization: K. G. Grønlien, M. E. Pedersen, J. Karlsen, H. H. Tønnesen.

Funding acquisition: J. Karlsen.

Investigation: K. G. Grønlien, K. W. Sanden, V. Høst.

Supervision: M. E. Pedersen, J. Karlsen, H. H. Tønnesen.

Visualization: K. G. Grønlien, V. Høst.

Writing: K. G. Grønlien, M. E. Pedersen, K. W. Sanden, V. Høst, J. Karlsen, H. H. Tønnesen.

Norilia AS provided the turkey tendon by-products and funded the isolation of collagen and kits for analysis of collagen, but was not involved in the study design, interpretation of the data, writing of the manuscript, or decision to publish.

References

Afseth, N.K., Kohler, A., 2012. Extended multiplicative signal correction in vibrational spectroscopy, a tutorial. Chemometr. Intell. Lab. 117, 92–99.
Ashokkumar, M., Cristian Chipara, A., Tharangattu Narayanan, N., Anumary, A., Sruthi, R., Thanikaivelan, P., Vajtai, R., Mani, S.A., Ajayan, P.M., 2016. Three-dimensional porous sponges from collagen biowastes. ACS Appl. Mater. Interfaces 8, 14836–14844.
Chattopadhyay, S., Raines, R.T., 2014. Collagen-based biomaterials for wound healing. Biopolymers 101, 821–833.
Cliche, S., Amiot, J., Avezard, C., Gariepy, C., 2003. Extraction and characterization of collagen with or without telopeptides from chicken skin. Poult. Sci. 82, 503–509.
Davidenko, N., Schuster, C.F., Bax, D.V., Raynal, N., Farndale, R.W., Best, S.M., Cameron, R.E., 2015. Control of crosslinking for tailoring collagen-based scaffolds stability and mechanics. Acta Biomater. 25, 131–142.
Delgado, L.M., Shologu, N., Fuller, K., Zeugolis, D.I., 2017. Acetic acid and pepsin result in high yield, high purity and low macrophage response collagen for biomedical applications. Biomed. Mater. 12, 065009.
Desimone, M.F., Hélary, C., Quignard, S., Rietveld, I.B., Bataille, I., Copello, G.J., Mosser, G., Giraud-Guille, M.-M., Livage, J., Meddahi-Pellé, A., Coradin, T., 2011. In vitro studies and preliminary in vivo evaluation of silicified concentrated collagen hydrogels. ACS Appl. Mater. Interfaces 3, 3831–3838.
Doyle, B.B., Bendit, E.G., Blout, E.R., 1975. Infrared spectroscopy of collagen and collagen-like polypeptides. Biopolymers 14, 937–957.
Farndale, R.W., 2006. Collagen-induced platelet activation. Blood Cells Mol. Dis. 36, 162–165.
Fauzi, M.B., Lokanathan, Y., Aminuddin, B.S., Ruszymah, B.H.I., Chowdhury, S.R., 2016. Ovine tendon collagen: extraction, characterisation and fabrication of thin films for tissue engineering applications. Mater. Sci. Eng. C 68, 163–171.
Gąsior-Głogowska, M., Komorowska, M., Hanuza, J., Ptak, M., Kobielarz, M., 2010. Structural alteration of collagen fibres - spectroscopic and mechanical studies. Acta Bioeng. Biomech. 12, 55–62.
Han, L., Zhang, Z.W., Wang, B.H., Wen, Z.K., 2018. Construction and biocompatibility of a thin type I/II collagen composite scaffold. Cell Tissue Bank. 19, 47–59.
Heo, J., Koh, R., Shim, W., Kim, H., Yim, H.-G., Hwang, N., 2016. Riboflavin-induced photo-crosslinking of collagen hydrogel and its application in meniscus tissue engineering. J. Control. Release 6, 148–158.
Jayathilakan, K., Sultana, K., Radhakrishna, K., Bawa, A.S., 2012. Utilization of byproducts and waste materials from meat, poultry and fish processing industries: a review. J. Food Sci. Technol. 49, 278–293.
Kane, R.J., Weiss-Bilka, H.E., Meagher, M.J., Liu, Y., Gargac, J.A., Niebur, G.L., Wagner, D.R., Roeder, R.K., 2015. Hydroxyapatite reinforced collagen scaffolds with improved architecture and mechanical properties. Acta Biomater. 17, 16–25.
Kulicke, W.-M., Clasen, C., 2004. Viscosimetry of Polymers and Polyelectrolytes. Springer, Berlin.
Leikina, E., Mertts, M.V., Kuznetsova, N., Leikin, S., 2002. Type I collagen is thermally unstable at body temperature. Proc. Natl. Acad. Sci. U.S.A. 99, 1314–1318.
Lewis, M.S., Piez, K.A., 1964. Sedimentation-equilibrium studies of the molecular weight of single and double chains from rat-skin collagen. Biochemistry 3, 1126–1131.
Li, H., Liu, B.L., Gao, L.Z., Chen, H.L., 2004. Studies on bullfrog skin collagen. Food Chem. 84, 65–69.
Li, J., Mooney, D.J., 2016. Designing hydrogels for controlled drug delivery. Nat. Rev. Mater. 1, 16071.
Liu, W., Li, G., 2010. Non-isothermal kinetic analysis of the thermal denaturation of type I collagen in solution using isoconversional and multivariate non-linear regression methods. Polym. Degrad. Stab. 95, 2233–2240.
Liu, Y., Liu, L., Chen, M., Zhang, Q., 2013. Double thermal transitions of type I collagen in acidic solution. J. Biomol. Struct. Dyn. 31, 862–873.
Loh, Q.L., Choong, C., 2013. Three-dimensional scaffolds for tissue engineering applications: role of porosity and pore size. Tissue Eng. B Rev. 19, 485–502.
Losso, J.N., Ogawa, M., 2014. Thermal stability of chicken keel bone collagen. J. Food Biochem. 38, 345–351.
Lumry, R., Eyring, H., 1954. Conformation changes of proteins. J. Phys. Chem. 58, 110–120.
Murphy, C.M., O'Brien, F.J., 2010. Understanding the effect of mean pore size on cell activity in collagen-glycosaminoglycan scaffolds. Cell Adhes. Migrat. 4, 377–381.
Nishihara, T., Doty, P., 1958. The sonic fragmentation of collagen macromolecules. Proc. Natl. Acad. Sci. U.S.A. 44, 411–417.
Noda, H., 1972. Partial specific volume of collagen. J. Biochem. 71, 699–703.
Pantin-Jackwood, M.J., Stephens, C.B., Bertran, K., Swayne, D.E., Spackman, E., 2017. The pathogenesis of H7N8 low and highly pathogenic avian influenza viruses from the United States 2016 outbreak in chickens, turkeys and mallards. PLoS One 12, e0177265.
Parenteau-Bareil, R., Gauvin, R., Cliche, S., Gariepy, C., Germain, L., Berthod, F., 2011. Comparative study of bovine, porcine and avian collagens for the production of a tissue engineered dermis. Acta Biomater. 7, 3757–3765.
Persikov, A.V., Ramshaw, J.A.M., Brodsky, B., 2005. Prediction of collagen stability from amino acid sequence. J. Biol. Chem. 280, 19343–19349.
Pietrucha, K., 2005. Changes in denaturation and rheological properties of collagen–hyaluronic acid scaffolds as a result of temperature dependencies. Int. J. Biol. Macromol. 36, 299–304.
Postlethwaite, A.E., Seyer, J.M., Kang, A.H., 1978. Chemotactic attraction of human fibroblasts to type I, II, and III collagens and collagen-derived peptides. Proc. Natl. Acad. Sci. U.S.A. 75, 871–875.
Prinzinger, R., Preßmar, A., Schleucher, E., 1991. Body temperature in birds. Comp. Biochem. Physiol. A: Physiol. 99, 499–506.
Rabotyagova, O.S., Cebe, P., Kaplan, D.L., 2008. Collagen structural hierarchy and susceptibility to degradation by ultraviolet radiation. Mater. Sci. Eng. C 28, 1420–1429.
Rider, P., Kačarević, Ž.P., Alkildani, S., Retnasingh, S., Barbeck, M., 2018. Bioprinting of tissue engineering scaffolds. J. Tissue Eng. 9, 2041731418802090-90.
Schmidt, A.C., Niederwanger, V., Griesser, U.J., 2004. Solid-state forms of prilocaine hydrochloride. J. Therm. Anal. Calorim. 77, 639–652.
Shikh Alsook, M.K., Gabriel, A., Salouci, M., Piret, J., Alzamel, N., Moula, N., Denoix, J. M., Antoine, N., Baise, E., 2015. Characterization of collagen fibrils after equine suspensory ligament injury: an ultrastructural and biochemical approach. Vet. J. 204, 117–122.
Shoulders, M.D., Raines, R.T., 2009. Collagen structure and stability. Annu. Rev. Biochem. 78, 929–958.
Silver, F.H., Garg, A.K., 1997. Collagen: characterization, processing and medical applications. In: Domb, A.J., Kost, J., Wiseman, D.M. (Eds.), Handbook of Biodegradable Polymers. Harwood Academic Publishers, Amsterdam, pp. 323–350.
Sotelo, C.G., Comesaña, M.B., Ariza, P.R., Pérez-Martín, R.I., 2016. Characterization of collagen from different discarded fish species of the west coast of the iberian peninsula. J. Aquat. Food Prod. Technol. 25, 388–399.
Telay Mekonnen, B., Meiyazhagan, A., Ragothaman, M., Kalirajan, C., Palanisamy, T., 2019. Bi-functional iron embedded carbon nanostructures from collagen waste for photocatalysis and Li-ion battery applications: a waste to wealth approach. J. Clean. Prod. 210, 190–199.
Terzi, A., Storelli, E., Bettini, S., Sibillano, T., Altamura, D., Salvatore, L., Madaghiele, M., Romano, A., Siliqi, D., Ladisa, M., De Caro, L., Quattrini, A., Valli, L., Sannino, A., Giannini, C., 2018. Effects of processing on structural, mechanical and biological properties of collagen-based substrates for regenerative medicine. Sci. Rep. 8, 1429.

Tihan, G.T., Rău, I., Zgârian, R.G., Ghica, M.V., 2016. Collagen-based biomaterials for ibuprofen delivery. C. R. Chim. 19, 390–394.
Tirella, A., Liberto, T., Ahluwalia, A., 2012. Riboflavin and collagen: new crosslinking methods to tailor the stiffness of hydrogels. Mater. Lett. 74, 58–61.
Varriale, A., Bernardi, G., 2006. DNA methylation and body temperature in fishes. Gene 385, 111–121.
Wang, L., Liang, Q., Chen, T., Wang, Z., Xu, J., Ma, H., 2014. Characterization of collagen from the skin of Amur sturgeon (Acipenser schrenckii). Food Hydrocolloids 38, 104–109.
Wilson, W.O., Woodard, A., 1955. Some factors affecting body temperature of turkeys. Poult. Sci. 34, 369–371.
Wright, N.T., Humphrey, J.D., 2002. Denaturation of collagen via heating: an irreversible rate process. Annu. Rev. Biomed. Eng. 4, 109–128.
Yousefi, M., Ariffin, F., Huda, N., 2017. An alternative source of type I collagen based on by-product with higher thermal stability. Food Hydrocolloids 63, 372–382.
Zhang, G., Young, B.B., Ezura, Y., Favata, M., Soslowsky, L.J., Chakravarti, S., Birk, D.E., 2005. Development of tendon structure and function: regulation of collagen fibrillogenesis. J. Musculoskelet. Neuronal Interact. 5, 5–21.

Supplementary material

Collagen from turkey (*Meleagris gallopavo*) tendon: a promising sustainable biomaterial for pharmaceutical use

Krister Gjestvang Grønlien[a,*], Mona Elisabeth Pedersen[b], Karen Wahlstrøm Sanden[b], Vibeke Høst[b], Jan Karlsen[a,†] and Hanne Hjorth Tønnesen[a]

[a]*Section for Pharmaceutics and Social Pharmacy, Department of Pharmacy, University of Oslo, P.O. Box 1068 Blindern, NO-0316 Oslo, Norway;*
[b]*Nofima AS, P.O. Box 210, NO-1431 Ås, Norway*

* Corresponding author. E-mail address: k.g.gronlien@farmasi.uio.no

† Deceased 21 March 2019

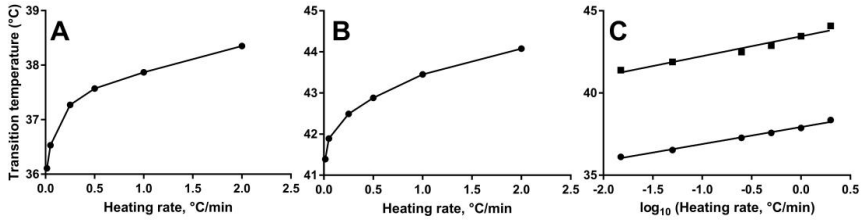

Figure S1. Relation between the transition temperature at the maximum of the denaturation peak and the DSC heating rate. A: minor transition (T_s), B: major transition (T_m), C: the logarithm of the heating rate for both transitions (lower curve = T_c, $r^2 = 0.99$; upper curve = T_m, $r^2 = 0.96$).

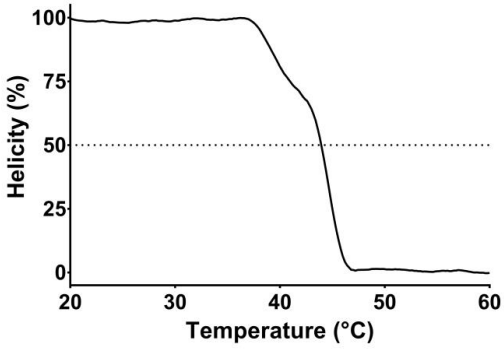

Figure S2. Changes in molecular ellipticity at 221 nm with heating at 2°C/min. 100% helicity corresponds to the triple helix content of native collagen, while 0% helicity corresponds to denaturated collagen.

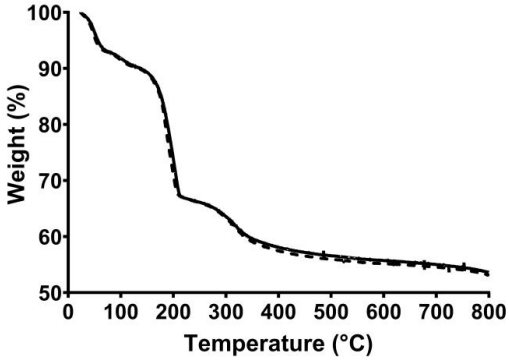

Figure S3. TGA thermograms of collagen freeze dried scaffolds. Irradiated collagen sponges (dashed line), non-irradiated collagen sponges (solid line).

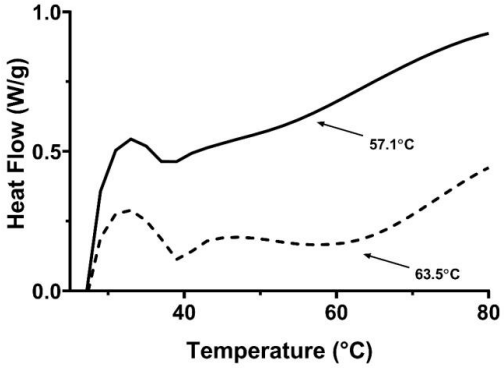

Figure S4. DSC thermograms of collagen freeze dried scaffolds. Irradiated collagen sponges (dashed line), non-irradiated collagen sponges (solid line).

Paper II

A natural deep eutectic solvent (NADES) as potential excipient in collagen-based products

Krister Gjestvang Grønlien, Mona Elisabeth Pedersen, Hanne Hjorth Tønnesen

Published in *International Journal of Biological Macromolecules*, August 2020, volume 156, pp. 394–402. DOI: 10.1016/j.ijbiomac.2020.04.026.

II

International Journal of Biological Macromolecules 156 (2020) 394–402

Contents lists available at ScienceDirect

International Journal of Biological Macromolecules

journal homepage: http://www.elsevier.com/locate/ijbiomac

A natural deep eutectic solvent (NADES) as potential excipient in collagen-based products

Krister Gjestvang Grønlien [a,*], Mona Elisabeth Pedersen [b], Hanne Hjorth Tønnesen [a]

[a] Section for Pharmaceutics and Social Pharmacy, Department of Pharmacy, University of Oslo, P.O. Box 1068 Blindern, NO-0316 Oslo, Norway
[b] Nofima AS, P.O. Box 210, NO-1431 Ås, Norway

ARTICLE INFO

Article history:
Received 17 December 2019
Received in revised form 26 March 2020
Accepted 5 April 2020
Available online 11 April 2020

Keywords:
Natural deep eutectic solvent (NADES)
Collagen
Rest raw material
Fluorescence
Thermostability

ABSTRACT

Natural deep eutectic solvents (NADES) have previously shown antibacterial properties alone or in combination with photosensitizers and light. In this study, we investigated the behavior of the structural protein collagen in a NADES solution. A combination of collagen and NADES adds the unique wound healing properties of collagen to the potential antibacterial effect of the NADES. The behavior of collagen in a NADES composed of citric acid and xylitol and aqueous dilutions thereof was assessed by spectroscopic, calorimetric and viscosity methods. Collagen exhibited variable unfolding properties dependent on the type of material (telo- or atelocollagen) and degree of aqueous dilution of the NADES. The results indicated that both collagen types were susceptible to unfolding in undiluted NADES. Collagen dissolved in highly diluted NADES showed similar results to collagen dissolved in acetic acid (i.e., NADES network possibly maintained). Based on the ability to dissolve collagen while maintaining its structural properties, NADES is regarded as a potential excipient in collagen-based products. This is the first study describing the solubility and structural changes of an extracellular matrix protein in NADES.

1. Introduction

We hereby propose a new sustainable concept for potential use in antimicrobial products, e.g., for treatment of infected wounds. This concept combines collagen from rest raw material and a natural deep eutectic solvent (NADES; used as both singular and plural in the following). This combination benefits the unique wound healing properties of collagen with the potential antibacterial effect of NADES [1,2]. The concept focuses on reducing environmental pollution and using sustainable resources, like "green", natural solvents and rest raw material. A successful combination depends on the molecular stability of collagen in the solvent while keeping the eutectic properties of NADES intact. The following paper addresses the structural and thermal properties of collagen in a selected NADES and maintenance of eutectic properties. Both issues are of great importance in the preformulation of a potential therapeutic product based on collagen and NADES.

Collagen is the major fibrillar component and protein in both human and animal connective tissue. Collagen has a triple helix structure formed by three α-chains held together by hydrogen bonds. The chains consist of repeating triplets of the amino acid glycine, followed by often proline and hydroxyproline. Collagen has nonhelical telopeptides attached to the ends of the molecule in its post-translational form [3,4]. The telopeptides can be cleaved off by pepsin digestion to produce atelocollagen. The amino acid tyrosine is located at the telopeptides, and cleavage of these will result in a low tyrosine content [4,5]. While telocollagen can produce immunogenicity, atelocollagen is considered biocompatible and well tolerated by the human body. Telocollagen is soluble in weak acids, while atelocollagen is soluble in both pepsin and in weak acids [6]. Both collagen and collagen peptides have demonstrated excellent wound healing properties by the attraction of cells involved in the rebuilding of the extracellular matrix and skin [2,7].

NADES are regarded as a third class of liquids in organisms, different from water and lipids, which is present in all living cells. NADES were first described by Choi et al. in 2011 [8]. They solely consist of natural compounds, i.e., primary metabolites (e.g., organic acids, amino acids, sugars, polyols, and tertiary amines). It is postulated that NADES have a central role in plants' ability to survive extreme conditions, such as cold and drought [8]. Apart from solubilizing plant metabolites, they have been reported to solubilize both small molecules such as itraconazole, curcumin and porphyrins, and proteins, such as gluten and laccases [9–16]. NADES are considered as "green" solvents compared to conventional organic solvents. NADES have shown antimicrobial effect in the absence and presence of light. The antimicrobial effect is present in pure NADES, in aqueous dilutions of NADES up to 1:200, or in combination with photosensitizers and light under the production of toxic reactive oxygen species. This was first reported by Wikene et al. in 2017 [1]. NADES have also shown antioxidative properties [17].

* Corresponding author.
E-mail address: k.g.gronlien@farmasi.uio.no (K.G. Grønlien).

https://doi.org/10.1016/j.ijbiomac.2020.04.026

A polyol compound is an important component of some NADES. Polyols have been reported to stabilize the triple helix of collagen to various extents, depending on the number of carbon atoms present in the polyol molecule. The stabilizing effect is suggested to be achieved through the binding of the polyol to the surface of the collagen molecule followed by the formation of additional hydrogen bonds [18,19]. Although this should indicate a stabilization of collagen in NADES, the properties of polyols when part of a eutectic mixture could be different from a polyol solution. In NADES, the components are tightly bound in a network of hydrogen bonds, which can affect the way the solutes reacts with the surrounding media.

NADES have been proposed as potential excipients in pharmaceutical preparations and drug delivery systems, particularly because of their solubilizing properties, varying viscosity and antibacterial properties [1,16]. Collagen has good biocompatibility, and both collagen and collagen peptides have as mentioned above, beneficial properties for wound healing. The combination of NADES and collagen has the potential to be included in different types of topical formulations, e.g., spray formulation, personalized products from 3D printing, and wound dressings. Collagen to be used in wound products should retain the chemotactic properties important for wound healing, either as a triple helix or in fragmented form as collagen peptides [2,7]. For other purposes like 3D printing, the collagen should be able to be crosslinked, either physically by pH and temperature, or by a crosslinker. This requires an intact triple helical structure [20].

The aim of the present study was to investigate the physicochemical properties of collagen in a selected NADES and aqueous dilutions thereof to identify potential combinations suitable in pharmaceutical preparations. Both pepsin soluble collagen (atelocollagen) and acid soluble collagen (telocollagen) were studied. The selected NADES contained an organic acid (citric acid) and a polyol (xylitol). This NADES has shown antibacterial effect combined with unique solvent properties and is, therefore, a candidate excipient in antimicrobial products [1]. The unfolding, thermal properties, fragmentation and viscosity of telo- and atelocollagen in NADES were assessed. Freeze-dried collagen sheets with NADES were prepared as a potential wound dressing. The structure and mechanical properties of the sheets were evaluated. Our data reveals the potential of the selected NADES and aqueous dilutions thereof as excipients in collagen-based products. This is to our knowledge the first study describing solubility and behavior of an extracellular matrix protein in NADES.

2. Materials and methods

All experiments were performed at 25 °C unless other stated. The data were presented as mean ± highest deviation from three independent experiments.

2.1. Materials

Pepsin soluble collagen (atelocollagen) isolated from industrially produced turkey (*Meleagris gallopavo*) rest raw materials was prepared as described in Grønlien et al. [21]. Acid soluble collagen (telocollagen) from calf skin (Sigma-Aldrich, C9791) and other reagents were of analytical grade and were purchased from either Sigma-Aldrich Chemical Company (St. Louis, MO, USA) or Merck KGaA (Darmstadt, Germany).

2.2. Preparation of the natural deep eutectic solvent (NADES)

The selected NADES was prepared by a solvent evaporation method, according to Wikene et al. [12]. The two components of the NADES were dissolved in warm Milli-Q water (~50 °C) and evaporated at 45 °C for 20 min with a rotary evaporator. The liquid obtained was transferred to polypropylene tubes with a tight cap. Water content was determined by Karl Fischer titration (C20 Coulometric KF Titrator, Mettler Toledo Inc., Schwerzenbach, Switzerland). The NADES prepared contained citric acid/xylitol (molar ratio 1:1) (abbreviated CX). The NADES was used in the undiluted form or after dilution in Milli-Q water 1:1, 1:10, 1:50, 1:100 and 1:200. The pH was measured using a pH 526 MultiCal® pH meter (WTW GmbH, Weilheim, Germany).

2.3. Intrinsic viscosity and estimated average molecular weight of collagen

Collagen isolated from turkey tendon was dissolved in 0.5 M acetic acid to a concentration of 0.5 mg/ml. The solution was diluted to concentrations between 0.1 and 0.5 mg/ml. Acetic acid (0.5 M) was used as negative control. The viscosity of the solutions was determined with an Anton Paar Rheometer (Anton Paar Physica MCR301 Rheometer, Germany). Samples of 10 ml were measured with a double gap concentric cylinder (DG 26.7) at 25 °C with a shear rate of 10 s^{-1}. The intrinsic viscosity of collagen was calculated from the dynamic viscosity [22]. The average molecular weight was then estimated from the intrinsic viscosity according to the Kuhn-Mark-Houwink-Sakurada equation (Eq. (1)):

$$[\eta] = KM^{\alpha} \quad (1)$$

where η is the intrinsic viscosity, M is the average molecular weight, K and α are values specific for the polymer or protein (1.86×10^{-19} and 1.8 for collagen, respectively) [23].

2.4. Sodium dodecyl sulfate-polyacrylamide gel electrophoresis (SDS-PAGE)

SDS-gel electrophoresis is a common method for determination of collagen polypeptide chains [24,25]. Collagen (both qualities) was solubilized in 0.02 M acetic acid or NADES diluted 1:10, 1:50, 1:100 and 1:200 with Milli-Q water to a final concentration of 2.0 mg/ml. Lower dilutions of NADES (1:1 or undiluted samples) were not tested for practical reasons (i.e., high viscosity). Further, 100 μl sample was mixed with 50 μl buffer to a final concentration of 0.05% Tris-HCl pH 6.8, 7% glycerol, 0.07 M dithiothreitol, 1% (*w*/*v*) SDS and 0.001% bromophenol blue. The samples were then pre-heated to 50 °C for 10 min and separated by SDS-PAGE by use of 4–12% Bis-Tris gels (Invitrogen, MD, USA), NuPAGE® MOPS SDS running buffer (Invitrogen, MD, USA) and Novex XCell II apparatus (Invitrogen, MD, USA). Protein bands were visualized by Coomassie Staining and molecular weight determined by use of Benchmark prestained protein ladder (Novex, Life technologies, 10748-010) run simultaneously on the gel.

2.5. Preparation of samples for spectroscopy

Collagen isolated from turkey filet tendon or collagen from calf skin was dissolved at 1.5 mg/ml in NADES, aqueous dilutions of NADES or 0.02 M acetic acid. The samples were gently stirred overnight at room temperature (IKA® RO 15, IKA Werke, GmbH, Staufen, Germany, 400 rpm) protected from light and filtered (5 μm Versapor® Membrane, Pall Corporation, MI, USA) prior to the spectroscopic measurements.

2.6. UV–Vis spectrophotometry

Absorption spectra were recorded between 190 and 700 nm on a Shimadzu UV-2101 PC (Kyoto, Japan) UV–Vis scanning spectrophotometer using a quartz cuvette with a 1 cm cell path.

2.7. Fluorescence spectroscopy

Fluorescence measurements were performed on a Photon Technology International modular fluorescence system (London, Ontario, Canada), Model 101 monochromator with f/4 0.2-m Czerny-Turner configuration. The instrument was equipped with a red-sensitive photomultiplier. The excitation source was a 75 W xenon lamp. The

emission and excitation spectra were automatically corrected for both the lamp spectral radiance and the detector quantum efficiency by means of the acquisition software (FeliX32, PTI). The excitation and emission monochromator bandpasses were set at 2 or 5 nm for recording of emission spectra and fluorescence quenching measurements respectively, and at 10 nm for anisotropy measurements. The excitation wavelength was 270 nm or 295 nm (anisotropy measurements of turkey collagen). Correction for the difference in absorbance between samples at the excitation wavelength was performed when relevant. The measurements were performed in quartz cuvettes with 1 × 1 cm cell path or in micro cuvettes at 25 ± 0.1 °C ($n = 3$). The anisotropy measurements were performed by the L-format (single channel) method.

2.8. Viscosity measurements

Viscosity measurements were performed on a Brookfield DV2T viscometer (Brookfield Engineering Laboratories, Inc., Middleboro, MA, USA) with spindles CPA-40Z (low viscosity samples < 10 mPa s; accuracy: ±0.1 mPa s; sample volume: 1.5 ml) and CPA-52Z (high viscosity samples ≥ 10 mPa·s; accuracy: ±3.1 mPa·s; sample volume: 0.5 ml). The temperature was kept constant at 25 ± 0.1 °C during the viscosity measurements (Grant LTD6G water bath, Grant Instruments, Cambridge, Ltd., Royston, UK). A single point viscosity measurement was performed with the end condition parameter fixed at 2 min and speed 30 rpm for all samples.

2.9. Differential scanning calorimetry

Differential scanning calorimetry (DSC) experiments were performed using a Nano DSC 602000 differential scanning calorimeter (TA Instruments, Lindon, UT, USA) with a capillary cell volume of 0.300 ml. DSC thermograms were recorded for 1.5 mg/ml collagen solutions in selected media at a constant heating rate of 2 °C/min and 3 atm in the temperature range of 20–60 °C. The respective NADES in their current dilutions were used as baseline references. The transition temperature of collagen was defined at the maximum of the transition peak after baseline subtraction and processing.

The results were processed by application of the NanoAnalyze software (TA Instruments). The partial specific heat capacity of collagen was determined from the estimated average molecular weight and a partial specific volume of 0.700 ml/g [26]. The results were fitted to a two-state trimer-to-monomer model. The deviation between the recorded data and the modulated data was ≤3%.

2.10. Preparation of collagen-NADES sheets

Collagen-NADES sheets were prepared by a freeze-drying method. Collagen (both qualities) was solubilized overnight in NADES CX diluted 1:1, 1:10, 1:50, 1:100 and 1:200 with Milli-Q water to a final concentration of 3.0 mg/ml. The solutions were transferred to a 6-well multiplate (Corning Life Sciences, Tewksbury, MA, USA) (2 ml) and freeze-dried in order to form the sheets. The solutions were frozen at −80 °C for 1 h prior to freeze-drying at 0.0019 mbar for 20 h, including 1 h final drying at 0.0010 mbar (Alpha 2-4 LD Plus Freeze Dryer, Martin Christ, Osterode am Harz, Germany). Collagen dissolved in undiluted NADES is not applicable, as undiluted NADES will neither freeze nor freeze-dry under the actual conditions.

2.11. Fourier transform infrared spectroscopy (FT-IR) of collagen-NADES sheets

FT-IR spectra of undiluted NADES CX and the freeze-dried collagen-NADES sheets were acquired using a Nicolet™ iS™ 5 FTIR Spectrometer (Thermo Fisher Scientific, Waltham, MA, USA) with an iD5 diamond ATR Accessory. For each sample, 16 scans from 4000 cm^{-1} to 550 cm^{-1} were collected in single beam mode with a spectral resolution of 4 cm^{-1}. The smoothed spectra are presented.

2.12. Mechanical force-displacement studies of collagen-NADES sheets

Mechanical properties (force-displacement) of the collagen-NADES sheets were studied using a TA-XT2i Texture Analyser (Stable Micro Systems, Haslemere, UK) in compression mode. The sheets were exposed to constant pressure at 0.5 mm/s with a 2 mm probe. Force-displacement curves of the collagen-NADES sheets were compared to collagen sheets without NADES ($n = 3$–6). The force was defined as the maximum force measured and displacement was defined as the displacement at the maximum force.

3. Results

3.1. Intrinsic viscosity and estimated average molecular weight of collagen

The intrinsic viscosity of collagen isolated from turkey tendon was found to be 1721 cm^3/g. The average molecular weight was estimated to be 445 kDa. Commercially available collagen from calf skin has no reported molecular weight, but the specified production method indicated an isolation without pepsin, producing acid soluble (telo) collagen. In the current experiments, the average molecular weight was set to 300 kDa.

3.2. SDS-PAGE

The SDS-PAGE pattern of collagen (both qualities) in acetic acid indicated the presence of α-chains from both collagen type I and III [25,27,28]. For collagen dissolved in aqueous dilutions of NADES, the pattern showed the most extensive fragmentation of the molecule in dilution 1:10 in case of calf skin collagen and dilutions ≤1:50 in case of turkey collagen. The pattern for dilutions >1:50 appeared similar to collagen dissolved in acetic acid (Fig. 1).

3.3. Absorption spectra

Collagen (both qualities) in acetic acid displayed an absorption maximum around 220 nm and a broad shoulder in the range 250–290 nm with a diffuse maximum around 275 nm (Table 1). Dissolution in undiluted NADES resulted in a broad peak with low absorbance and a maximum at 265 nm and shoulders at 258, 268, 275, and 281 nm (calf) or 281 nm with shoulders at 269, 265, and 259 nm (turkey). Dissolution in NADES diluted 1:1 induced a blue shift of the main peak of 32 nm and 16 nm for turkey and calf skin collagen, respectively. The resulting absorption maximum was similar in both samples (249 nm). The absorption maximum was further blue-shifted upon further dilution (Fig. 2). The absorption maximum in the individual NADES dilutions was similar for both collagen qualities. A hyperchromic effect occurred at dilutions ≥1:50 in the case of calf collagen and ≥1:1 in case of collagen from turkey. A shoulder at approximately 280 nm remained virtually constant in all the diluted samples (Fig. 2). There was a linear relationship ($r^2 = 0.998$, turkey collagen; $r^2 = 0.975$, calf skin collagen) between the absorption maximum (Table 1) of collagen and the pH of the NADES solution (Table 2) in the dilution range 1:1–1:100.

3.4. Fluorescence spectra

An excitation wavelength (270 nm) corresponding to the tyrosine absorption was selected. The emission maximum was 297–303 nm in all the samples containing collagen from calf skin. The emission maximum in samples made from turkey collagen showed a bathochromic shift and was detected between 319 nm and 339 nm with a shoulder around 298 nm (Table 1, Fig. 3). The fluorescence excitation spectrum at emission 340 nm was recorded in acetic acid and in NADES diluted

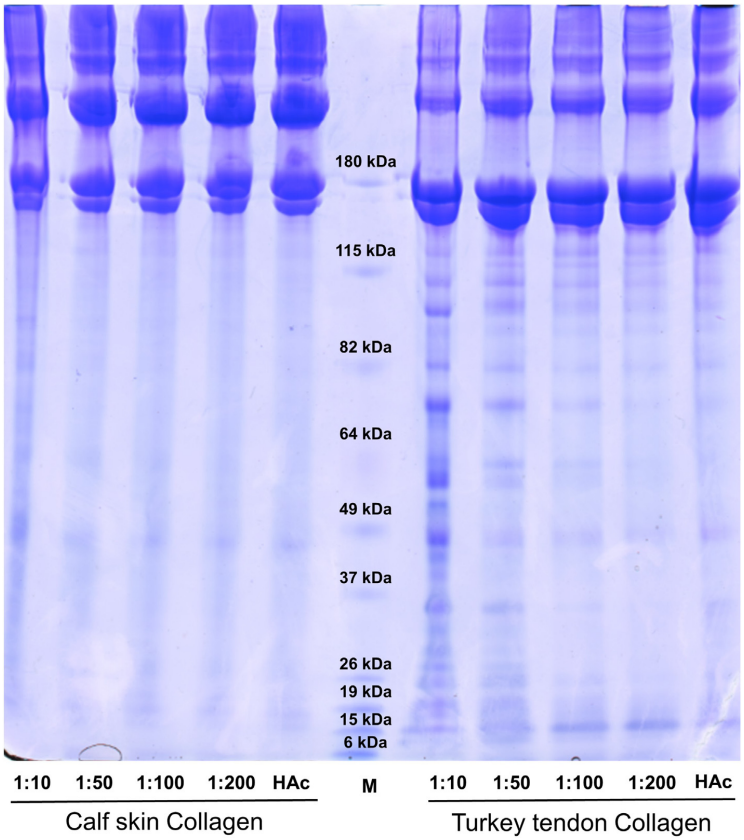

Fig. 1. SDS-PAGE of collagen from turkey tendon and calf skin dissolved in either 0.02 M acetic acid (HAc) or aqueous dilutions of NADES and stained with Coomassie Brilliant Blue. Molecular weight standard (Benchmark prestained protein ladder) is shown in the middle (M).

Table 1
Spectral and thermal properties of collagen from turkey tendon and calf skin dissolved in NADES CX and aqueous solutions thereof.

Sample	Solvent	λ_{Abs}[a] (nm)	λ_{Em}[b] (nm) (λ_{Ex} 270 nm)	Anis.[c] (λ_{Ex} 270 nm)	Viscosity (mPa·s)	FI[d]/Abs[e] (270 nm) (x10^5)	T_s (°C)[f]	T_m (°C)[g]
Turkey tendon collagen (isolated in-house)	NADES CX	281 (259, 265, 269)	319	0.12 ± 0.01	–	6.40	–	–
	NADES CX (1:1)	249 (280)	335	0.12 ± 0.04	8.35	4.23	–	–
	NADES CX (1:10)	242 (280)	(297), 333	0.13 ± 0.01	6.50	2.52	33.8	38.3
	NADES CX (1:50)	234 (280)	(297), 334	0.12 ± 0.01	5.69	2.36	34.8	40.3
	NADES CX (1:100)	231 (280)	(301), 339	0.12 ± 0.01	5.12	3.08	35.1	40.9
	NADES CX (1:200)	228 (280)	(297), 336	0.12 ± 0.01	4.64	1.48	35.7	41.7
	0.02 M Acetic acid	223 (~275)	(298), 333	0.10 ± 0.02	5.42	3.30	38.5	44.2
Calf skin collagen (Sigma-Aldrich)	NADES CX	265 (258, 268, 275, 281)	303	0.12 ± 0.02	–	3.26	–	–
	NADES CX (1:1)	249 (278)	300	0.13 ± 0.02	6.67	0.68	–	–
	NADES CX (1:10)	243 (278)	301	0.18 ± 0.02	5.52	0.29	–	35.7
	NADES CX (1:50)	231 (282)	297	0.20 ± 0.01	5.19	1.01	34.1	39.6
	NADES CX (1:100)	230 (280)	298	0.20 ± 0.01	4.86	0.46	34.4	39.9
	NADES CX (1:200)	230 (279)	300	0.21 ± 0.01	4.54	0.32	34.1	40.0
	0.02 M Acetic acid	221 (~275)	296	0.22 ± 0.01	5.43	1.33	36.9	42.6

[a] Absorption wavelength.
[b] Emission wavelength.
[c] Anisotropy.
[d] Fluorescence intensity.
[e] Absorption intensity.
[f] Minor transition.
[g] Major transition.

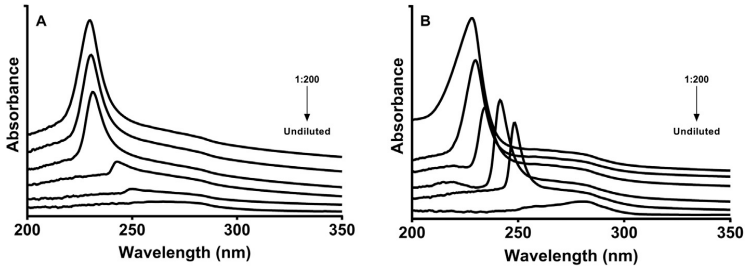

Fig. 2. Absorption spectra of collagen dissolved in NADES and aqueous dilutions thereof. The concentration of collagen was 1.5 mg/ml in all samples. A: calf skin collagen; B: turkey tendon collagen.

1:1 and 1:50 (emission 335 nm) in case of turkey collagen and emission at 300 nm in case of calf skin collagen. The excitation maximum kept constant in the range 272–278 nm, characteristic of tyrosine (data not shown). The fluorescence intensity corrected for differences in absorption at the excitation wavelength was highest in undiluted NADES and at dilution 1:1 in case of turkey collagen and exceeded the intensity in acetic acid. The intensity showed a linear decrease as a function of sample viscosity ($r^2 = 0.973$, dilution 1:1–1:200; 1:100 excluded) in case of collagen from turkey but was virtually independent of NADES concentration in case of calf skin collagen (Table 1).

3.5. Steady state fluorescence anisotropy

The fluorescence anisotropy was independent of the solvent in samples containing turkey collagen but did increase upon dilution of the NADES in calf skin samples. The latter showed a linear increase as a function of NADES dilution ($r^2 = 0.992$; except 1:50); i.e., by a decrease in sample viscosity (Table 1).

3.6. Differential scanning calorimetry

The thermal transitions of collagen from turkey tendon and calf skin were dependent on the dissolution medium. Collagen exhibited both a minor (T_s) and a major thermal transition (T_m) in acetic acid and aqueous dilutions of NADES > 1:50. In NADES diluted 1:10 in the case of calf skin collagen, only T_m was present (Table 1). No signals were detected in undiluted and 1:1 dilution of NADES. The denaturation temperature showed a linear increase as a function of increased pH between dilution 1:10 and 1:100 ($r^2 \geq 0.999$, turkey: T_s and T_m; calf: T_m).

3.7. Characterization of collagen-NADES sheets

Freeze-drying of collagen dissolved in aqueous dilutions of NADES CX between 1:50 and 1:200 formed sheet-like sponges with different plasticity. Dilution 1:10 resulted in a sticky fibrous layer, which was difficult to handle. Dilution 1:1 resulted in a transparent product (i.e., no sheet formation).

The FT-IR spectrum of calf skin (Fig. 4a) and turkey tendon (Fig. 4b) collagen included the bands of amide A (3313/3324 cm^{-1}), amide B (2942/2938 cm^{-1}), amide I (1648/1658 cm^{-1}), amide II (1542/1548 cm^{-1}) and amide III (1237/1234 cm^{-1}) for calf skin collagen/turkey tendon collagen, respectively [21,29]. The FT-IR spectrum of undiluted NADES CX included a broad band at 3360 cm^{-1}, a band at 1630 cm^{-1} and a band at 1710 cm^{-1}.

Force-displacement studies demonstrated a plasticizing effect by aqueous dilutions of NADES on collagen sheets. However, the mechanical strength of the sheets was also dependent on the collagen source. Only sheets made from turkey tendon collagen could be handled, whereas sheets made from calf skin collagen were sticking to the container and appeared too fragile to be tested. The results are summarized in Table 3 and representative figures are shown in Supplementary Material, Fig. S1a–d.

Table 2
Aqueous dilutions of NADES CX and corresponding pH values.

Sample	pH
NADES CX	0.2
NADES CX (1:1)	1.0
NADES CX (1:10)	1.6
NADES CX (1:50)	2.2
NADES CX (1:100)	2.4
NADES CX (1:200)	2.4

4. Discussion

Type I collagen has a low content of aromatic amino acids, which are represented by tyrosine and phenylalanine. The tyrosine residues are located at the non-helical telopeptides [30,31]. Collagen from calf skin contains telopeptides, while turkey collagen has been treated with pepsin to remove these peptides. It has, however, been demonstrated that telopeptides are not completely excised by pepsin treatment [30]. This can explain why tyrosine was detected in both types of collagen. An absorption peak at ~276 nm and a shoulder at ~282 nm would reflect the presence of tyrosine residues while peaks at 268, 265, and 258 nm indicate the presence of phenylalanine [30]. All these peaks were identified in collagen samples dissolved in undiluted NADES. The absorption peak of phenylalanine (i.e., 265 nm) emerged as the highest intensity peak in the calf collagen spectrum in undiluted NADES, while the tyrosine absorption (i.e., 281 nm) was dominating in samples of turkey collagen under similar conditions. The hypsochromic effect showed a linear

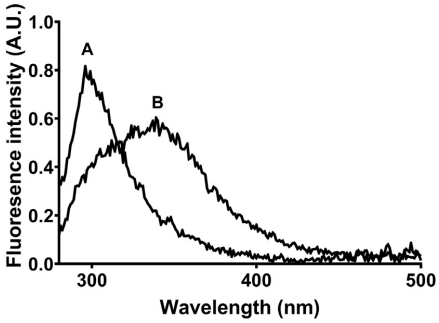

Fig. 3. Representative fluorescence spectra of collagen dissolved in NADES with calf skin collagen (A) and turkey tendon collagen (B) exhibiting λ_{Em} = 298 and 339 nm, respectively.

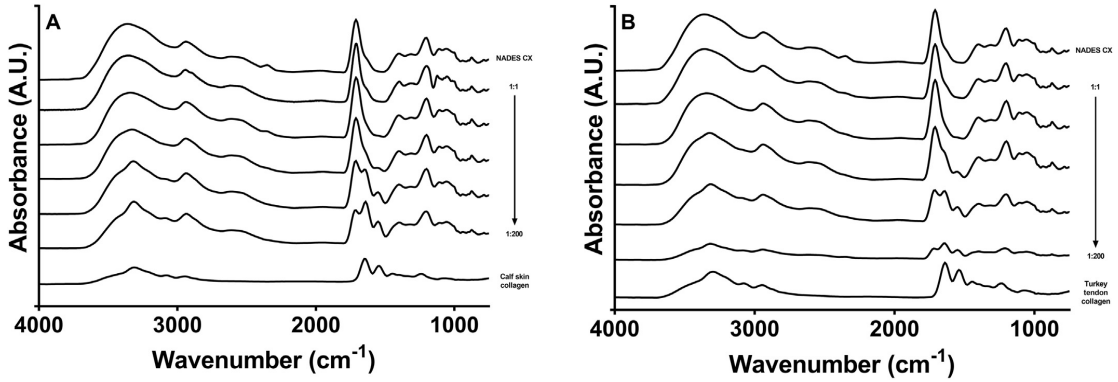

Fig. 4. FT-IR spectra of NADES CX, collagen and freeze-dried collagen-NADES sheets (prepared with aqueous dilutions of NADES CX 1:1–1:200). A: calf skin collagen; B: turkey tendon collagen.

dependency of the solution pH which increased from 1.0 to 2.4 upon NADES dilution. The pK_a value of tyrosine and phenylalanine is approximately 2.2 and 2.0, respectively. A hyperchromic effect in turkey collagen occurred at dilutions ≥1:50 which corresponded to a pH similar to the tyrosine pK_a value. A similar hyperchromic effect in calf collagen was observed at lower dilutions, i.e., at a pH closer to the pK_a value of phenylalanine. It has previously been reported that hypsochromic and hyperchromic shifts in collagen samples could indicate an uncoiling of the triple helix, i.e., a denaturation of the protein [31,32]. However, since the components in NADES and the solutes are tightly bound together in a network of hydrogen bonds, the hyperchromic effect observed upon dilution could also indicate a weakening in the hydrogen bonding between collagen and the NADES network, leading to collagen stabilization as observed in acetic acid. This is consistent with a bathochromic shift in fluorescence in the case of turkey collagen (i.e., tyrosine/tyrosinate fluorescence). Tyrosine side chains are often distributed from the interior to the surface of a protein, while phenylalanine residues are highly apolar and thereby buried in the interior of the protein, making them less sensitive to changes in the solvent (e.g., polarity, H-bonding) [33].

Collagen belongs to the group of tryptophan-free proteins. Excitation at 270 nm should, therefore, induce tyrosine fluorescence (maximum emission near 305 nm) without any interference from tryptophan (maximum emission near 350 nm). However, unusual tyrosine emission at longer wavelengths has previously been reported in proteins [34]. This can be observed as a weak shoulder on the tyrosine band in the range 330–350 nm and has been ascribed to tyrosinate emission [35]. In the present study, the tyrosinate emission was intense and emerged as the main peak in turkey collagen samples while absent in calf skin collagen. Ground state tyrosine has a pK_a value of 10.3 and tyrosinate fluorescence is, therefore, most easily observed at high pH. The pK_a value does, however, decrease to about 4 in the excited state. Tyrosinate emission can for that reason occur at neutral pH from the singlet excited tyrosine [36]. This is facilitated by the presence of proton acceptors like acetate in the solvent but is also dependent on to which extent the tyrosine is exposed to the aqueous phase. Tyrosinate emission can also be achieved by excited-state proton transfer to adjacent acceptor groups within the protein, e.g., carboxylate, histidyl, and lysyl residues or the side chains of aspartate and glutamate residues [35,37]. The excitation spectrum for the tyrosinate emission is expected to be independent of pH below the pK_a of ground-state tyrosine if the emission arises from singlet excited tyrosine. This was the case in the present study when the pH varied from 1.0 to 3.2. The intensity of the tyrosinate emission (corrected for variation in absorbance) showed a linear decrease as a function of decreased viscosity in the diluted NADES samples. The fact that tyrosinate emission occurred only in turkey collagen (including samples in 0.02 M acetic acid) might indicate that tyrosine was more exposed to the aqueous phase than in calf skin collagen, which is in agreement with the UV absorption measurements (see above) and/or the presence of nucleophilic group(s) in the tyrosyl microenvironment in turkey collagen. Further, it has previously been reported that tyrosine residues in calf skin collagen mainly are located in hydrophobic regions of the protein that are poorly accessible to the surrounding solvent, which supported the above results [38]. The intensity of the tyrosine emission from calf skin collagen was quite independent of NADES concentration (i.e., viscosity and pH). This emphasized that the rate of deactivation of the tyrosine excited state in calf skin collagen was fast relative to the rate of deprotonation (i.e., formation of tyrosinate).

The anisotropy in dilute non-viscous solutions is primarily determined by the rotational motion of the fluorophore. In the case of proteins, these motions will rely on e.g., the size, shape, and extent of aggregation of the molecule. The samples in the present study varied from low to medium viscosity dependent on the extent of NADES dilution, which complicated the interpretation of the results. Further, all the samples were slightly turbid in spite of filtration prior to the spectroscopic measurements. The observed anisotropy can be expected to decrease linearly with an increase in turbidity. The contribution of scattering to depolarization can be evaluated by changing into a cuvette with smaller dimensions. Both conventional cuvettes (1×1 cm) and micro cuvettes (2×2 mm) were applied in the present work giving similar results (data not shown). It is therefore unlikely that depolarization due to scattering made a major contribution to the observed values.

The steady-state fluorescence anisotropy of tyrosinate emission in turkey collagen remained constant independent of NADES dilution; i.e., independent of the supramolecular structure, pH, and viscosity of the solvent. Further, the anisotropy was virtually independent of the excitation wavelength, which indicated that the angle between the absorption and emission dipoles did not change upon changes in the macro environment. Fluorophores bound to proteins can be independent of the overall rotational diffusion by displaying fast segmental

Table 3
Force-displacement data for collagen-NADES sheets.

Sheet	Force (N)	Displacement (mm)
Turkey tendon collagen	0.10 ± 0.01	1.80 ± 0.12
+NADES CX (1:50)	0.28 ± 0.08	4.49 ± 1.04
+NADES CX (1:100)	0.46 ± 0.07	4.94 ± 0.65
+NADES CX (1:200)	0.31 ± 0.15	3.70 ± 0.59

motions [39]. The result is that the anisotropy becomes rather insensitive to macroscopic viscosity [34]. This could explain the observations on turkey collagen and emphasized the assumption that the tyrosine residues were not deeply embedded in this protein. On the other hand, the fluorescence anisotropy from tyrosine emission in calf skin collagen was dependent on the NADES dilution and was apparently an inverse function of the viscosity. It is evident from the calorimetric measurements that the conformation of calf skin collagen changed upon dilution of the NADES. This had apparently a palpable effect on the emission properties of the tyrosine fluorophores in calf skin collagen. Collagen normally exhibits two thermal transitions when heated. The minor transition has previously been ascribed to collagen fibril depolymerization, unfolding and melting of small parts of the triple helix structure or been related to the thermally labile regions with hydroxyproline deficient sequences, while the major transition has been ascribed to denaturation of the triple helix to form monocoils [40,41]. The thermograms demonstrated a lack of protein unfolding prior to denaturation in undiluted NADES and samples diluted 1:1 and 1:10 in case of calf skin collagen; i.e., only the denaturation temperature could be detected. This indicated either that collagen is thermostable in concentrated NADES, or that unfolding of the triple helix had occurred at room temperature in these solvents. The latter hypothesis was supported by SDS-PAGE, where collagen in NADES diluted 1:10 showed higher fragmentation than dilutions ≥1:50. It is reasonable to infer that dilution of NADES will cause conformational changes in the protein due to changes in the supramolecular network formed in deep eutectic solvents combined with the change in pH. The triple helix, therefore, seemed to be maintained at dilutions ≥1:10 illustrated by the occurrence of two peaks in the thermograms that are typical for unfolding and denaturation, respectively. Further, this is consistent with the increase in fluorescence anisotropy observed by dilution of the NADES, best illustrated by calf skin collagen. In very dilute NADES samples (i.e., 1:200); the anisotropy was virtually similar to samples in 0.02 M acetic acid representing a stable collagen structure. This is as well consistent with the hypothesis that the hyperchromic effect observed upon dilution of the NADES was caused by a weakening of the eutectic network, rather than denaturation of collagen. The presence of xylitol in the eutectic mixture had apparently no stabilizing effect on the collagen triple helix, which was an effect hypothesized from studies where collagen exhibited increased thermostability in the presence of polyols [18,19].

The denaturation temperature showed a linear increase as a function of increased pH between dilution 1:10 and 1:100. This was valid for both the minor and major transition of turkey tendon collagen, but only for the major transition of calf skin collagen. Collagen has shown low protein solubility, water binding capacity and apparent viscosity at pH ≤ 1, caused by a partial denaturation [42]. This can explain why the collagen lacked an unfolding transition prior to denaturation in the thermograms and the fragmentation observed by the SDS.

The correlations demonstrated by the overall results were valid up to a NADES dilution between 1:100 and 1:200 with water, e.g., the hyperchromic effect of collagen absorbance at the absorption maximum observed upon dilution of NADES was present up to a 1:200 dilution. Further, at this dilution, the anisotropy became virtually similar to collagen dissolved in 0.02 M acetic acid. Together, these results indicated that the eutectic network was preserved upon dilution to this ratio. This is in accordance with previous results obtained in our lab where the eutectic network appeared to be preserved upon dilution ≤1:200 [1]. However, a report in the literature claims that the network was absent in dilutions ≥1:1 [43]. The NADES network structure is probably dependent on a series of factors, e.g., ionic strength, pH and chemical properties of the solute.

The results on collagen-NADES sheets were consistent with the spectroscopic and thermal observations on collagen dissolved in NADES solutions, indicating that the structural properties of collagen was maintained when the NADES was diluted ≥1:10. This can be illustrated by e.g., comparing the FT-IR spectra of the freeze-dried sheets with the undiluted NADES. The main peaks of collagen (amide A, B, I, II and II) were clearly present in collagen-NADES sheets prepared with NADES diluted 1:50–1:200, whereas the sheets prepared with NADES diluted 1:1 and 1:10 showed weak or no amide I or II signals. Conformational changes in the secondary structure of the collagen molecule can be followed by the changes in the amide profile in the FT-IR spectrum. The profile of amide I is associated to the α-helix conformation, the β-sheet conformation and the β-turn. An apparent loss in these structures is indicated by the lower intensity of this peak, which was observed for collagen-NADES sheets prepared with NADES diluted 1:1 and 1:10. A shift of the C═O stretching signal of the citric acid component of the NADES (i.e., from 1692 to approximately 1714 cm^{-1}) can be a measure of hydrogen bonding between the reagents [44]. Such a shift was observed in the plain NADES (undiluted) and in all the NADES samples containing collagen. The water will evaporate upon freeze-drying of the collagen sheets and leave concentrated NADES within the protein structure. This was confirmed by the FT-IR results obtained for collagen-NADES sheets when compared to the undiluted NADES. The presence of concentrated NADES within the sheets will maintain the solubilizing properties and potential antibacterial properties of this solvent.

Mechanical force-displacement studies of the formed sheets clearly showed a plasticizing effect by the NADES and aqueous dilutions thereof compared to a sponge of collagen without NADES. The plasticizing effect can be attributed to the high concentration of NADES, the presence of polyols, a crosslinking effect of the NADES components or a combination of all. Some of the force-displacement results expressed quite large standard deviations. This can be caused by a variation in the organization of the collagen fibers formed during freeze-drying or how the NADES is organized within the collagen structure. Highly concentrated NADES may dissolve the collagen and result in varying mechanical properties. The mechanical properties of collagen sheets prepared with highly diluted NADES seem to approach the properties of collagen sheets prepared in acetic acid, although some of the plasticizing effects by the NADES are maintained. Further, the NADES may work as a plasticizer as demonstrated by the force-displacement results discussed above, to form bioplastics, offering an alternative to toxic or non-biodegradable plasticizers [45]. Citric acid has previously been investigated as a potential natural crosslinker for collagen, increasing the mechanical properties of collagen sheets. Andonegi et al. [46] investigated how compressed collagen sheets were influenced by different concentrations of citric acid. Addition of low amounts of citric acid did not change the structure, but higher contents changed the structural order of the collagen sheets [46]. In a NADES based on citric acid, the acid is maintained within a hydrogen-bonded network, resulting in supersaturated solutions. The high concentration of citric acid may induce a change in the collagen structure. Xylitol has previously been tested for a plasticizing effect on squid protein films, where it showed promising properties, although the films became brittle over time [47]. It is however, likely that the properties of xylitol or other components can be modified when they are part of a NADES network. A choline chloride and glycerol based NADES has been evaluated for a potential plasticizing effect on pectin films and showed promising properties as excipients in bio-based plastics formulations [48]. The addition of plasticizers to a collagen sheet can be used to control the mechanical properties of the constructs. It appeared that a 1:100 dilution of the NADES was the optimal concentration in this study, maintaining both the collagen structure and a plasticizing effect. A collagen-NADES sheet formulation has to be optimized further to find the optimal NADES composition and concentration.

Based on the above results and previous knowledge about the antibacterial properties of NADES and the unique wound healing properties of collagen, a combination of NADES CX and collagen represents a promising formulation strategy for topical preparations. Inclusion of a photosensitizer could allow for additional application in antimicrobial

photodynamic therapy (aPDT). In cases where there is a need to preserve the collagen triple helical structure, an aqueous dilution of the NADES between 1:10 and 1:200 can be selected. Although collagen seems fragmented in undiluted NADES, it is still possible that the chemotactic properties are preserved. The application of undiluted or slightly diluted NADES in collagen preparations should therefore not be ruled out.

5. Conclusions

Collagen exhibited variable unfolding properties based on the type and method of isolation and the degree of aqueous dilution of the added NADES. The results indicated that both telo- and atelocollagen were more susceptible to molecular changes when dissolved in undiluted NADES than in acetic acid. However, a formulation based on undiluted NADES and collagen can benefit from both chemotactic properties by the attraction of cells involved in wound healing by collagen peptides and the unique antibacterial properties of the NADES. The results obtained in highly diluted samples approached the data obtained in acetic acid. Further, the results indicated that the intramolecular NADES network was maintained up to a dilution ≤1:200, which preserves the unique effects of NADES. The eutectic solvents have previously shown antibacterial properties in aqueous dilutions up to 1:200 [1]. Further, an increased mechanical strength of freeze-dried collagen-NADES sheets and a plasticizing effect of NADES at low concentration, were demonstrated in the present work. The combination of diluted NADES and collagen seemed suitable for further development into a topical preparation.

Supplementary data to this article can be found online at https://doi.org/10.1016/j.ijbiomac.2020.04.026.

CRediT authorship contribution statement

Krister Gjestvang Grønlien: Conceptualization, Investigation, Visualization, Writing - original draft, Writing - review & editing. **Mona Elisabeth Pedersen:** Conceptualization, Supervision, Writing - review & editing. **Hanne Hjorth Tønnesen:** Conceptualization, Funding acquisition, Investigation, Supervision, Writing - original draft, Writing - review & editing.

Declaration of competing interest

The authors declare that they have no conflict of interest.

Acknowledgments

The authors are grateful to Bente Amalie Breiby, Department of Pharmacy, University of Oslo and Vibeke Høst, Nofima AS for technical support, and Karen Wahlstrøm Sanden, Nofima AS for isolation of collagen from turkey tendon. Turkey tendon by-products and financial support for isolation of collagen from turkey were contributed by Norilia AS.

Funding

This work was supported by Norilia AS (Oslo, Norway).

References

[1] K.O. Wikene, H.V. Rukke, E. Bruzell, H.H. Tonnesen, Investigation of the antimicrobial effect of natural deep eutectic solvents (NADES) as solvents in antimicrobial photodynamic therapy, J. Photochem. Photobiol. B 171 (2017) 27–33, https://doi.org/10.1016/j.jphotobiol.2017.04.030.
[2] S. Chattopadhyay, R.T. Raines, Collagen-based biomaterials for wound healing, Biopolymers 101 (2014) 821–833, https://doi.org/10.1002/bip.22486.
[3] M.D. Shoulders, R.T. Raines, Collagen structure and stability, Annu. Rev. Biochem. 78 (2009) 929–958, https://doi.org/10.1146/annurev.biochem.77.032207.120833.
[4] M. Meyer, Processing of collagen based biomaterials and the resulting materials properties, Biomed. Eng. Online 18 (2019) 24, https://doi.org/10.1186/s12938-019-0647-0.
[5] J. Zhang, R. Duan, Characterisation of acid-soluble and pepsin-solubilised collagen from frog (*Rana nigromaculata*) skin, Int. J. Biol. Macromol. 101 (2017) 638–642, https://doi.org/10.1016/j.ijbiomac.2017.03.143.
[6] L.M. Delgado, N. Shologu, K. Fuller, D.I. Zeugolis, Acetic acid and pepsin result in high yield, high purity and low macrophage response collagen for biomedical applications, Biomed. Mater. 12 (2017), 065009. https://doi.org/10.1088/1748-605X/aa838d.
[7] F.F. Felician, R.-H. Yu, M.-Z. Li, C.-J. Li, H.-Q. Chen, Y. Jiang, T. Tang, W.-Y. Qi, H.-M. Xu, The wound healing potential of collagen peptides derived from the jellyfish *Rhopilema esculentum*, Chin. J. Traumatol. 22 (2019) 12–20, https://doi.org/10.1016/j.cjtee.2018.10.004.
[8] Y.H. Choi, J. van Spronsen, Y. Dai, M. Verberne, F. Hollmann, I.W.C.E. Arends, G.-J. Witkamp, R. Verpoorte, Are natural deep eutectic solvents the missing link in understanding cellular metabolism and physiology? Plant Physiol. 156 (2011) 1701–1705, https://doi.org/10.1104/pp.111.178426.
[9] H.G. Morrison, C.C. Sun, S. Neervannan, Characterization of thermal behavior of deep eutectic solvents and their potential as drug solubilization vehicles, Int. J. Pharm. 378 (2009) 136–139, https://doi.org/10.1016/j.ijpharm.2009.05.039.
[10] K.O. Wikene, E. Bruzell, H.H. Tonnesen, Characterization and antimicrobial phototoxicity of curcumin dissolved in natural deep eutectic solvents, Eur. J. Pharm. Sci. 80 (2015) 26–32, https://doi.org/10.1016/j.ejps.2015.09.013.
[11] K.O. Wikene, H.V. Rukke, E. Bruzell, H.H. Tonnesen, Physicochemical characterisation and antimicrobial phototoxicity of an anionic porphyrin in natural deep eutectic solvents, Eur. J. Pharm. Biopharm. 105 (2016) 75–84, https://doi.org/10.1016/j.ejpb.2016.06.001.
[12] K.O. Wikene, E. Bruzell, H.H. Tonnesen, Improved antibacterial phototoxicity of a neutral porphyrin in natural deep eutectic solvents, J. Photochem. Photobiol. B 148 (2015) 188–196, https://doi.org/10.1016/j.jphotobiol.2015.04.022.
[13] H. Lores, V. Romero, I. Costas, C. Bendicho, I. Lavilla, Natural deep eutectic solvents in combination with ultrasonic energy as a green approach for solubilisation of proteins: application to gluten determination by immunoassay, Talanta 162 (2017) 453–459, https://doi.org/10.1016/j.talanta.2016.10.078.
[14] S. Khodaverdian, B. Dabirmanesh, A. Heydari, E. Dashtban-Moghadam, K. Khajeh, F. Ghazi, Activity, stability and structure of laccase in betaine based natural deep eutectic solvents, Int. J. Biol. Macromol. 107 (2018) 2574–2579, https://doi.org/10.1016/j.ijbiomac.2017.10.144.
[15] R. Esquembre, J.M. Sanz, J.G. Wall, F. del Monte, C.R. Mateo, M.L. Ferrer, Thermal unfolding and refolding of lysozyme in deep eutectic solvents and their aqueous dilutions, Phys. Chem. Chem. Phys. 15 (2013) 11248–11256, https://doi.org/10.1039/c3cp44299c.
[16] M.H. Zainal-Abidin, M. Hayyan, G.C. Ngoh, W.F. Wong, C.Y. Looi, Emerging frontiers of deep eutectic solvents in drug discovery and drug delivery systems, J. Control. Release 316 (2019) 168–195, https://doi.org/10.1016/j.jconrel.2019.09.019.
[17] K. Radosevic, I. Canak, M. Panic, K. Markov, M.C. Bubalo, J. Frece, V.G. Srcek, I.R. Redovnikovic, Antimicrobial, cytotoxic and antioxidative evaluation of natural deep eutectic solvents, Environ. Sci. Pollut. Res. Int. 25 (2018) 14188–14196, https://doi.org/10.1007/s11356-018-1669-z.
[18] R. Usha, T. Ramasami, Stability of collagen with polyols against guanidine denaturation, Colloids Surf. B Biointerfaces 61 (2008) 39–42, https://doi.org/10.1016/j.colsurfb.2007.07.005.
[19] R. Usha, S.S. Raman, V. Subramanian, T. Ramasami, Role of polyols (erythritol, xylitol and sorbitol) on the structural stabilization of collagen, Chem. Phys. Lett. 430 (2006) 391–396, https://doi.org/10.1016/j.cplett.2006.09.023.
[20] M.K. Wlodarczyk-Biegun, A. Del Campo, 3D bioprinting of structural proteins, Biomaterials 134 (2017) 180–201, https://doi.org/10.1016/j.biomaterials.2017.04.019.
[21] K.G. Grønlien, M.E. Pedersen, K.W. Sanden, V. Høst, J. Karlsen, H.H. Tønnesen, Collagen from turkey (*Meleagris gallopavo*) tendon: a promising sustainable biomaterial for pharmaceutical use, Sustain. Chem. Pharm. 13 (2019) 100166, https://doi.org/10.1016/j.scp.2019.100166.
[22] W.-M. Kulicke, C. Clasen, Viscosimetry of Polymers and Polyelectrolytes, Springer, Berlin, 2004.
[23] T. Nishihara, P. Doty, The sonic fragmentation of collagen macromolecules, Proc. Natl. Acad. Sci. U. S. A. 44 (1958) 411–417, https://doi.org/10.1073/pnas.44.5.411.
[24] S. Cliche, J. Amiot, C. Avezard, C. Gariepy, Extraction and characterization of collagen with or without telopeptides from chicken skin, Poult. Sci. 82 (2003) 503–509, https://doi.org/10.1093/ps/82.3.503.
[25] O.S. Rabotyagova, P. Cebe, D.L. Kaplan, Collagen structural hierarchy and susceptibility to degradation by ultraviolet radiation, Mater. Sci. Eng. C 28 (2008) 1420–1429, https://doi.org/10.1016/j.msec.2008.03.012.
[26] H. Noda, Partial specific volume of collagen, J. Biochem. 71 (1972) 699–703, https://doi.org/10.1093/oxfordjournals.jbchem.a129815.
[27] L. Han, Z.W. Zhang, B.H. Wang, Z.K. Wen, Construction and biocompatibility of a thin type I/II collagen composite scaffold, Cell Tissue Bank. 19 (2018) 47–59, https://doi.org/10.1007/s10561-017-9653-2.
[28] M.K. Shikh Alsook, A. Gabriel, M. Salouci, J. Piret, N. Alzamel, N. Moula, J.M. Denoix, N. Antoine, E. Baise, Characterization of collagen fibrils after equine suspensory ligament injury: an ultrastructural and biochemical approach, Vet. J. 204 (2015) 117–122, https://doi.org/10.1016/j.tvjl.2015.02.011.
[29] B.B. Doyle, E.G. Bendit, E.R. Blout, Infrared spectroscopy of collagen and collagen-like polypeptides, Biopolymers 14 (1975) 937–957, https://doi.org/10.1002/bip.1975.360140505.
[30] G.C. Na, UV spectroscopic characterization of type I collagen, Collagen Rel. Res. 8 (1988) 315–330, https://doi.org/10.1016/S0174-173X(88)80003-7.
[31] J.M. Menter, Temperature dependence of collagen fluorescence, Photochem. Photobiol. Sci. 5 (2006) 403–410, https://doi.org/10.1039/B516429J.

[32] S. Lindy, T. Sorsa, K. Suomalainen, A. Lauhio, H. Turto, Hyperchromic effect of collagen induced by human collagenase, Eur. J. Biochem. 156 (1986) 1–4, https://doi.org/10.1111/j.1432-1033.1986.tb09539.x.
[33] L.H. Lucas, B.A. Ersoy, L.A. Kueltzo, S.B. Joshi, D.T. Brandau, N. Thyagarajapuram, L.J. Peek, C.R. Middaugh, Probing protein structure and dynamics by second-derivative ultraviolet absorption analysis of cation-{pi} interactions, Protein Sci. 15 (2006) 2228–2243, https://doi.org/10.1110/ps.062133706.
[34] J.R. Lakowicz, Principles of Fluorescence Spectroscopy, 3rd ed. Springer, New York, 2006.
[35] S. Pundak, R.S. Roche, Tyrosine and tyrosinate fluorescence of bovine testes calmodulin: calcium and pH dependence, Biochemistry 23 (1984) 1549–1555, https://doi.org/10.1021/bi00302a032.
[36] D.M. Rayner, D.T. Krajcarski, A.G. Szabo, Excited state acid–base equilibrium of tyrosine, Can. J. Chem. 56 (1978) 1238–1245, https://doi.org/10.1139/v78-206.
[37] K.J. Willis, A.G. Szabo, Fluorescence decay kinetics of tyrosinate and tyrosine hydrogen-bonded complexes, J. Phys. Chem. 95 (1991) 1585–1589, https://doi.org/10.1021/j100157a015.
[38] Z. Deyl, R. Praus, H. Sulcova, J.N. Goldman, Fluorescence of collagen - properties of tyrosine residues and another fluorescent element in calf skin collagen, FEBS Lett. 5 (1969) 187–191, https://doi.org/10.1016/0014-5793(69)80328-5.
[39] E. Feinstein, G. Deikus, E. Rusinova, E.L. Rachofsky, J.B.A. Ross, W.R. Laws, Constrained analysis of fluorescence anisotropy decay: application to experimental protein dynamics, Biophys. J. 84 (2003) 599–611, https://doi.org/10.1016/S0006-3495(03)74880-2.
[40] Y. Liu, L. Liu, M. Chen, Q. Zhang, Double thermal transitions of type I collagen in acidic solution, J. Biomol. Struct. Dyn. 31 (2013) 862–873, https://doi.org/10.1080/07391102.2012.715042.
[41] L. He, C. Mu, D. Li, W. Lin, Revisit the pre-transition of type I collagen denaturation in dilute solution by ultrasensitive differential scanning calorimetry, Thermochim. Acta 548 (2012) 1–5, https://doi.org/10.1016/j.tca.2012.08.024.
[42] P. Montero, F. Jiménez-Colmenero, J. Borderìas, Effect of pH and the presence of NaCl on some hydration properties of collagenous material from trout (Salmo irideus Gibb) muscle and skin, J. Sci. Food Agric. 54 (1991) 137–146, https://doi.org/10.1002/jsfa.2740540115.
[43] Y. Dai, G.-J. Witkamp, R. Verpoorte, Y.H. Choi, Tailoring properties of natural deep eutectic solvents with water to facilitate their applications, Food Chem. 187 (2015) 14–19, https://doi.org/10.1016/j.foodchem.2015.03.123.
[44] A.P.R. Santana, D.F. Andrade, J.A. Mora-Vargas, C.D.B. Amaral, A. Oliveira, M.H. Gonzalez, Natural deep eutectic solvents for sample preparation prior to elemental analysis by plasma-based techniques, Talanta 199 (2019) 361–369, https://doi.org/10.1016/j.talanta.2019.02.083.
[45] W. Qu, R. Häkkinen, J. Allen, C. D'Agostino, P.A. Abbott, Globular and fibrous proteins modified with deep eutectic solvents: Materials for drug delivery, Molecules 24 (2019) https://doi.org/10.3390/molecules24193583.
[46] M. Andonegi, K. de la Caba, P. Guerrero, Effect of citric acid on collagen sheets processed by compression, Food Hydrocoll. 100 (2020) 105427, https://doi.org/10.1016/j.foodhyd.2019.105427.
[47] C. Murrieta-Martínez, H. Soto-Valdez, R. Pacheco-Aguilar, W. Torres-Arreola, F. Rodríguez-Felix, B. Ramírez-Wong, H. Santacruz-Ortega, I. Santos-Sauceda, G. Olibarría-Rodríguez, E. Márquez-Ríos, Effect of different polyalcohols as plasticizers on the functional properties of squid protein film (*Dosidicus gigas*), Coatings 9 (2019) 77, https://doi.org/10.3390/coatings9020077.
[48] T.I.A. Gouveia, K. Biernacki, M.C.R. Castro, M.P. Gonçalves, H.K.S. Souza, A new approach to develop biodegradable films based on thermoplastic pectin, Food Hydrocoll. 97 (2019) 105175, https://doi.org/10.1016/j.foodhyd.2019.105175.

Supplementary material

A natural deep eutectic solvent (NADES) as potential excipient in collagen-based products

Krister Gjestvang Grønlien[a,] *, Mona Elisabeth Pedersen[b] and Hanne Hjorth Tønnesen[a]

[a]*Section for Pharmaceutics and Social Pharmacy, Department of Pharmacy, University of Oslo, P.O. Box 1068 Blindern, NO-0316 Oslo, Norway;*
[b]*Nofima AS, P.O. Box 210, NO-1431 Ås, Norway*

* Corresponding author. E-mail address: k.g.gronlien@farmasi.uio.no

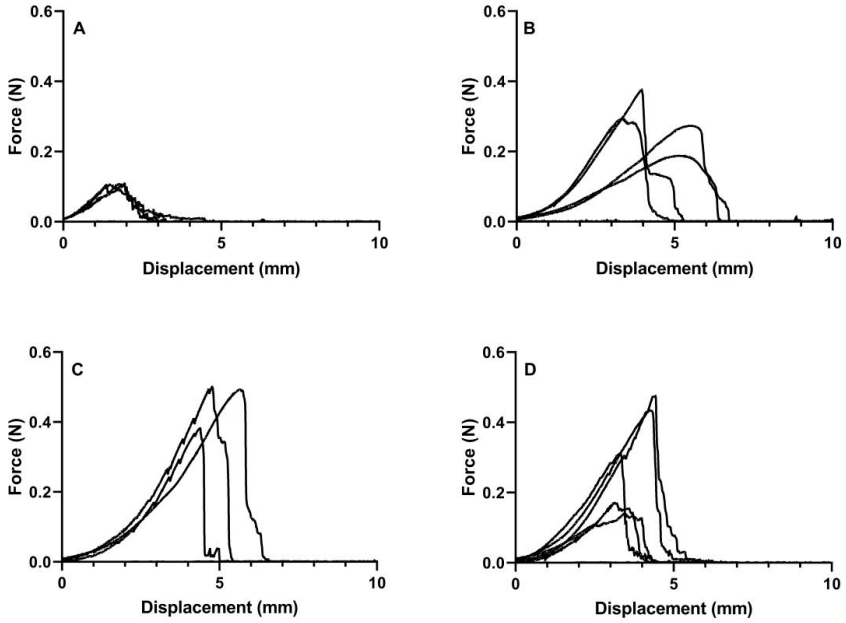

Fig. S1. Representative force-displacement curves for turkey tendon collagen (A), freeze-dried collagen-NADES sheets with NADES CX diluted 1:50 (B), 1:100 (C) and 1:200 (D).

Paper III

Tuning of 2D cultured human fibroblast behavior using lumichrome photocrosslinked collagen hydrogels

Krister Gjestvang Grønlien, Mona Elisabeth Pedersen, Sissel Beate Rønning, Nina Solberg, Hanne Hjorth Tønnesen

Submitted to *International Journal of Biological Macromolecules*.

III

Tuning of 2D cultured human fibroblast behavior using lumichrome photocrosslinked collagen hydrogels

Krister Gjestvang Grønlien[a]*, Mona Elisabeth Pedersen[b], Sissel Beate Rønning[b], Nina Solberg[b] and Hanne Hjorth Tønnesen[a]

[a]*Section for Pharmaceutics and Social Pharmacy, Department of Pharmacy, University of Oslo, P.O. Box 1068 Blindern, NO-0316 Oslo, Norway;*
[b]*Department of Raw Material and Process Optimization, Nofima AS, P.O. Box 210, NO-1431 Ås, Norway*

*Corresponding author. E-mail address: k.g.gronlien@farmasi.uio.no

Tuning of 2D cultured human fibroblast behavior using lumichrome photocrosslinked collagen hydrogels

Abstract

Biomedical application of collagen is limited by its slow gelation and crosslinking (via chemical or photochemical methods) could tailor these properties. Collagen has previously been crosslinked by chemical or photochemical methods. Chemical crosslinkers are often toxic, and the crosslinking reaction is difficult to control. Photochemical crosslinkers are usually biocompatible compounds that are activated upon irradiation. Riboflavin (vitamin B_2), a photochemical crosslinker of collagen, photodegrades to lumichrome upon irradiation. Cyclodextrins have previously been used to increase the aqueous solubility of lumichrome and regulate collagen self-assembly. In this study, lumichrome dissolved by cyclodextrin complexation was used as a photochemical crosslinker of collagen. Lumichrome photocrosslinking reduced the gelation time to 10 s, compared to 90 min for physical crosslinking. The formed hydrogels exhibited increased elasticity and water holding capacity compared to physically crosslinked collagen hydrogels and riboflavin photocrosslinked collagen hydrogels. Fibroblasts achieved a myofibroblastic phenotype alongside with an apparent migratory behavior when cultivated in 2D on lumichrome photocrosslinked gels as observed from real-time PCR and ELISA results. These biocompatible photocrosslinked hydrogels could have potential applications in biomedical applications, such as wound healing.

Keywords: collagen; lumichrome; fibroblasts

1. Introduction

Collagen is a structural protein that is considered as a good material candidate for fabrication of biocompatible and biodegradable scaffolds. Collagen is composed of three α-chains forming the characteristic triple helix structure of the protein. The α-chains consists of repeating triplets of the amino acids Glycine-X-Y, where X and Y are often proline and its metabolite hydroxyproline [1]. As the main structural protein in the extracellular matrix and connective tissue, collagen serves important functions in the body as support for cell growth and migration in various biological processes [2].

The production of scaffolds suitable for cell growth can be used in tissue engineering techniques. These techniques are considered as emerging technologies for production and engineering of tissue and biomimicking constructs and organs [3-5]. In tissue engineering, scaffolds are fabricated to serve as synthetic extracellular matrices to organize cells into three dimensional architectures, providing mechanical support and allowing for optimal growth, nutrition and biological signaling [6, 7]. Examples of scaffold fabrication techniques are electrospinning, bioprinting, production of hybrid scaffolds and hydrogels [8]. Constructs can be fabricated with cells seeded within the material, or used without cells to mimic biological constructs and scaffolds where seeding of cells on the scaffolds can be performed after the fabrication [9, 10]. The use of collagen in such applications has been considered somewhat limited due to low viscosity and slow gelation. Previous attempts to overcome these challenges include increasing collagen concentration, using protein or polymer blends, forming the structures directly into a supportive gelatin slurry bath (commonly known as FRESH bioprinting) or chemically modifying the collagen with methacrylate [11-15]. Recently, the effects of riboflavin (Vitamin B_2, RF) photocrosslinking on the printability of collagen bioinks for bioprinting have been studied. Diamantides *et al.* (2017) reported

that blue light-activated RF crosslinking improved the viscoelastic properties and printability of the bioink [16]. The study found that the RF photocrosslinking increased the storage modulus even before the bioink was brought to 37 °C, which is normally necessary for collagen to physically crosslink. RF photocrosslinking of collagen is commonly used in corneal crosslinking (CXL) for the treatment of the eye disease keratoconus [17]. Irradiation of RF results in photodegradation to lumichrome (LC) and lumiflavin (LF) in acidic and neutral, and alkaline solutions, respectively [18, 19]. Both LC and LF are considered as more photostable than RF and are efficient photogenerators of singlet oxygen in aqueous media [19-21]. LC has previously been investigated as a potential photosensitizer for inactivation of pathogens by antimicrobial photodynamic therapy (aPDT). The photosensitizer absorbs in both UVA and the blue region of the electromagnetic spectrum. The use of these metabolites as photosensitizers are, however, limited due to their low aqueous solubility [20].

Cyclodextrins (CDs) have been used to increase the water solubility of LC by a tenfold [20]. This increases the potential for LC as a photosensitizer. CDs are cyclic oligosaccharides with a hydrophobic inner and a hydrophilic outer structure [22]. They are stable in bases and weak organic acids but may be hydrolyzed in strong acids [23, 24]. Collagen has previously been modulated with CDs in order to regulate the collagen self-assembly and producing materials similar to native cornea [25]. CDs will bind to aromatic residues on the collagen molecule resulting in increased viscosity through collagen self-assembly [25]. Potential aromatic residues are phenylalanine and tyrosine, where the latter is almost completely eliminated if the protein is isolated by pepsin digestion [1]. CDs have as well been incorporated into collagen scaffolds to promote binding of growth factors and modulate stem cell activity [26]. In drug delivery systems, CDs have been incorporated into collagen membranes for controlled delivery

and increased bioavailability of ofloxacin for the treatment of bacterial keratitis [27].

Collagen is a protein interesting for tissue engineering applications, including the treatment of dermal loss and wound healing, mimicking the native structure of the skin. During wound healing, collagen is degraded by proteolytic enzymes to peptides, which are chemotactic to cells involved in the remodeling of the skin. This makes collagen an excellent candidate as an excipient in products for wound healing purposes [28, 29]. The invasion of cells, among other fibroblasts, is important for migration and proliferation into the wound site and synthesis of extracellular macromolecules. In granulation tissue, the fibroblasts are activated further into myofibroblasts, expressing α-smooth muscle actin (α-SMA). Myofibroblasts are involved in the wound healing by production and organization of the extracellular matrix [30]. It is further involved in wound contraction and scarring [31]. In all steps of the wound healing process, proteolytic enzymes play a major role modifying the wound matrix allowing cell migration and remodeling of the skin. These include matrix metalloproteinases (MMPs) and tissue inhibitors of MMPs (TIMPs). MMPs are important for collagen in wound healing, digesting the collagen to fragments, that may work chemotactically to cells involved in the healing process [32]. Syndecan-4 (SDC-4) is a cell receptor protein, which is a target for MMP-2 activity. Its extracellular domain is cleaved by this protease among others, thereby fine tuning the biological activity of the receptor protein [33]. SDC-4 belongs to a family of transmembrane heparan sulfate proteoglycans, and functions as co-receptors for growth factor activities, or signaling by itself via the cytoplasmatic domain regulating cell activities [34]. SDC-4 is shown to be important for the wound healing process [35]. The importance is highlighted by the ability to also interact with extracellular matrix ligands, morphogens and cytokines that are important regulators of tissue regeneration [34]. SDC-4 is a prominent regulator of focal adhesion

and actin-cytoskeletal organization formation in fibroblasts, and therefore a regulator of fibroblast cell adhesion and migration [36-38].

In the present study, the aim was to investigate the effects of CD modulation and LC photocrosslinking on collagen hydrogels. The physical properties of the hydrogels were studied with respect to water retention, mechanical properties and enzyme mediated scaffold degradation. Cell studies were conducted with fibroblasts seeded on top of the hydrogels. Cell morphology, cell viability, enzyme expression and secretion of proteins involved in extracellular matrix production and differentiation were monitored, as well as expression of corresponding genes. To our knowledge, this is the first paper describing the use of LC as a photochemical crosslinker for collagen.

2. Materials and methods

All experiments were performed at 25 °C unless other stated. LC photocrosslinked collagen hydrogels were crosslinked at 4 °C and used directly, or further physically crosslinked at 37 °C. Physically crosslinked collagen hydrogels, RF photocrosslinked collagen hydrogels and CD modulated collagen hydrogels were crosslinked at 37 °C.

2.1. Raw materials, chemicals, and reagents

Collagen isolated from industrially produced turkey (*Meleagris gallopavo*) rest raw materials was prepared as described in Grønlien *et al.* 2019 [39]. In brief, turkey tendons were manually cleaned and freeze dried for 48 h. A 0.5 M acetic acid solution with pepsin (1:10) was added to enzymatically hydrolyze the material. The hydrolyzed material was centrifuged, and the supernatant was collected. The collagen was precipitated by the addition of 4 M NaCl (1:3) and centrifuged. The collagen was re-solubilized in 0.5 M acetic acid and dialyzed against distilled water for 3 days. The

dialyzed solution was further freeze dried to obtain dry collagen. Other reagents were of analytical grade and were purchased from Merck KGaA (Darmstadt, Germany). Cell medium and components were all purchased from Thermo Fischer Scientific (Waltham, MA, USA).

2.2. Preparation of collagen hydrogels

The preparation of collagen hydrogels by physical crosslinking, lumichrome photocrosslinking, collagen photocrosslinking and CD modulations is described below. The preparation parameters are summarized in Table 1.

2.2.1. Hydrogels prepared by lumichrome photocrosslinking (LC gels)

LC photocrosslinked hydrogels (LC gels) were prepared by a direct photocrosslinking method. (2-Hydroxypropyl)-Beta-cyclodextrin (HPβCD) was dissolved in 20 mM acetic acid to a final concentration of 5% (w/v). LC was dissolved in the acidic HPβCD-solution to a final concentration of 250 µM. Collagen was dissolved in the acidic HPβCD-solution over 24 h to a final concentration of 5 mg/ml. The collagen solution was neutralized to pH 7.4 by the addition of 10X phosphate buffered saline (PBS) (0.1 × final volume of the combined solution), 1 M NaOH (0.023 × volume of added collagen-HPβCD solution) and Milli-Q water to give a final concentration of 4 mg/ml collagen, 200 µM LC and 1X PBS. The neutralized solutions were crosslinked by irradiation with either UVA (λ_{max} = 365 nm, 16.0 mW/cm^2) or blue light (λ_{max} = 405 nm, 17.8 mW/cm^2) (Bio X, Cellink, Gothenburg, Sweden) for 10 s. The gels were incubated at 37 °C for 90 min to complete the crosslinking procedure.

To distinguish the effects of lumichrome and HPβCD in cell studies, CD modulated collagen hydrogels (CD gels) were prepared with 5% (w/v) HPβCD added to 20 mM

acetic acid without the addition of LC and photocrosslinking.

2.2.2. Hydrogels prepared by physical crosslinking (Col gels)

Physically crosslinked hydrogels (Col gels) were prepared by a direct gelation method. Collagen was dissolved in 20 mM acetic acid over 24 h to a concentration of 5 mg/ml. The collagen solution was neutralized to pH 7.4 by the addition of 10X PBS (0.1 × final volume of the combined solution) and 1 M NaOH (0.023 × volume of added collagen solution) and diluted with Milli-Q water to give a final concentration of 4 mg/ml collagen and 1X PBS. The neutralized solution was incubated in the dark at 37 °C for 90 min to initiate gelling and self-assembly of the collagen.

2.2.3. Hydrogels prepared by riboflavin photocrosslinking (RF gels)

RF photocrosslinked hydrogels (RF gels) were prepared by a two-step gelation and photocrosslinking method. The hydrogels were prepared as for the Col gels, except with the addition of riboflavin 5'-monophosphate sodium salt to a final concentration of 0.01% (w/v) (265 µM). The neutralized solution was incubated in the dark at 37 °C for 1 h to initiate gelling and self-assembly of the collagen. The collagen hydrogels were irradiated with UVA (λ_{max} = 365 nm, 2.94 mW/cm^2) (Polylux-PT, Dreve, Germany), for 4 min to form interhelical crosslinks. The crosslinking procedure was then completed by incubating the hydrogels in the dark at 37 °C for 30 min.

2.3. Viscosity measurements

Viscosity measurements were performed on a Brookfield DV2T viscometer (Brookfield Engineering Laboratories, Inc., Middleboro, MA, USA) with spindles CPA-40Z (low viscosity samples < 10 mPa s; accuracy: ± 0.1 mPa·s; sample volume: 0.5 ml) and CPA-52Z (medium viscosity samples 10 – 300 mPa·s; accuracy: ± 3.1 mPa·s and high

viscosity samples ≥ 1500 mPa·s; accuracy: ± 31.0 mPa·s; sample volume: 0.5 ml). For the HPβCD-collagen samples, the temperature was kept constant at 4 °C, while for the neutralized and irradiated samples, the temperature was kept constant at 25 °C during the viscosity measurements (Grant LTD6G water bath, Grant Instruments, Cambridge, Ltd., Royston, UK). An average measurement was performed with the end condition parameter fixed at 2 min and speed depending on the expected viscosity (30 rpm for samples ≤ 300 mPa·s, 5 rpm for samples 300 – 1500 mPa·s, and 3 rpm for samples ≥ 1500 mPa·s).

2.4. Water holding capacity (centrifugal dehydration)

Col, RF, LC and CD gels were compared according to their water holding capacity. The hydrogels were placed in a Corning™ Costar™ Spin-X™ Centrifuge Tube Filter (Corning Inc. Life Sciences, Corning, NY, USA) with 0.45 µm pores and centrifuged at 2000 rpm (394*g*) [40]. The water retention at fixed time points between 2 and 240 min were calculated based on the weight ratio after and before centrifugation (W/W_0). The water holding capacity was defined as the percentage of weight remaining after centrifugation for 240 min.

2.5. Enzyme-mediated scaffold degradation

Enzyme-mediated scaffold degradation was studied by collagenase digestion of the prepared hydrogels. Type I collagenase from *Clostridium histolyticum* (C0130, Sigma-Aldrich, Saint Louis, MO, USA) was dissolved in Dulbecco's Phosphate Buffered Saline (DPBS) with 100 mg/l $MgCl_2$ and 100 mg/l $CaCl_2$ (Gibco, Life Technologies Corp., Grand Island, NY, USA) to a concentration of 5 CDU/ml. Hydrogels prepared were first soaked in DPBS for 30 min. Further, the hydrogels were treated with the collagenase solution and incubated at 37 °C. Remaining hydrogels were weighed and

compared with untreated hydrogels at fixed time points between 2 and 24 h. The collagenase solution was changed at every 3rd sampling.

2.6. Mechanical properties (macroindentation)

Mechanical properties of the prepared hydrogels were studied using TA-XTplusC Texture Analyser (Stable Micro Systems, Godalming, UK) in compression mode. The hydrogels were prepared in 24-well plates (VWR International., Radnor, PA, USA) according to the described preparation procedures. The resulting cylindrical gels equilibrated in PBS overnight (4 °C) and exposed to constant pressure at 0.1 mm/s with a maximum strain set to 60% by a cylindrical flat-ended indenter (ø = 6 mm) attached to a 500 g load cell. The probe was positioned approximately 2 mm above the sample prior to analysis. The stress (kPa) was calculated by the force and load-bearing area (A) of the gels and plotted against the strain. The elastic moduli (*E*) were calculated using Equation 1.

$$E = \frac{(1-v^2)\,F_c}{2\partial r}, \qquad \text{(Equation 1)}$$

where *v* is the Poisson's ratio, F_c is the applied force (N), δ is the indentation depth and *r* is the indenter radius [41]. Poisson's ratio was estimated to 0.5 for the hydrogels.

2.7. Cell studies

The cell studies consisted of three independent biological experiments, each performed in triplicates.

2.7.1. Cell culture

Human primary dermal fibroblasts (ATCC, Manassas, VA, USA) were cultured in Dulbecco's modified Eagle's medium (DMEM) supplemented with 10% (v/v) fetal

bovine serum (FBS), 100 U/ml penicillin, 100 µg/ml streptomycin and 250 µg/ml fungizone in tissue culture flasks. The cells were maintained at 37 °C in a humidified atmosphere of 5% CO_2. The cells were routinely sub-cultivated twice a week. The cells were examined by a Leica DM IL LED light microscope (Leica Microsystems Nussloch GmbH, Nußloch, Germany) during incubation. Cells between passages 3-10 were used in these experiments.

2.7.2. Cell behavior on hydrogels

Evaluation of the suitability of the hydrogels as cell matrices was conducted for 48 h on proliferating cells. The different hydrogels (prepared as described above) were prepared in the wells of 24-well plates with glass bottom (MatTek Corp., Ashland, MA, USA). Fibroblasts were seeded on top of the hydrogels at a concentration of 50 000 cells/well. To monitor cell nuclei and dead cells, the cells were stained with NucBlue™ Live ReadyProbes™ (Hoechst 33342, bisbenzimide) and Propidium Iodide ReadyProbes™ (Life Technologies Corp., Eugene, OR, US), respectively. The dyes were used according to the manufacturer's instructions. Media was replaced prior to staining. The cells were examined and imaged with a Zeiss Axio Observer Z1 microscope and the ZEN 2.6 blue edition microscopy software suite (Zeiss, Jena, Germany). If necessary, the brightness and contrast of the image were manually adjusted across the entire image using Adobe Photoshop Elements 11.

2.7.3. Immunofluorescence

Hydrogels (prepared as previously described) were prepared on the glass bottom of uncoated petri dishes with the area of the glass bottom corresponding to the size of the wells of a 24-well plate (MatTek Corp., Ashland, MA, USA). Fibroblasts were seeded on top of the hydrogels at a concentration of 50 000 cells/well. After 48 h, the cells were

washed twice with PBS, fixed with 4% (v/v) formaldehyde solution (252549, Sigma-Aldrich, Saint Louis, MO, USA) for 15 min. The cells were washed three times with 0.1% (v/v) Tween 20 in PBS (PBS-t) before permeabilizing with 0.1% (v/v) Triton X-100 in PBS for 10 min. After washing with PBS-t, the cells were blocked for 1 h (25 °C) or overnight (4 °C) using blocking buffer (ab126587, Abcam, Cambridge, UK) diluted in PBS-t before incubation with the primary antibody (Anti-alpha smooth muscle Actin antibody, ab5694, Abcam, Cambridge, UK or, Monoclonal Anti-Pan Cadherin antibody, C1821, Sigma, St. Louis, MO, USA, both 1:100 dilution) for 1 h (25 °C) or overnight (4 °C). Subsequent incubation with secondary antibody (Goat anti-Rabbit IgG (H+L) Cross-Adsorbed Secondary Antibody, Alexa Fluor™ 546, A-11010 or Goat anti-Mouse IgG, IgM, IgA (H+L) Secondary Antibody, Alexa Fluor™ 488, A-10667 both 1:400 dilution) for 1 h was performed after washing three times with PBS-t for 10 min. The cells were washed again thrice for 10 min before mounting the gels with Dako Fluorescence Mounting Medium (Dako North America, Carpinteria, CA, USA) or ProLong™ Diamond Antifade Mountant (P36961, Life Technologies Corp., Eugene, OR, US). For staining of the F-actin filaments, Alexa Fluor™ Phalloidin 488 or 555 (A12379 and A34055, Life Technologies Corp., Eugene, OR, US, 1:200 and 1:400 dilution, respectively) was added together with the secondary antibody. Hoechst (1:1000 dilution, Invitrogen, Carlsbad, CA, USA) was used to counterstain cell nuclei. The cells were examined and imaged with a Zeiss Axio Observer Z1 microscope and the ZEN microscopy software suite (Zeiss, Jena, Germany). If necessary, the brightness and contrast of the image were manually adjusted across the entire image using Adobe Photoshop Elements 11. Integrated density of fluorescence signal was quantified using ImageJ for staining of pan-cadherin [42]. Presented values for integrated densities are calculated from the sum of pixel values in section × area of section of 10 randomly

chosen cells.

2.7.4. Sandwich enzyme-linked immunosorbent assays (ELISAs)

The protein secretion of matrix metalloproteinase-2 (MMP-2), tissue inhibitor of metalloproteinase-2 (TIMP-2) and shed syndecan-4 (SDC-4) was measured in the cell media supernatants. Fibroblasts were cultured on hydrogels in 24-well plates (VWR, Radnor, PA, USA) for 48 h and the protein secretion was measured with commercial sandwich ELISA Kits (KHC3081 and EHTIMP2, Thermo Fisher Scientific, Inc., Waltham, MA, USA and ab213830, Abcam, Cambridge, UK). The ELISA kits were used according to the manufacturer's instructions. The optical density was detected using a Synergy H1 Hybrid Multi-Mode Microplate Reader (Biotek, Bad Friedrichshall, Germany).

2.7.5. RNA extraction and reverse transcriptase quantitative polymerase chain reaction (RT-qPCR)

After sampling the supernatant for the Sandwich ELISA, the remaining gels were washed two times with PBS and preserved at -80 °C for RT-qPCR experiments. The cells within the hydrogels were lysed and homogenized with a Precellys Evolution (Bertin Technologies SAS, Montigny-le-Bretonneux, France) for 2 cycles of 30 sec in RLT-lysis buffer (RNeasy® Plus Micro Kit, Qiagen, Hilden, Germany). The RNA was further purified using the RNeasy® Plus Micro Kit according to the manufacturer's protocol. cDNA was generated from the entire mRNA sample using TaqMan® Reverse Transcription Reagents (Applied Biosystem, Life Technologies, Carlsbad, CA, USA) according to the manufacturer's protocol. The cDNA (40 µl) was diluted to 65 µl with RNase-free water before aliquots were subjected to real-time qPCR by QuantStudio 5 Real-Time PCR System (Applied Biosystem, Life Technologies, Carlsbad, CA, USA).

Amplification of cDNA by 45 two-step cycles (15 sec at 95 °C for denaturation of DNA, 1 min at 60 °C for primer annealing and extension) was performed, and cycle threshold (Ct) values were obtained graphically (QuantStudio 5, Applied Biosystem, Design and Analysis Software version 1.5.1). The TaqMan® Gene Expression Assays used in this study are listed in Table 2. Gene expression of the samples was normalized against the average value of the housekeeping gene *EEF1A1*, and the ΔCt values were calculated according to the MIQE guidelines [43]. Comparison of the relative gene expression (fold change) of the fibroblasts between Col gels, LC gels and CD gels was derived by using the comparative Ct method. In short, values were generated by subtracting ΔCt values between two samples which gave a ΔΔCt value. The relative gene expression (fold change) was then calculated by the formula $2^{-\Delta\Delta Ct}$ [44]. The ΔΔCt value of LC gels and CD gels were calculated based on the mean ΔCt value of collagen. The real-time qPCR was performed with three technical replicates in three independent cell culture experiments seeded out in triplicates.

2.8. Statistical analysis

The data was presented as mean ± standard deviation from three independent experiments. Statistical analyses were performed by one-way ANOVA with Tukey's multiple comparisons using GraphPad Prism version 8.0.1 for Windows (GraphPad Software, La Jolla, CA, USA, www.graphpad.com). Differences were considered significant at $P < 0.05$.

2.9. Graphics

Illustrations were prepared in Microsoft PowerPoint. Graphs were created with GraphPad Prism version 8.0.1 for Windows (GraphPad Software, La Jolla, CA, USA, www.graphpad.com). Microscopy images were modulated with Adobe Illustrator CS6.

3. Results

3.1. Physical properties of collagen hydrogels are dependent on the preparation method and the crosslinking procedures

LC gels were formed directly after photocrosslinking of the neutralized collagen solution. A simplified illustration of the photocrosslinking by lumichrome is illustrated in Fig. 1a. To evaluate the optimal irradiation source for LC gels, the viscosity of gels before and directly after irradiation was measured. Collagen solutions with 5% (w/v) HPβCD and 250 µM LC exhibited a viscosity of 29.15 ± 0.44 mPa·s before crosslinking and 998.6 ± 55.2 mPa·s after irradiation by UVA (10 s, λ_{max} = 365 nm), while exposing the solution to blue light (10 s, λ_{max} = 405 nm) increased the viscosity to 1818 ± 83.8 mPa·s. Due to a superior viscosity and low deviation compared to the other formulations, we decided to continue with the formulation irradiated by blue light for 10 s. The collagen hydrogels prepared by physical crosslinking appeared translucent with a low water retention (2.67 ± 0.53 %). LC photocrosslinking of collagen resulted in gels with high water retention (44.97 ± 3.04 %), which appeared slightly yellow and transparent. RF photocrosslinking of collagen resulted in gels appearing yellow and translucent with a low water retention (2.57 ± 0.06 %). CD gels had a low water retention (5.12 ± 2.80 %) and appeared translucent after complete crosslinking procedure (Fig. 1b-c). Exposing the gels to collagenase resulted in complete degradation within 24 hours for all the gels, except RF gels. The weight of the LC gels became significantly reduced compared to the weight of the RF gels already after 3 h (Fig. 1d). After 24 h, 18.5 ± 1.9% of the RF gels were still intact (data not shown).

Compression tests illustrated the difference in the mechanical properties for the gels. Values for Young's moduli, ultimate compressive strengths and fracture points are

presented in Table 3. Stress-strain curves are presented in Fig. 1e.

3.2. Fibroblasts seeded in 2D on LC gels exhibited a myofibroblastic phenotype and collective migratory behavior

Light microscopy investigation of the fibroblasts cultured on the different hydrogels showed different cell behavior dependent on type of crosslinking. Fibroblasts seeded on Col gels and CD gels were evenly distributed throughout the hydrogel surface (Fig. 2a left and right), however no cell clustering was observed, despite cell contact. Cells seeded on hydrogels with LC photocrosslinking, on the other hand, were self-organized into cell clusters and the fibroblast had a more elongated morphology (Fig. 2a, middle). The cell viability was high, demonstrated by the low appearance of dead cells on either of the hydrogels (Fig. 2b). Cells seeded on top of hydrogels photocrosslinked using RF did, however, lead to dramatically reduced cell viability and were therefor not included in the following cell behavior experiments (Fig. S1).

When examining filamentous actin (F-actin) we clearly observed more prominent intracellular stress fibers in the Col and CD gels, while cells seeded onto LC gels demonstrated stronger staining of peripheral stress fibers (Fig. 3a). All the hydrogels seemed to stimulate the expression of the common myofibroblast marker α-SMA (Fig. 3b), however, cells seeded onto the LC hydrogel displayed a more mature organization of α-SMA visualized as long aligned fibers, whereas the other hydrogels displayed immature, less organized and prominent punctured structures (Fig. 3c). Immunostaining against cadherin, a cell adhesion protein related to myofibroblast differentiation, revealed a more prominent expression in fibroblasts on LC gels with significantly higher level ($P < 0.001$) than in the Col gels and CD gels (Fig. 4). Secondary antibody controls were included in the experiments to verify specific staining of α-SMA and

cadherin (Fig. S2 and S3). On the gene level, the fibroblasts seeded on Col gels had a significantly higher mRNA expression of α-SMA (*ACTA2*) ($P < 0.001$) compared to both LC gels and CD gels (Fig. 5a). Fibroblasts cultured on Col gels and LC gels showed a lower expression of collagen type 1 mRNA expression (*COL1A2*) compared to cells cultured on CD gels (Fig. 5b).

The mRNA expression of the *SDC4* gene in fibroblasts seeded on Col gels was significantly higher than the other gels ($P < 0.001$) (Fig. 5c). The levels of SDC-4 shed by fibroblasts on the different collagen gels were variable, both within the same gel samples and between gel types, indicating a spontaneous shedding. The experiment was repeated with two different ELISA kits, with similar results. Despite no significant differences between the different gels, the LC and CD gel seemed to have a slightly higher level of shed SDC-4 (Fig. 5d). The ratio between secreted MMP-2 and its inhibitor TIMP-2 is presented (Fig. 5e). The ratio can be used as an indication for the enzyme activity and was calculated based on the results from the ELISA experiments for MMP-2 and TIMP-2. The MMP-2/TIMP-2 ratio for the cells on LC gels was significantly higher than Col gels and CD gels ($P \leq 0.01$ and $P \leq 0.001$, respectively). The difference between the Col gels and CD gels was not significant. The MMP-2 and TIMP-2 raw data are included in the supplementary material (Fig. S4). The cells seeded on Col gels showed significantly higher MMP-2 protein secretion than the LC gels ($P \leq 0.05$). There was no significant difference in the MMP-2 protein secretion between LC gels and the gels made with HPβCD. The cells seeded on LC gels had the lowest TIMP-2 protein secretion of all samples. There was no significant difference in the TIMP-2 secretion between Col gels and CD gels.

4. Discussion

In this study, we developed a hydrogel based on CD modulated collagen and LC photocrosslinking to tailor the properties of the material. CDs are known to interact with collagen by binding with hydrophobic amino acids in the protein chain. This has previously been shown to reduce the fibril diameter during gelation, and provide increased viscosity, mechanical strength and transparency [25]. The LC gels were clearly more transparent compared to Col gels and RF gels after completed photocrosslinking and incubation. The CD gels without LC did, however, become translucent, similar to the Col gels. A change in the crosslinking procedure from irradiation before to irradiation after incubation for 1 h (as used in the RF photocrosslinking procedure) resulted in more translucent gels but quite similar mechanical strength (data not shown). The ability of LC photocrosslinking to achieve gelling already after 10 s of irradiation may be crucible for the organization of collagen fibrils and transparency. This will further increase the potential for use in biofabrication applications. Transparent materials may be desirable for certain applications, like in the eye [45]. Based on these observations, and the ease of the crosslinking procedure, the further photocrosslinking irradiation was performed directly after neutralization and before the final incubation.

The water holding capacity, enzymatic resistance and mechanical properties of the hydrogels depended on the crosslinking procedure. The RF gels exhibited a surprisingly low water holding capacity, despite a high Young's modulus and a high enzymatic resistance to collagenase. This indicates that RF gels have higher crosslinking density than the other gels [46, 47]. The water holding capacity of the LC gels was superior. This is probably due to a more organized alignment of the collagen molecules by CD modulation before photocrosslinking, and stabilization of the structure after

photocrosslinking [25, 48]. The potential water absorption properties by CD was eliminated by including and comparing the significantly lower water holding capacity of CD gels with LC gels. The LC gels were, however, least resistant to the collagenase degradation. In cases where there is an elevated level of MMPs, like collagenases, the LC gels may be broken down to smaller fragments in a shorter time than collagen hydrogels prepared by other crosslinking procedures. Further, this indicates a good biodegradability. The collagenase effect is dependent on the availability of the site of cleavage and may be influenced by the apparent difference in fibril organization after crosslinking [49]. The water holding capacity is on the other side a measurement on the hydrogen bonding ability and may be an indication of a change in crosslinking [50-52]. The difference in water holding capacity between the gels indicates a variation in crosslinking of the structures. The variation in crosslinking is supported by the difference in resistance to collagenase. The crosslinking will further change the mechanical strength [53]. This resulted in more brittle LC gels, but with a high Young's modulus (higher elasticity). The high water retention may be desirable in tissue engineering applications, as it will facilitate the diffusion and retention of nutrition and provide elasticity and flexibility similar to the native extracellular matrix [54].

Fibroblasts were seeded on top of the produced gels. By examining the cell distribution, some of the cells seemed to migrate into the gels. Most of the cells were, however, still distributed on the gel surface after 48 h (results not shown). The 3D migration through the gels were not studied further. The cell viability was high on Col gels, LC gels and CD gels, illustrated by a higher number of live cell nuclei compared to the low number of dead cells. The RF gels did, however, not allow for cell growth. The reason for the low viability is unknown but was confirmed in three independent experiments. The only differences between the RF gels and the Col gels, were the addition of 0.01% (w/v) RF

and a photocrosslinking procedure after 1 h incubation in the former. The gels were incubated for 30 min after irradiation to complete crosslinking, before addition of cells. Gels prepared with the same RF concentration and similar photocrosslinking procedure, have previously been tested as a scaffold for fibrochondrocytes with excellent viability. This revealed most likely cell specific effects of RF in our study [55]. Another potential explanation is the formation of hydrogen peroxide (H_2O_2) during irradiation of riboflavin in the presence of certain amino acids [56]. This suggested the need for a reduction in irradiation time during the preparation of collagen constructs. Based on these results, the RF gels were not included in the further cell studies.

All cells cultured on the different hydrogels expressed α-SMA, as demonstrated by the immunofluorescence staining. RT-qPCR was further used to quantify the expression of α-SMA by the cells in the gels after 48 h. The differentiation of fibroblasts into myofibroblasts on gels is known to be dependent on, among other factors, the gel rigidity [57]. The myofibroblasts play an important role in the wound healing process, promoting matrix synthesis and wound contraction [58]. Cells cultured on a rigid surface, like the bottom of a well plate or a rigid gel, can differentiate into myofibroblasts at low seeding densities [59, 60]. The cells were seeded with similar density for all samples, and with a density more than 3-fold higher than the reported values in the literature. Further, this indicates that the differentiation was a result of the material and not the seeding density. The LC gels exhibited remarkably higher stress at lower strains, which can influence the myofibroblast differentiation. Even though the mRNA expression of α-SMA by fibroblasts seeded on LC gels and CD gels was somewhat low and the fibroblasts seeded on the Col gels expressed higher α-SMA expression at the time of sampling, the immunofluorescence results indicated that the LC gels contained fibroblasts with more organized α-SMA. This may indicate that the

onset of myofibroblast differentiation was earlier in fibroblasts grown on LC gels, reflecting the observed downregulation of α-SMA at mRNA level. This was further supported by the appearance of α-SMA in Col gels and CD gels, expressed as an unorganized grainy pattern, rather than fibers. The formation of cadherin-type cell-cell adherens junctions (AJs) are related to the differentiation of fibroblasts to myofibroblasts. Cadherins were expressed in fibroblasts on LC gels, significantly higher than in cells seeded on the other gels. The cadherins were detected throughout the cells on the LC gels, including focal adhesion points. AJs are normally absent in normal fibroblasts, which do not develop prominent stress fibers and α-SMA [61]. The increased expression of cadherins for cells seeded on LC gels may be connected with the more prominent myofibroblastic phenotype [61].

SDC-4 is a regulator of fibroblast cell adhesion and migration by regulating focal adhesion and actin-cytoskeletal organization formation in fibroblasts. SDC-4 shedding of its ectodomain results in an altered distribution of cytoskeletal components, functional loss of adhesion, and gain of migratory capacities [62]. Our results showed a redistribution of stress fibers in LC gels, which is a morphological characteristic observed in less adhesive and more migratory cells [63, 64]. An increased SDC-4 shedding, although not significant, was observed from cells grown on LC gels. Together with less SDC-4 production and reorganized actin-cytoskeletal organization of less adhesive cells, this supports a more migratory fibroblast phenotype when grown on LC gels.

MMP-2 is known as an enzyme involved in wound healing and remodeling of the extracellular matrix by promoting migration of fibroblasts to the wound site [65]. The ratio between the protein secretion of MMP-2 and its inhibitor, TIMP-2, indicated a

balance of the expression of the proteins leaning towards MMP-2 for cells seeded on all of the gels. Fibroblasts seeded on LC gels had the highest MMP-2/TIMP-2 ratio. The MMP-2 and TIMP-2 levels were, however, lower in cells grown on the LC and CD gels, indicating a lower release or complexation of the enzyme. A possible explanation is complexation of MMPs with TIMPs or that the protein is shielded by complexation with CDs. The ratio of MMP-2/TIMP-2 was significantly higher for cells seeded on LC compared to the other gels, suggesting that complexation with TIMPs may explain the lower enzyme levels.

The tendency of increased SDC-4 shedding from fibroblasts seeded on collagen hydrogels can potentially be due to an elevated MMP-2/TIMP-2 ratio, whereas MMP-2 is known to cleave SDC-4 [66]. SDC-4 is a target for MMP-2 activity, and shedding of syndecan-4 is necessary for migration, therefore also indirectly an indication of migratory behavior [62]. The *COL1A2* mRNA expression for fibroblasts seeded on CD gels was significantly higher than both LC gels and Col gels. LC gels also tended to have a higher expression than Col gels (although not significant). The levels of TIMP-2 were highest in Col gels, which can explain the somewhat lower *COL1A2* mRNA expression for the same gels, whereas the addition of TIMP-2 has shown to suppress collagen synthesis and mRNA expression in keloid fibroblasts [67]. In cardiac fibroblasts, SDC-4 is shown to increase *COL1A2* mRNA expression and, as well as increasing α-SMA protein expression and fiber organization, correlating with the results in our study [68].

The fibroblasts seeded on LC gels exhibited an apparent cell clustering, despite results on mRNA and protein expression for SDC-4 and MMP-2 indicating a low adhesively and a more migratory behavior. Cell clustering is depended on extracellular matrix

properties, growth factors and cell-cell interaction stabilization. Formation of fibroblast clusters can further be promoted by procontractile conditions, i.e., presence of growth factors that activate signaling proteins, like Rho (e.g., growth factors in FBS), whereas growth factors that activate Rac (e.g., platelet-derived growth factor, PDGF) will promote promigratory conditions where fibroblasts migrate as individuals without clustering [69]. FBS was used as an additive with growth factors in the present study. Rac will stimulate the protrusion of fibroblast dendritic extensions [69, 70]. The clustering can be independent on the SDC-4, which leads to the involvement of other receptors, like cadherins, which are important for cell-cell interactions [71]. As discussed above, cadherin was used to assess AJs expression in myofibroblasts. Cadherins can further be addressed to clustering properties. Cadherin has also been studied as a mechanotransducer to stimulate the polarization of cell clusters and their collective forward-directed migration movement [72]. This behavior may be important for applications, such as in wound healing [73]. The promigratory versus procontractile behavior was not studied further.

The mechanisms of RF photocrosslinking of collagen have previously been discussed and thoroughly studied [74]. LC photocrosslinking of collagen to a firm gel can as demonstrated in the present work, be performed at 4 °C without further crosslinking. Photocrosslinking with RF needs to be performed after incubation at 37 °C to form a firm gel [16, 55, 75]. RF is rapidly photodecomposed to LC within minutes under certain experimental conditions [19]. This might indicate that the photocrosslinking by RF actually is a result of the photochemical degradation of the photosensitizer. This hypothesis is further supported by studies on the phototoxic effect of RF, being a hydrophilic substance, while LC is lipophilic and can penetrate the bacterial membrane [20]. Further, the crosslinking effect can be due to the formation of ROS and singlet

oxygen ($^1O_2$) by excitation of RF, supported by the ability of quenchers to inhibit the photocrosslinking properties of RF [75, 76]. Similar mechanisms can occur in the presence of LC. The quantum yield of $^1O_2$ formation by LC at 365 nm exposure is more than 30% higher than for RF in aqueous media ($\Phi_{RF} = 0.48$, $\Phi_{LC} = 0.63$) [19].

The CD is a multifunctional excipient in the current formulation, increasing viscosity, decreasing fiber diameter and securing transparent gels. CDs are also applied to increase solubility of components with poor aqueous solubility, like LC in the present formulation. The application of LC as a photosensitizer has been limited due to the low aqueous solubility, as described in the introduction. Complexation of LC with HPβCD has increased the aqueous solubility of LC by a tenfold and has previously been demonstrated a photoinactivation effect on certain bacteria [20]. By combining a CD-LC complex with a collagen delivery system, we have developed a potential formulation strategy, e.g., for the treatment of localized infections. Treatment of the eye disease keratoconus is another possible application of the collagen-LC-CD formulation. The conventional therapy for this disease consists of RF photocrosslinking by application of RF eye drops and UVA irradiation, and was first described by Wollensak *et al.* in 2003 [17]. The procedure requires a long UVA irradiation procedure, up to 30 minutes [17]. A recent study has, however, shown that an accelerated crosslinking of 10 minutes is comparable to the conventional procedure [77]. CXL of the cornea painful for some patients, especially postoperative, and requires active pain management [78]. Based on our results, an eye drop formulation containing CDs and LC can possibly be used in CXL. HPβCD is considered safe for use in eye drop formulations [79]. Further, the mechanical properties and transparency of the LC-collagen gels, combined with facilitated cell growth make them suitable as, among others, corneal transplants or shields with controlled release of relevant drugs added to the device [45]. Recently,

ultra-stiff compressed collagen constructs have been developed for corneal perforation patch grafts using *in situ* RF photochemical crosslinking combined with compression to make nearly transparent constructs with enhanced mechanical properties [80]. It should be possible to substitute RF with LC for the preparation of similar constructs.

In addition to good physical properties, i.e., good mechanical properties and excellent water holding capacity, it is important that scaffolds for tissue engineering, e.g., eye applications and in wound treatment allow for sufficient exchange of nutrients and oxygen. The fibroblasts in the present work were seeded on top of the hydrogels. The translation of the present results (in 2D) to the proposed applications (in 3D) can, however, be challenging. The LC photocrosslinked scaffolds are currently further developed in our lab and will therefore be assessed for their suitability in tissue engineering (3D cultures) and wound healing in future work.

5. Conclusions

This study has demonstrated the effects of photocrosslinking of collagen hydrogels by LC on human fibroblasts cultured in 2D. LC photocrosslinking reduced the gelation time to 10 s prior to optional physical crosslinking. The gels exhibited stronger water holding capacity and higher elasticity compared to Col gels and RF gels. The use of CDs in the hydrogel formulation increased the solubility of LC and potentially contributed to increased transparency and good physical properties of the hydrogel. CD modulation of collagen gels combined with LC photocrosslinking can further be utilized in drug delivery. Cell studies indicated good biocompatibility and an apparent migratory behavior of fibroblasts seeded on the gel. The fibroblasts seeded on LC gels seemed to differentiate into myofibroblasts. LC is an endogenous compound and LC photocrosslinking of collagen offers an alternative to other potentially toxic

crosslinkers. Further studies of fibroblast behavior in 3D and *in vivo* have to be performed to assess the suitability in tissue engineering and wound healing.

Acknowledgments

The authors are grateful to Bente Amalie Breiby, Department of Pharmacy, University of Oslo, Ulrike Böcker, Silje Kristine Bergum and R. Christel Andreassen, Nofima AS for technical support, Karen Wahlstrøm Sanden, Nofima AS for isolation of collagen from turkey tendon and Raj Kumar Thapa, Department of Pharmacy, University of Oslo, for valuable discussions. Turkey tendon by-products and financial support for isolation of collagen from turkey were contributed by Norilia AS.

Conflict of interest

The authors declare that they have no conflict of interest.

Funding

This work was partially supported by a grant from Norwegian Fund for Research Fees for Agricultural Products (NFR 262300) and Norilia AS (Oslo, Norway). The funder had no role in study design, data collection and analysis, decision to publish, or preparation of the manuscript.

CRediT authorship contribution statement

K. G. Grønlien: Conceptualization, Investigation, Visualization, Writing – original draft, Writing – review & editing.

M. E. Pedersen: Conceptualization, Supervision, Investigation, Writing – original draft, Writing – review & editing.

S. B. Rønning: Supervision, Investigation, Visualization, Writing – original draft, Writing – review & editing.

N. Solberg: Supervision, Investigation, Writing – review & editing

H. H. Tønnesen: Conceptualization, Funding acquisition, Supervision, Writing – original draft, Writing – review & editing.

Disclosure statement

Norilia AS provided the turkey tendon by-products and funded the isolation of collagen, but was not involved in the study design, interpretation of the data, writing of the manuscript, or decision to publish.

References

[1] M.D. Shoulders, R.T. Raines, Collagen structure and stability, Annu. Rev. Biochem. 78 (2009) 929-958. https://doi.org/10.1146/annurev.biochem.77.032207.120833.

[2] C. Frantz, K.M. Stewart, V.M. Weaver, The extracellular matrix at a glance, J. Cell Sci. 123(24) (2010) 4195-4200. https://doi.org/10.1242/jcs.023820.

[3] W. Aljohani, M.W. Ullah, X. Zhang, G. Yang, Bioprinting and its applications in tissue engineering and regenerative medicine, Int. J. Biol. Macromol. 107 (2018) 261-275. https://doi.org/10.1016/j.ijbiomac.2017.08.171.

[4] P. Abdollahiyan, B. Baradaran, M. de la Guardia, F. Oroojalian, A. Mokhtarzadeh, Cutting-edge progress and challenges in stimuli responsive hydrogel microenvironment for success in tissue engineering today, J. Control Release 328 (2020) 514-531. https://doi.org/10.1016/j.jconrel.2020.09.030.

[5] X. Cui, J. Li, Y. Hartanto, M. Durham, J. Tang, H. Zhang, G. Hooper, K. Lim, T. Woodfield, Advances in Extrusion 3D Bioprinting: A Focus on Multicomponent Hydrogel-Based Bioinks, Adv. Healthc. Mater. 9(15) (2020) 1901648. https://doi.org/10.1002/adhm.201901648.

[6] J.A. Hunt, R. Chen, T. van Veen, N. Bryan, Hydrogels for tissue engineering and regenerative medicine, J. Mater. Chem. B 2(33) (2014) 5319-5338. https://doi.org/10.1039/C4TB00775A.

[7] J.L. Drury, D.J. Mooney, Hydrogels for tissue engineering: scaffold design variables and applications, Biomaterials 24(24) (2003) 4337-4351. https://doi.org/10.1016/S0142-9612(03)00340-5.

[8] A. De Mori, M. Peña Fernández, G. Blunn, G. Tozzi, M. Roldo, 3D Printing and Electrospinning of Composite Hydrogels for Cartilage and Bone Tissue Engineering, Polymers (Basel) 10(3) (2018) 285. https://doi.org/10.3390/polym10030285.

[9] J. Groll, J.A. Burdick, D.W. Cho, B. Derby, M. Gelinsky, S.C. Heilshorn, T. Jüngst, J. Malda, V.A. Mironov, K. Nakayama, A. Ovsianikov, W. Sun, S. Takeuchi, J.J. Yoo, T.B.F. Woodfield, A definition of bioinks and their distinction from biomaterial inks, Biofabrication 11(1) (2018) 013001. https://doi.org/10.1088/1758-5090/aaec52.

[10] S.R. Caliari, J.A. Burdick, A practical guide to hydrogels for cell culture, Nat. Methods 13(5) (2016) 405-414. https://doi.org/10.1038/nmeth.3839.

[11] T.J. Hinton, Q. Jallerat, R.N. Palchesko, J.H. Park, M.S. Grodzicki, H.-J. Shue, M.H. Ramadan, A.R. Hudson, A.W. Feinberg, Three-dimensional printing of complex biological structures by freeform reversible embedding of suspended hydrogels, Sci. Adv. 1(9) (2015) e1500758. https://doi.org/10.1126/sciadv.1500758.

[12] N. Ashammakhi, S. Ahadian, C. Xu, H. Montazerian, H. Ko, R. Nasiri, N. Barros, A. Khademhosseini, Bioinks and bioprinting technologies to make heterogeneous and biomimetic tissue constructs, Mater. Today Bio 1 (2019) 100008. https://doi.org/10.1016/j.mtbio.2019.100008.

[13] J. Gopinathan, I. Noh, Recent trends in bioinks for 3D printing, Biomater Res 22 (2018) 11-11. https://doi.org/10.1186/s40824-018-0122-1.

[14] E.O. Osidak, P.A. Karalkin, M.S. Osidak, V.A. Parfenov, D.E. Sivogrivov, F.D.A.S. Pereira, A.A. Gryadunova, E.V. Koudan, Y.D. Khesuani, V.A. Kasyanov, S.I. Belousov, S.V. Krasheninnikov, T.E. Grigoriev, S.N. Chvalun, E.A. Bulanova, V.A. Mironov, S.P. Domogatsky, Viscoll collagen solution as a novel bioink for direct 3D bioprinting, J. Mater. Sci. Mater. Med. 30(3) (2019) 31. https://doi.org/10.1007/s10856-019-6233-y.

[15] G. Tronci, C.A. Grant, N.H. Thomson, S.J. Russell, D.J. Wood, Multi-scale mechanical characterization of highly swollen photo-activated collagen hydrogels, J. R. Soc. Interface 12(102) (2015) 20141079. https://doi.org/10.1098/rsif.2014.1079.

[16] N. Diamantides, L. Wang, T. Pruiksma, J. Siemiatkoski, C. Dugopolski, S. Shortkroff, S. Kennedy, L.J. Bonassar, Correlating rheological properties and printability of collagen bioinks: the effects of riboflavin photocrosslinking and pH, Biofabrication 9(3) (2017) 034102. https://doi.org/10.1088/1758-5090/aa780f.

[17] G. Wollensak, E. Spoerl, T. Seiler, Riboflavin/ultraviolet-A–induced collagen crosslinking for the treatment of keratoconus, Am. J. Ophthalmol. 135(5) (2003) 620-627. https://doi.org/10.1016/s0002-9394(02)02220-1.

[18] R. Huang, H.J. Kim, D.B. Min, Photosensitizing Effect of Riboflavin, Lumiflavin, and Lumichrome on the Generation of Volatiles in Soy Milk, J. Agric. Food Chem. 54(6) (2006) 2359-2364. https://doi.org/10.1021/jf052448v.

[19] C.K. Remucal, K. McNeill, Photosensitized Amino Acid Degradation in the Presence of Riboflavin and Its Derivatives, Environ. Sci. Technol. 45(12) (2011) 5230-5237. https://doi.org/10.1021/es200411a.

[20] V.J.V. Bergh, E. Bruzell, A.B. Hegge, H.H. Tønnesen, Influence of formulation on photoinactivation of bacteria by lumichrome, Pharmazie 70(9) (2015) 574-580. https://doi.org/10.1691/ph.2015.5006.

[21] A.M. Edwards, C. Bueno, A. Saldano, E. Silva, K. Kassab, L. Polo, G. Jori, Photochemical and pharmacokinetic properties of selected flavins, J. Photochem. Photobiol. B 48(1) (1999) 36-41. https://doi.org/10.1016/s1011-1344(99)00006-8.

[22] S.V. Kurkov, T. Loftsson, Cyclodextrins, Int. J. Pharm. 453(1) (2013) 167-180. https://doi.org/10.1016/j.ijpharm.2012.06.055.

[23] A. Hedges, Chapter 22 - Cyclodextrins: Properties and Applications, in: J. BeMiller, R. Whistler (Eds.), Starch (Third Edition), Academic Press, San Diego, 2009, pp. 833-851.

[24] R. Vaitkus, G. Grinciene, E. Norkus, Peculiarities of β-cyclodextrin acid hydrolysis, Chemija 19 (2008).

[25] S. Majumdar, X. Wang, S.D. Sommerfeld, J.J. Chae, E.-N. Athanasopoulou, L.S. Shores, X. Duan, L.M. Amzel, F. Stellacci, O. Schein, Q. Guo, A. Singh, J.H. Elisseeff, Cyclodextrin Modulated Type I Collagen Self-Assembly to Engineer Biomimetic Cornea Implants, Adv. Funct. Mater. 28(41) (2018) 1804076. https://doi.org/10.1002/adfm.201804076.

[26] W.K. Grier, A.S. Tiffany, M.D. Ramsey, B.A.C. Harley, Incorporating β-cyclodextrin into collagen scaffolds to sequester growth factors and modulate mesenchymal stem cell activity, Acta Biomater. 76 (2018) 116-125. https://doi.org/10.1016/j.actbio.2018.06.033.

[27] Y. Chen, W. Song, X. Zhao, Q. Han, L. Ren, An antibacterial collagen membrane crosslinked by the inclusion complex of β-cyclodextrin dialdehyde and ofloxacin for bacterial keratitis, RSC Adv. 8(32) (2018) 18153-18162. https://doi.org/10.1039/C8RA02160K.

[28] A.E. Postlethwaite, J.M. Seyer, A.H. Kang, Chemotactic attraction of human fibroblasts to type I, II, and III collagens and collagen-derived peptides, Proc. Natl. Acad. Sci. U. S. A. 75(2) (1978) 871-875. https://doi.org/10.1073/pnas.75.2.871.

[29] S. Chattopadhyay, R.T. Raines, Collagen-based biomaterials for wound healing., Biopolymers 101(8) (2014) 821-833. https://doi.org/10.1002/bip.22486.

[30] B. Hinz, The role of myofibroblasts in wound healing, Curr. Res. Transl. Med. 64(4) (2016) 171-177. https://doi.org/10.1016/j.retram.2016.09.003.

[31] B. Hinz, G. Gabbiani, Cell-matrix and cell-cell contacts of myofibroblasts: role in connective tissue remodeling, Thromb. Haemost. 90(12) (2003) 993-1002. https://doi.org/10.1160/TH03-05-0328.

[32] M.P. Caley, V.L.C. Martins, E.A. O'Toole, Metalloproteinases and Wound Healing, Adv. Wound Care 4(4) (2015) 225-234. https://doi.org/10.1089/wound.2014.0581.

[33] T. Manon-Jensen, Y. Itoh, J.R. Couchman, Proteoglycans in health and disease: the multiple roles of syndecan shedding, FEBS J. 277(19) (2010) 3876-89. https://doi.org/10.1111/j.1742-4658.2010.07798.x.

[34] H. Chung, H.A.B. Multhaupt, E.-S. Oh, J.R. Couchman, Minireview: Syndecans and their crucial roles during tissue regeneration, FEBS Lett. 590(15) (2016) 2408-2417. https://doi.org/10.1002/1873-3468.12280.

[35] T.T. Vuong, T.M. Reine, A. Sudworth, T.G. Jenssen, S.O. Kolset, Syndecan-4 Is a Major Syndecan in Primary Human Endothelial Cells In Vitro, Modulated by Inflammatory Stimuli and Involved in Wound Healing, J. Histochem. Cytochem. 63(4) (2015) 280-292. https://doi.org/10.1369/0022155415568995.

[36] R. Brooks, R.C. Williamson, M.D. Bass, Syndecan-4 independently regulates multiple small GTPases to promote fibroblast migration during wound healing, Small GTPases 3(2) (2012) 73-79. https://doi.org/10.4161/sgtp.19301.

[37] S. Gopal, A. Bober, J.R. Whiteford, H.A. Multhaupt, A. Yoneda, J.R. Couchman, Heparan sulfate chain valency controls syndecan-4 function in cell adhesion, J. Biol. Chem. 285(19) (2010) 14247-58. https://doi.org/10.1074/jbc.M109.056945.

[38] S. Gopal, H.A.B. Multhaupt, R. Pocock, J.R. Couchman, Cell-extracellular matrix and cell-cell adhesion are linked by syndecan-4, Matrix Biol. 60-61 (2017) 57-69. https://doi.org/10.1016/j.matbio.2016.10.006.

[39] K.G. Grønlien, M.E. Pedersen, K.W. Sanden, V. Høst, J. Karlsen, H.H. Tønnesen, Collagen from turkey (Meleagris gallopavo) tendon: a promising sustainable biomaterial for pharmaceutical use, Sustain. Chem. Pharm. 13 (2019) 100166. https://doi.org/10.1016/j.scp.2019.100166.

[40] R. Mao, J. Tang, B.G. Swanson, Water holding capacity and microstructure of gellan gels, Carbohydr. Polym. 46(4) (2001) 365-371. https://doi.org/10.1016/S0144-8617(00)00337-4.

[41] D. Lee, H. Zhang, S. Ryu, Elastic Modulus Measurement of Hydrogels, in: M.I.H. Mondal (Ed.), Cellulose-Based Superabsorbent Hydrogels, Springer International Publishing, Cham, 2018, pp. 1-21.

[42] C.A. Schneider, W.S. Rasband, K.W. Eliceiri, NIH Image to ImageJ: 25 years of image analysis, Nat. Methods 9(7) (2012) 671-675. https://doi.org/10.1038/nmeth.2089.

[43] S.A. Bustin, J.-F. Beaulieu, J. Huggett, R. Jaggi, F.S.B. Kibenge, P.A. Olsvik, L.C. Penning, S. Toegel, MIQE précis: Practical implementation of minimum standard guidelines for fluorescence-based quantitative real-time PCR experiments, BMC Mol. Biol. 11(1) (2010) 74. https://doi.org/10.1186/1471-2199-11-74.

[44] T.D. Schmittgen, K.J. Livak, Analyzing real-time PCR data by the comparative CT method, Nat. Protoc. 3(6) (2008) 1101-1108. https://doi.org/10.1038/nprot.2008.73.

[45] G.M. Fernandes-Cunha, K.M. Chen, F. Chen, P. Le, J.H. Han, L.A. Mahajan, H.J. Lee, K.S. Na, D. Myung, In situ-forming collagen hydrogel crosslinked via

multi-functional PEG as a matrix therapy for corneal defects, Sci. Reports 10(1) (2020) 16671. https://doi.org/10.1038/s41598-020-72978-5.

[46] C. Yang, Enhanced physicochemical properties of collagen by using EDC/NHS-crosslinking, Bull. Mater. Sci. 35(5) (2012) 913-918. https://doi.org/10.1007/s12034-012-0376-5.

[47] V. Charulatha, A. Rajaram, Influence of different crosslinking treatments on the physical properties of collagen membranes, Biomaterials 24(5) (2003) 759-67. https://doi.org/10.1016/s0142-9612(02)00412-x.

[48] S. Hayes, P. Lewis, M.M. Islam, J. Doutch, T. Sorensen, T. White, M. Griffith, K.M. Meek, The structural and optical properties of type III human collagen biosynthetic corneal substitutes, Acta Biomater. 25 (2015) 121-30. https://doi.org/10.1016/j.actbio.2015.07.009.

[49] S. Perumal, O. Antipova, J.P.R.O. Orgel, Collagen fibril architecture, domain organization, and triple-helical conformation govern its proteolysis, Proc. Natl. Acad. Sci. U. S. A. 105(8) (2008) 2824-2829. https://doi.org/10.1073/pnas.0710588105.

[50] V.M. Gun'ko, I.N. Savina, S.V. Mikhalovsky, Properties of Water Bound in Hydrogels, Gels 3(4) (2017). https://doi.org/10.3390/gels3040037.

[51] S. Mani, F. Khabaz, R.V. Godbole, R.C. Hedden, R. Khare, Structure and Hydrogen Bonding of Water in Polyacrylate Gels: Effects of Polymer Hydrophilicity and Water Concentration, J. Phys. Chem. B 119(49) (2015) 15381-15393. https://doi.org/10.1021/acs.jpcb.5b08700.

[52] K. Nam, T. Kimura, A. Kishida, Physical and biological properties of collagen-phospholipid polymer hybrid gels, Biomaterials 28(20) (2007) 3153-3162. https://doi.org/10.1016/j.biomaterials.2007.03.001.

[53] S. Lin, L. Gu, Influence of Crosslink Density and Stiffness on Mechanical Properties of Type I Collagen Gel, Materials 8(2) (2015) 551-560.

[54] S. Mantha, S. Pillai, P. Khayambashi, A. Upadhyay, Y. Zhang, O. Tao, H.M. Pham, S.D. Tran, Smart Hydrogels in Tissue Engineering and Regenerative Medicine, Materials 12(20) (2019) 3323. https://doi.org/10.3390/ma12203323.

[55] J. Heo, R. Koh, W. Shim, H. Kim, H.-G. Yim, N. Hwang, Riboflavin-induced photo-crosslinking of collagen hydrogel and its application in meniscus tissue

engineering, J. Control Release 6(2) (2016) 148-158. https://doi.org/10.1007/s13346-015-0224-4.

[56] S. Yoshimoto, N. Kohara, N. Sato, H. Ando, M. Ichihashi, Riboflavin Plays a Pivotal Role in the UVA-Induced Cytotoxicity of Fibroblasts as a Key Molecule in the Production of H(2)O(2) by UVA Radiation in Collaboration with Amino Acids and Vitamins, Int. J. Mol. Sci. 21(2) (2020). https://doi.org/10.3390/ijms21020554.

[57] E.E. Charrier, K. Pogoda, R.G. Wells, P.A. Janmey, Control of cell morphology and differentiation by substrates with independently tunable elasticity and viscous dissipation, Nat. Commun. 9(1) (2018) 449. https://doi.org/10.1038/s41467-018-02906-9.

[58] U.H. Ko, J. Choi, J. Choung, S. Moon, J.H. Shin, Physicochemically Tuned Myofibroblasts for Wound Healing Strategy, Sci. Reports 9(1) (2019) 16070. https://doi.org/10.1038/s41598-019-52523-9.

[59] S.K. Masur, H.S. Dewal, T.T. Dinh, I. Erenburg, S. Petridou, Myofibroblasts differentiate from fibroblasts when plated at low density, Proc. Natl. Acad. Sci. U. S. A. 93(9) (1996) 4219-4223. https://doi.org/10.1073/pnas.93.9.4219.

[60] A.M. Ruiz-Zapata, A. Heinz, M.H. Kerkhof, C. van de Westerlo-van Rijt, C.E.H. Schmelzer, R. Stoop, K.B. Kluivers, E. Oosterwijk, Extracellular Matrix Stiffness and Composition Regulate the Myofibroblast Differentiation of Vaginal Fibroblasts, Int. J. Mol. Sci. 21(13) (2020) 4762. https://doi.org/10.3390/ijms21134762.

[61] B. Hinz, P. Pittet, J. Smith-Clerc, C. Chaponnier, J.J. Meister, Myofibroblast development is characterized by specific cell-cell adherens junctions, Mol. Biol. Cell 15(9) (2004) 4310-20. https://doi.org/10.1091/mbc.e04-05-0386.

[62] J.C. Rodríguez-Manzaneque, D. Carpizo, C. Plaza-Calonge Mdel, A.X. Torres-Collado, S.N. Thai, M. Simons, A. Horowitz, M.L. Iruela-Arispe, Cleavage of syndecan-4 by ADAMTS1 provokes defects in adhesion, Int. J. Biochem. Cell Biol. 41(4) (2009) 800-10. https://doi.org/10.1016/j.biocel.2008.08.014.

[63] P.S. Acharya, S. Majumdar, M. Jacob, J. Hayden, P. Mrass, W. Weninger, R.K. Assoian, E. Puré, Fibroblast migration is mediated by CD44-dependent TGF beta activation, J. Cell Sci. 121(Pt 9) (2008) 1393-402. https://doi.org/10.1242/jcs.021683.

[64] J.L. Rodríguez Fernández, B. Geiger, D. Salomon, A. Ben-Ze'ev, Suppression of vinculin expression by antisense transfection confers changes in cell morphology, motility, and anchorage-dependent growth of 3T3 cells, J. Cell Biol. 122(6) (1993) 1285-94. https://doi.org/10.1083/jcb.122.6.1285.

[65] E. Olaso, J.P. Labrador, L. Wang, K. Ikeda, F.J. Eng, R. Klein, D.H. Lovett, H.C. Lin, S.L. Friedman, Discoidin domain receptor 2 regulates fibroblast proliferation and migration through the extracellular matrix in association with transcriptional activation of matrix metalloproteinase-2, J. Biol. Chem. 277(5) (2002) 3606-13. https://doi.org/10.1074/jbc.M107571200.

[66] T. Manon-Jensen, H.A. Multhaupt, J.R. Couchman, Mapping of matrix metalloproteinase cleavage sites on syndecan-1 and syndecan-4 ectodomains, FEBS J. 280(10) (2013) 2320-31. https://doi.org/10.1111/febs.12174.

[67] T. Dohi, K. Miyake, M. Aoki, R. Ogawa, S. Akaishi, T. Shimada, T. Okada, H. Hyakusoku, Tissue Inhibitor of Metalloproteinase-2 Suppresses Collagen Synthesis in Cultured Keloid Fibroblasts, Plast Reconstr Surg Glob Open 3(9) (2015) e520-e520. https://doi.org/10.1097/GOX.0000000000000503.

[68] K.M. Herum, I.G. Lunde, B. Skrbic, G. Florholmen, D. Behmen, I. Sjaastad, C.R. Carlson, M.F. Gomez, G. Christensen, Syndecan-4 signaling via NFAT regulates extracellular matrix production and cardiac myofibroblast differentiation in response to mechanical stress, J. Mol. Cell Cardiol. 54 (2013) 73-81. https://doi.org/10.1016/j.yjmcc.2012.11.006.

[69] B. da Rocha-Azevedo, F. Grinnell, Fibroblast morphogenesis on 3D collagen matrices: The balance between cell clustering and cell migration, Exp. Cell Res. 319(16) (2013) 2440-2446. https://doi.org/10.1016/j.yexcr.2013.05.003.

[70] H. Jiang, S. Rhee, C.-H. Ho, F. Grinnell, Distinguishing fibroblast promigratory and procontractile growth factor environments in 3-D collagen matrices, FASEB J. 22(7) (2008) 2151-2160. https://doi.org/10.1096/fj.07-097014.

[71] K.L. Mui, C.S. Chen, R.K. Assoian, The mechanical regulation of integrin–cadherin crosstalk organizes cells, signaling and forces, J. Cell Sci. 129(6) (2016) 1093-1100. https://doi.org/10.1242/jcs.183699.

[72] D. Cai, S.C. Chen, M. Prasad, L. He, X. Wang, V. Choesmel-Cadamuro, J.K. Sawyer, G. Danuser, D.J. Montell, Mechanical feedback through E-cadherin

promotes direction sensing during collective cell migration, Cell 157(5) (2014) 1146-59. https://doi.org/10.1016/j.cell.2014.03.045.

[73] L. Li, Y. He, M. Zhao, J. Jiang, Collective cell migration: Implications for wound healing and cancer invasion, Burns Trauma 1(1) (2013) 21-6. https://doi.org/10.4103/2321-3868.113331.

[74] L.A. Hapach, J.A. VanderBurgh, J.P. Miller, C.A. Reinhart-King, Manipulation of in vitro collagen matrix architecture for scaffolds of improved physiological relevance, Phys. Biol. 12(6) (2015) 061002. https://doi.org/10.1088/1478-3975/12/6/061002.

[75] A. Tirella, T. Liberto, A. Ahluwalia, Riboflavin and collagen: New crosslinking methods to tailor the stiffness of hydrogels, Mater. Lett. 74 (2012) 58-61. https://doi.org/10.1016/j.matlet.2012.01.036.

[76] S. Sel, N. Nass, S. Pötzsch, S. Trau, A. Simm, T. Kalinski, G.I. Duncker, F.E. Kruse, G.U. Auffarth, H.J. Brömme, UVA irradiation of riboflavin generates oxygen-dependent hydroxyl radicals, Redox Rep. 19(2) (2014) 72-9. https://doi.org/10.1179/1351000213y.0000000076.

[77] R.A. Stock, G. Brustollin, R.A. Mergener, E.L. Bonamigo, Efficacy of Standard and Accelerated (10 Minutes) Corneal Crosslinking in Keratoconus Stabilization, Clin. Ophthalmol. 14 (2020) 1735-1740. https://doi.org/10.2147/opth.S258205.

[78] J.C. Serna-Ojeda, O. Santana-Cruz, N. Quiroz-Casian, E. González-Mendoza, J.L. Mercado-Orozco, A. Navas, A. Lichtinger, E.O. Graue-Hernandez, Pain Management in Corneal Collagen Crosslinking for Keratoconus: A Comparative Case Series, J. Ocul. Pharmacol. Ther. 35(6) (2019) 325-330. https://doi.org/10.1089/jop.2019.0021.

[79] T. Loftsson, M.E. Brewster, Pharmaceutical applications of cyclodextrins: basic science and product development, J. Pharm. Pharmacol. 62(11) (2010) 1607-1621. https://doi.org/10.1111/j.2042-7158.2010.01030.x.

[80] H. Hong, J. Kim, H. Cho, S.M. Park, M. Jeon, H.K. Kim, D.S. Kim, Ultra-stiff compressed collagen for corneal perforation patch graft realized by in situ photochemical crosslinking, Biofabrication 12(4) (2020) 045030. https://doi.org/10.1088/1758-5090/abb52a.

Figure legends

Fig. 1. Physical properties of hydrogels. a) Schematic illustration of LC photocrosslinking showing organization and crosslinking of collagen after irradiation. b) Gel appearance depended on crosslinking procedure. Upper left; LC gel with slightly yellow and transparent appearance, upper right; CD gel with translucent appearance, lower left; RF gel with yellow and translucent appearance, lower right; Col gel with translucent appearance. c) Water holding capacity of hydrogels subjected to 394*g* centrifugal force, with LC gels having a superior water holding capacity compared to Col gels, CD gels and RF gels, where the latter had the lowest capacity. d) Enzyme-mediated scaffold degradation by collagenase, showing highest resistance to collagenase for RF gels (points marked with a dagger (†) for LC gels had only one replicate due to low mechanical strength after collagenase digestion). e) Representative stress-strain curves of hydrogels between 0-30% strains. Col gels (green), LC gels (blue), RF gels (red), CD gels (purple).

Fig. 2. Fibroblast morphology and viability on hydrogels. a) Light microscopy images of fibroblasts seeded on the hydrogels showing even dispersion of fibroblasts on Col gels and CD gels, while fibroblasts on LC gels seemed to cluster or collectively migrate through the gel. b) Staining of cell nuclei (blue) and dead cells (red, marked with arrows) mainly showing viable cells for fibroblasts seeded on Col gels, LC gels and CD gels.

Fig. 3. Hydrogel crosslinking procedures influences fibroblast F-actin stress fibers and myofibroblast differentiation. a) Fluorescence microscopy of F-actin (Phalloidin) showing more prominent intracellular stress fibers in the Col and CD gels, while cells seeded onto LC gels had stronger staining of peripheral stress fibers. b) Immunostaining of α-SMA (red) and cell nuclei (blue). c) Higher magnification of α-SMA, showing organized smooth muscle actin fibers (marked by arrow heads) for LC gels rather than immature fibers as seen for Col and CD gels.

Fig. 4. Hydrogel crosslinking procedure influences the production and expression of cadherins by fibroblasts. a) Fluorescence microscopy of cadherins (pan-cadherin) showing a clearly higher fluorescence intensity of cadherins from fibroblasts seeded onto LC gels. b) Merged fluorescence image of pan-cadherin (green) and F-actin stress

fibers (red) emphasizing that the focal adhesions of LC are expressing cadherins, boxed magnification of cells seeded on LC hydrogels. c) Total cadherin expression in cells was quantified using ImageJ, based on fluorescence intensity on images of immunostaining, as presented in b. A total of 10 randomly chosen cells were quantified for each hydrogel. Presented values are Integrated Densities (sum of pixels values in selection x area of selection). Asterisks (*) indicate significant differences (*** $P < 0.001$ in LC gels compared to the other gels). Statistics assessed by one-way ANOVA with Tukey's multiple comparison test.

Fig. 5. mRNA expression and secretion of proteins related to fibroblast differentiation and migration are changed upon crosslinking of the hydrogels. mRNA expression is presented as the relative and normalized mRNA (fold change) in cells seeded on hydrogels compared to cells seeded on Col gels. Protein secretion is presented as the average protein concentration. The hydrogel crosslinking procedure affects the expression of a) *ACTA2* (α-SMA), b) *COL1A2* (collagen type I alpha 2 chain) mRNA expression, c) *SDC4* mRNA expression, d) SDC-4 shedding and e) MMP-2/TIMP-2 ratio calculated based on the secretion of protein into the cell media. The data was collected from three independent biological experiments, each with three technical replicates. Asterisks (*) denote significant differences. Statistical analysis was performed by one-way ANOVA with Tukey's multiple comparison test (* $P \leq 0.05$, ** $P \leq 0.01$, *** $P \leq 0.001$).

Table legends

Table 1. Summary of preparation parameters of collagen hydrogels.

Table 2. List of TaqMan Gene Expression Assay probes used in RT-qPCR experiments.

Table 3. Results from macroindentation of collagen hydrogels.

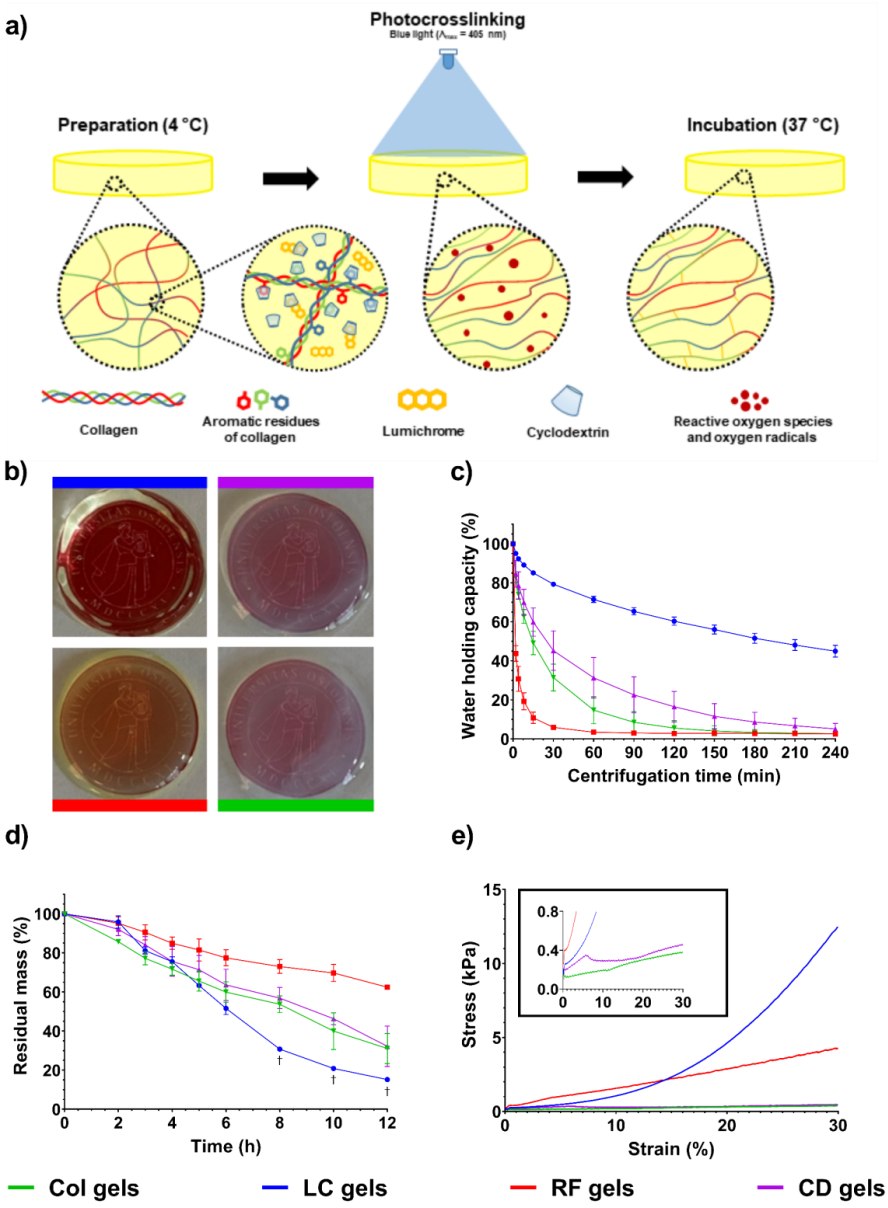
a)
Photocrosslinking
Blue light (λmax = 405 nm)
Preparation (4 °C)
Incubation (37 °C)
Collagen
Aromatic residues of collagen
Lumichrome
Cyclodextrin
Reactive oxygen species and oxygen radicals
b)
c)
Water holding capacity (%)
Centrifugation time (min)
d)
Residual mass (%)
Time (h)
e)
Stress (kPa)
Strain (%)
Col gels
LC gels
RF gels
CD gels

Fig. 1

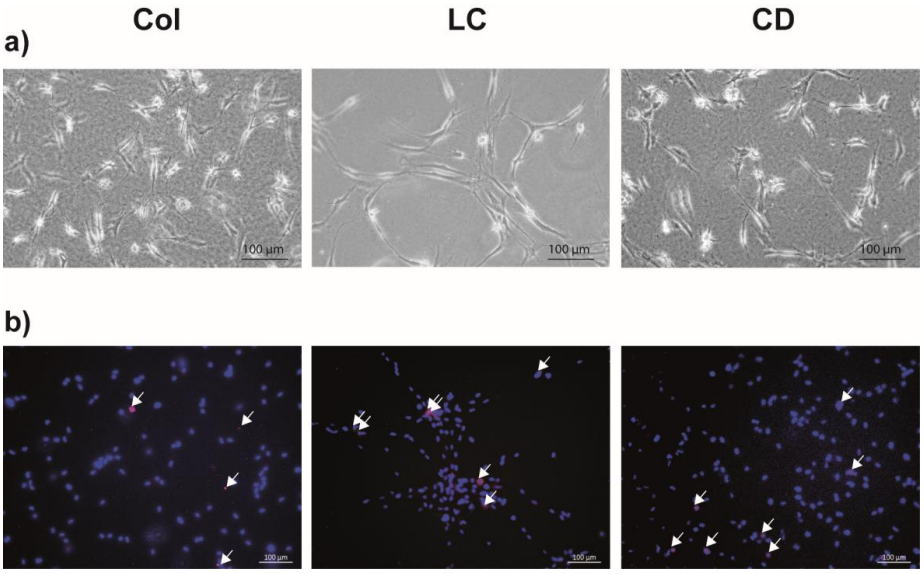

Fig. 2

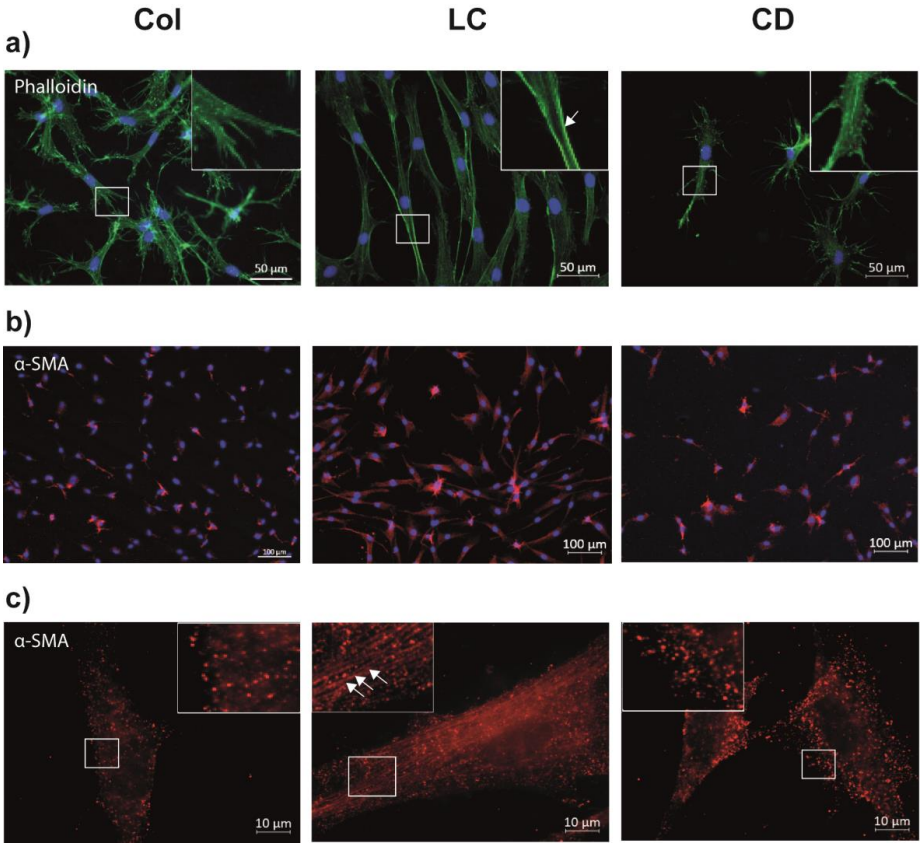
Col
LC
CD
a)
Phalloidin
50 µm
50 µm
50 µm
b)
α-SMA
100 µm
100 µm
c)
α-SMA
10 µm
10 µm
10 µm

Fig. 3

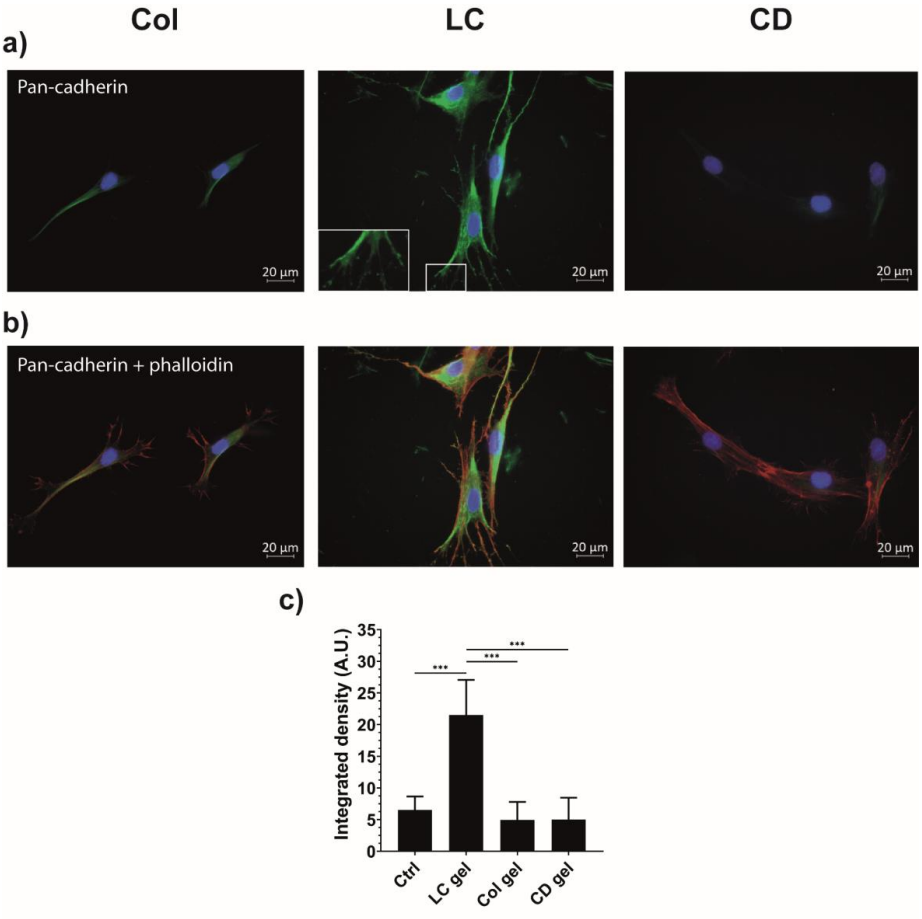
Col
LC
CD
a)
Pan-cadherin
20 µm
b)
Pan-cadherin + phalloidin
c)
Integrated density (A.U.)
35
30
25
20
15
10
5
0
***
***
***
Ctrl
LC gel
Col gel
CD gel

Fig. 4

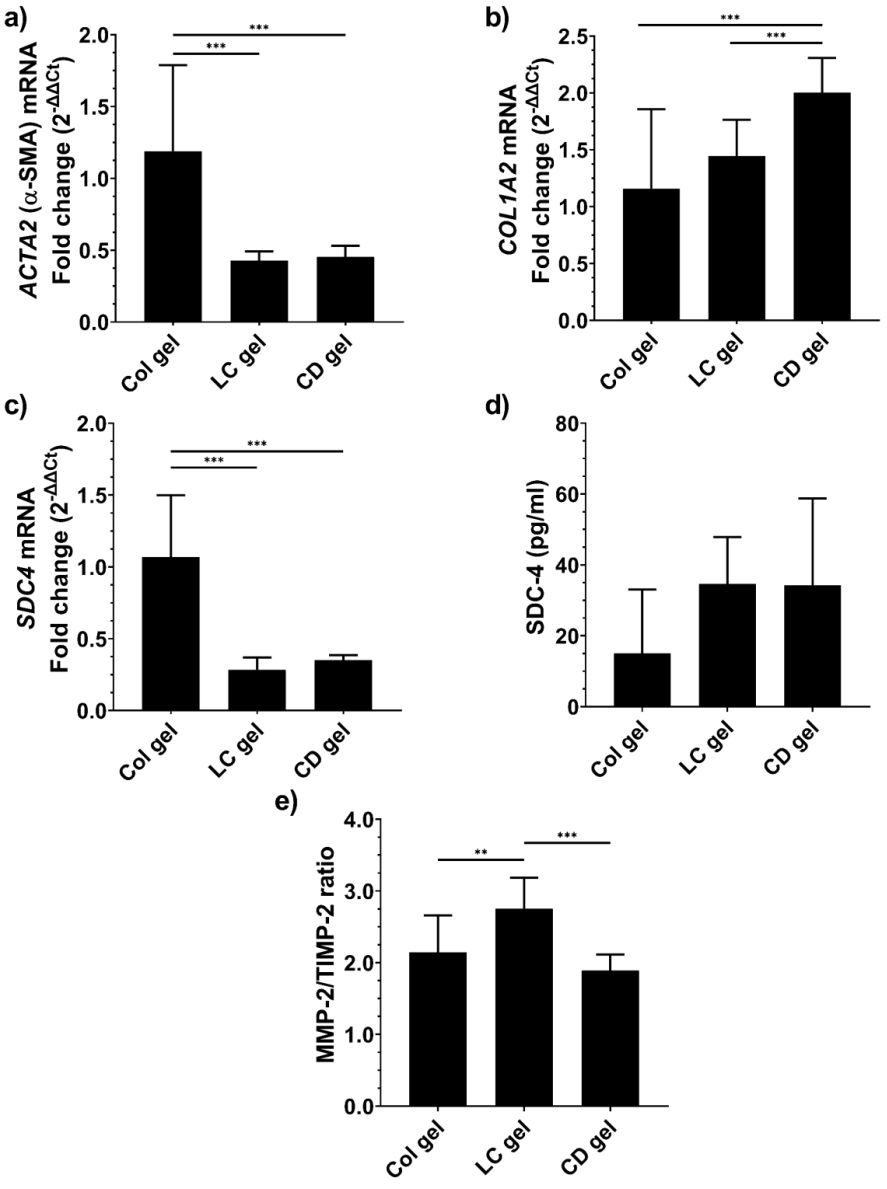
a)
ACTA2 (α-SMA) mRNA
Fold change (2-ΔΔCt)
2.0
1.5
1.0
0.5
0.0
***
***
Col gel
LC gel
CD gel
b)
COL1A2 mRNA
Fold change (2-ΔΔCt)
2.5
2.0
1.5
1.0
0.5
0.0
***
***
Col gel
LC gel
CD gel
c)
SDC4 mRNA
Fold change (2-ΔΔCt)
2.0
1.5
1.0
0.5
0.0
***
***
Col gel
LC gel
CD gel
d)
SDC-4 (pg/ml)
80
60
40
20
0
Col gel
LC gel
CD gel
e)
MMP-2/TIMP-2 ratio
4.0
3.0
2.0
1.0
0.0
**
***
Col gel
LC gel
CD gel

Fig. 5

Tables

Table 1. Summary of preparation parameters of collagen hydrogels.

Gel sample	Final collagen concentration	Final cyclodextrin concentration	Final photocrosslinker concentration	Final pH	Incubation	Irradiation parameters	Post-irradiation incubation
Col gels	4 mg/ml	N. A.	N. A.	7.4	37 °C, 90 min	N. A.	N. A.
LC gels	4 mg/ml	4%	200 µM LC	7.4	N. A.	10 s, λ_{max} = 405 nm	37 °C, 90 min
RF gels	4 mg/ml	N. A.	265 µM RF	7.4	37 °C, 60 min	4 min, λ_{max} = 365 nm	37 °C, 30 min
CD gels	4 mg/ml	4%	N. A.	7.4	37 °C, 90 min	N. A.	N. A.

Table 2. List of TaqMan Gene Expression Assay probes used in RT-qPCR experiments.

Gene	TaqMan Description	TaqMan assay ID
EEF1A1	Eukaryotic translation elongation factor 1 alpha 1	Hs00265885_g1
ACTA2	Actin, alpha 2, smooth muscle, aorta	Hs00909449_m1
SDC4	Syndecan 4	Hs00161617_m1
COL1A2	Collagen type I alpha 2 chain	Hs01028939_g1

Table 3. Results from macroindentation of collagen hydrogels.

Gel sample	Young's modulus (20% strain)	Ultimate compressive strength	Fracture point
Col gels	3.50 ± 0.21 kPa	≥ 0.43 ± 0.04 kPa	≥ 60% strain
LC gels	62.30 ± 7.95 kPa	16.05 ± 4.93 kPa	25-35% strain
RF gels	30.88 ± 0.51 kPa	≥ 11.89 ± 0.49 kPa	≥ 60% strain
CD gels	3.90 ± 0.40 kPa	≥ 0.57 ± 0.05 kPa	≥ 60% strain

Supplementary Material

Tuning of 2D cultured human fibroblast behavior using lumichrome photocrosslinked collagen hydrogels

Krister Gjestvang Grønlien[a]*, Mona Elisabeth Pedersen[b], Sissel Beate Rønning[b], Nina Solberg[b] and Hanne Hjorth Tønnesen[a]

[a]*Section for Pharmaceutics and Social Pharmacy, Department of Pharmacy, University of Oslo, P.O. Box 1068 Blindern, NO-0316 Oslo, Norway;*
[b]*Department of Raw Material and Process Optimization, Nofima AS, P.O. Box 210, NO-1431 Ås, Norway*

*Corresponding author. E-mail address: k.g.gronlien@farmasi.uio.no

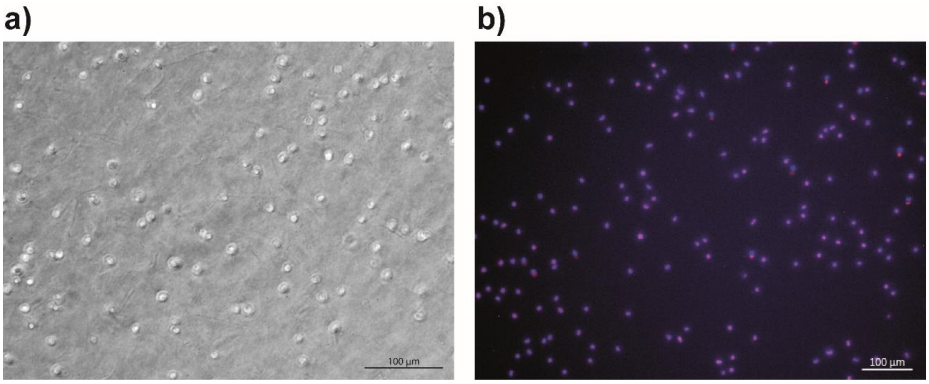

Fig. S1. Fibroblast morphology and viability on hydrogels. a) Light microscopy images of fibroblasts seeded on the hydrogels. b) Staining of cell nuclei (blue) and dead cells (red). Dead cells were only detected for fibroblasts seeded on RF photocrosslinked collagen gels.

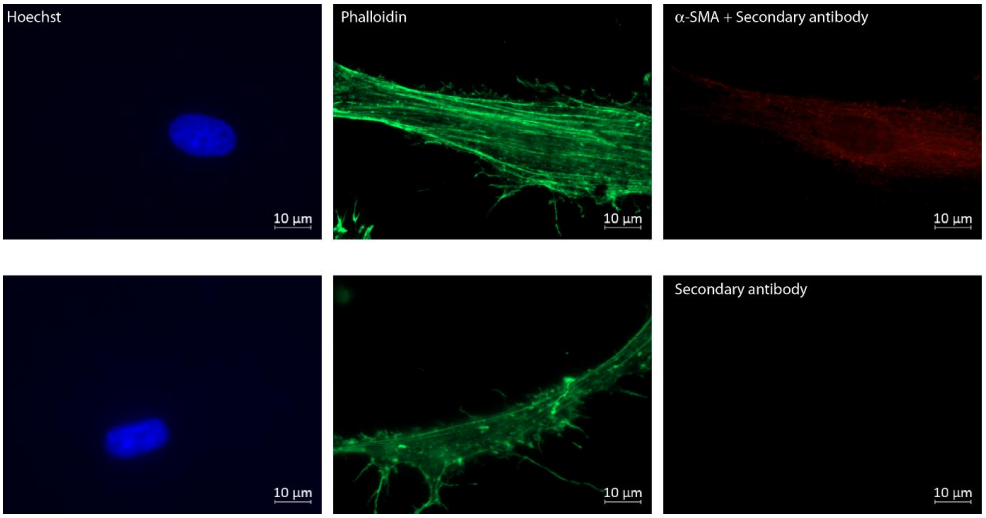

Fig. S2. Control experiments with secondary antibody show no unspecific binding for cells stained with anti-α-SMA followed by incubation with secondary antibody (Goat anti-Rabbit IgG (H+L) Cross-Adsorbed Secondary Antibody, Alexa Fluor™ 546, A-11010, 1:400 dilution, red) (upper panel) or staining with secondary antibody alone (lower panel) before fluorescence microscopy analysis (Zeiss Axio Observer Z1 microscope). Nuclei were stained with Hoechst (blue) and F-actin filaments were stained with phalloidin (green). All pictures were captured under the similar experimental conditions.

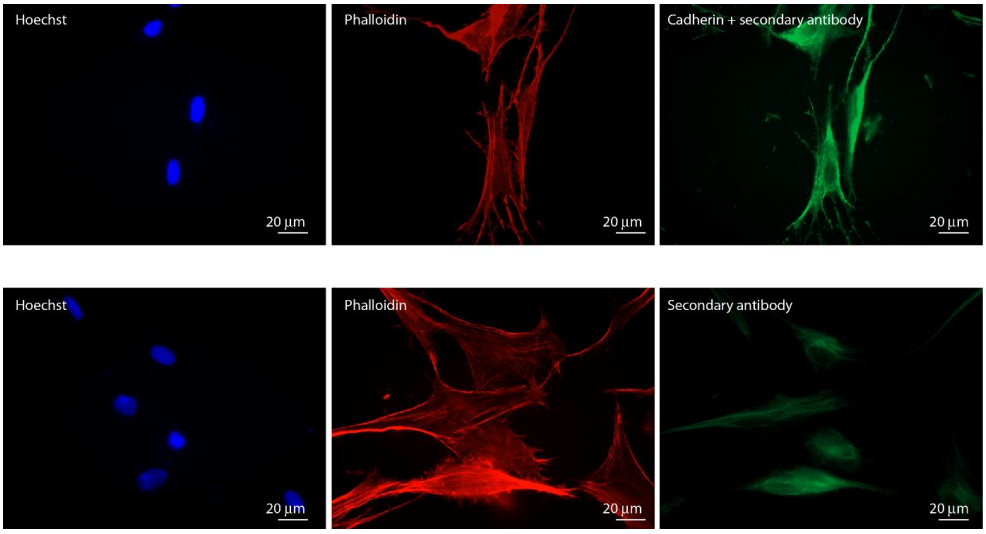

Fig. S3. Control experiments with secondary antibody show some unspecific binding for cells stained with anti-pan cadherin followed by incubation with secondary antibody (Goat anti-Mouse IgG, IgM, IgA (H+L) Secondary Antibody, Alexa Fluor™ 488, A-10667, 1:400 dilution, green) (upper panel) or staining with secondary antibody alone (lower panel) before fluorescence microscopy analysis (Zeiss Axio Observer Z1 microscope). Nuclei were stained with Hoechst (blue) and F-actin filaments were stained with phalloidin (red). All pictures were captured under the similar experimental conditions.

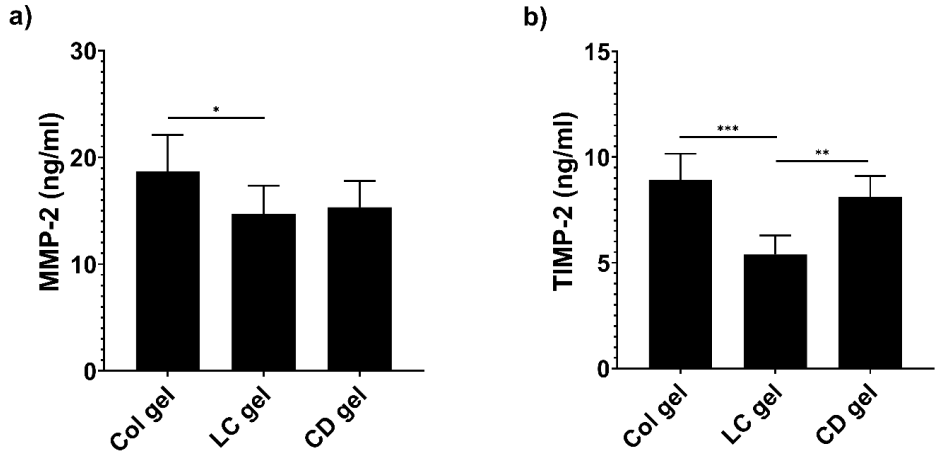

Fig. S4. Secretion of a) MMP-2 and b) TIMP-2 into the cell media of fibroblasts cultured on hydrogels. Asterisks (*) denote significant differences. Statistical analysis was performed by one-way ANOVA with Tukey's multiple comparison test (* $P \leq 0.05$, ** $P \leq 0.01$, *** $P \leq 0.001$).

Paper IV

Bacterial phototoxicity of lumichrome photocrosslinked collagen hydrogels

Krister Gjestvang Grønlien, Håkon Valen, Ellen Bruzell, Hanne Hjorth Tønnesen

Manuscript in preparation for *Photochemical & Photobiological Sciences*.

Communication

Bacterial phototoxicity of lumichrome photocrosslinked collagen hydrogels

Krister Gjestvang Grønlien[a]*, Håkon Valen[b], Ellen Bruzell[b] and Hanne Hjorth Tønnesen[a]

[a]*Section for Pharmaceutics and Social Pharmacy, Department of Pharmacy, University of Oslo, P.O. Box 1068 Blindern, NO-0316 Oslo, Norway;*
[b]*Nordic Institute of Dental Materials, Sognsveien 70A, NO-0855 Oslo, Norway;*

*Corresponding author. E-mail address: k.g.gronlien@farmasi.uio.no

Communication

Bacterial phototoxicity of lumichrome photocrosslinked collagen hydrogels

Abstract

Lumichrome (LC), an endogenous, lipophilic degradation product of riboflavin, is both a photocrosslinker of collagen and a photosensitizer for antimicrobial applications. Preliminary results demonstrated improved aqueous solubility of LC by the formation of cyclodextrin (CD) inclusion complexes. Therefore, collagen hydrogels were prepared with two types of CDs, namely (2-hydroxypropyl)-β-CD (HPβCD) and -γ-CD (HPγCD). The release of LC from the gels and the phototoxic effect of UVA-irradiated LC against planktonic *Staphylococcus aureus* were investigated. Irradiation of LC hydrogels complexed with either CD resulted in similar levels of bacterial death despite a 2-fold lower LC concentration in the gel containing HPγCD. This effect was ascribed to the higher complexation efficiency and stability of the LC-HPβCD complex. The results indicated an excipient-dependent formation of $^1O_2$. The study is a proof of concept for possible application of an endogenous photocrosslinker in combination with a biopolymer in applications such as antimicrobial photodynamic therapy (aPDT) after further optimization.

Keywords: collagen; lumichrome; photocrosslinking; phototoxicity; antimicrobial photodynamic therapy

1. Introduction

Collagen preparations may be efficient in the treatment of chronic wounds by facilitating chemotaxis of cells involved in remodeling of the skin [1-3]. Collagen hydrogels, characterized by a high degree of biocompatibility and high moisture content, contribute to a humid healing environment [4]. Such hydrogels have been identified as sacrificial materials against proteolytic enzymes and protection against secondary infections [5]. However, the collagen by itself has no antibacterial properties [6]. A disadvantage of the biomedical use of collagen hydrogels is their low mechanical strength. Photochemical crosslinking with photosensitizers can increase the mechanical strength without compromising biocompatibility. This method is used for, e.g., *in vivo* corneal photocrosslinking with riboflavin (Vitamin B_2; RF) in combination with UVA irradiation in the treatment of the eye disease keratoconus [7]. UVA irradiation is advantageous for treatment in the adult eye due to its limited penetration depth. RF has also been used as a photosensitizer in photocrosslinking of collagen gels [8]. Irradiation of RF results in photodegradation to lumichrome (LC) in acidic and neutral solutions or lumiflavin (LF) in alkaline solutions [9,10]. Studies in our lab have shown that LC acts as a photocrosslinker of collagen gels [11]. When used as a photosensitizer in bacterial phototoxicity studies a reduction in the number of bacteria was achieved. The reduction was dependent on the solubilization method [12]. LC is nearly 100 times more photostable than its precursor and will not be consumed in either the photocrosslinking or the aPDT process [10].

The application of aPDT has been postulated as an alternative or supplement to antibiotics in the treatment of localized infections [13]. An aqueous solubility of ~ 10^{-5} M has been the major limitation for the use of LC as a photosensitizer. Solubilization can be increased by a tenfold through the formation of inclusion complexes with

cyclodextrins (CDs) [12]. CDs are cyclic oligosaccharides with a hydrophobic inner and a hydrophilic outer structure [14]. Furthermore, collagen has been complexed with cyclodextrins (CD) to regulate the collagen self-assembly and produce materials similar to native cornea [15]. CDs have also been incorporated into collagen membranes for controlled delivery and increased bioavailability of conventional antibiotics, such as ofloxacin for the treatment of bacterial keratitis [16].

The aim of the present work was to investigate the bacterial phototoxic effect of the photocrosslinked hydrogels following LC release.

2. Materials and methods

2.1. Raw materials, chemicals and reagents

Pepsin soluble collagen isolated from industrially produced turkey (*Meleagris gallopavo*) rest raw materials was prepared as described in Grønlien et al. 2019 [17]. In brief, turkey tendons were manually cleaned and freeze dried for 48 h. A 0.5 M acetic acid solution with pepsin (1:10) was added to enzymatically hydrolyze the material. The hydrolyzed material was centrifuged, and the supernatant was collected. The collagen was precipitated by the addition of 4 M NaCl (1:3) and centrifuged. The collagen was re-solubilized in 0.5 M acetic acid and dialyzed against distilled water for 3 days. The dialyzed solution was further freeze dried to obtain dry collagen. Other reagents were of analytical grade and were purchased from Merck KGaA (Darmstadt, Germany). Bacterial medium and components were all purchased from Thermo Fischer Scientific (Waltham, MA, USA) or VWR International, LLC (Radnor, PA, USA).

2.2. Preparation of LC photocrosslinked collagen hydrogels

LC photocrosslinked collagen hydrogels were prepared by a direct photocrosslinking

method as described in Grønlien et al. 2021 [11]. In short, (2-hydroxypropyl)-β-cyclodextrin (HPβCD, International Specialty Products, Köln, Germany) and (2-hydroxypropyl)-γ-cyclodextrin (HPγCD, Wacker Chemie AG, Burghausen, Germany) were both dissolved in 20 mM acetic acid to a final concentration of 5% (w/v). LC was dissolved in the acidic HPβCD- and HPγCD-solutions to final concentrations of 250 µM and 100 µM in, respectively. Collagen was dissolved in the acidic LC-CD-solution for 24 h to a final concentration of 5 mg/ml. The solution was neutralized to pH 7.4 on ice by the addition of 10X phosphate buffered saline (PBS) (0.1 × final volume of the combined solution), 1 M NaOH (0.023 × volume of added collagen solution) and Milli-Q water to give a final concentration of 4 mg/ml collagen and 200 µM or 80 µM LC in the mixed solution. The solutions were further crosslinked by irradiation with blue light from a light emitting diode source (λ_{max} = 405 nm; 17.8 mW/cm^2 at solution surface) (Bio X, Cellink, Gothenburg, Sweden) for 10 s directly after neutralization. The gels were incubated at 37°C for 90 min before further use.

2.3. Antibacterial phototoxicity studies

2.3.1. Bacteria and media

The model bacterium, *Staphylococcus aureus* strain Newman, was cultured overnight in brain heart infusion (BHI, Oxoid Ltd., Basingstoke, UK) broth at 37°C in a 5% CO_2 supplemented atmosphere. The bacteria were centrifuged at 5000*g* for 5 min and redispersed in Dulbecco's PBS (DPBS, Lonza, Verviers, Belgium) to an optical density at 600 nm (OD_{600}) of 1.0, corresponding to approximately 3.0×10^8 colony-forming units (CFU)/ml. Agar plates were made of BHI and bacteriological agar.

2.3.2. Antibacterial assay on planktonic bacteria

A gel diffusion method was applied to evaluate the antibacterial phototoxicity of LC photocrosslinked collagen hydrogels on planktonic bacteria. Hydrogels were prepared as described in section 2.2 in 24-well cell culture inserts (Falcon®, Corning Inc. Life Sciences, Corning, NY, USA) with 3.0 µm pores and 8.0×10^5 pores/cm^2 placed in 24-well plates. The diffusion area of the inserts was 0.33 cm^2.

One ml of a 1:10 dilution of OD_{600} 1.0 inoculum was added to each well before the inserts containing hydrogels were added. The gels were incubated with the bacteria for 3 h, followed by the removal of the inserts containing the remaining gel. The bacterial suspension was subjected to UVA irradiation from three fluorescent tubes (Ralutec 9W/78, Radium, Germany) in a chamber (Polylux-PT, Dreve, Germany) (λ_{max} = 365 nm; full width at half maximum: 19 nm; mean spectral irradiance: 5.1 ± 0.3 mW/cm^2 at level of wells) for 30 min. Irradiance was measured immediately prior to experiments with a radiometer (United Detector Technology, 371 Optical Power Meter, Hawthorne, CA, USA with probes 268 Blue and 222 UVA). Spectral data were obtained by a Bentham spectroradiometer (model DTM300, Bentham Instruments Ltd., Reading, UK). The absorption spectrum of LC partly overlapped the emission spectrum of the irradiation source [12]. Colonies of surviving bacteria were calculated after serial dilution in PBS and plating on BHI agar plates incubated overnight at 37 °C in 5% CO_2 supplemented atmosphere. Experiments were performed in triplicate and repeated three times. The experimental setup is schematized in Fig. 1.

2.4. In vitro release of LC from photocrosslinked collagen hydrogels

The photocrosslinked collagen hydrogels were tested for *in vitro* release of LC. The LC photocrosslinked gels were prepared directly in the 24-well inserts (section 2.3.2).

The wells were filled with 1 ml receptor medium (DPBS). The inserts containing the gels were placed in the wells followed by addition of 0.5 ml receptor medium. The well plates were continuously stirred at 50 rpm at 37 ± 1°C. The inserts were transferred to a new well containing fresh medium at fixed time points in order to maintain sink conditions throughout a 4 h release period. Samples (200 µl) were collected from each well and diluted 1:1 with the HPLC mobile phase (Milli-Q water and methanol (MeOH) in the ratio 65:35 (v/v)) prior to LC quantification by isocratic reversed phase HPLC (Shimadzu Prominence modular system equipped with a LC-20AD pump, a SIL-20AC HT auto sampler, a CTO-20A column oven, a SPD-M20A diode array detector and a CBM-20A communication bus module, Shimadzu Corp., Kyoto, Japan). A C_{18} column (Nova-pak®, Waters Corporation, Milford, MA, USA) was used with a flow rate of 1.0 ml/min and column temperature of 30°C. The calibration curves were prepared from a stock solution of 250 µM LC in 5% HPβCD and 100 µM LC in 5% HPγCD. The retention time of LC was approximately 7 min under the given experimental conditions. The experiments were performed in triplicate. The accumulative amount of released LC was calculated.

2.5. Statistical analysis

The data were presented as mean ± standard deviation (SD) from three independent experiments. Statistical analyses were performed by using one-way ANOVA followed by the Tukey's multiple comparison test using GraphPad Prism version 8.0.1 for Windows (GraphPad Software, La Jolla, CA, USA; www.graphpad.com). Differences were considered significant at $P < 0.05$.

3. Results

The exposure with LC photocrosslinked collagen hydrogels (prepared with HPβCD and HPγCD) combined with UVA irradiation reduced *S. aureus* survival compared to non-irradiated samples ($P < 0.05$) (Fig. 2A). The bacterial survival was not dependent on the LC concentration of the hydrogels ($P > 0.05$) (Fig. 2B). Control experiments with and without UVA irradiation in the absence of hydrogels gave no reduction in the number of CFU/ml ($P < 0.05$; data not shown).

The amount of LC released from collagen hydrogels prepared with HPβCD and HPγCD increased more than 3-fold between 30 min and 4 h (Fig. 2C). The percentage LC release was similar for the two hydrogels after 4 h ($P > 0.05$), and analysis showed that LC remaining in the donor compartment was almost equally distributed between the gel and the supernatant (Table 1). LC retained in the hydrogels was dependent on the gel characteristics and choice of CD with a higher retention in the HPβCD gels (Table 1).

4. Discussion

The dual function of LC, namely as a photocrosslinker in the formulation of collagen hydrogels and as a photosensitizer in antimicrobial applications is facilitated by the fact that LC is photostable, i.e., not consumed during irradiation. LC has proven photostable in both HPβCD and HPγCD complexes [10,18]. No differences in mechanical behavior between the resulting hydrogels were observed, indicating that the hydrogels prepared with HPγCD complexes were crosslinked in a similar way as hydrogels previously studied with HPβCD [11].

The bacterial phototoxic effect in *S. aureus* of the LC released from the two gels was similar despite a more than 2-fold higher concentration of LC in hydrogels containing

HPβCD (Fig. 2A and B). The complexation efficiency (CE) and stability constant ($K_{1:1}$) of LC in HPβCD are more than twice the values in HPγCD (CE = 0.0165 compared to 0.0034 and $K_{1:1}$ = 412 compared to 85 M^{-1}, respectively) [19,20]. The pore size of the semipermeable inserts used to separate the gels from the bacterial suspension, allowed for the release of both free LC and LC-CD complexes into the receptor medium. The higher $K_{1:1}$ of HPβCD compared to HPγCD indicated that LC was retained to a greater extent in the HPβCD cavity after the release from the hydrogels than its counterpart. Studies on the complexation of photosensitizers by CDs have reported that the production of $^1O_2$ was reduced in the presence of CDs. This effect was explained by the lower diffusion rate of ground state oxygen in CD solutions resulting in diffusion-limited formation of $^1O_2$ [21,22]. The difference in antibacterial effect between the two gels in the current study may further be explained by the longer diffusion path of $^1O_2$ generated within the CD cavity compared to $^1O_2$ formed in the surrounding solution and, thereby, in close proximity to the bacterial membrane. Furthermore, $^1O_2$ can be quenched by the CDs to a various extent. As LC-HPβCD complexes are more stable than LC-HPγCD, a relatively higher phototoxicity per dose of the latter could be expected despite the lower concentration of LC. This was consistent with our results (Fig. 2B).

Despite the similar percentage cumulative release of LC after 4 h, the release profiles indicated a higher percentage release from HPγCD earlier in the process (i.e., compared to HPβCD after 1 h, $P < 0.05$) (Fig. 2c). This was expected due to difference in the CE and $K_{1:1}$ between the LC-CD complexes. Studies on the material properties of LC photocrosslinked collagen hydrogels containing HPβCD have shown a water retention ability of more than 40% [11]. A high water retention capacity will favor the retention of hydrophilic compounds such as LC-CD complexes dissolved in the water phase of

the hydrogels. This is consistent with the observed amount of LC retained in the HPβCD gels (Table 1). A previous study in our lab on the phototoxicity of LC complexed with CD demonstrated a stagnation of the phototoxic effect above a certain LC concentration due to radiation attenuation in highly absorbing solutions (inner filter effect) [12]. However, the low amount of LC released from the gels in the present work excluded an inner filter effect.

In vitro phototoxicity studies on antibiotic resistant bacteria strains with photosensitizers and irradiation have shown promising effect. Studies on the development of resistance against aPDT treatment have shown conflicting results [23,24]. However, only a few studies have so far tried to induce resistance [24]. The use of CDs in topical formulations will allow for co-inclusion of lipophilic antimicrobial substances in addition to the photosensitizers, thereby facilitating a combined therapy when needed. A combined effect may be achieved by a weakening of the bacteria by phototoxicity and attack by a conventional antimicrobial agent, which may result in a complete eradication of the bacteria. Further *in vitro* and *in vivo* testing of the formulation and evaluation of the phototoxicity have to be performed prior to clinical translation. This will include, e.g., other bacteria and biofilms as well as optimization of the irradiation dosimetry (wavelengths and radiant exposure) and LC doses.

4. Conclusions

The maximum LC concentration in the hydrogels was dependent on the complexation efficiency and stability of the inclusion complexes. The high LC-HPβCD complexation constant indicated that LC was retained in the CD cavity even when the inclusion complex was released from the hydrogels. The dual effect of LC in collagen hydrogels, both as a photocrosslinker of collagen and photosensitizer for antimicrobial applications

was demonstrated. The results are a proof of concept for the possible application of an endogenous photocrosslinker in combination with a biopolymer in UVA-activated aPDT after further optimization.

Acknowledgments

The authors are grateful to Bente Amalie Breiby, Department of Pharmacy, University of Oslo and Inger Sofie Dragland, NIOM for technical support and Karen Wahlstrøm Sanden, Nofima AS for isolation of collagen from turkey tendon. Turkey tendon by-products and financial support for isolation of collagen from turkey were contributed by Norilia AS.

Declarations

Funding

This work was supported by Norilia AS (Oslo, Norway). Norilia AS provided the turkey tendon by-products and funded the isolation of collagen, but was not involved in the study design, interpretation of the data, writing of the manuscript, or decision to publish.

Conflict of interest

The authors declare that they have no conflict of interest.

Availability of data and material

The datasets generated during and/or analyzed during the current study are available from the corresponding author on reasonable request.

Code availability

Not applicable

Authors' contributions

Conceptualization: K. G. Grønlien, H. Valen, E. Bruzell, H. H. Tønnesen;

Funding acquisition: H. H. Tønnesen;

Investigation: K. G. Grønlien;

Supervision**:** H. Valen, E. Bruzell, H. H. Tønnesen;

Visualization: K. G. Grønlien;

Writing: K.G. Grønlien, H. Valen, E. Bruzell, H. H. Tønnesen.

Ethics approval

Not applicable

Consent to participate

Not applicable

Consent for publication

Not applicable

References

1. Chattopadhyay, S., & Raines, R. T. (2014). Collagen-based biomaterials for wound healing. *Biopolymers, 101*(8), 821-833. https://doi.org/10.1002/bip.22486.
2. Caley, M. P., Martins, V. L. C., & O'Toole, E. A. (2015). Metalloproteinases and Wound Healing. *Adv. Wound Care, 4*(4), 225-234. https://doi.org/10.1089/wound.2014.0581.
3. Brett, D. (2008). A Review of Collagen and Collagen-based Wound Dressings. *Wounds, 20*(12), 347-356.
4. Xiang, J., Shen, L., & Hong, Y. (2020). Status and future scope of hydrogels in wound healing: Synthesis, materials and evaluation. *European Polymer Journal, 130*, 109609. https://doi.org/10.1016/j.eurpolymj.2020.109609.

5. Fleck, C. A., & Simman, R. (2010). Modern Collagen Wound Dressings: Function and Purpose. *The Journal of the American College of Certified Wound Specialists, 2*(3), 50-54. https://doi.org/10.1016/j.jcws.2010.12.003.

6. Michalska-Sionkowska, M., Walczak, M., & Sionkowska, A. (2017). Antimicrobial activity of collagen material with thymol addition for potential application as wound dressing. *Polymer Testing, 63*, 360-366. https://doi.org/10.1016/j.polymertesting.2017.08.036.

7. Wollensak, G., Spoerl, E., & Seiler, T. (2003). Riboflavin/ultraviolet-A–induced collagen crosslinking for the treatment of keratoconus. *American Journal of Ophthalmology, 135*(5), 620-627. https://doi.org/10.1016/s0002-9394(02)02220-1.

8. Tirella, A., Liberto, T., & Ahluwalia, A. (2012). Riboflavin and collagen: New crosslinking methods to tailor the stiffness of hydrogels. *Materials Letters, 74*, 58-61. https://doi.org/10.1016/j.matlet.2012.01.036.

9. Huang, R., Kim, H. J., & Min, D. B. (2006). Photosensitizing Effect of Riboflavin, Lumiflavin, and Lumichrome on the Generation of Volatiles in Soy Milk. *Journal of Agricultural and Food Chemistry, 54*(6), 2359-2364. https://doi.org/10.1021/jf052448v.

10. Remucal, C. K., & McNeill, K. (2011). Photosensitized Amino Acid Degradation in the Presence of Riboflavin and Its Derivatives. *Environmental Science & Technology, 45*(12), 5230-5237. https://doi.org/10.1021/es200411a.

11. Grønlien, K. G., Pedersen, M. E., Rønning, S. B., Solberg, N., & Tønnesen, H. H. (2021). Tuning of 2D cultured human fibroblast behavior using lumichrome photocrosslinked collagen hydrogels. Submitted to *Int. J. Biol. Macromol.*

12. Bergh, V. J. V., Bruzell, E., Hegge, A. B., & Tønnesen, H. H. (2015). Influence of formulation on photoinactivation of bacteria by lumichrome. *Pharmazie, 70*(9), 574-580. https://doi.org/10.1691/ph.2015.5006.

13. Jori, G., Fabris, C., Soncin, M., Ferro, S., Coppellotti, O., Dei, D., et al. (2006). Photodynamic therapy in the treatment of microbial infections: basic principles and perspective applications. *Lasers in Surgery and Medicine, 38*(5), 468-481. https://doi.org/10.1002/lsm.20361.

14. Kurkov, S. V., & Loftsson, T. (2013). Cyclodextrins. *International Journal of Pharmaceutics, 453*(1), 167-180. https://doi.org/10.1016/j.ijpharm.2012.06.055.

15. Majumdar, S., Wang, X., Sommerfeld, S. D., Chae, J. J., Athanasopoulou, E.-N., Shores, L. S., et al. (2018). Cyclodextrin Modulated Type I Collagen Self-Assembly to Engineer Biomimetic Cornea Implants. *Advanced Functional Materials, 28*(41), 1804076. https://doi.org/10.1002/adfm.201804076.
16. Chen, Y., Song, W., Zhao, X., Han, Q., & Ren, L. (2018). An antibacterial collagen membrane crosslinked by the inclusion complex of β-cyclodextrin dialdehyde and ofloxacin for bacterial keratitis. *RSC Advances, 8*(32), 18153-18162. https://doi.org/10.1039/C8RA02160K.
17. Grønlien, K. G., Pedersen, M. E., Sanden, K. W., Høst, V., Karlsen, J., & Tønnesen, H. H. (2019). Collagen from turkey (*Meleagris gallopavo*) tendon: a promising sustainable biomaterial for pharmaceutical use. *Sustainable Chemistry and Pharmacy, 13*, 100166. https://doi.org/10.1016/j.scp.2019.100166.
18. Bergh, V. J. V., & Tønnesen, H. H. (2017). Interaction between the photosensitizer lumichrome and human serum albumin: effect of excipients. *Pharmaceutical Development and Technology, 22*(8), 992-1000. https://doi.org/10.1080/10837450.2016.1212883.
19. Bergh, V. J. V. (2017). *Pharmaceutical preformulation and formulation of an alloxazine and a porphyrin-type photosensitizer*. University of Oslo, Faculty of Mathematics and Natural Sciences, School of Pharmacy, Oslo.
20. Terekhova, I. V., Kumeev, R. S., Alper, G. A., & Agafonov, A. V. (2011). Thermodynamic characteristics of the formation of α- and β-cyclodextrin complexes with lumichrome, lumazine, and uracil in aqueous solution. *Russian Journal of Physical Chemistry A, 85*(10), 1844. https://doi.org/10.1134/S0036024411100293.
21. Slavětínská, L., Mosinger, J., & Kubát, P. (2008). Supramolecular carriers of singlet oxygen: Photosensitized formation and thermal decomposition of endoperoxides in the presence of cyclodextrins. *Journal of Photochemistry and Photobiology A: Chemistry, 195*(1), 1-9. https://doi.org/10.1016/j.jphotochem.2007.09.007.
22. Lang, K., Mosinger, J., & Wagnerová, D. M. (2004). Photophysical properties of porphyrinoid sensitizers non-covalently bound to host molecules; models for photodynamic therapy. *Coordination Chemistry Reviews, 248*(3), 321-350. https://doi.org/10.1016/j.ccr.2004.02.004.

23. Rapacka-Zdonczyk, A., Wozniak, A., Pieranski, M., Woziwodzka, A., Bielawski, K. P., & Grinholc, M. (2019). Development of Staphylococcus aureus tolerance to antimicrobial photodynamic inactivation and antimicrobial blue light upon sub-lethal treatment. *Scientific Reports, 9*(1), 9423. 10.1038/s41598-019-45962-x.
24. Cieplik, F., Deng, D., Crielaard, W., Buchalla, W., Hellwig, E., Al-Ahmad, A., et al. (2018). Antimicrobial photodynamic therapy – what we know and what we don't. *Critical Reviews in Microbiology, 44*(5), 571-589. https://doi.org/10.1080/1040841X.2018.1467876.

Figure legends

Figure 1. Schematic of the bacterial phototoxicity experiment. *In vitro* release experiments were performed with similar setup, except for *S. aureus* which was replaced by PBS in the acceptor compartment.

Figure 2. a) Viable counts (CFU/ml) of *S. aureus* in planktonic form after incubation with LC photocrosslinked collagen hydrogels for 3 h with and without UVA irradiation (~ 9 J/cm^2). Dark and UVA are the dark control and UVA-irradiated hydrogels prepared with HPβCD (200 μM LC) and HPγCD (80 μM LC), respectively. b) Percentage bacterial survival as a function of LC content in the respective hydrogels. c) *In vitro* cumulative release curves of LC from LC-photocrosslinked collagen hydrogels. Dots: hydrogels prepared with HPβCD; squares: hydrogels prepared with HPγCD. Mean released LC (μg) to the acceptor compartment is presented beside the respective timepoints. All results are the mean of three experiments. Asterisks (*) denote significant differences.

Table legends

Table 1. Hydrogel characteristics and summary of the results from the release of LC from the hydrogels.

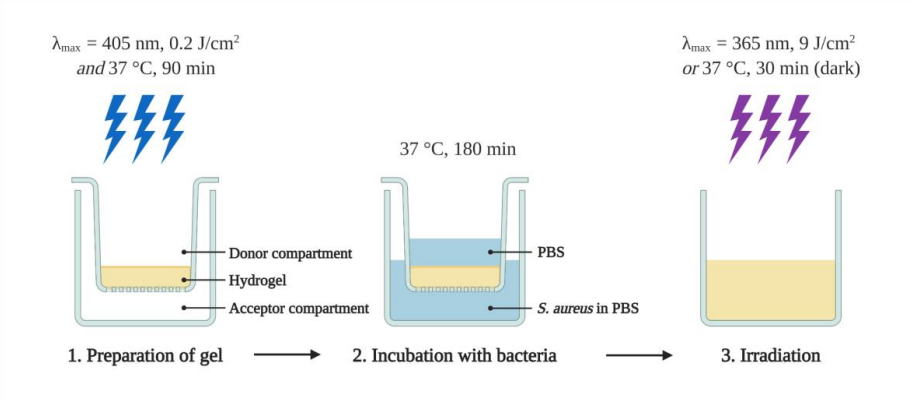

Figure 1. Schematic of the bacterial phototoxicity experiment. *In vitro* release experiments were performed with similar setup, except for *S. aureus* which was replaced by PBS in the acceptor compartment.

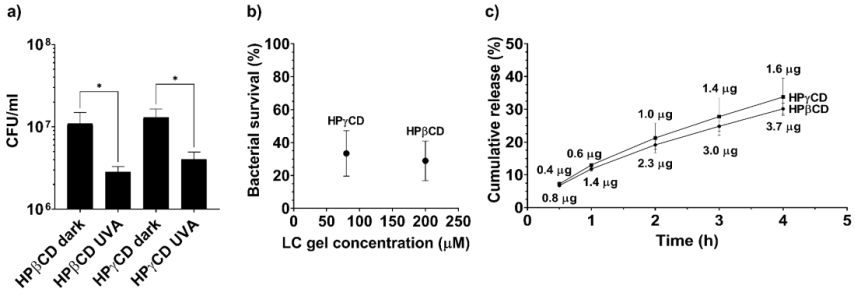

Figure 2. a) Viable counts (CFU/ml) of *S. aureus* in planktonic form after incubation with LC photocrosslinked collagen hydrogels for 3 h with and without UVA irradiation (~ 9 J/cm^2). Dark and UVA are the dark control and UVA-irradiated hydrogels prepared with HPβCD (200 μM LC) and HPγCD (80 μM LC), respectively. b) Percentage bacterial survival as a function of LC content in the respective hydrogels. c) *In vitro* cumulative release curves of LC from LC-photocrosslinked collagen hydrogels. Dots: hydrogels prepared with HPβCD; squares: hydrogels prepared with HPγCD. Mean released LC (μg) to the acceptor compartment is presented beside the respective timepoints. All results are the mean of three experiments. Asterisks (*) denote significant differences.

Table 1. Hydrogel characteristics and summary of the results from the percentage release of LC from the hydrogels.

Hydrogel sample	**Total LC concentration**	**LC release to acceptor compartment**	**LC release to donor compartment**	**LC retained in hydrogel**
HPβCD	200 µM	30.15 ± 1.67%	32.60 ± 0.15%	37.16 ± 1.79%
HPγCD	80 µM	33.76 ± 5.71%	35.47 ± 0.77%	30.77 ± 5.13%